

UNCLASSIFIED

NYO-2131

FUEL CYCLES IN NUCLEAR REACTORS

by

R. T. Shanstrom, M. Benedict, and C. T. McDaniel

Massachusetts Institute of Technology

Nuclear Engineering Department

Contract No. AT(30-1)-2073

August 24, 1959

September 1957-August 1959

UNCLASSIFIED

NYO-2131

FUEL CYCLES IN NUCLEAR REACTORS

by

R. T. Shanstrom, M. Benedict, and C. T. McDaniel

Massachusetts Institute of Technology

Nuclear Engineering Department

Contract No. AT(30-1)-2073

August 24, 1959

September 1957 - August 1959

**This work was done in part at the
MIT Computation Center, Cambridge, Mass.**

<u>Distribution</u>	<u>No. of copies</u>
New York Office, USAEC	20
Dr. Paul C. Fine	2
AEC TIS	1
Division of Sponsored Research, MIT	1
MIT Library	2
MIT Computation Center	1
R. T. Shanstrom	20
MIT Industrial Liason Office	20
MIT Files	30
Total Distribution	<u>97</u>

The contents of this report have been submitted by Mr. R.T. Shanstrom to the Massachusetts Institute of Technology in partial fulfillment of the requirements for the degree of Doctor of Science.

This work was done in part at the MIT Computation Center, Cambridge, Mass.

TABLE OF CONTENTS

<u>Section</u>	<u>Page</u>
CHAPTER I. ABSTRACT	1
CHAPTER II. INTRODUCTION	3
CHAPTER III. SUMMARY	8
A. SUMMARY OF THE CALCULATIONAL PROCEDURE	8
1. FUELCYC Code	8
2. Fuel Scheduling Methods	8
3. Nuclear Data	9
4. Limitations of Code	9
5. Objectives of Code	10
6. Outline of Steps in Code	10
B. SUMMARY OF IMPORTANT RESULTS	14
1. Comparison with Experimental Data	14
2. Comparison with Results of a Simpler Code	17
3. Fuel Cycle Study of Pressurized Light-Water Reactor	18
CHAPTER IV. CALCULATIONAL PROCEDURE	31
A. PHYSICAL MODEL	31
1. Energy Considerations	31
2. Spatial Considerations	42
3. Solution of the Nuclide Concentration Equations	63
4. Nuclear Data	69
B. BASES FOR THE COST CALCULATIONS	71
1. Background and Assumptions	71
2. The Partial Fuel Cost Equations	73
C. DESCRIPTION OF FUELCYC	83
1. General Description	83
2. Fuel Scheduling Procedures Handled by Present FUELCYC Code	85
3. Solution Procedure	96
4. Machine and Time Requirements	109
CHAPTER V. REACTOR DESIGN DATA	112
A. PRESSURIZED LIGHT-WATER REACTOR	112
1. General Description	112
2. Calculation of FUELCYC Nuclear Input Data for the Pressurized Light-Water Reactor	116

<u>Section</u>	<u>Page</u>
B. NRX REACTOR AND THE GLEEP	121
1. Long Term Irradiations in the NRX Reactor	121
2. Calculation of FUELCYC Nuclear Input Data for the NRX Reactor	123
3. Calculation of the Reactivity of the NRX Samples as Measured in the GLEEP	128
C. THE SIMPLER MODEL.....	131
CHAPTER VI. DISCUSSION OF RESULTS	134
A. PRESSURIZED LIGHT-WATER REACTOR.....	134
1. Material Properties of the Fuel Depending on Initial Enrichment and Flux-time	134
2. Material Properties of the Fuel for Different Fuel Scheduling Methods.....	141
3. Cost Results	170
B. COMPARISON WITH EXPERIMENTAL DATA.....	182
1. Buildup of Plutonium Nuclides	182
2. The Reactivity of the NRX Samples.....	184
3. Effect of Changes on Pressurized Light-Water Results..	201
C. COMPARISON OF THE FUELCYC CALCULATIONS WITH THOSE OF A SIMPLER CODE.....	205
CHAPTER VII. CONCLUSIONS.....	208
A. COMPARISONS OF FUELCYC CALCULATIONS WITH EXPERIMENT.....	208
B. PERFORMANCE OF CODE	209
C. STUDY OF ALTERNATE FUELING METHODS	209
D. FUEL CYCLE COSTS IN PRESSURIZED WATER REACTOR.....	210
CHAPTER VIII. RECOMMENDATIONS FOR FUTURE WORK...	212
A. USE OF FUELCYC.....	212
B. EXTENSION OF FUELCYC	212
C. OPERATIONS ANALYSIS STUDY	213
D. COMPARISON WITH EXPERIMENTAL DATA.....	214

<u>Section</u>	<u>Page</u>
CHAPTER VIII. (continued)	
E. EXPERIMENTAL WORK IN THE M.I.T. REACTOR.....	214
F. FURTHER THEORETICAL INVESTIGATION	215
CHAPTER IX. APPENDICES.....	216
A. NUMERICAL SOLUTION OF THE WILKINS EQUATION..	216
B. A CONDENSED CROUT REDUCTION THAT MINIMIZES THE STORAGE AND TIME REQUIREMENTS	220
C. FUELCYC SUBPROGRAMS.....	227
1. LOADER	228
2. MAIN	228
3. READ-PRINT	228
4. TIMECK.....	229
5. TIME-CLOCK	230
6. CONST	231
7. PTCS	232
8. AVGCS2	234
9. WILK2	236
10. FLF2	238
11. CSF2.....	239
12. SQRT	240
13. EXP.....	240
14. NUCON.....	241
15. RKY3	244
16. DERIV	245
17. RESPRB.....	247
18. SPACON.....	248
19. SPACE2	249
20. SPFUN	251
21. SPACFX.....	253
22. SPFUN2	256
23. SPPROP	259
24. NCGTHV	261
25. NEWIMV	262
26. AVGFTH	263
27. COST.....	265
28. CPF.....	270
29. LOG	270
30. BATCH.....	271
31. INOUT	275
32. OUTIN	275
33. GRADED	281
34. (WTPE)	282

<u>Section</u>	<u>Page</u>
CHAPTER IX. (continued)	
35. MI CPM2.....	283
36. MI CTH2.....	283
D. OPERATIONAL INFORMATION FOR FUELCYC.....	284
1. Input Data Preparation.....	284
2. Octal Correction Cards.....	301
3. Program Stops in FUELCYC.....	303
E. ERROR ESTIMATION FOR THE NUMERICAL METHODS.....	305
1. Truncation Errors in Computing Average Cross Sections.....	306
2. Truncation Errors in Computing Nuclide Con- centrations as Functions of Flux-Time.....	309
3. Errors in the Spatial Calculations.....	312
F. TABULATED RESULTS FOR THE PRESSURIZED LIGHT-WATER REACTOR.....	318
G. NOMENCLATURE.....	351
1. English Letters.....	351
2. Greek Letters.....	360
3. Subscripts.....	363
4. Superscripts.....	366
H. BIBLIOGRAPHY.....	367
1. Index.....	367
2. Reference Citations.....	369

LIST OF TABLES

<u>Table No.</u>	<u>Title</u>	<u>Page</u>
3.1	Isotopic Composition of Plutonium in an NRX Sample	14
3.2	Comparison of the Measured Reactivity of NRX Samples with That Calculated in FUELCYC	16
3.3	Performance Characteristics of Pressurized Light-Water Reactor for Various Fuel Scheduling Methods	20
3.4	Fuel Cycle Costs for Various Fuel Scheduling Methods in Pressurized Light-Water Reactor	26
3.5	Principal Components of Fuel Cycle Costs in Pressurized Light-Water Reactor	28
4.1	Nuclear Data	70
4.2	Parameters for Cost Calculation	74
5.1	Reference Design Data for Pressurized Light-Water Reactor	114
5.2	FUELCYC Nuclear Input Data for the Pressurized Light-Water Reactor	117
5.3	Reference Design Data for NRX	124
5.4	FUELCYC Nuclear Input Data for NRX	124
5.5	Nuclear Parameters for the Simpler Model	133
6.1	Local Properties of Fuel, Initial Enrichment of 3.441 a/o U235	139
6.2	Results of Runs for Batch Fuel Scheduling	166
6.3	Results of Runs for Inout Fuel Scheduling	167
6.4	Results of Runs for Outin Fuel Scheduling	168
6.5	Results of Runs for Graded Fuel Scheduling	169
6.6	Fuel Cycle Costs, Batch Fuel Scheduling, 3.441 a/o U235	171

<u>Table No.</u>	<u>Title</u>	<u>Page</u>
6.7	Isotopic Composition of Plutonium in an Irradiated NRX Sample	183
6.8	Nuclide Concentrations for an NRX Sample	185
6.9	Effective Macroscopic Cross Section Changes for the NRX Reactor	188
6.10	Effective Thermal Macroscopic Cross Section Changes for the NRX Reactor	189
6.11	Effective Resonance Macroscopic Cross Section Changes for the NRX Reactor	190
6.12	Reactivity Change Term, R, for the NRX Samples for Different Spectra and for Different Assumptions for Basic Parameters	194
6.13	The Samarium Group of Fission Products	196
6.14	Approximate Values of Different Scaling Ratios for the Pressurized Light-Water Reactor	202
6.15	Values for the Maximum and Average Burnup Predicted by Different Physical Models	206
D1	Input Data Required by MAIN	287
D2	Input Data Required by Fuel Movement Subprograms and for Initialization for a New Run	293
D3	Cost Input Data	295
D4	Sample Input Data for FUELCYC	300
D5	Program Stops in FUELCYC	304
F1-F7	Local Properties of Fuel for Initial Enrichments from 2.876 to 6.452 a/o U235	319
F8-F11	Fuel Cycle Costs, Batch Fuel Scheduling, Initial Enrichments from 2.876 to 6.452 a/o U235	333
F12-F15	Fuel Cycle Costs, Inout Fuel Scheduling, Initial Enrichments from 2.876 to 4.272 a/o U235	337

<u>Table No.</u>	<u>Title</u>	<u>Page</u>
F16-F20	Fuel Cycle Costs, Outin Fuel Scheduling, Initial Enrichments from 2.876 to 4.272 a/o U235	341
F21-F25	Fuel Cycle Costs, Graded Fuel Scheduling, Initial Enrichments from 2.876 to 4.272 a/o U235	346

LIST OF FIGURES

<u>Fig. No.</u>	<u>Title</u>	<u>Page</u>
3.1	Two-Dimensional Contour Plot of the Initial Spatial Distribution of the Relative Thermal Flux or the Power Density, for Batch Fuel Scheduling	22
3.2	Two-Dimensional Contour Plots of the Final Spatial Distributions of the Relative Thermal Flux and the Relative Power Density, for Batch Fuel Scheduling	23
3.3	Two-Dimensional Contour Plots of the Spatial Distributions of the Relative Thermal Flux and the Relative Power Density, for Outin Fuel Scheduling	24
3.4	Net Fuel Cost as a Function of Maximum Local Burnup for Different Cost Bases, Batch Irradiation	30
4.1	Variation of the Microscopic Total Cross Sections of the Fuel Nuclides with Energy	33
4.2	Schematic Diagram of the Energy Model and Neutron Balance	39
4.3	Non-Escape Probability for a Sphere of Radius u , Neutrons Born at the Origin	45
4.4	Schematic Diagram of Material Regions, Mesh Lines, and Mesh Point Numbering	49
4.5	Process Flowsheet for Cost Assumptions	73
6.1	Thermal Flux Spectrum as a Function of Velocity	135
6.2	Relative Change in the Average Thermal Microscopic Absorption Cross Sections for Fuel Nuclides as Functions of Flux-Time	137
6.3	Changes in Fuel Composition with Flux-Time	142
6.4	Relative Change in Space Properties with Flux-Time	143
6.5	Average Enrichment as a Function of Average Burnup	145
6.6	Maximum Burnup as a Function of Average Burnup	146
6.7	Variation of On-Stream Time with Average Burnup	147

<u>Fig. No.</u>	<u>Title</u>	<u>Page</u>
6.8	Variation of Maximum-to-Average Power Density Ratio with Average Burnup	148
6.9	Variation of the Maximum-to-Average Power Density Ratio During a Batch Irradiation	150
6.10	Variation of the Average Non-Leakage Probability for the Fast Group with Average Burnup	151
6.11	Initial Criticality Factors for Batch Irradiation as Functions of Average Burnup; with and without Xenon and Samarium Group Poison	152
6.12	Variation of the Criticality Factor During a Batch Irradiation	154
6.13	Variation of the Final Flux-Time at the Center of the Discharged Fuel with the Initial Concentration of U235	155
6.14	Thermal Neutron Flux as a Function of Radius at the Axial Center Plane of the Core	156
6.15	Ratio of the Thermal Neutron Flux in Fuel to Flux at Midplane of Reactor	158
6.16	Two-Dimensional Contour Plot of the Initial Spatial Distribution of the Relative Thermal Flux or the Power Density, for Batch Irradiation	159
6.17	Two-Dimensional Contour Plots of the Final Spatial Distributions of the Relative Thermal Flux and the Relative Power Density, for Batch Fuel Scheduling	160
6.18	Two-Dimensional Contour Plots of the Spatial Distributions of the Relative Thermal Flux and the Relative Power Density, for Graded Fuel Scheduling	161
6.19	Two-Dimensional Contour Plots of the Spatial Distributions of the Relative Thermal Flux and the Relative Power Density, for Inout Fuel Scheduling	162
6.20	Two-Dimensional Contour Plots of the Spatial Distributions of the Relative Thermal Flux and the Relative Power Density, for Outin Fuel Scheduling	163

<u>Fig. No.</u>	<u>Title</u>	<u>Page</u>
6. 21	Net Fuel-Cycle Cost as a Function of the Average Burnup of the Discharged Fuel	172
6. 22	Net Fuel-Cycle Cost as a Function of the Maximum Burnup of the Discharged Fuel	173
6. 23	Material Cost as a Function of Average Burnup	175
6. 24	Fabrication and Reprocessing Costs as Functions of Average Burnup	176
6. 25	Interest Charges as Functions of Average Burnup	177
6. 26	Breakdown of Fuel-Cycle Cost for Different Values of Average Burnup	178
6. 27	Net Fuel-Cycle Cost as a Function of the Maximum Burnup of the Fuel, for Current Prices, Operation with Constant Maximum Power Density	180
6. 28	Variation of R for NRX Fuel as Measured in GLEEP	195
6. 29	Comparison of Nuclide Concentrations: the "Simpler Code" Versus FUELCYC	207
B1	Schematic Diagram of the Coefficient Matrix for the Spatial Flux Shape	222
B2	Schematic Diagram of the Crout Coefficient Auxiliary Matrix	223

I. ABSTRACT

FUEL CYCLES IN NUCLEAR REACTORS

by

Raymond T. Shanstrom, Manson Benedict, and Charles T. McDaniel

A new IBM 704 computer code, FUELCYC, has been developed for studying the effect on the fuel cycle of different methods of scheduling replacement of fuel and movement of control poisons. Four alternate fuel scheduling methods have been built into the current code and provision is made for the addition of other methods. The fueling techniques available in the current code are: 1) "Batch," the replacement of the entire fuel charge at one time, with uniform control poisoning during the irradiation; 2) "Inout," the progressive shifting of fuel rods from inner positions to outer positions; 3) "Outin," the progressive shifting of fuel rods from outer positions to inner positions; and 4) "Graded," the periodic replacement of the most irradiated fuel rod among different local groups of rods.

FUELCYC is designed for the study of fuel cycles in large power reactors with azimuthal symmetry, which are fueled with U235, U238 and the higher nuclides in their irradiation chains. It is a two-dimensional code in which neutron leakage occurs from two energy groups and neutron absorptions are allowed in the thermal group and also in one of four resonance groups for each fuel nuclide. Local properties are homogenized into cells.

FUELCYC calculates the criticality factor, the flux distribution, the power density distribution, the burnup, the fuel cycle cost, and other properties during the life history of the fuel, taking into account the buildup and decay of nuclides in the fuel irradiation chains. An iterative method for solution of the flux distribution has been developed which converges even for very coarse mesh spacings, and allows a typical fuel cycle problem to be solved, with good accuracy, in from three to five minutes.

The code has been compared with experimental data for the irradiation of natural uranium metal in the NRX reactor. Excellent agreement was obtained with a plutonium isotopic analysis when the base value for the Pu240 disadvantage factor, in the FUELCYC input data, was normalized to experimental data. Fair agreement was obtained with the experimental measurements of reactivity, within 0.6% $\delta k/k$, for irradiations up to 3000 MWD/ton. The comparison of the FUELCYC calculations with the experimental data suggested several changes to improve the agreement. These are:

- 1) a reduction in the value for the Sm 149 yield from U235 fission

from the conventional value of 1.15% to 0.8%. The proposed value is in agreement with a measurement by Littler, L23, of $0.9 \pm 0.2\%$.

2) a few percent increase in the value of the ratio $\sigma_9(\eta_9 - 1)/\sigma_5(\eta_5 - 1)$ over that of the "World Consistent Values"

3) a few percent reduction in the cross section of Pu239 as calculated by FUELCYC at high flux-times due to self shielding in the 0.3 eV resonance.

The effect of the above changes was calculated for the longer irradiations of interest for power reactors. It was found that the effect was small and therefore, (on the basis of this experimental check) that the FUELCYC calculations can be relied on for prediction of the composition changes and reactivity changes for fuel cycle studies in power reactors.

It was found that the flux and power density distributions in an irradiated reactor core are grossly different from that of the uniformly loaded core, and that this has an important effect on the calculation of burnup and costs. A simpler code which assumed a time-invariant chopped-cos, chopped- J_0 thermal flux distribution gave values for average burnup which were approximately 25% lower than those of FUELCYC.

FUELCYC was used for a study of the effect of different methods of fuel scheduling for variations in the initial U235 enrichment in a pressurized light-water reactor similar to the one being developed by Westinghouse Electric Corporation for Yankee Electric Company. It was found that Outin fuel movement was particularly attractive economically. This is because "Outin" gives a high ratio of average to maximum burnup, which is desirable in increasing the total power output of a given charge of fuel, and it also gives a low ratio of maximum to average power density, which would enable the core to be operated at high power. High power operation reduces both the fuel cycle cost and the capital charges. Graded fuel scheduling is also attractive, but Inout produces prohibitively high flux peaking.

The trend of the fuel cycle cost with variations in burnup gives incentive for the development of fuel elements which can withstand average burnups of from 20-25,000 MWD/ton and maximum burnups from 30-40,000 MWD/ton. If burnups of this order could be obtained the fuel-cycle cost in the pressurized light-water reactor could be reduced to 3.5 mills/kwh for simple Batch irradiation and 2.5 mills/kwh for the Graded or Outin fuel scheduling methods.

II INTRODUCTION

Fuel cycle analysis is concerned with the changes that occur in the properties of nuclear fuels and nuclear reactors during long term irradiation. The properties that are of greatest interest are: the burnup attainable from a given charge of fuel, the excess reactivity produced, and the power density distribution. Fuel cycle analysis is also concerned with the cost of fuel and of the processes to which fuel is subjected before and after irradiation in the reactor. A typical fuel cycle study involves the following steps: 1) the choice of fuel material, where fuel is used to mean both fissionable and fertile materials; 2) evaluation of the costs involved in the "purchase" of the fuel and in the fabrication of the fuel elements (or for a homogeneous reactor, the preparation of the fuel slurries or solutions); 3) selection of the method of fuel scheduling, i. e., whether to replace the entire charge fuel as a single batch or to replace a portion of the fuel at more frequent intervals, and whether to leave the fuel in one place in the reactor or periodically to shift the position of partially irradiated fuel elements; 4) calculation of the changes in composition of the fuel during irradiation; 5) calculation of the criticality factor without control poison, the flux distribution, and the power density distribution periodically as the irradiation progresses; 6) choice of the method of control of the reactor so as to maintain criticality during the irradiation; and 7) evaluation of the costs involved in the reprocessing or in the disposal of the spent fuel and in the "sale" or recycling of the fissile material.

It can be seen that in principle the part of fuel cycle analysis dealing

with changes taking place in the reactor involves nearly all of nuclear reactor statics theory. In practice, simplifications are made by limiting consideration to certain reactor types and, by assuming that certain properties of the reactor remain constant during irradiation of the fuel. In reality, a measure of the refinement of a fuel cycle calculation method is its lack of assumptions of time-invariant properties.

Many of the fundamental characteristics of fuel cycles can be determined by calculation of the composition changes that occur in a local section of fuel as it is irradiated. If neutron leakage is assumed to be constant, reactivity changes can be obtained from the calculation of cross section changes. This method is usually referred to as the constant-flux, or zero-dimensional, approximation, and was used in basic papers by Dunworth, D10; Lewis, L20; Spinrad, Carter, and Egger, S6; and Weinburg, W7. Benedict and Pigford, B4, have published a very comprehensive discussion of fuel cycles using this model, and consider not only batch-irradiated, uranium-fueled reactors but also plutonium recycle, methods of fuel scheduling, and thorium breeders.

This zero-dimensional model was still used for most of the fuel cycles papers presented at the Second Geneva Conference on the Peaceful Uses of Atomic Energy although considerable refinements had been made in other aspects. Greebler, Harker, Harriman, and Zebroski, G11, took into account the energy spectrum of the flux and depression of the flux in cylindrical fuel elements. (The energy model proposed by Greebler et al was adopted in part for this work.) Pigford, Benedict, Shanstrom, Loomis, and Van Ommeslaghe, P3, treated spatial non-uniformity of the flux by perturbation methods, assuming a time-independent chopped-cos,

chopped- J_0 flux distribution for various fuel scheduling methods in both uranium and thorium reactors, and considered the recycle of plutonium and of U233. Feinberg, Antsiferov, Katkov, Komissarov, Levina, Nicolsky, Novikov, Osmachkin, Stolarov, and Shevelev, F2, also considered various fuel scheduling methods and applied the heterogeneous method to the calculation of fuel burnup.

Spatial variations in the flux distribution during the irradiation history are important in fuel cycle calculations; however, there has been little work published in which these variations were considered. One-dimensional fuel cycle calculations have been made for different fuel scheduling methods by Minton, M7, and for initially non-uniformly loaded cores and for different control rod programming techniques by Graves, Arnold, Eich, Minton, and Wolf, G15, using various Westinghouse IBM 704 computer codes, namely: the zero-dimensional burnup code CAP-1; the one-dimensional, few-group, diffusion-theory, criticality code WANDA; the one-dimensional fuel-cycle code MERLIN, which is a combination of CAP-1 and WANDA; the one-dimensional, few-group, diffusion-theory, criticality and burnup code CANDLE; and the two-dimensional, few-group, diffusion-theory, criticality code PDQ. Mention should be made of a British two-dimensional fuel cycle study for Batch irradiation; that of Hitchcock, Price, and Shenton, H11, performed on the Elliott 402 digital computer. The operable two-dimensional computer codes in the U.S., except for FUELCYC, are primarily designed to calculate criticality. The KAPL IBM 704 code system CUREBO, A16, however, has an additional option allowing depletion of a single fissionable nuclide in each core region, but no buildup of higher isotopes

is accounted for. More elaborate codes are under development at various laboratories; the most elegant of these is the three-dimensional Monte Carlo and diffusion theory, criticality and burnup code RBU for the IBM 709 computer, which is being developed by Leshan, Burr, Morrison, Temme, and Thompson of American-Standard and by Triplett of Hanford Laboratories, L26.

As the interest of different power reactor design groups has settled on particular reactor types, more emphasis has been placed on fuel cycle variations in order to optimize the operation of these reactors. The FUELCYC computer code has been developed specifically as a tool for the solution of these fuel cycle problems. The attempt has been made to develop a code which will be of general applicability to many reactor types with the emphasis on large power reactors.

Implicit in the effort that has gone into the code is the faith that these power reactors have a future in the competitive power market. This economic breakthrough seems certain eventually due to the abundance of potential nuclear fuel and to the rapidity of the dissipation of fossil fuels.* The question of how soon the breakthrough can be made is up to the ingenuity of the reactor designers. Since reactors can be expected to cost more than fossil-fueled boilers for some time, a requirement for economic nuclear power is a reduction in the cost of the nuclear fuel cycle. It is hoped that FUELCYC will be of some use in the development

*Baumeister, B3, estimates the total world energy reserves of uranium and thorium assuming full utilization of fertile as well as fissionable material to be twenty-five times that of fossile fuels. Davis, D2, estimates that the usable U. S. fossil fuel reserves will be exhausted within fifty years.

of a nuclear fuel cycle that will do this.

This work has been carried out under the M. I. T. Fuel Cycles Project, AEC Contract No. AT(30-1)-2073 which was initiated at M. I. T. in September 1957.

III SUMMARY

A. SUMMARY OF THE CALCULATIONAL PROCEDURE

1. FUELCYC Code

A new fuel-cycle code, FUELCYC, has been written for the IBM 704 computer. This code computes the distribution of neutron flux with respect to energy and position in the reactor, derives effective cross sections for each nuclide at each point in the reactor, uses the flux and effective cross sections to project the change of nuclide concentration at each point with time, determines the conditions under which the reactor is just critical, and evaluates fuel-cycle costs.

The physical model for FUELCYC is two-dimensional diffusion theory in an axially-symmetric cylinder. Four major energy groups are treated: fast fission, fast, resonance, and thermal, with the resonance group further divided into four sub-groups. Leakage is assumed to occur in the fast and in the thermal group, and each fuel nuclide is assumed to absorb neutrons in one of the resonance sub-groups as well as in the thermal group.

2. Fuel Scheduling Methods

Four methods of charging and discharging fuel have been written into the code:

(1) "Batch" irradiation of fuel fixed in place in the reactor, with control poison distributed uniformly throughout the reactor.

(2) "Inout" irradiation, in which fuel rods are moved from the center of the reactor to the periphery, with no control poison and with the reactor just critical.

(3) "Outin" irradiation, in which fuel rods are moved from the periphery of the reactor to the center, with no control poison and with the reactor just critical.

(4) "Graded" irradiation, in which fuel rods, fixed in place in the reactor, are discharged individually and replaced by fresh rods on such a schedule that the average composition of fuel in each region of the reactor remains time-independent and the reactor, with no control poison, remains just critical.

Provision is made for writing into the code other methods of charging and discharging fuel and managing control poison.

3. Nuclear Data

Nuclear data presently written into the code comes principally from the following sources:

(1) The dependence of cross sections of non $1/v$ absorbers on energy is represented by a series of equations of the Breit-Wigner form, with parameters recommended by Westcott, W11. Cross sections at 2200 m/sec from these equations are consistent with BNL-325, 2nd edition, H29.

(2) Cross sections of other nuclides and neutron yield data have been taken from BNL-325, 2nd edition.

(3) Yields and cross sections of fission products are calculated from Walker's report, W4.

4. Limitations of Code

The code is limited in applicability to:

(1) Reactors sufficiently well moderated to have the majority of fissions caused by thermal neutrons.

(2) Large reactors, in which thermal leakage is small compared to thermal absorption.

(3) Reactors with azimuthal symmetry.

(4) Reactors in which the spatial variation of flux and nuclide concentrations may be adequately approximated by specification of values in 200 regions, 10 radial by 20 axial.

(5) Homogeneous reactors or heterogeneous reactors whose lattice properties may be represented by an equivalent homogeneous reactor.

(6) Reactor fuel consisting of any mixture of U235, U238 and their irradiation products.

All of the large, uranium-fueled power reactors under development in the United States at the present time, except the fast Enrico Fermi reactor, meet these conditions and may be handled by this code.

5. Objectives of Code

Development of this code has had as its objectives the reliable prediction of fuel composition, reactivity changes, flux and power-density distributions, reactivity lifetimes, and fuel cycle costs without calling for excessive amounts of computer input data or computer time.

FUELCYC requires an IBM 704 computer with a 32,768-word fast memory and two magnetic tape units. Calculation of the above fuel cycle properties for fuel of a specified initial enrichment in a fifty region reactor uses about three minutes of computer time.

6. Outline of Steps in Code

The computation sequence followed by the code is as follows:

(1) For a fuel of specified composition, the energy distribution of neutrons below 0.45 eV is computed by a fifth order difference solution of the Wilkins equation, H24.

(2) From this energy distribution, and the dependence of cross sections on energy which has been written into the code, effective thermal cross sections are computed.

(3) Absorptions at resonance energies are computed by the standard resonance escape probability formulation, using experimentally determined effective resonance integrals for U238 and Pu240 and infinite-dilution resonance integrals for U235, U236, Pu239, Pu241 and Pu242.

(4) The change of nuclide concentrations over the first flux-time interval is computed by solving the differential equations expressing nuclide material balances by a fourth-order Runge-Kutta-Gill technique.

(5) The neutron energy spectrum and effective cross sections of fuel at the end of the first flux-time interval is computed by a repetition of steps (1), (2) and (3).

(6) The change of nuclide concentrations over the second flux-time interval is computed by a repetition of step (4). This process is repeated until the entire flux-time interval of interest is covered.

(7) The concentration of each nuclide and certain functions of these concentrations which appear in the neutron balance equation are represented by polynomials in flux-time.

(8) The neutron balance equation in each region of the reactor is expressed as a linear difference equation in the flux in the region in question and the four adjacent regions. Parameters in the equation are functions of the nuclide concentrations and effective cross sections, both

of which depend on the flux-time to which the fuel has been exposed, which depend in turn on the flux distribution in the reactor and the previous history of the fuel.

(9) The procedure for solving this set of neutron-balance difference equations will be outlined for the batch irradiation case. At time zero in this case the reactor is assumed to be charged with fuel of specified uniform composition. A value for the uniform concentration of control poison which makes the reactor critical is computed. The set of linear, second-order difference equations for all regions of the reactor is solved for the relative thermal-neutron flux distribution by an iterative technique employing the Crout reduction procedure.

(10) A criticality factor for the entire reactor, defined as the ratio of the over-all production rate of neutrons to the over-all consumption rate excluding control poisons, is computed.

(11) A time step is then taken, the new flux-time in each region of the reactor is determined, functions of the nuclide concentrations at this flux-time are evaluated from the polynomials (7), and a new set of neutron balance difference equations for each region of the reactor is written.

(12) A new control poison concentration is computed and the set of difference equations is solved by iteration as in step (9) to find the new relative flux distribution.

(13) Steps (10), (11), and (12) are repeated until the reactor is just critical without control poison.

(14) The average composition of spent fuel is determined by averaging local concentrations, using the polynomials (7).

(15) The cost of the fuel cycle is determined from the weight and composition of a charge of fuel, the time it spends in the reactor, and the composition of spent fuel (14).

For the other methods of charging and discharging fuel a repeated iterative solution of the neutron-balance difference equations somewhat similar to steps (9)-(13) is carried out, to find the rate at which fuel of a specified initial composition may be moved through a reactor just critical without control poison.

B. SUMMARY OF IMPORTANT RESULTS

1. Comparison with Experimental Data

FUELCYC results were compared with experimental data for natural uranium samples irradiated in the NRX reactor. Comparison was possible for build-up of plutonium isotopes and for reactivity changes of the samples with irradiation. The available experimental measurements were for irradiations of less than 3000 MWD/ton. (Reference C11)

1.1. Comparison of the Plutonium Content in the NRX Samples with FUELCYC Calculations. Results of one isotopic analysis were available for the relative amounts of plutonium nuclides in an NRX sample, which had been irradiated to a flux-time (for 2200 m/s flux) of 0.63 n/kb. This is equivalent to about 2500 MWD/ton. The experimental results are compared with those of FUELCYC in Table 3.1.

Table 3.1 Isotopic Composition of Plutonium in an NRX Sample Irradiated to 0.633 n/kb, Comparison of Experimental and FUELCYC Values.

Isotope	Isotopic Composition, %		
	Measured (Mass Spectrometer)	Run NRX1*	Run NRX2†
Pu239	87.117 ± 0.052	87.22	87.30
Pu240	11.244 ± 0.051	11.19	10.72
Pu241	1.521 ± 0.010	1.47	1.84
Pu242	0.118 ± 0.005	0.12	0.14

* $\sum_{s, fl} = 230$. bifa

† $\sum_{s, fl} = 1160$. bifa

The macroscopic scattering cross section* of the fuel, $\Sigma_{s,fl}$, is used in computing the Pu240 disadvantage factor as recommended in Reference C13. When the true value of 1160 bifa (Run NRX2) is used, the agreement between the experimental results and the FUELCYC calculations is fair. If the reduced value of 230. bifa is used (which increases the Pu240 resonance disadvantage factor from 1.2 to 2.0 at a flux-time of 0.6) the agreement is excellent for all nuclides. These results are further discussed and compared with "blackness" theory calculations in Section VI. B. 1.

1.2. Comparison of the Experimental Measurements of the Reactivity of NRX Samples with FUELCYC Calculations. The reactivity of NRX samples, irradiated from 0.05 to 0.6 n/kb, was determined by oscillator measurements in the Harwell GLEEP.

In these experiments the signal produced due to variations in the neutron density by the alternate oscillation of irradiated and unirradiated uranium fuel was compared to that of a standard boron absorber. This gives a "reactivity change term," R, which is proportional to the change in reactivity of the irradiated sample from that of the unirradiated sample. (The true reactivity change is related to changes in R by, $\delta\rho \sim \delta R/1600$ if the units of R are bifa.)

The results for the comparison of these experimental measurements with the FUELCYC calculations are given in Table. 3.2. Xenon-135 has

* The Canadian system has been adopted in which the units of microscopic cross sections are barns and in which nuclide concentrations are normalized to the initial concentration of U235. This gives macroscopic cross sections in barns per initial fissile atom, abbreviated as bifa.
 $(\Sigma_{s,fl} = N_{fl} \sigma_{s,fl} / N_5^0)$

Table 3.2 Comparison of the Measured Reactivity of NRX Samples with That Calculated in FUELCYC

Reactivity change term, R (bifa)	Flux-time (n/kb)					
	0.0	0.0822	0.164	0.246	0.411	0.575
Observed in GLEEP	0.0	0.0	3.1	2.6	-4.3	-15.4
Calculated by FUELCYC						
1.15% yield of Sm 149	0.0	-5.5	-4.7	-5.2	-13.5	-21.7
0.80% yield of Sm 149	0.0	-3.5	-2.7	-3.2	-11.5	-19.7
Above case plus increase in R.c.r. of 6% initially reducing to 2% increase at a flux-time of 0.575	0.0	0.0	3.1	2.6	-4.3	-15.4

decayed to a negligible amount by the time the measurements were made, however, the measurements do include the Samarium group transients. This causes an initial reduction in reactivity but saturates at about 0.05 n/kb. Table 3.2 shows that values from the FUELCYC calculations using the normal built-in data, which includes a 1.15% U235 fission yield for Sm 149, are from zero to nine bifa below the experimental values for R. (The yield value of 1.15% was recommended in Reference C11.) This represents a reactivity difference of from zero to 0.6%. The behavior of the measured and calculated results at low flux-times indicates that the yield value for Sm 149 should be reduced to 0.8%. The latter value is in agreement with a measurement by Littler, L23. Using the value of 0.8% improves the agreement by 2 bifa.

The curve is very sensitive to the following ratio of Pu239 and U235 parameters. This ratio has been called the R.c.r., for reactivity change ratio,

$$\text{R. c. r} = -\frac{\delta N_9 \sigma_9 (\eta_9 - 1)}{\delta N_5 \sigma_5 (\eta_5 - 1)} \quad (3.1)$$

where $-\delta N_9/\delta N_5$ is the initial conversion ratio (at zero flux-time). The FUELCYC results can be forced to fit the experimental curve within the standard deviations of measurements for the 2200 m/s values of the σ 's and η 's in Eq. (3.1). The change required to fit the experimental data is a 6% increase in R.c.r. initially reducing to a 2% increase at a flux-time of 0.575 n/kb.

The most likely changes to bring the FUELCYC calculations into agreement with the NRX experimental data appear to be:

- 1) Adoption of a U235 fission yield value for Sm 149 of 0.8%
- 2) An increase in the value of the ratio $\sigma_9(\eta_9 - 1)/\sigma_5(\eta_5 - 1)$ over that of the "World Consistent Values" for fission parameters.
- 3) A reduction in the value calculated by FUELCYC for the Pu239 cross section as flux-time increases due to progressive spatial self-shielding in its 0.29 ev resonance.

2. Comparison with Results of a Simpler Code

FUELCYC calculations were compared with those of a simpler code for Batch and Graded fuel scheduling. The simpler code was that used in a former fuel-cycle paper by Pigford et al, P3. The spatial model for this "simpler" code assumed a time-independent chopped-cos, chopped- J_0 flux distribution, where reactor average properties were calculated from the constant-flux properties by perturbation methods. Average burn-ups calculated by FUELCYC differed in some cases by as much as 25% from those calculated by the simpler code. This difference is due to the marked departure of the spatial distribution of neutron flux from a chopped-cos, chopped- J_0 distribution when the fuel composition becomes non-uniform.

3. Fuel Cycle Study of Pressurized Light-Water Reactor

This fuel-cycle code has been applied to a pressurized light-water reactor similar to one being developed by Westinghouse Electric Corporation for Yankee Atomic Electric Company (Reference Y1). Fuel for this reactor consists of slightly enriched UO_2 rods 0.3 inches in diameter and eight feet long clad in stainless steel. The total uranium inventory of the reactor is 21,000 kgm. Its rated heat output is 480 Mw, and the net electric output of the power plant is 134 Mw.

3.1 Operating Variables Considered. The principal operating variables considered were:

- (1) The U235 enrichment of feed to the reactor, and
- (2) The procedure for scheduling and recharging of reactor fuel.

The fuel scheduling procedures, (1) Batch, (2) Inout, (3) Graded, and (4) Outin, described in Section III. A. 2. above were the four procedures studied.

3.2 Performance Characteristics. For each of these fuel scheduling procedures it was assumed that the reactor would be so operated as to obtain the maximum amount of heat allowed by the initial excess reactivity of the fuel. The principal performance characteristics of the reactor under these conditions evaluated with the aid of the fuel cycle code were:

- 1) The maximum local burnup experienced by fuel.
- 2) The average burnup experienced by a complete charge of fuel,

and

- 3) The ratio of maximum to average power density in the reactor.

The maximum local burnup is important because radiation-damage

considerations usually set an upper limit to the local burnup which can be taken without distortion or rupture of fuel cladding serious enough to interfere with safe operation of the reactor.

The average burnup is important because it sets the amount of heat and power which can be produced from a given quantity of fuel. It and the feed enrichment are the two factors with principal effect on fuel-cycle costs.

The ratio of maximum to average power density is important because of the critical effect of this variable on temperatures in the reactor and on the maximum thermal power at which it may be operated safely. The higher this ratio, the lower the safe power level.

Table 3.3 summarizes the interrelationships found between these operating variables and performance characteristics of the pressurized-water reactor. Results have been tabulated as functions of the fuel-scheduling method and the maximum local burnup. because these are the two factors on which the reactor designer or operator is most apt to wish to exercise choice.

The first part of this table shows the feed enrichment needed to permit attainment of the specified maximum local burnup for each of the four fuel-scheduling methods. The enrichment increases nearly linearly with burnup. Batch fueling requires the highest enrichment for a given burnup because of the use of neutron-absorbing control poisons during the early part of the batch cycle. None of the other three fueling methods need control poisons, because their fuel composition remains steady during irradiation. The small differences in enrichment needed for the three steady-state methods are due to differences in fuel

Table 3.3 Performance Characteristics of Pressurized Light-Water Reactor for Various Fuel Scheduling Methods.

<u>Fuel Sch'd. Method:</u> <u>Max. Local Burnup</u> <u>(MWD/ton)</u>	<u>Batch</u>	<u>Inout</u> <u>Atom %U235 in Feed</u>	<u>Graded</u>	<u>Outin</u>
10,000	3.14	2.93	2.95	3.02
20,000	3.58	3.17	3.20	3.39
30,000	4.10	3.42	3.53	3.79
40,000	4.71	3.70	3.88	4.20
50,000	5.34	4.06	4.24	-
60,000	6.09	-	-	-
		<u>Average Burnup, MWD/ton</u>		
10,000	4,200	7,900	7,900	7,900
20,000	10,000	16,300	16,300	16,300
30,000	16,800	25,100	25,100	25,100
40,000	24,200	34,400	34,400	34,400
50,000	32,200	44,000	44,000	-
60,000	41,200	-	-	-
		<u>Ratio of Max. to Avg. Power Density</u>		
10,000	1.90*	3.28	2.54	1.80
20,000	1.49*	4.20	2.39	1.47
30,000	1.37*	5.16	2.30	1.38
40,000	1.29*	6.17	2.23	1.35
50,000	1.25*	7.20	2.18	-
60,000	1.23*	-	-	-

*At end of batch cycle

composition distributions.

The second part of the table shows the average burnup attainable from a complete charge of fuel initially of such an enrichment as to permit attainment of the specified maximum local burnup. The average burnup attainable in the last three, steady-state fuel scheduling procedures at a given maximum local burnup are equal and are much greater than the average burnup attainable in batch irradiation. For a given maximum local burnup important advantages for the steady-state fueling methods compared with batch irradiation are: the higher average burnup attainable, the lower feed enrichment needed, and elimination of control poison. The ratio of average to maximum burnup increases as burnup increases, because of flattening of reactor flux in regions of high burnup.

The third part of this table lists the ratio of maximum to average power density. In the case of batch irradiation the values are for the end of the cycle; at the beginning of the cycle the ratio has the value 2.70 independent of burnup. The Outin method of fueling has a great advantage over the other steady-state fueling methods in having the lowest maximum-to-average power density ratio.

3.3 Flux and Power-Density Distributions. Fig. 3.1 shows a two-dimensional contour plot of the initial thermal flux or power density distribution for Batch fuel scheduling. The power density distribution is initially the same as that of the flux since the fuel is loaded uniformly. The initial distribution is slightly more flattened than that of the familiar chopped $\cos-J_0$ distribution due to the uneven distribution of equilibrium Xe-135.

Fig. 3.2 shows the flux and the power-density that would exist at the

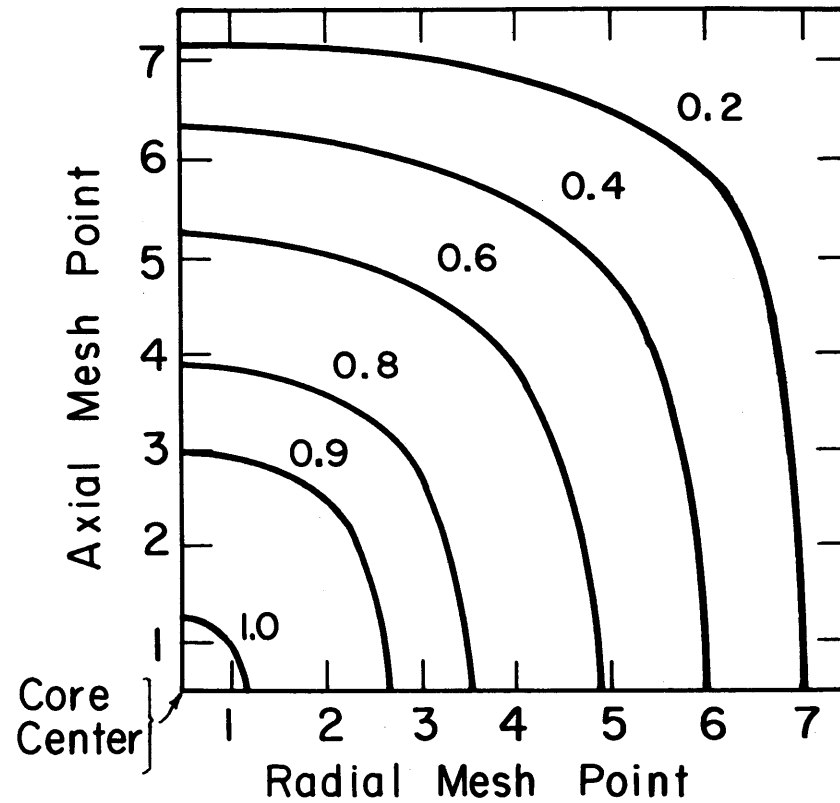


FIG. 3.1 TWO-DIMENSIONAL CONTOUR PLOT OF THE INITIAL SPATIAL DISTRIBUTION OF THE RELATIVE THERMAL FLUX OR THE POWER DENSITY FOR BATCH IRRADIATION, WITH EQUILIBRIUM Xe AND Sm (ONE QUADRANT OF THE CORE IS SHOWN)

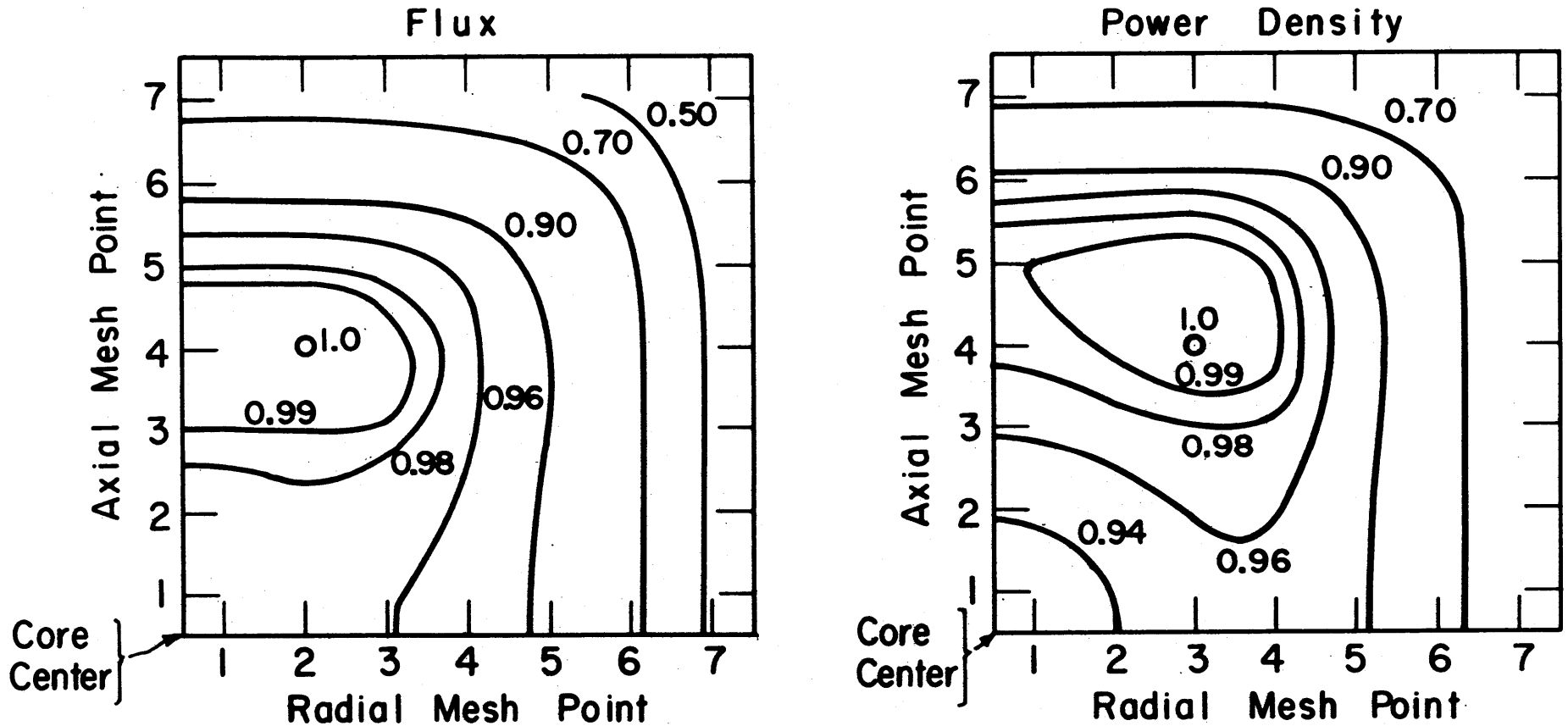


FIG. 3.2 TWO-DIMENSIONAL CONTOUR PLOTS OF THE FINAL SPATIAL DISTRIBUTIONS OF THE RELATIVE THERMAL FLUX AND THE POWER DENSITY, FOR BATCH FUEL SCHEDULING, AVERAGE BURNUP OF APX. 23,000 MWD/TON (ONE QUADRANT OF THE CORE IS SHOWN)

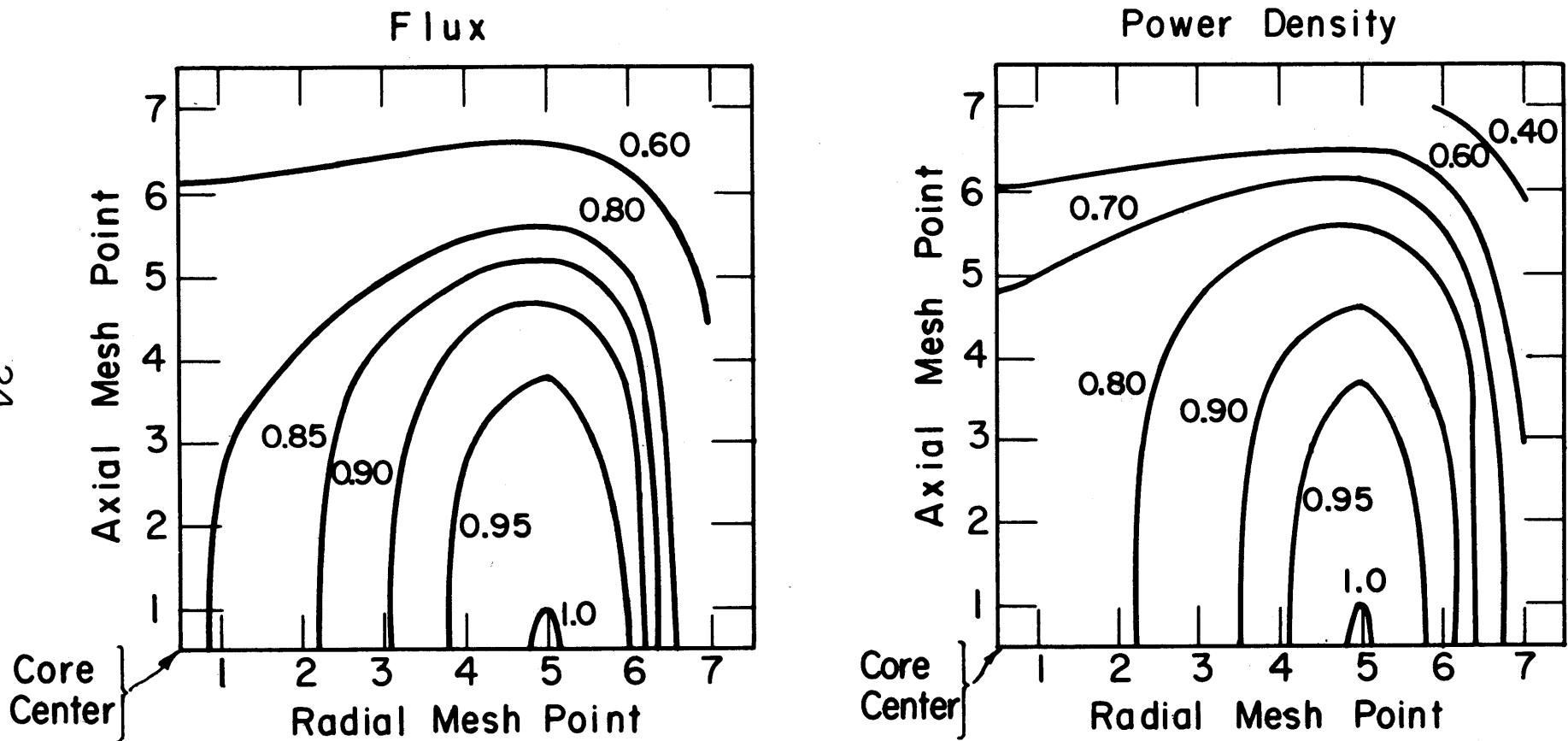


FIG. 3.3 TWO-DIMENSIONAL CONTOUR PLOTS OF THE SPATIAL DISTRIBUTIONS OF THE RELATIVE THERMAL FLUX AND THE RELATIVE POWER DENSITY FOR OUTIN FUEL SCHEDULING, AVERAGE BURNUP OF APX. 23,000 MWD/TON (ONE QUADRANT OF THE CORE IS SHOWN)

end of a Batch irradiation if the average burnup had been 23,000 MWD/ton. The point of maximum flux has shifted off the center line both axially and radially. It is apparent that the final flux shape has little resemblance to a chopped $\cos-J_0$ distribution. The final power density distribution is even more distorted with the maximum shifted further outwards radially than for the flux.

Fig. 3.3 shows the steady-state thermal flux and power-density distributions for Outin fuel scheduling for the same average burnup (23,000 MWD/ton) as the previous Batch case. The distributions peak on the axial center line but far out radially. The Outin method of fueling, however, gives considerably flatter distributions than those of the uniformly loaded reactor (Fig. 3.1).

Similar plots are given for Graded and Inout fuel scheduling in Chapter VI, Figs. 6.18 and 6.19.

It is seen that the heat transfer characteristics of the core will be strongly dependent on the fuel scheduling method used and that this should be taken into consideration in the initial core design.

3.4 Fuel Cycle Costs. Fuel cycle costs evaluated from the data of Table 3.3 are listed in Table 3.4, for two operating conditions. In the top half of the table, it has been assumed that the power level of the reactor can be kept constant at the design value of 480 thermal Mw, no matter how the power density distribution changes. In the bottom half of the table it is assumed that the maximum power density remains constant at the value of 190 kw/l occurring at the beginning of the cycle in Batch irradiation. In actual operation of the reactor, conditions (and fuel cycle costs) will probably fall between these two cases as extremes.

Table 3.4 Fuel Cycle Costs for Various Fuel Scheduling Methods in Pressurized Light-Water Reactor.

		<u>Fuel Cycle Costs, mills/kwhe</u>			
<u>Fuel Scheduling Method:</u>		<u>Batch</u>	<u>Inout</u>	<u>Graded</u>	<u>Outin</u>
<u>Max. Local Burnup, MWD/ton</u>		<u>Constant Power Output of 480 tMw</u>			
10,000		8.90	5.48	5.48	5.48
20,000		4.95	3.52	3.52	3.58
30,000		4.00	2.90	2.94	3.08
40,000		3.62	2.62	2.68	2.86
50,000		3.48	2.50	2.58	-
60,000		3.48	-	-	-
		<u>Constant Max. Power Density of 190kw/l</u>			
10,000		8.88	5.70	5.50	5.25
20,000		4.88	3.81	3.49	3.34
30,000		3.87	3.41	2.88	2.78
40,000		3.44	3.36	2.59	2.51
50,000		3.24	3.48	2.48	-

Nothing more precise can be stated without detailed knowledge of the reactor-cooling, steam-producing and power-generating systems. For instance, if the output of the power-generating system is limited to 134 ekw, it will not be useful to operate the reactor at more than 480 tkw even in the Outin case with its low maximum-to-average ratio, and costs for this case will not be lower than in the top half of the table. On the other hand if maximum heat flux rather than maximum heat production rate limits reactor operation, the costs of the bottom half of the table are appropriate.

Both parts of the table show the striking cost advantage gained in having fuel elements which will permit local burnups of 30-40,000 MWD/ton, no matter which fueling method is used. Beyond this burnup, the apparent cost advantages are too small to offset possible operating interruptions due to increased frequency of fuel failure. The cost advantage of the Graded and Outin fueling methods compared with Batch irradiation are large. Although the Inout method appears to have important cost advantages for operation at constant power output, this method is not practical because of the extreme non-uniformities in power density cited earlier.

Table 3.5 show the contribution to overall fuel-cycle costs of each of the principal components of the fuel cycle for batch fueling with four different feed enrichments and burnups. The initial decrease in overall cost with increasing burnup is due to reduction in fabrication and re-processing charges, which are nearly inversely proportional to average burnup. The leveling off of overall cost and its ultimate slight increase is due to the reduction in the plutonium credit and the increase in the

Table 3.5 Principal Components of Fuel Cycle Costs in Pressurized Light-Water Reactor, Batch Fuel Scheduling, 480 Mw Heat Production.

% U235 in Feed	3.44	4.38	5.59	6.45
Avg. Burnup, MWD/ton	8,650	20,500	35,400	45,400
Max. Burnup, MWD/ton	17,900	35,000	53,300	64,500
Mills/kwhe				
Uranium feed	7.71	4.36	3.37	3.09
Credit for U in spent fuel	-5.23	-2.17	-1.28	-1.02
Credit for Pu in spent fuel	<u>-0.91</u>	<u>-0.70</u>	<u>-0.57</u>	<u>-0.51</u>
Net material cost	1.57	1.49	1.52	1.56
Fabrication	1.94	0.87	0.54	0.44
Fuel reprocessing	0.73	0.35	0.21	0.18
UF ₆ lease charge	0.96	0.89	1.04	1.17
Working Capital charges	<u>0.21</u>	<u>0.17</u>	<u>0.17</u>	<u>0.17</u>
Overall fuel cycle cost	5.41	3.77	3.48	3.52

UF₆ lease charge at the higher enrichments.

3.5 Cost Bases and their Consequences. The principal cost bases used for the above fuel cycle costs are

(1) Uranium price as a function of enrichment from the AEC's current schedule of UF₆ prices (Reference U5), tied to \$39.27/kgmU for natural UF₆.

(2) Credit for plutonium in spent fuel, \$12/gm.

(3) Costs for mechanical fabrication of fuel, \$90/kgmU.

(4) Cost for producing UF₆ from the spent fuel from AEC's present charges for this service (Reference U6), approximating \$25/kgmU for this reactor.

(5) UF₆ inventory lease charge, 4% of value per year, in accordance with present AEC charges.

(6) Interest charges on working capital tied up in initial fuel fabrication expenses, 9%/year.

To illustrate the effect of changes in these bases, fuel-cycle costs have been computed on the three different bases listed in the key of Fig. 3.4 This figure shows the variation of overall fuel-cycle cost with maximum local burnup for batch irradiation at a constant thermal power of 480 Mw. Although the level of fuel cycle costs are quite different for the three bases, their trends with burnup are similar; the optimum maximum local burnup is in the range of 30-40,000 MWD/ton for every basis.

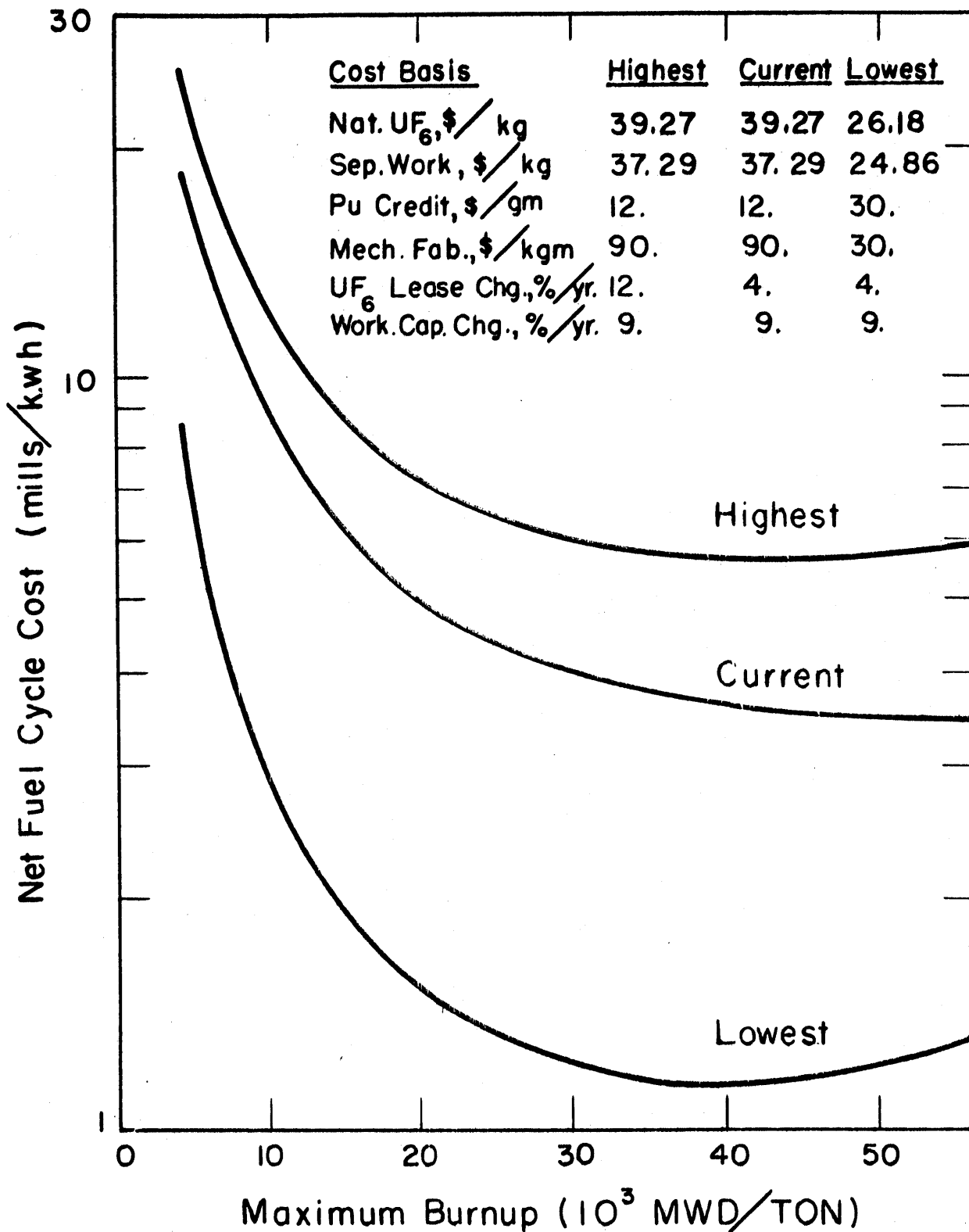


FIG. 34 NET FUEL CYCLE COST AS A FUNCTION OF THE MAXIMUM BURNUP OF THE FUEL, BATCH IRRADIATION, FOR DIFFERENT COST BASES

IV. CALCULATIONAL PROCEDURE

A. PHYSICAL MODEL

1. Energy Considerations

The nuclear events have been divided into four major energy groups: thermal, resonance, fast, and fast fission; with the resonance group further subdivided as explained in Section 1.2.

1.1 The Thermal Cutoff Energy. The thermal group is characterized by the occurrence of collisions which increase the energy of the neutrons as well as those which decrease their energy, so the upper bound on this group should equal or exceed the cutoff energy for pure slowing down. This cutoff energy depends on the hardening parameter Δ , see Eq. (4.5), as well as the moderator temperature, as shown by Hurwitz, Nelkin, and Habetler, H24. On the basis of typical core average values of Δ for different thermal reactors, the cutoff will fall in the range of from 5 to 10 kT.*

For many thermal reactors a cutoff energy of .45 ev is sufficiently high, since this is approximately 10 kT for 500° K and 5 kT for 1000° K, and is also a convenient break point for the following three reasons:

- 1) This is within the energy region in which molecular binding effects become important, C7, so as a first approximation it can be considered that the scattering unit in the thermal region is a chemically bound molecule and above thermal is a free atom.

*For a more exact value for a specific reactor, the reader is referred to Fig. 11.6 given by Weinberg and Wigner in Reference W8.

- 2) It is a convenient energy for separating thermal and fast effects from an experimental standpoint since 0.45 eV is approximately the cadmium cutoff energy and is specifically the cutoff used by Westcott, W11, in normalizing his resonance integrals.
- 3) This is near the low spot between the important Pu239, Pu241, and Pu240 resonances, and as such is a natural division line, as can be seen by referring to Fig. 4.1, a superimposed plot of microscopic cross sections of the fuel nuclides as functions of energy.

For reactors in which the thermal cutoff falls above 0.45 eV, the thermal region should be extended as necessary, and resonance integrals reduced accordingly.

1.2 The Thermal Spectrum. The energy distribution of the thermal flux is dependent upon the degree of moderation, becoming progressively more distorted from that of a Maxwell-Boltzmann as the ratio of absorber to moderator increases. Because of these flux shape changes, it is difficult to prescribe a consistent method of hardening a Maxwell-Boltzmann spectrum and blending in a $1/E$ epithermal tail so as to yield correct average cross sections. This has been discussed by Cohen, C6, for various mixtures of moderator plus $1/v$ absorber. The difficulty is increased in the case of non $1/v$ absorbers such as are present in the fuel of a reactor, mainly due to flux perturbations introduced by the resonances in the vicinity of 0.3 eV.

The results of several workers in the thermalization field point towards the Wilkins distribution, in which the moderator is assumed to behave as heavy monatomic gas, as an attractive model for the

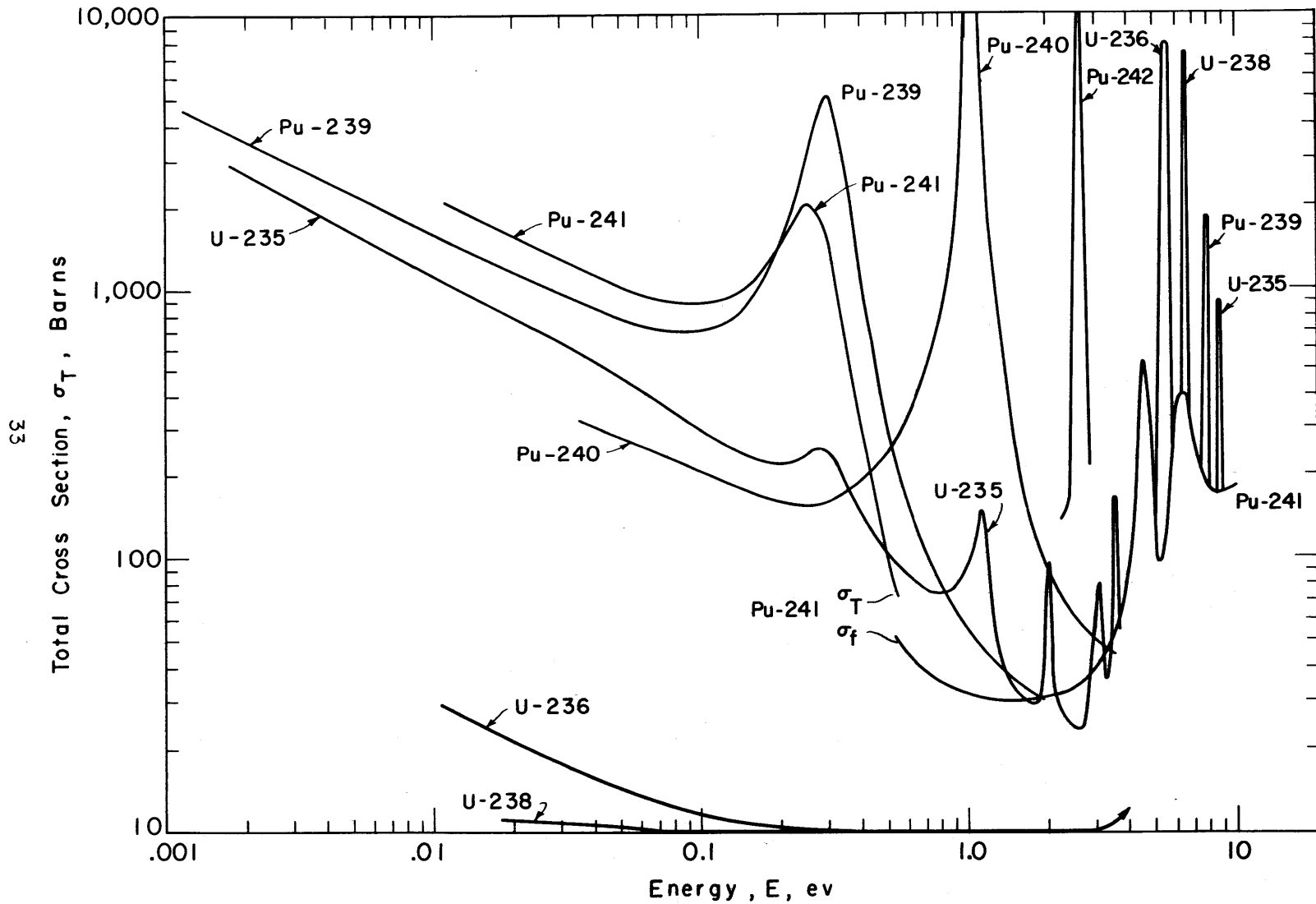


FIG. 4.1 VARIATION OF THE MICROSCOPIC TOTAL CROSS SECTIONS OF THE FUEL NUCLIDES WITH ENERGY. (EXCEPT σ_f IS GIVEN FOR Pu 241 ABOVE 0.55 ev)

moderators of most interest, e. g. , light and heavy water, graphite and beryllium. This model is, of course, better for some of these moderators than for others, but in any case should give better results than a modified Maxwellian. The original derivation of the Wilkins equation, by Wilkins, is unpublished; however, it has been rederived in published work by Hurwitz, Nelkin, and Habetler, H24. In terms of Y, the flux per unit velocity, and x, the normalized velocity of the neutrons, this equation is as follows:

$$x^2 \frac{d^2 Y}{dx^2} + (2x^3 - 3x) \frac{dY}{dx} + [2x^2 - 4x^2 A(x) + 3] Y(x) = 0 \quad (4.1)$$

where,

$$x = \left(\frac{E}{kT_{md}} \right)^{1/2} \quad (4.2)$$

$$Y = \frac{d\phi}{dx} \quad (4.3)$$

$$A(x) = \Sigma(x) / (\xi \Sigma_s)_{\text{eff}} \quad (4.4)$$

$$\Delta(x) = 4x A(x) \quad (4.5)$$

The single term A(x), the inverse moderating ratio of the lattice, determines the flux spectrum. The term Δ is often used rather than A in the thermalization literature dealing with 1/v absorbers since, in this case, Δ is a constant. For high energies, i. e. , large x, the solution reduces to a 1/E flux per unit energy and for low energies, as A(x) goes to zero, the solution reduces to a Maxwell-Boltzmann flux. A description of the numerical method used for solution of Eq. (4.1) is given in Appendix A.

Criteria for the use of the Wilkins equation are that the atoms or

molecules of the moderator which act as the scattering units have negligible binding to each other and that the square of the mass of these units be large compared to one. For crystalline moderators the former requirement restricts the use of the Wilkins equation to lattices with small intra-crystalline binding. For light and heavy water moderators the latter requirement restricts use to that energy region in which the chemically bound molecule is the scattering unit.

Cohen and Nelkin, C7, state that chemical binding is important below 1 ev and that below 0.2 ev light water scatters with the effective mass of 18, i. e., the mass of the water molecule. The mass of 18 for light water is recommended also by Brockhouse, B16. This would indicate that the previously mentioned energy of .45 ev is a reasonable one for a step change in scattering properties from that of the unbound atom to that of the chemical molecule. H. D. Brown's Monte Carlo thermalization studies for light water compare favorably with Cohen's heavy moderator work and the similarity in behavior between his light and heavy water results indicate that this would also be a reasonable cutoff for heavy water, B20.

For light water it appears that the thermal spectrum is fairly insensitive to the thermalization model, due mainly to the opposing variations of ξ and σ_s which leaves the product, $(\xi\sigma_s)_{\text{eff}}$, relatively constant. The Wigner-Wilkins model for a moderator with a mass of one is a possible alternate for light water, W13; however, Amster, A5, and Poole, P4, have shown that the Wigner-Wilkins equation gives fluxes which are lower than experimental in the 0.1 to 0.3 ev region. This is an important region because of the large resonances in Pu239,

Pu241, and U235, and as such presents another argument for the use of the Wilkins equation, since Greebler, G13 and G11, has shown that the Wilkins equation gives a better fit to Poole's experimental data than does the Wigner-Wilkins, and particularly so in this 0.1 to 0.3 ev region.

Support for the use of the heavy-moderator model with crystalline moderators is given by Nelkin, N1; however, in later work, C7, he points out that the spectrum in graphite will be somewhat more hardened than that of a heavy gas. In addition, de Sobrino's work, D12, leads one to expect that Be should moderate similarly to a gas. It is thought, therefore, that the Wilkins model will give satisfactory results for these two crystalline moderators, but may require a reduction in the effective $\xi\Sigma_s$ term for carbon to give increased hardening.

The values of $A(x)$ obtained by homogenizing each fuel element with the moderator region are used in Eq. (4.1) for an approximation to the average energy spectrum in the fuel.* This average energy spectrum is calculated periodically throughout the life history of the fuel element, and the thermal cross sections for the fuel are obtained as averages over these spectra.

Resonance absorption by materials in the moderator region are taken into account by using an effective cross section for these materials in the thermal group. This cross section is assumed to be constant throughout the life of the reactor. This effective thermal cross section is calculated for the fresh fuel as the average over a hardened Maxwell-Boltzmann thermal flux plus a resonance contribution. The thermal flux hardening is estimated by the relationship,

*A more detailed description of the variation of energy spectrum with position in the cell is given in Honeck's thesis, H-26.

$$T_{\text{neutron}} = T_{\text{md}} (1 + .46\Delta) \quad (4.6)$$

due to Coveyou, Bate, and Osborn, C10. In Eq. (4.6) Δ is calculated as the homogenized cell value which gives the initial neutron temperature in the fuel. The moderator cross section is then given by

$$\Sigma_{\text{md}} = \Sigma_{\text{md},0} \sqrt{\frac{\pi T_0}{4T_{\text{neutron}}}} \quad (4.6A)$$

In calculating the neutron absorption rate in moderator materials, the neutron temperature of the fuel region is used rather than that of the moderator region, because the neutron flux used throughout the code is that of the fuel region, $\phi_{fl} \equiv n_{fl} \bar{v}_{fl}$, rather than that of the moderator region, $\phi_{md} \equiv \psi n_{fl} \bar{v}_{md}$. ψ is the thermal disadvantage factor, defined as $\psi \equiv n_{md}/n_{fl}$. Neutron absorption by moderator materials is not dependent on the choice of neutron temperature because of the assumed $1/v$ dependence of moderator cross section on velocity.

1.3 The Resonance Group. The resonance group accounts for all absorption in the fuel other than that of the thermal group and, in the case of U238, the fast fission group. This group is divided into subgroups in which absorptions occur in one or more of the fuel nuclides and the slowing down density, q , is depleted by these resonance absorptions according to the energy sequence of the subgroups. Fig. 4.1 shows clearly the order of the main resonances in Pu240, Pu242, and U236. The first and largest U238 resonance is seen at 6.7 ev, but above this is a region not shown by Fig. 4.1 in which there are multiple inseparable resonances in U235, U238, Pu239, and Pu241.

For this reason (and recalling that the resonances in the vicinity of 0.3 ev have been included in the thermal group), four resonance subgroups have been defined as follows, in order of decreasing energy: (1) concurrent absorptions in U235, U238, Pu239, and Pu241; (2) absorptions in U236; (3) absorptions in Pu242; (4) absorptions in Pu240. A hand calculation was made to check this assumption for a fuel mixture of Pu239, U235, and U238 typical of discharge compositions in a light water reactor irradiated to about 6000 MWD/tonne. Resonance absorptions calculated by the above prescription were essentially identical with results of a twenty-five group calculation using the Eyewash, OCOSOL-A, group cross sections.* Fig. 4.2 is a schematic diagram of this energy model showing the neutron balance.

In calculating fast leakage the age to thermal is used but it is assumed that all this leakage, i. e., from birth to thermal, occurs prior to the resonance region. The arguments for this assumption follow:

- 1) The main resonance absorptions are at relatively low energies. Taking 2 Mev for birth, 10 ev for the mid resonance energy, and .45 ev for the thermal cutoff, one finds that 80 per cent of the leakage occurs prior to 10 ev if leakage is assumed proportional to the lethargy span (i. e., leakage proportional to $DB_g^2 \phi$ where $\phi(u)$ and DB_g^2 are constant).
- 2) The leakage prior to resonance is greater than that indicated by the previous argument due to the decrease in scattering cross sections at high energies.

* See Reference A13 for a tabulation of the Eyewash group constants.

PRODUCTION

ABSORPTION

LEAKAGE

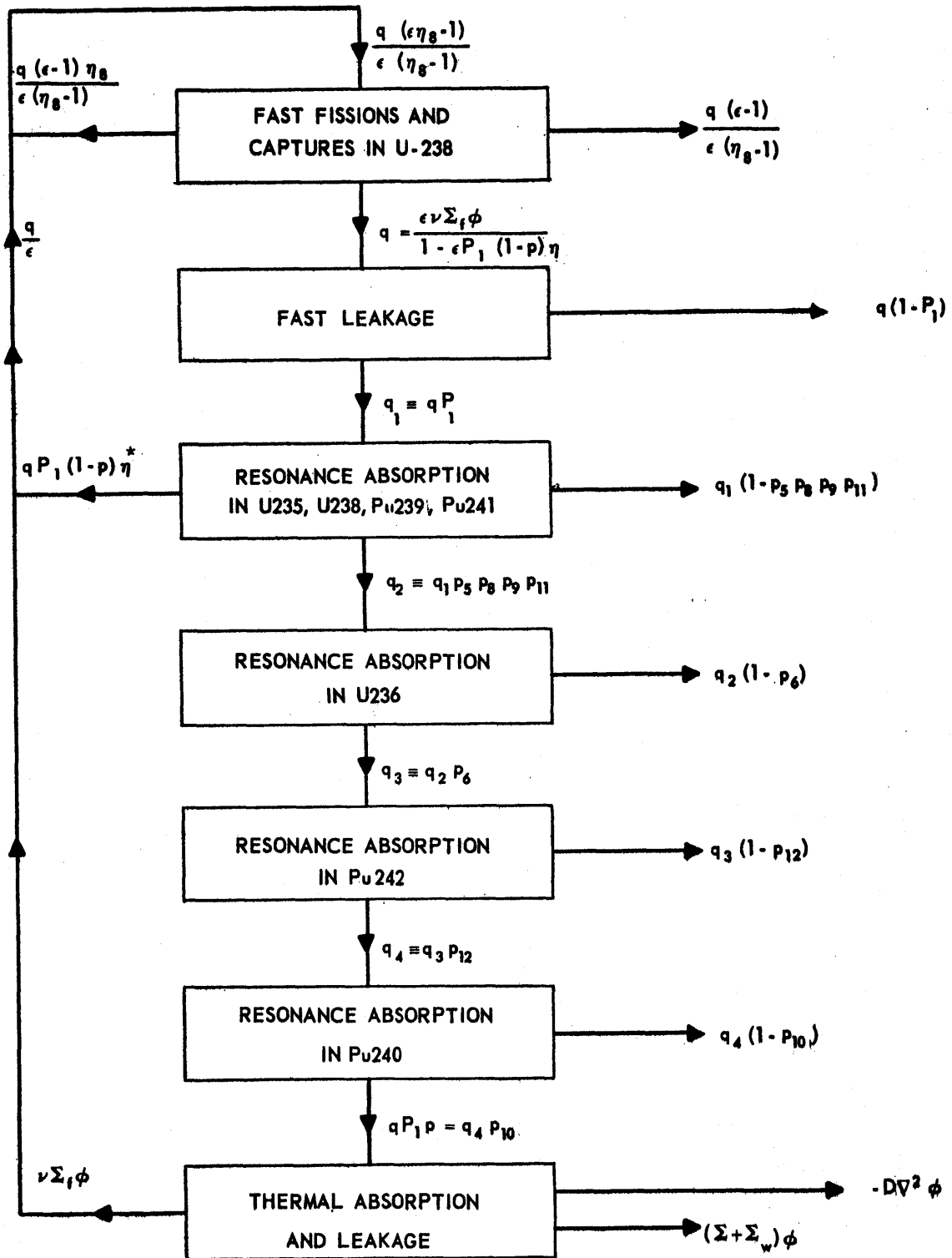


FIG. 4.2 SCHEMATIC DIAGRAM OF THE ENERGY MODEL AND NEUTRON BALANCE.

* $(1-p) \eta$ is defined by Eqs. (4.101) and (4.10)

3) We are concerned with the error involved in calculating the resonance absorptions. The absorptions are proportional to q , but for large power reactors the fast leakage causes only a few per cent reduction in q from its initial value, so small errors in leakage cause negligible errors in values for resonance absorptions.

The flux is taken to be $1/E$ immediately above each resonance subgroup and resonance escape probabilities are of the standard form:

$$p_m = \exp - \left[C_1 \frac{N_m I_m^\infty}{\psi_{1,m}} \right] \quad (4.7)$$

where

$$C_1 \equiv \frac{V_{fl}}{\xi \Sigma_s V_{md}} \quad (4.8)$$

I_m^∞ is the infinite dilution resonance integral and $\psi_{1,m}$ is the epithermal disadvantage factor for nuclide m . The disadvantage factors for the calculations of this thesis have been taken as unity, except for U238 and Pu240, for which shielding is important. $\psi_{1,8}$ is assumed constant throughout the life of the fuel and has been given a value such that the resulting p_8 agrees with experimental data for the fresh fuel. $\psi_{1,10}$ is dependent on the concentration of Pu240 and is re-evaluated periodically throughout the fuel's history using a simple approximation by Crowther and Weil, C13, namely

$$\psi_{1,10} \sim \frac{I_m^\infty}{I_m^{\text{eff}}} \sim 1 + \frac{N_{10} I_{10}^\infty}{\Sigma_{s,fl}} \quad (4.8A)$$

which they have shown to compare favorably with experimental data.*

Resonance absorption probabilities, denoted by $\langle 1 - p_m \rangle$, are of the standard form for U236, Pu240, and Pu242, namely:

$$\langle 1 - p_m \rangle = (1 - p_m) \quad \text{for } m = 6, 10, 12 \quad (4.9)$$

Because of the concurrence of their absorptions, the resonance absorption probabilities for U235, U238, Pu239, and Pu241 are of the following form:

$$\langle 1 - p_m \rangle = \frac{\frac{N_m I_m^\infty}{\psi_{1,m}}}{\sum_{m=5,8,9,11} \frac{N_m I_m^\infty}{\psi_{1,m}}} (1 - p_5 p_8 p_9 p_{11}) \quad (4.10)$$

1.4 Miscellany. The fast leakage region, as mentioned previously, occurs above the resonance groups and is a domain of leakage and slowing down only. The choice of one fast group for the slowing down model is discussed in Sub-Section 2.2 of Spatial Considerations. The fast fission group is the normal one in which fast captures and fissions occur in U238.

*The standard form for the disadvantage factor for nuclide m , $\psi_{1,m}$, is,

$$\psi_{1,m} = \frac{I_m^\infty}{I_m^{\text{eff}}} [1 + X C_1 N_m I_m^{\text{eff}}]$$

In cases where the flux has negligible buildup in the moderator over that of the fuel surface flux, the excess absorption, X , is zero and $\psi_{1,m}$ reduces to,

$$\psi_{1,m} = \frac{I_m^\infty}{I_m^{\text{eff}}}$$

2. Spatial Considerations

2.1 Homogenization. The model for the transport of neutrons throughout the core is that of two-group diffusion theory. Fuel, moderator, and other core materials are homogenized into cells according to their relative volumes, with the thermal cross sections for materials in the moderator region weighted by a disadvantage factor appropriate for the fresh core. This is a simplifying assumption to avoid the additional complexities and specificities involved in considering flux changes within the fuel element. The change is not merely one of the gross average cross section change during the fuel's history but also involves such things as change in the energy dependence of the total cross section and preferential building up of Pu239 towards the edge of the fuel element. Consideration of these effects would in general require considerably more computer time, since a method more elaborate than diffusion theory is required for these local effects, and would require consideration of specific shapes of fuel elements, both of which are antagonistic to the purpose of FUELCYC. The most elaborate treatment of these local effects is by the Monte Carlo method in the I. B. M. 709 computer code RBU, L26. Another approach that has been used primarily for cylindrical fuel elements is that of blackness theory; see S10, T2, G11, K11.

2.2 The Number of Groups. One fast group is provided to allow transport of the neutrons in slowing down. The relationship of this distribution to that of other slowing down models can be illustrated by calculation of P_r , the probability that a neutron born at the origin will be thermalized within a radius r . Given the slowing down kernel, $K(r)$, or the probability per unit volume that a neutron born at the origin will

be thermalized at r , we can obtain P_r as the volume integral of $K(r)$.

$$P_r = \int_r 4\pi r^2 K(r) dr \quad (4.14)$$

The one group diffusion kernel, which is the model used in this study, is,

$$K(r) = \frac{\kappa^2 e^{-\kappa r}}{4\pi r} \quad (4.15)$$

which, replacing κ^2 by τ^{-1} , its age equivalent, and substituting in Eq. (4.14) gives,

$$P_u = 1 - e^{-u} (1+u) \quad (4.16)$$

where,

$$u \equiv \frac{r}{\sqrt{\tau}} \quad (4.17)$$

In the limit of an infinite number of groups one obtains the Fermi Age, or Gaussian, kernel, applicable to a heavy moderator:

$$K(r) = \frac{e^{-\frac{r^2}{4\tau}}}{(4\pi\tau)^{3/2}} \quad (4.18)$$

which gives the non escape probability,

$$P_u = \operatorname{erf} \frac{u}{2} - \frac{u}{\sqrt{\pi}} e^{-\frac{u^2}{4}} \quad (4.19)$$

with u defined as before.

Weinberg and Wigner suggest the single collision kernel as a rough approximation for the slowing down kernel in water, W8, p. 402. This is given by,

$$K(r) = \frac{\Sigma_1 e^{-\Sigma_1 r}}{4\pi r^2} \quad (4.19)$$

The customary definition of the Fermi Age as one-sixth of the mean displacement yields the relationship,

$$\tau = \frac{1}{3\Sigma^2} \quad (4.20)$$

which then gives for P_u ,

$$P_u = 1 - e^{-\frac{u}{\tau}} \quad (4.21)$$

These three non-escape probabilities are plotted in Fig. 4.3, which shows that the single collision kernel tends to concentrate the thermalized neutrons more at short radii than does the Fermi Age kernel. The one-group kernel gives an intermediate distribution which lends support to its use as a general model for different moderators. It should be noted, however, that a three-group model fits some experimental data for water better than the single collision results, W8, p. 373, and the distribution characteristic of this model would be between that of the one-group curve and the Fermi Age curve in Fig. 4.3. In any case, the simplicity of the one fast-group model is a strong argument for its use.

2.3 Development of the Condensed Two-Group Diffusion Equation.

Using the subscript 1 for the fast group and no subscript for the thermal group we have the fast diffusion equation,

$$q + D_1 \nabla^2 \phi_1 - \Sigma_1 \phi_1 = 0 \quad (4.22)$$

q/ϵ equals the combination of thermal and resonance production terms, see Fig. 4.2,

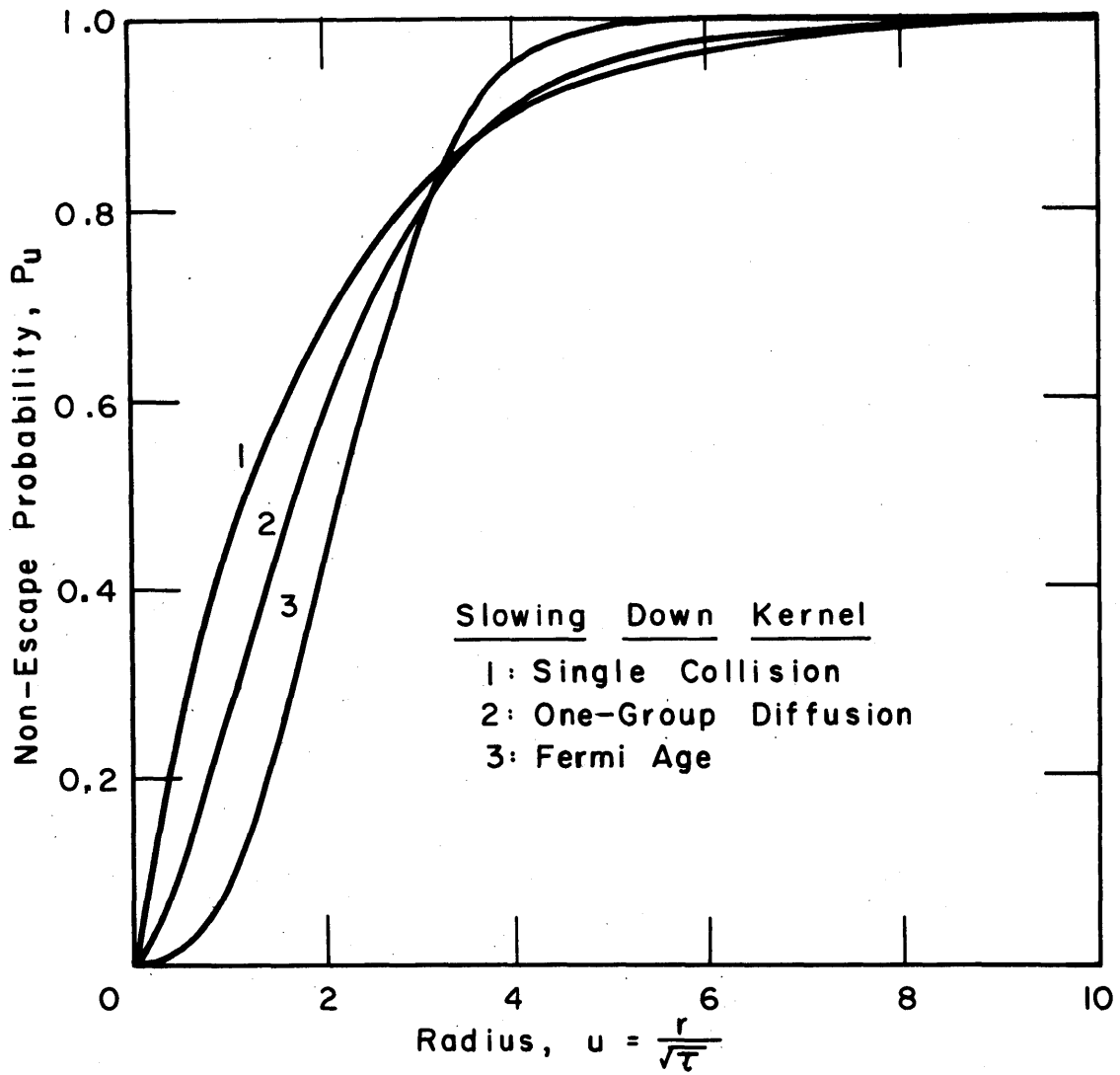


FIG. 4.3 NON-ESCAPE PROBABILITY, P_u , FOR A SPHERE OF RADIUS u ; NEUTRONS BORN AT THE ORIGIN

$$\frac{q}{\epsilon} = \nu \Sigma_f \phi + (q + D_1 \nabla^2 \phi_1) (1 - p) \eta \quad (4.23)$$

where η is an average for the resonance group as defined by Eq. (4.101).

When solved for q this gives,

$$q = \frac{\epsilon [\nu \Sigma_f \phi + (1-p) \eta D_1 \nabla^2 \phi_1]}{1 - \epsilon(1-p) \eta} \quad (4.24)$$

Substitution of (4.24) for q into Eq. (4.22) yields the fast group equation,

$$C_2 (\epsilon \nu \Sigma_f \phi + D_1 \nabla^2 \phi_1) - \Sigma_1 \phi_1 = 0 \quad (4.25)$$

where,

$$C_2 = \frac{1}{1 - \epsilon(1-p) \eta} \quad (4.26)$$

C_2 is unity in the absence of resonance fissions.

The thermal diffusion equation is,

$$D \nabla^2 \phi - (\Sigma + \Sigma_w) \phi + p \Sigma_1 \phi_1 = 0 \quad (4.27)$$

where the portion of the thermal macroscopic absorption cross section due to removable poisons, as control rods, is called Σ_w .

For large power reactors the thermal leakage is very small compared to thermal absorptions which permits a convenient reduction of the two diffusion equations to one. This is done as follows. Eliminate $\Sigma_1 \phi_1$ between Eqs. (4.25) and (4.27) giving

$$D \nabla^2 \phi - (\Sigma + \Sigma_w) \phi + p C_2 (\epsilon \nu \Sigma_f \phi + D_1 \nabla^2 \phi_1) = 0 \quad (4.28)$$

Solve Eq. (4.27) for ϕ_1 assuming that $D \nabla^2 \phi$ is negligible in magnitude compared to $(\Sigma + \Sigma_w) \phi$, which gives,

$$\phi_1 \sim \frac{(\Sigma + \Sigma_w) \phi}{p \Sigma_1} \quad (4.29)$$

Assuming Σ_1 to be constant and replacing D_1/Σ_1 by the Fermi Age, τ , we obtain the following equation in only the one unknown ϕ by substituting (4.29) for ϕ_1 in Eq. (4.28). The result of this is the condensed two group equation,

$$D\nabla^2 \phi - (\Sigma + \Sigma_w) \phi + C_2 p \left\{ \epsilon \nu \Sigma_f \phi + \tau \nabla^2 \left[\frac{(\Sigma + \Sigma_w) \phi}{p} \right] \right\} = 0 \quad (4.30)$$

which contains terms for both fast and thermal leakage within the single equation. Finally it is useful to derive an expression for the fast non-leakage probability, P_1 , which is defined by,

$$P_1 \equiv \frac{q + D_1 \nabla^2 \phi_1}{q} \quad (4.31)$$

Substituting (4.24) for q gives,

$$P_1 = \frac{\epsilon \nu \Sigma_f \phi + D_1 \nabla^2 \phi_1}{\epsilon [\nu \Sigma_f \phi + (1-p) \eta D_1 \nabla^2 \phi_1]} \quad (4.32)$$

or solving for the fast leakage term, $-D_1 \nabla^2 \phi_1$

$$-D_1 \nabla^2 \phi_1 = \frac{(1 - P_1) \epsilon \nu \Sigma_f \phi}{1 - P_1 \epsilon (1-p) \eta} \quad (4.33)$$

finally, substitution of (4.33) in Eq. (4.24) gives the useful expression for q in terms of P_1 :

$$q = \frac{\epsilon \nu \Sigma_f \phi}{1 - \epsilon P_1 (1-p) \eta} \quad (4.34)$$

2.4 The Difference Form of the Diffusion Equation. We wish to consider reactor cores in which properties change from cell to cell in a manner which is always complicated and often impossible to express

analytically, such as the changes involved in the life history of the fuel with the initial charging not necessarily uniform, so we cannot solve Eq. (4. 30) in its exact form. The approximation made is to assume symmetry in the azimuthal direction and to replace Eq. (4. 30) by the two-dimensional five-point difference equation for cylindrical geometry. The core is divided by a mesh of grid lines running radially and axially, and the difference equation approximation for the differential equation (4. 30) is written for the flux, $\phi_{r, z}$, at each point where these lines intersect, commonly referred to as a mesh point. This gives a set of n linear homogeneous equations for the n unknown fluxes where n is the number of mesh points. This points out the advantage of the single "condensed two group equation", Eq. (4. 30), since solving the normal two equations, Eqs. (4. 25) and (4. 27), would have resulted in a set of $2 n$ difference equations for the n thermal and n fast fluxes. This is an important simplification since the spatial solution part of the code is the most time-consuming, the time required being roughly proportional to the number of mesh points. Fig. 4.4 shows the system of mesh point spacing and numbering for a typical (r, z) section through the reactor. Each mesh point is at the approximate center of the material region that it represents. The point $(r' = 0, z' = 0)$ is at the radial center of the reactor, and also at the axial center if there is axial symmetry, but at the end of the axis in the absence of axial symmetry (here lengths are distinguished from the radial, r , and axial, z , indices by prime marks).

In order to develop the difference approximation to Eq. (4. 30) consider first the exact expression for $\nabla^2 \phi(r, z)$:

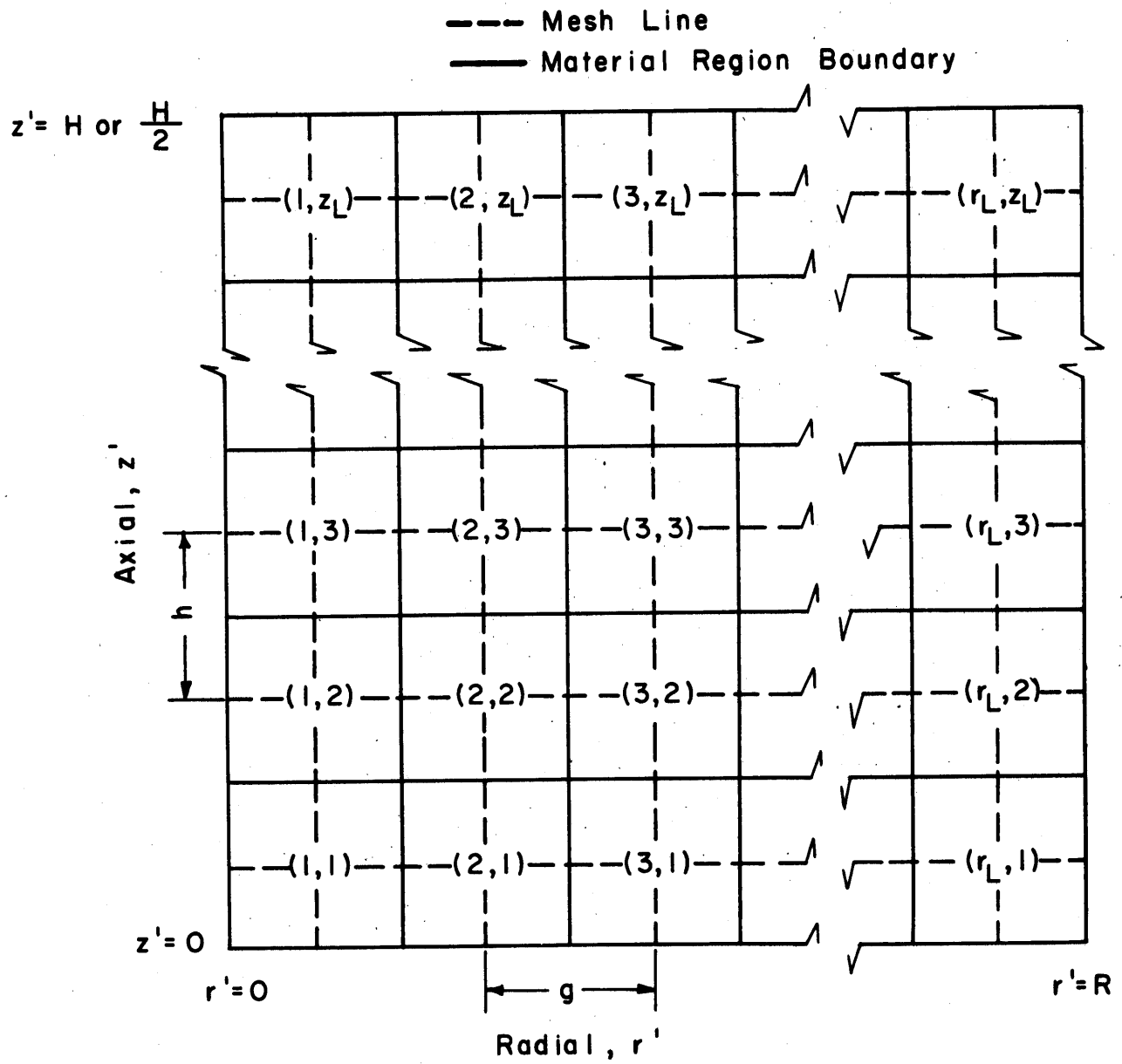


FIG. 4.4 SCHEMATIC DIAGRAM OF MATERIAL REGIONS, MESH LINES, AND MESH POINT NUMBERING

$$\nabla^2 \phi(r, z) = \frac{\partial^2 \phi(r, z)}{\partial r^2} + \frac{1}{r} \frac{\partial \phi(r, z)}{\partial r} + \frac{\partial^2 \phi(r, z)}{\partial z^2} \quad (4.35)$$

The five point difference approximation to Eq. (4.35) with constant radial spacing, g , and constant axial spacing, h , is:

$$\begin{aligned} \nabla^2 \phi_{r,z} = & \frac{\phi_{r+1,z} - 2\phi_{r,z} + \phi_{r-1,z}}{g^2} + \frac{\phi_{r+1,z} - \phi_{r-1,z}}{(2r-1)g^2} \\ & + \frac{\phi_{r,z+1} - 2\phi_{r,z} + \phi_{r,z-1}}{h^2} + 0(g^2) + 0(h^2) \end{aligned} \quad (4.36)$$

or combining terms

$$\begin{aligned} \nabla^2 \phi_{r,z} = & -2 \left(\frac{1}{g^2} + \frac{1}{h^2} \right) \phi_{r,z} + \frac{2(r-1)}{g^2(2r-1)} \phi_{r-1,z} + \frac{2r}{g^2(2r-1)} \phi_{r+1,z} \\ & + \frac{1}{h^2} \phi_{r,z-1} + \frac{1}{h^2} \phi_{r,z+1} + 0(g^2) + 0(h^2) \end{aligned} \quad (4.37)$$

Applying this rule to Eq. (4.30) we obtain the difference form of the condensed two-group diffusion equation, at the mesh point (r, z) , as,

$$\begin{aligned} d_{r,z,1} \phi_{r,z} + d_{r,z,2} \phi_{r-1,z} + d_{r,z,3} \phi_{r+1,z} + d_{r,z,4} \phi_{r,z-1} \\ + d_{r,z,5} \phi_{r,z+1} = e_{r,z} \phi_{r,z} + 0(g^2) + 0(h^2) \end{aligned} \quad (4.38)$$

or to condense the nomenclature, and dropping the error terms,

$$\sum_{u=1}^5 d_{r,z,u} \phi_u = e_{r,z} \phi_{r,z} \quad (4.39)$$

where u replaces the mesh point indices in the ϕ terms with the under-standing,

when, <u>u</u> is	:	then, <u>the radial index is</u>	and, <u>the axial index is</u>
1		r	z
2		r-1	z
3		r+1	z
4		r	z-1
5		r	z+1

Eq. (4.39), or (4.38), is the basic equation for the numerical solution for the spatial flux-shape in which terms of second degree and higher in g or h are neglected, and where each mesh point "feels" the flux at its own mesh point and at the four neighboring mesh points. The terms in Eq. (4.39) are defined below:

$$e_{r,z} = \epsilon(C_2 p \nu \Sigma_f)_{r,z} - (\Sigma + \Sigma_w)_{r,z} \quad (4.40)$$

$$d_{r,z,u} = -C_{3,r,z,u} C_{4,r,z,u} \quad (4.41)$$

where,

$$C_{4,r,z,u} = D + \tau(C_2 p)_{r,z} \left(\frac{\Sigma + \Sigma_w}{p} \right)_u, \quad u = 1, 2, 3, 4, 5 \quad (4.42)$$

$$C_{3,r,z,u} = \frac{1}{h^2}, \quad u = 4, 5 \quad (4.43)$$

$$C_{3,r,z,3} = \frac{2r}{g^2(2r-1)} \quad (4.44)$$

$$C_{3,r,z,2} = \frac{2(r-1)}{g^2(2r-1)} \quad (4.45)$$

$$C_{3,r,z,1} = \frac{1}{g^2} (C_{7,r} - 2) + \frac{1}{h^2} (C_{8,\bar{z}} - 2) \quad (4.46)$$

Terms of Eq. (4.39) are omitted when their mesh points fall outside of the material region being calculated, i. e., the core or reflector.

The boundary conditions are accounted for by the terms $C_{7,r}$ and $C_{8,h}$ in Eq. (4.46). These terms are zero within the mesh and take values at the border mesh points so that a straight line interpolation between the flux value just within the material region edge and that at a pseudo mesh point just outside the region gives the proper boundary condition on the flux or current. In the radial direction the boundary conditions are that the current equals zero at the center and that the flux goes

to zero at a radial distance δ_R beyond the edge of the material region.

This gives for $C_{7,r}$:

$$C_{7,r_L} = \left(\frac{2\delta_R - g}{2\delta_R + g} \right) \frac{2r}{2r - 1} \quad (4.47)$$

$$C_{7,r} = 0 \quad 1 \leq r \leq (r_L - 1) \quad (4.48)$$

In the axial direction the flux goes to zero at an axial distance δ_H beyond the material boundary. This gives,

$$C_{8,z_L} = \frac{2\delta_H - h}{2\delta_H + h} \quad (4.49)$$

$$C_{8,z} = 0 \quad 2 \leq z \leq (z_L - 1) \quad (4.50)$$

If there is symmetry in the axial direction, then we have a zero current at the center of the reactor for the second boundary condition, giving

$$C_{8,1} = 1 \quad (4.51)$$

For no symmetry in the axial direction the second boundary condition is again one of zero flux and we have instead of Eq. (4.51),

$$C_{8,1} = \frac{2\delta_H - h}{2\delta_H + h} \quad (4.52)$$

2.5 Method of Solving the Set of Difference Equations. The set of linear homogeneous equations generated by Eq. (4.39) can be written in matrix form as

$$G\phi = 0 \quad (4.53)$$

where, if the number of mesh points is n , G is the $n \times n$ coefficient matrix of the $d_{r,z,u}$ and $e_{r,z}$ terms, and ϕ represents the unknown column matrix of the n unknown fluxes. The problem is to solve for the $n - 1$ flux ratios, say $\frac{\phi_{r,z}}{\phi_{1,1}}$ & arbitrarily normalizing to $\phi_{1,1}$.

The requirement that Eq. (4.53) have a solution is that the determinant of G , $|G|$, equals zero, or physically, given a super-critical system with known material properties, at each point in the reactor, that we adjust the values of control poison, $\Sigma_{w,r,z}$, so that the reactor is just critical. Let us assume that the ratios of control poison, $\frac{\Sigma_{w,r,z}}{\Sigma_{w,1,1}}$ have been previously specified, so that the standard method of solution would be to solve for the value of $\Sigma_{w,1,1}$ so that

$$|G| = 0 \tag{4.54}$$

Then having satisfied this condition, any one of the n sets of $n - 1$ independent equations from (4.53) could be solved for the $n - 1$ flux ratios, $\frac{\phi_{r,z}}{\phi_{1,1}}$. This standard method of solution is too time-consuming for large matrices. This fact can be appreciated by considering that the formation of a determinant of a $n \times n$ matrix requires on the order of $(n!)$ arithmetic operations and the subsequent matrix inversion of an $(n-1) \times (n-1)$ matrix requires on the order of $(n-1)(n-1)!$ operations. DON'T Believe it

An alternate technique is the so called iterative method in which guesses are made for a convenient group of the terms in (4.53), henceforth referred to as the source terms, and the resulting linear inhomogeneous set of equations is solved for an approximation to the fluxes. The new fluxes are used to adjust the values of the original source terms and the procedure is repeated until the flux ratios converge. To illustrate this

method let us choose the removable poison terms as source terms and rewrite (4.53) as

$$G_2 \phi^{(i+1)} = \Sigma_{w, 1, 1} Q \phi^{(i)} \quad (4.55)$$

where G_2 and Q are known matrices, the Q matrix being composed of the terms $\frac{\Sigma_{w, r, z}}{\Sigma_{w, 1, 1}}$, and $\Sigma_{w, 1, 1}$ is the unknown eigenvalue. The procedure then is to guess initial values for the ϕ vector on the right hand side of (4.55), say $\phi^{(0)}$. Eq. (4.55) can then be solved by a Crout reduction for the new solution vectors $\phi^{(1)}$, and this procedure iterated until the ϕ vectors converge. Due to the arrangement of Eq. (4.55) the flux ratios $\frac{\phi_{r, z}}{\phi_{1, 1}}$ are independent of the magnitude of $\Sigma_{w, 1, 1}$, so one doesn't have to solve for this value.

The complete Crout reduction takes on the order of $2n^3$ arithmetic operations for a $n \times n$ matrix so presents a considerable advantage over the matrix inversion technique, provided the convergence rate of the fluxes is sufficiently fast. An abridged Crout reduction applicable to reactor matrices is described in Appendix B and it further reduces the solution time required.

In other popular iteration methods source terms are taken in groups which involve only a portion of the fluxes. In these techniques, the complete Crout reduction is not used to generate new fluxes but instead a technique of mesh sweeping is used which generates new fluxes in only a portion of the mesh at one time. These methods converge more slowly than the Crout reduction techniques since repeated mesh sweepings are required to propagate the effect of revisions in flux shape from one part of the mesh to another, while in the Crout reduction each mesh point

feels the new flux at every other mesh point for each revision. The disadvantage of the Crout reduction method is that it requires more computer space than the "mesh sweeping" techniques. The set of equations in Appendix B for an abridged Crout reduction considerably reduces the storage requirement and permits the use of the Crout technique for mesh sizes up to several hundred mesh points, which is adequate for this work. *

Even though the arrangement of Eq. (4.55) eliminates the need for calculating $\Sigma_{w, 1, 1}$, a more advantageous method, due to the reasons of convergence mentioned in the next section, is to keep the terms derived from the ∇^2 terms in Eq. (4.35) on the left side and the other terms on the right hand side as source terms. Calling the matrix for the first group, d, and the second, e, we have instead of Eq. (4.53),

$$d\phi^{(i+1)} = e\phi^{(i)} \quad (4.56)$$

which is the matrix form of the set of equations given by Eq. (4.39). (d will be used throughout this section as a matrix symbol, not the differential symbol.) The $\Sigma_{w, 1, 1}$ term can't be separated out of the e matrix, see Eq. (4.40), so the iteration is not independent of its magnitude, as was Eq. (4.55).

While it is time-consuming to calculate $\Sigma_{w, 1, 1}$ exactly, a close

*The main storage requirement is that of the auxiliary matrix which requires approximately $2n^{3/2}$ spaces, when the method of Appendix B is used, where n is the number of mesh points. (Fast memory of the MIT I. B. M 704 is approximately 32000 words.)

estimate can easily be made from the results of the solution at the preceding time step. Since the resulting reactor will be slightly off critical, the flux will rise or fall, eventually with a constant flux shape. The estimate of $\Sigma_{w, 1, 1}$ can be made well enough so that this persisting time-dependent flux distribution is sufficiently close to the steady-state flux. So, accepting this distribution we have, instead of Eq. (4.56),

$$d\phi - e\phi = \lambda\phi \quad (4.57)$$

where λ is a constant proportional to the inverse period of the reactor, or in terms of differential operator,

$$\lambda = \frac{1}{\nabla} \frac{\partial}{\partial t} \quad (4.58)$$

Due again to convergence reasons, it is preferable not to solve Eq. (4.57) but rather the following approximation to it,

$$d\phi^{(i+1)} = \gamma e\phi^{(i)} \quad (4.59)$$

where γ is now the eigenvalue such that Eq. (4.59) has a solution.

If we use Eq. (4.59) for iteration with the right hand side as the source term, the flux ratios, $\frac{\phi_{r, z}}{\phi_{1, 1}}$, are independent of the magnitude of γ . The question then arises: what is the relationship of γ to the true physical eigenvalue λ and under what conditions is it a constant, (or at least nearly constant)? Considering Eqs. (4.57) and (4.59) as single equations rather than matrices, for simplicity, we can solve for γ as,

$$\gamma = \frac{1}{1 - \frac{\lambda\phi}{d\phi}} \quad (4.60)$$

which reduces to the constant, unity, as $\lambda\phi$ becomes small relative to $d\phi$. Now $\lambda\phi$ represents the excess neutrons (or deficiency, if negative) and, in the absence of resonance fissions, $d\phi$ represents the leakage terms, so the requirement that γ be a constant is met as the excess neutrons available become small compared to the leakage. In the limit, using the correct value of $\Sigma_{w, 1, 1}$, this results in $\lambda\phi = 0$ and $\gamma=1$ for which case, Eqs. (4.57) and (4.59) reduce to the steady state relationship Eq. (4.56). The advantage of using Eq. (4.59) for iteration instead of Eq. (4.55) is discussed in the following sub-section and the error involved is further discussed in Appendix E.3.2. It should be noted that for the steady-state types of fuel movements discussed in IV.C.2, the exact value for $\Sigma_{w, 1, 1}$ is known, namely, zero, and the solution gives the true steady-state flux.

2.6 Convergence Considerations. It is a characteristic of iterative solutions that the convergence is very sensitive to the arrangement of the equation. The arrangement (4.59) of the set of equations (4.39) is chosen so that the iteration will converge rapidly even with large mesh spacing. This occurs because the terms obtained from ∇^2 terms are separated from the others. The value of this method can be illustrated simply for the case of a 1 group, 1 dimension, 2 mesh point case.

Here the critical condition,

$$\nabla^2 \phi + \frac{k-1}{M^2} \phi = 0 \quad (4.61)$$

has the difference form,

$$\phi_{r+1} - 2\phi_r + \phi_{r-1} + (k-1) \left(\frac{h}{M}\right)^2 \phi_r = 0 \quad (4.62)$$

taking,

$$\frac{(k-1)}{M^2} = \text{const.} \quad (4.63)$$

with the boundary condition,

$$\phi_0 = \phi_1 \quad (4.64)$$

$$\phi_3 = -\phi_2 \quad (4.65)$$

equivalent to zero central current and $\delta_R = 0$. For arrangement 1, equivalent to (4.59), we have

$$\phi_1^{(i+1)} - \phi_2^{(i+1)} = (k-1) \left(\frac{h}{M}\right)^2 \phi_1^{(i)} \quad (4.66)$$

$$-\phi_1^{(i+1)} + 3\phi_2^{(i+1)} = (k-1) \left(\frac{h}{M}\right)^2 \phi_2^{(i)} \quad (4.67)$$

Defining,

$$S^{(i)} = \left(\frac{\phi_2}{\phi_1}\right)^{(i)} \quad (4.68)$$

solving Eqs. (4.66) and (4.67) for ϕ_1 and ϕ_2 , and taking the ratio yields:

$$S^{(i+1)} = \frac{S^{(i)} + 1}{S^{(i)} + 3} \quad (4.69)$$

now the true value of S must satisfy,

$$S = \frac{S + 1}{S + 3} \quad (4.70)$$

From (4.69) and (4.70) we can derive the convergence factor for the first arrangement, ρ_1 , which is defined as the ratio of the error in $S^{(i+1)}$ to that in $S^{(i)}$, as $S^{(i)}$ approaches S ,

$$\rho_1 = \frac{S - S^{(i+1)}}{S - S^{(i)}} = \frac{2}{(S+3)(S^{(i)} + 3)} \sim \frac{2}{(S+3)^2} \quad (4.71)$$

Now for this simple problem it is easy to calculate S , from Eq. (4.70), as 0.414 which gives,

$$\rho_1 = .17 \quad (4.72)$$

It is, of course, desired that ρ be small for fast convergence.

For an alternate arrangement of Eq. (4.62), in which the ∇^2 terms aren't isolated, consider,

$$\left[1 + \left(\frac{h}{M} \right)^2 \right] \phi_1^{(i+1)} + \phi_2^{(i+1)} = k \left(\frac{h}{M} \right)^2 \phi_1^{(i)} \quad (4.73)$$

$$-\phi_1^{(i+1)} + \left[3 + \left(\frac{h}{M} \right)^2 \right] \phi_2^{(i+1)} = k \left(\frac{h}{M} \right)^2 \phi_2^{(i)} \quad (4.74)$$

By the preceding method the convergence factor for this second arrangement is found to be,

$$\rho_2 = \frac{\left[3 + \left(\frac{h}{M}\right)^2\right] \left[1 + \left(\frac{h}{M}\right)^2\right]^{-1}}{\left[S + 3 + \left(\frac{h}{M}\right)^2\right]^2} \quad (4.75)$$

It is seen that ρ_2 depends on the dimensionless ratio of mesh spacing to migration length, ρ_2 has been calculated below for $S = 0.414$:

$\left(\frac{h}{M}\right)$	ρ_2
0	0.17
1	0.36
3	0.77
5	0.89
10	0.97
∞	1.

It is seen that ρ_2 is higher than ρ_1 , the amount depending on the ratio of spacing to migration length. It should be noted that not only does Arrangement 1 always give faster convergence than Arrangement 2 but also that its convergence rate is independent of the spacing. In the two dimensional case, the ratio of $\frac{h}{g}$ appears but this causes no trouble so long as $\frac{h}{g}$ is reasonably near unity.

Because the errors eventually tend to reduce exponentially, the Aiken δ^2 process, (see p.445 of H27) is used to estimate the true fluxes for the source terms, after the initial adjustment period, rather than the direct substitution of the last calculated flux values. This technique further reduces the number of iterations required. Instead of substituting $\phi^{(i)}$, $\phi^{(i)}$ would be substituted where,

$$\phi', (i) \equiv \phi^{(i)} - \frac{(\phi^{(i)} - \phi^{(i-1)})^2}{(\phi^{(i)} - 2\phi^{(i+1)} + \phi^{(i+2)})} \quad (4.75A)$$

2.7 Core Average Properties. After the flux distribution has been obtained, region values and core average values are calculated for the fast and thermal leakage terms, thermal production and absorption terms, and the criticality factor with and without control poison. The core averages are defined as flux volume averages of the cell properties where the region properties undergo step changes at the boundaries. In particular, the criticality factor without control poison, C, is defined as

$$C = \frac{\text{total thermal production rate}}{\text{total thermal absorption rate less control absorption} + \text{total thermal leakage rate}} \quad (4.76)$$

which gives,

$$C = \frac{\sum_{r=1}^{r_L} V_r \sum_{z=1}^{z_L} \left(\frac{q}{\phi} P_{1p} \right)_{r,z} \left(\frac{\phi_{r,z}}{\phi_{1,1}} \right)}{\sum_{r=1}^{r_L} V_r \sum_{z=1}^{z_L} \left[\Sigma_{r,z} \left(\frac{\phi_{r,z}}{\phi_{1,1}} \right) - D \nabla^2 \left(\frac{\phi_{r,z}}{\phi_{1,1}} \right) \right]} \quad (4.77)$$

where V_r is the volume of a region with the radial position r .

The flux level is determined by the specified value for the average power density, P_d , in terms of kw/liter of core. This gives the value of the central flux in n/cm^2 sec,

$$\phi_{11} = \frac{P_d z_L \sum_r V_r}{3.14 \times 10^{-11} \sum_r V_r \sum_z \left(\frac{dN_{FP}}{d\theta} \right)_{r,z} \left(\frac{\phi_{r,z}}{\phi_{1,1}} \right)} \quad (4.78)$$

where the fission energy release is assumed constant and equal to 196 Mev/fission, or in the units of Eq. (4.78), 3.14×10^{-11} watt sec/fission. $\left(\frac{dN_{FP}}{d\theta} \right)_{r,z}$ is the fissions per unit volume per unit of flux time given by Eq. (4.89) and has units of cm^{-1} .

The average burnup is given by:

$$E = 0.917 \times 10^6 \frac{\bar{N}_{FP}}{\sum_{m=5}^{12} N_m^0} \frac{\text{MWD}}{\text{ton of fuel fed}} \quad (4.79)$$

where ton means metric ton and the fission energy constant is $.917 \times 10^6 \frac{\text{MWD}}{\text{ton of fuel fissioned}}$, which is strictly consistent with 196 Mev/fission if the fissioned material has an average atomic weight of 238. \bar{N}_{FP} is the volume-average for the discharged fuel. The on-stream reactor time, t_R , or the average time that the fuel would spend in the reactor if operated at full power is then,

$$t_R = 0.993 \times 10^6 \bar{N}_{FP} \frac{V_{fl}}{P_d} \text{ years} \quad (4.80)$$

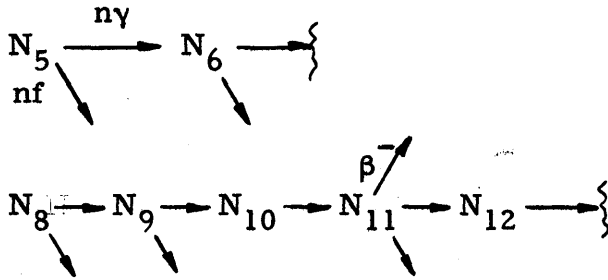
where \bar{N}_{FP} has the units $\frac{\text{atoms fissioned}}{\text{barn cm of fuel}}^*$

$$* t_R = \left(\bar{N}_{FP} \frac{\text{fissions}}{\text{b cm of fuel}} \right) \left(\frac{10^{24} \text{ b}}{\text{cm}^2} \right) \left(V_{fl} \frac{\text{cm}^3 \text{ fuel}}{\text{cm}^3 \text{ core}} \right) \left(\frac{10^3 \text{ cm}^3 \text{ core}}{P_d \text{ k-watts}} \right)$$

$$\left(3.14 \times 10^{-14} \frac{\text{k-watt sec}}{\text{fission}} \right) \left(\frac{1}{3.154 \times 10^7} \frac{\text{year}}{\text{sec}} \right) = 0.993 \times 10^6 \bar{N}_{FP} \frac{V_{fl}}{P_d}$$

3. Solution of the Nuclide Concentration Equations

The effective composition changes for fuel of U235, U238 and daughter nuclides are considered in this work. These changes are schematically given by the chains:



where, subscript 5 designates U235; 9, Pu239; etc. U239 has been considered to decay instantaneously. This results in the below listed set of first order differential equations which are nonlinear since all the terms except for a_m , ϵ , η_8 , and λ_{11} are functions of the N_m . The most convenient independent variable is flux time, θ , where

$$\theta \equiv \int_0^t \phi dt \tag{4.81}$$

The resonance terms p_m and $\langle 1 - p_m \rangle$ are defined in Section IV. A. 1.3. Also, Fig. 4.2 is useful for a diagram of the neutron balance. The a_m and η_m are averages for nuclide m in the resonance group, or fast fission group for U238; the ν_m refer to thermal group fission and are considered constant. The differential equations are:

$$\text{U235: } \frac{dN_5}{d\theta} = -N_5 \sigma_5 - \left(\frac{q}{\phi} \right) P_1 \langle 1 - p_5 \rangle \tag{4.82}$$

$$\text{U236: } \frac{dN_6}{d\theta} = N_5(\sigma_5 - \sigma_{f,5}) - N_6\sigma_6 + \left(\frac{q}{\phi}\right) P_1 \left[\frac{a_5}{1+a_5} \langle 1-p_5 \rangle - p_5 p_8 p_9 p_{11} (1-p_6) \right] \quad (4.83)$$

$$\text{U238: } \frac{dN_8}{d\theta} = -N_8\sigma_8 - \left(\frac{q}{\phi}\right) \left[P_1 \langle 1-p_8 \rangle + \frac{(\epsilon-1)}{\epsilon(\eta_8-1)} \right] \quad (4.84)$$

$$\text{Pu239: } \frac{dN_9}{d\theta} = N_8\sigma_8 - N_9\sigma_9 + \left(\frac{q}{\phi}\right) \left[P_1 (\langle 1-p_8 \rangle - \langle 1-p_9 \rangle) + \frac{a_8(\epsilon-1)}{(1+a_8)\epsilon(\eta_8-1)} \right] \quad (4.85)$$

$$\text{Pu240: } \frac{dN_{10}}{d\theta} = N_9(\sigma_9 - \sigma_{f,9}) - N_{10}\sigma_{10} + \frac{q}{\phi} P_1 \left[\frac{a_9}{1+a_9} \langle 1-p_9 \rangle - p_5 p_8 p_9 p_{11} p_6 p_{12} (1-p_{10}) \right] \quad (4.86)$$

$$\text{Pu241: } \frac{dN_{11}}{d\theta} = N_{10}\sigma_{10} - N_{11} \left(\sigma_{11} + \frac{\lambda_{11}}{\phi} \right) + \left(\frac{q}{\phi}\right) P_1 \left[p_5 p_8 p_9 p_{11} p_6 p_{12} (1-p_{10}) - \langle 1-p_{11} \rangle \right] \quad (4.87)$$

$$\text{Pu242: } \frac{dN_{12}}{d\theta} = N_{11}(\sigma_{11} - \sigma_{f,11}) - N_{12}\sigma_{12} + \frac{q}{\phi} P_1 \left[\frac{a_{11}}{1+a_{11}} \langle 1-p_{11} \rangle - p_5 p_8 p_9 p_{11} p_6 (1-p_{12}) \right] \quad (4.88)$$

N_{FP} represents the number of fission product pairs produced or, equivalently, the total number of fissions, and in differential form is given by,

$$\frac{dN_{FP}}{d\theta} = \sum_{m=5, 9, 11} N_m \sigma_{f, m} + \left(\frac{q}{\phi}\right) \left[\frac{1}{(1 + a_8)} \frac{(\epsilon - 1)}{\epsilon(\eta_8 - 1)} + P_1 \sum_{m=5, 9, 11} \frac{\langle 1 - p_m \rangle}{1 + a_m} \right] \quad (4.89)$$

σ_{FP} is defined as the average microscopic cross section per fission, due to fission products with cross section less than 10,000 barns, so that the macroscopic poisoning cross section of this group is simply,

$$\Sigma_{FP} = N_{FP} \sigma_{FP} \quad (4.90)$$

The value of σ_{FP} is given in Reference S3 for different fissionable materials, flux-times, fluxes, and methods of irradiation.

The macroscopic Xenon cross section is:

$$\Sigma_{Xe} = \frac{\sigma_{Xe} \phi}{\sigma_{Xe} \phi + \lambda_{Xe}} \Sigma_{Xe, \max} \quad (4.91)$$

where,

$$\Sigma_{Xe, \max} = \sum_{m=5, 9, 11} y_{Xe, m} N_m \sigma_{f, m} + \left(\frac{q}{\phi}\right) \left[\frac{y_{Xe, 8}}{(1 + a_8)} \frac{(\epsilon - 1)}{\epsilon(\eta_8 - 1)} + P_1 \sum_{m=5, 9, 11} \frac{y_{Xe, m} \langle 1 - p_m \rangle}{(1 + a_m)} \right] \quad (4.92)$$

The remaining fission products with cross sections greater than 10,000 barns have relatively long β decay half life and can be grouped together in what is called here the Samarium group, designated by the subscript Sm. The macroscopic absorption cross section for this group is,

$$\Sigma_{Sm} = \sum_{m=5, 9, 11} y_{Sm, m} N_m \sigma_{f, m} + \left(\frac{q}{\phi}\right) \left[\frac{y_{Sm, 8} (\epsilon - 1)}{(1 + a_8) \epsilon (\eta_8 - 1)} + P_1 \sum_{m=5, 9, 11} \frac{y_{Sm, m} \langle 1 - p_m \rangle}{(1 + a_m)} \right] \quad (4.93)$$

Values for $y_{Xe, m}$ and $y_{Sm, m}$ are also given in Table 4.1

In simplified form the eight nuclide concentrations related by Eqs. (4.82) to (4.89) can be written as a function of the following variables,

$$N_m = f \left[N, \sigma, p, \left(\frac{q}{\phi}\right), \phi, P_1, \theta \right] \quad (4.94)$$

where N , σ , and p represent the sets of these terms. Now p and $\left(\frac{q}{\phi}\right)$ depend only upon N and σ , and σ in turn depends only upon N , see Subsections 1.2 and 1.3, so the dependence can be condensed to,

$$N_m = f_2(N, \phi, P_1, \theta) \quad (4.95)$$

The dependence on ϕ is weak since ϕ occurs only in Eq. (4.87) for Pu241 and there in the term $\left(\frac{\lambda_{11}}{\phi}\right)$ which is small compared to σ_{11} , so a constant value for ϕ is used here as a representative core and life-history average for Pu241. The true value of the flux at each mesh point is used, however, in evaluating Σ_{Xe} . Eq. (4.91).

The only spatial dependence now remaining in the nuclide concentration equations is in the epithermal nonleakage probability, P_1 , which enters as a multiple of the slowing-down-density term in the resonance-capture part of the equations. However, the variation of P_1 from point

to point in the core is small for the loadings considered, so for this reason, and because of the considerable simplification it affords, an average value is also used for P_1 in the solution of the nuclide concentration equations. The true variation of P_1 is considered, however, in the calculation of flux shape and criticality.

With these assumptions, the nuclide concentrations are dependent only upon flux time. The equations are nonlinear, however, due to the N dependence of σ , p , and $\left(\frac{q}{\phi}\right)$. Therefore, the eight equations are numerically solved, using a fourth-order Runge-Kutta-Gill method. The variation of $\left(\frac{q}{\phi}\right)$ and p with N is considered in the first derivative evaluation part of this method, which results in their being recalculated four times for each flux time step. The average microscopic cross sections, σ , vary more slowly so are reevaluated between flux time steps only.

The concentrations are then fitted versus flux time as power series in θ and in addition the following seven properties of the fuel, which are required for the spatial flux shape and criticality calculation, are computed and fitted:

$$1) \quad \Sigma_{Xe, \max} \equiv \text{Eq. (4.92)} \quad (4.96)$$

$$2) \quad (\Sigma_{fl} - \Sigma_{Xe}) \equiv \sum_{\substack{m=5 \\ m \neq 7}}^{12} \Sigma_m + \Sigma_{FP} + \Sigma_{Sm} \quad (4.97)$$

$$3) \quad \Sigma_f \equiv \sum_{m=5, 9, 11} \Sigma_{f, m} \quad (4.98)$$

$$4) \quad \nu \Sigma_f \equiv \sum_{m=5, 9, 11} \nu_m \Sigma_{f, m} \quad (4.99)$$

$$5) \quad \left(\frac{1-p}{1+a} \right) \equiv \sum_{m=5, 9, 11} \frac{\langle 1 - p_m \rangle}{(1 + a_m)} \quad (4.100)$$

$$6) \quad (1-p)\eta \equiv \sum_{m=5, 9, 11} \langle 1 - p_m \rangle \eta_m \quad (4.101)$$

$$7) \quad p \equiv p_5 p_8 p_9 p_{11} p_6 p_{12} p_{10} \quad (4.102)$$

The power-series fit is by the Lagrange collocation method, H27, p. 62. Truncation errors in this fit and recommendations for the number of fit points are discussed in Appendix E.

Thus the numerical solution of the concentration equations need be carried out only once for a given initial fuel composition. Thereafter, the properties at different points in the reactor can be obtained from the above fitted properties knowing only the cumulative flux time of the fuel at each mesh point. For the Xenon poisoning the magnitude of the flux is also needed, and given this, Σ_{Xe} can be calculated at each mesh point from $\Sigma_{Xe, \max}$ according to Eq. (4.91), where $\Sigma_{Xe, \max}$ has only flux-time dependence.

4. Nuclear Data

Table 4.1 lists the principal nuclear data that is built into the code and is intended for use for any uranium-fueled thermal reactor. The source of these data unless specified otherwise was C. H. Westcott's report, AECL 670, Reference W11. Westcott's report gives equations, for the calculation of thermal cross sections as functions of energy for all the non - $1/v$ nuclides required for this study. These equations are composed of a series of terms of the Breit-Wigner form,

$$\sigma(E) = E^{-\frac{1}{2}} \left[a + \sum_{j=1}^n \frac{c_j}{b_j + (E - e_j)^2} \right] \quad (4.102A)$$

The parameters a , b_j , c_j , and e_j , are tabulated in AECL 670. They are the resolved resonance parameters for the term in the series (4.102A) which dominates in the energy range of a large resonance, and are otherwise empirically chosen so that the sum of the terms in (4.102A) fits the BNL-325 curves in regions away from the resonances. These calculated curves give the σ_{2200} values of Table 4.1 for non - $1/v$ nuclides.

The absorption cross sections for U238 and U236 are assumed to be $1/v$ in the thermal region and are normalized to the 2200 m/s σ_{abs} values given in BNL-325. Values of ν_5 and ν_9 are from the World Consistent Set of BNL-325. Also values for ν_{11} and the beta decay half lives of Xenon and Pu241 are taken from BNL-325. α and ν for fast fission and capture in U238 are from ANL-5800, Reference A13. The fission yields of Xenon and the "Samarium group" of fission products (with cross section greater than 10,000 b) are calculated from Walker's report, W4, and are itemized in S3 and in C11.

Table 4.1 Nuclear Data

Nuclide	σ_{2200}, b	Inf. Dilution Res. Integral, I^∞, b	α	ν	Fission Yields	
					y_{Xe}	y_{Sm}
U235(abs)	693.52	370.				
U235(f)	582.78	271.	0.365(res.)	2.47	0.064	0.01649
U236(abs)	7.	257.				
U238(abs)	2.71	289.				
U238(fast f)	—	—	0.0687(fast)	2.60	0.06	0.03154
Pu239(abs)	1031.1	478.5				
Pu239(f)	747.73	319.	0.5(res.)	2.90	0.053	0.03315
Pu240(abs)	300.0	8850.				
Pu241(abs)	$(1.3765 \sigma_{f,11})$	781.				
Pu241(f)	1015.2	567.5	0.3765(res.)	3.06	0.06	0.035
Pu242(abs)	30.09	1015.				

70

$$T_{\frac{1}{2}, Xe} = 9.13 \text{ h}$$

$$T_{\frac{1}{2}, 11} = 13.2 \text{ y}$$

B: BASES FOR THE COST CALCULATIONS

1. Background and Assumptions

The procedure used to calculate costs is essentially that used by Pigford, Benedict, Shanstrom, Loomis, and Van Ommeslaghe, P3, Section 8. Since this paper, however, the Technical Appraisal Task Force on Nuclear Power of the Edison Electrical Institute has published a report E8, which should help in standardizing the method of fuel cycle cost calculations. For this reason the method of Pigford, et. al., has been slightly modified so that the cost breakdown is directly comparable with the Edison Electrical Institute method. The main modification is the adoption of the "fixed charge on working capital" technique of roughly approximating the cost due to interest considerations. This method is a simplified substitute for the accurate accounting technique involving the calculation of the interest debit or credit due to each step in the fuel cycle, depending on the time difference between the payment for that step and receipt of revenue when the fuel is utilized in the reactor. The other modifications are essentially ones of nomenclature and of the grouping of the items in the fuel-cycle pipe line. A constant cost item has been provided which can be used for the cost of replaceable core structures or items not covered by the other terms; however, it has been taken as zero for the calculations of this work.

The processes in the fuel cycle have been divided into the steps shown in Fig. 4.5. Each step is given a number which is used as an index for the costs, recovery terms, and weight ratios in the cost equations. These equations are written in general form for the processes of Fig. 4.5. If a

step is not required in the chosen fuel cycle, the cost of that step can be eliminated by setting its material adjustment factor, f , or unit cost equal to zero. Steps 1, 3, 4, 5, 7, and 15, were not needed for the calculations of this work.

The parameters used in the cost equations are listed in Table 4.2. The current prices were taken from published sources or producers estimates and the references for these values are also listed in Table 4.2. In addition to the current prices, alternative cases of interest have been calculated for each fuel cycle system to indicate the effect of variations in certain of the unit prices. When no value is given for an alternate unit price, the current price is used. The alternate costs that produce the highest total fuel-cycle cost have been grouped together and, likewise those that produce the lowest cost have been grouped together.

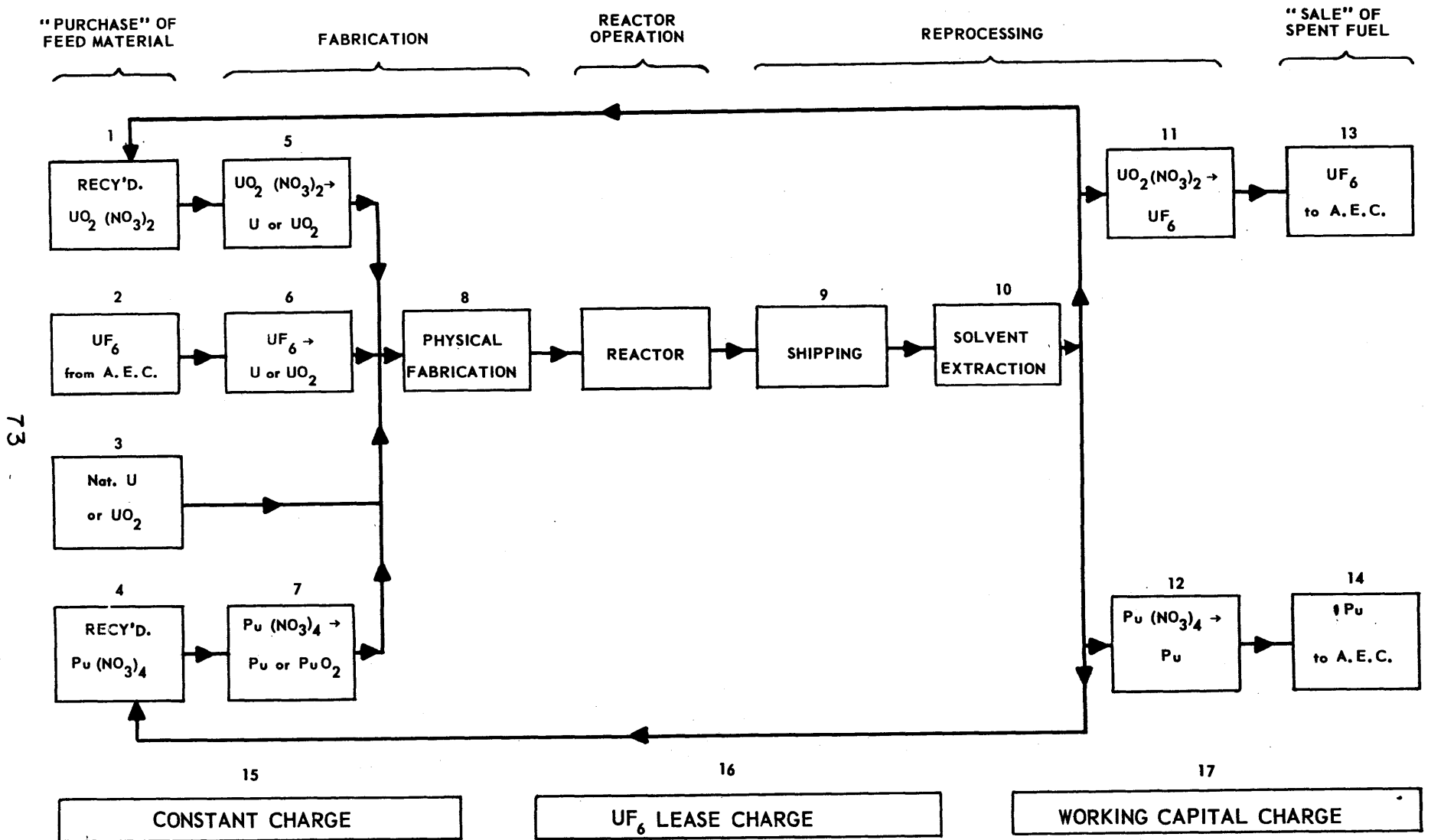


FIG. 4.5 PROCESS FLOWSHEET FOR COST ASSUMPTIONS

TABLE 4.2 PARAMETERS FOR COST CALCULATION ✓

STEP NUMBER (i)	ITEM	UNIT PRICES, (C)					MATERIAL ADJUST. FACTORS (ii)	REFERENCES	
		1. "CURRENT"	2. HIGH ALTERNATE	3. LOW ALTERNATE	4. OTHER	IN $\frac{1}{kg}$ OF			
1	UO ₂ (NO ₃) ₂ , recycled	Eqs. (4.124) and (4.125)					U		
2	UF ₆ from A.E.C.	Eq. (4.121) and (4.122)					U	1.02 U5, U15, B4	
for 1, 2, and 13	Separative Work, (C _E)	37,286	*	24,857	*	U		B4	
"	Optimum Waste Comp., (x ₀)	.0022138 ✓	*	.0022138 ✓	.0026700 ✓	(wt. fract. U235)		B4	
3	Natural U					U		U4	
4	Pu (NO ₃) ₄ , recycled					Pu			
5	UO ₂ (NO ₃) ₂ → UO ₂					U235			
6	UF ₆ → UO ₂ powder	660.	1320.	*	*	U235	1.01	W3, Z1	
7	Pu (NO ₃) ₄ → PuO ₂					Pu			
8	Physical Fabrication	90.	*	30.	45.	fuel	1.00	W3, Z1, R7, E5, U14	
9	Shipping	9.	*	5.	*	fuel	1.00	C14, N5	
10	Solvent Extraction	Eq. (4.129)					fuel	.99	U6, U9, E8
for 10	Daily Rate for Solv. Ext., (d ₁₀)	15,300.	*	*	*	(\$/day)		U6, U9, E8	
11	UO ₂ (NO ₃) ₂ { ≤ 5%, (d _{11,1}) → UF ₆ { > 5%, (d _{11,2})	5.60 32.	*	*	*	U	0.99	U10	
12	Pu (NO ₃) ₄ → Pu	1,500.	*	*	*	Pu	0.99	U10	
13	UF ₆ to A.E.C.	Eqs (4.138) and (4.139)					U	0.99	U5, B4
14	Pu to A.E.C.	12,000	*	30,000.	*	Pu	0.99	U7	
15	Constant Charge					fuel			
16	UF ₆ Lease Charge, (F _L)	.04	.12	*	*	(fract./yr.)		U5	
17	Working Cap. Charge, (F _W)	.09	*	*	*	(fract./yr.)		E8	

Load Factor, L 0.8
 Fraction of new feed U235 from Nat. U, f_{nat} 0.
 Net thermal efficiency, γ 0.2791
 Non-reactor lease charge time, t_L, years 1.67
 Non-reactor working cap. charge time, t_w years 0.458
 Weight of fuel charged to reactor, W_{f1}, kg 24,395.

✓ Blanks mean step not used.

✗ Cost of UF₆ feed corresponding to optimum waste composition is \$39.27/Kg.U.

✗ Cost of UF₆ feed corresponding to optimum waste composition is \$26.18/Kg.U.

* An asterisk means same value as "current" price.

2. The Partial Fuel Cost Equations

It is useful in condensing the cost equations to define an energy yield term, G , as the grams of fuel fed to the reactor per kwh of electricity produced. G is related to E , the average burnup in Mwd per ton of fuel fed to the reactor, by the equation,

$$G = \frac{10^3}{24 \bar{E} \gamma} \quad (4.103)$$

where γ is the net thermal efficiency.

$\bar{C}_{i,j}$ is defined as the cost for the i^{th} step in the fuel cycle for input cost set j ; (see Fig. 4.5 and Table 4.2). For a given set of input data the j index can be dropped and these costs can be expressed in the general form,

$$\bar{C}_i = f_i W_i C_i G \frac{\text{mills}}{\text{Kwh}} \quad (4.104)$$

where C_i is the unit price for process i , in $\frac{\$}{\text{kg of "material i"}}$, (or $\frac{\text{mills}}{\text{gm}}$); W_i is the weight ratio of "material i ", the material on which the price C_i is based, to the fuel fed to the reactor for no process losses; and f_i is a dimensionless material adjustment factor, to account for process losses. f_i is the ratio of "material i " leaving the step to "material i " entering the reactor for steps preceding the reactor, and is the ratio of material "i" leaving the step to "material i " leaving the reactor for steps following the reactor. It is seen that the product of the four terms on the right side of Eq. (4.104) gives the partial fuel cycle cost, \bar{C}_i , in mills per electrical kwh.

We can now proceed to write the equations for the individual terms required by Eq. (4.104). In the following equations N_m^0 refers to the concentration of nuclide m in the fuel fed to the reactor; $N_{R,m}$ to that part of N_m^0 which was obtained from recycled fuel; and $N_{m'}$ to the discharge fuel concentration. A term proportional to the weight of the fuel fed to the reactor, W_d , is given by:

$$W_d = \sum_{\substack{m=5 \\ m \neq 7}}^{12} (230 + m) N_m^0 \quad (4.105)$$

With this common term the weight ratios can be written, referring to Table 4.1 for the materials on which the unit prices are based.

$$W_1 = \frac{235 N_{R,5} + 236 N_{R,6} + 238 N_{R,8}}{W_d} \quad (4.106)$$

f_{nat} is defined as the fraction of the fresh (non-recycled) U235 required that is obtained from natural uranium. Then,

$$W_3 = \frac{235 f_{nat} (N_5^0 - N_{R,5})}{.007115 W_d} \quad (4.107)$$

$$W_2 = 0, \quad \text{for } f_{nat} = 1 \quad (4.108)$$

$$W_2 = \frac{235 N_5^0 + 236 N_6^0 + 238 N_8^0}{W_d} - W_1 - W_3, \quad \text{for } f_{nat} \neq 1 \quad (4.109)$$

$$W_4 = \frac{\sum_{m=9}^{12} (230 + m) N_{R,m}}{W_d} \quad (4.110)$$

$$W_5 = \frac{235 N_{R,5}}{W_d} \quad (4.111)$$

$$W_6 = .007115 W_2 \quad (4.112)$$

$$W_7 = W_4 \quad (4.113)$$

$$W_8 = W_9 = W_{10} = W_{15} = 1 \quad (4.114)$$

$$W_{11} = \frac{235 N_5 + 236 N_6 + 238 N_8}{W_d} \quad (4.115)$$

$$W_{12} = \frac{\sum_{m=9}^{12} (230 + m) N_m}{W_d} \quad (4.116)$$

$$W_{13} = W_{11} \quad (4.117)$$

$$W_{14} = W_{12} \quad (4.118)$$

The following equations for the product cost, C_P , from an ideal separation cascade, see B4, Eq. (10.119), fits the A.E.C. price schedule for UF_6 and is used to calculate C_1 , C_2 , C_{13} :

$$C_P(x_P) = C_E \left[(2x_P - 1) \ln \frac{x_P(1 - x_0)}{x_0(1 - x_P)} + \frac{(x_P - x_0)(1 - 2x_0)}{x_0(1 - x_0)} \right] \quad (4.119)$$

Where the unit cost of separative work, C_E , and the optimum waste composition, x_0 , are specified as input data. x_0 is obtained from C_E and the unit cost of feed, C_F , of weight fraction x_F of U235, according to a similar equation, B4, Eq. (10.118), namely,

$$C_F = C_E \left[(2x_F - 1) \ln \frac{x_F(1-x_0)}{x_0(1-x_F)} + \frac{(x_F - x_0)(1-2x_0)}{x_0(1-x_0)} \right] \quad (4.120)$$

For this work x_0 is calculated taking C_F as the unit price of natural UF_6 feed, \$39.27/kg for "current" prices. This is somewhat less than the \$40/kg price for natural uranium since the cost for the metal preparation is slightly more than for the hexafluoride. The x_F for natural uranium of .007115 is used.

Equations for the unit prices not provided as input data can now be developed.

$$C_2 = 0, \quad f_{nat} = 1. \quad (4.121)$$

$$C_2 = C_P(x_P), \quad f_{nat} \neq 1. \quad (4.122)$$

where,

$$x_P = \frac{235 (1 - f_{nat})(N_5^0 - N_{R,5})}{W_d W_2} \quad (4.123)$$

and, $C_P(x_P)$ is given by Eq. (4.119).

$$C_1 = 0, \quad W_1 = 0 \quad (4.124)$$

$$C_1 = C_P(x_P) - d_1 \quad (4.125)$$

where,

$$x_P = \frac{235 N_{R,5}}{W_d W_1} \quad (4.126)$$

$$d_1 = d_{11,1} \quad x_P \leq .05 \quad (4.127)$$

$$d_1 = d_{11,2} \quad x_p > .05 \quad (4.128)$$

Values for $d_{11,1}$ and $d_{11,2}$ are listed in Table 4.1. The solvent extraction cost, C_{10} , is calculated according to the prescription of Reference E8 for the A.E.C. price data of References U6 and U9,

$$C_{10} = \frac{d_{10} \left(\frac{W_{fl}}{r} + t \right)}{W_{fl}} \quad (4.129)$$

where,

$$b = \frac{40 W_d W_{11}}{235 N_5} \quad (4.130)$$

and the reprocessing rate, r , in kg/day is given by

$$r = b, \quad b \leq 1000 \quad (4.131)$$

$$r = 1000, \quad b > 1000 \quad (4.132)$$

$$\left(b = 1000 \frac{\text{kg}}{\text{day}} \text{ for an enrichment of } 4\% \right)$$

and, the "turnaround" time, t , in days is,

$$t = 3, \quad \frac{W_{fl}}{r} < 3 \quad (4.133)$$

$$t = \frac{W_{fl}}{r}, \quad 3 \leq \frac{W_{fl}}{r} < 8 \quad (4.134)$$

$$t = 8, \quad \frac{W_{fl}}{r} > 8 \quad (4.135)$$

W_{fl} is the weight of the fuel in kg and d_{10} is the daily reprocessing charge, \$15,300/day for "current" prices. The uranyl nitrate conversion unit price is,

$$C_{11} = d_{11,1}, \quad x_P \leq .05 \quad (4.136)$$

$$C_{11} = d_{11,2}, \quad x_P > .05 \quad (4.137)$$

where x_P is defined by Eq. (4.140). For return of the UF_6 to the A.E.C.,

$$C_{13} = 0, \quad f_{13} = 0 \quad (4.138)$$

(Separate criteria are specified if zero unit prices are desired for C_1 , C_2 , or C_{13} to avoid the computer's attempting to calculate the ln of zero in the C_P calculation.)

$$C_{13} = C_P(x_P), \quad f_{13} \neq 0 \quad (4.139)$$

where

$$x_P = \frac{W_d W_{11}}{235 N_5} \quad (4.140)$$

The partial fuel cycle costs, \bar{C}_i for i from 1 to 17, can now be calculated. As given previously,

$$\bar{C}_i = f_i W_i C_i G, \quad \text{for } 1 \leq i \leq 15 \quad (4.141)$$

The lease charge on UF_6 is given by

$$\bar{C}_{16} = F_N \left(t_L + \frac{t_R}{L} \right) \bar{C}_2 \quad (4.142)$$

where: F_N is the lease charge rate on UF_6 , $\frac{\text{fraction}}{\text{year}}$; $\frac{t_R}{L}$ is the reactor holdup time in years, L being the load factor and t_R the time at full power; and t_L is the non-reactor lease charge time in years. The working capital charge, essentially as recommended in E8, is calculated from

$$\bar{C}_{17} = F_W \left(t_W + \frac{t_R}{2L} \right) \left(\sum_{\substack{i=1 \\ i \neq 2}}^8 \bar{C}_i \right) \quad (4.143)$$

where, F_W is charge rate on working capital, $\frac{\text{fraction}}{\text{year}}$, and t_W is the non-reactor working capital charge time, years, taken here as one-half of the reactor lead time. (In Ref. E8, $\frac{t_R}{L}$ is used for the time instead of $t_W + \frac{t_R}{2L}$.)

Finally, some of the partial unit costs are then combined in groups according to the Edison Electric system, E8.

The net fuel material cost, \bar{C}_{mt} , is,

$$\bar{C}_{mt} = \sum_{i=1}^4 \bar{C}_i - \bar{C}_{13} - \bar{C}_{14} \quad (4.144)$$

where \bar{C}_{13} and \bar{C}_{14} are subtracted since they represent credits for returned fissionable material. The fabrication cost, \bar{C}_{fb} , is defined by,

$$\bar{C}_{fb} = \sum_{i=5}^8 \bar{C}_i \quad (4.145)$$

and the spent fuel reprocessing cost, \bar{C}_{rp} , is

$$\bar{C}_{rp} = \sum_{i=9}^{12} \bar{C}_i \quad (4.146)$$

The latter two combinations are in accord with the current trend to include the related conversion and shipping costs with the cost of physical fabrication and with that of solvent extraction when reporting "fabrication" costs.

Thus we have two sets of partial fuel cycle costs that add up to the net

cost: 1) the set of seventeen partial costs, \bar{C}_i for $i = 1$ to 17, (only eleven of these are used for in this work), and 2) the set of six costs: \bar{C}_{mt} , \bar{C}_{fb} , \bar{C}_{rp} , \bar{C}_{15} , \bar{C}_{16} , and \bar{C}_{17} . Cost results will be presented in both forms in this study.

C. DESCRIPTION OF FUELCYC

1. General Description

FUELCYC is an IBM 704 computer code which will simulate the life history of a reactor for various ways of moving the fuel. It will calculate the criticality, the material composition changes, and the cost of the fuel cycle for most of the reactors that are of current interest. More specifically, FUELCYC will perform the above fuel cycle calculations for the following conditions:

1. Cylindrical reactors with azimuthal symmetry, see IV. A. 2.
2. Fuels of U235, U238 and daughter nuclides, see IV. A. 3.
3. Moderators of water, heavy water, graphite, or beryllium, see IV. A.1. 2.
4. Specification of different nuclear compositions and properties in a maximum of 200 regions, 10 radial by 20 axial, IV. A. 2.
5. Arbitrary concentration of control poison within the different regions, IV. A. 2.
6. Arbitrary axial symmetry, IV. A. 2.

These conditions are general bounds on the range of fuel cycles and reactor systems that can be calculated due to the basic assumptions of the physical model which was developed in Part A. of this chapter.

Within these general bounds of reactor design one, can, of course, propose many different ways of operating the reactor, involving variations in the regional properties, in the charging of the fuel, and in the programming of the control poison. For this reason, FUELCYC has been written so as to minimize the coding effort required for the addition of

new reactor operational methods as they come of interest. The operational methods now available in FUELCYC are discussed in the next section.

There are many different numerical methods employed in the code, all of which, of course, introduce truncation errors. The magnitudes of these errors are estimated and discussed in Appendix E.

2. Fuel Scheduling Procedures Handled by Present FUELCYC Code

For the purpose of this study control subroutines have been added to the basic code to permit treatment of four different methods of scheduling fuel movement which are of interest in the large power reactors being developed in the United States. The four methods treated are:

- (1) Batch irradiation, in which a complete fresh load of fuel is charged to the reactor, irradiated without movement, and discharged completely when the reactor ceases to be critical.
- (2) Inout irradiation, in which fresh fuel elements are charged continuously to the axis of the reactor, moved steadily radially outward, and discharged continuously from the periphery of the reactor core, with all elements having been irradiated to the same degree.
- (3) Outin irradiation, in which fresh fuel elements are charged continuously to the periphery of the reactor core, moved steadily radially inward, and discharged continuously from the axis of reactor, with all elements at discharge having been irradiated to the same degree.
- (4) Graded irradiation, in which individual fuel elements are irradiated while fixed in place in the reactor and are removed after exposure to a specified degree, and charging and discharging of fuel is scheduled that each region of the reactor contains some fresh fuel, some partially irradiated fuel, and some fully irradiated fuel.

Assumptions made in all of these four fuel scheduling methods, are:

the fresh fuel fed to the reactor has uniform concentration; the reactor has axial symmetry; and the reflector's effect can be adequately approximated by axial and radial reflector savings which are then included in the zero flux extrapolation distances of the problem input data. The latter assumption is good for the large power reactors studies and permits all the cell mock-ups to be core regions.

One of the fuel-scheduling methods, Batch, gives a core with time-dependent properties; the other three are steady-state methods of fuel movement. These methods are discussed in the following subsection.

2.1 Batch Irradiation. This is the normal technique of starting up the reactor with a uniformly loaded core, and with all the fuel elements remaining fixed in position during the life of the core. It is assumed that the excess reactivity in the core is controlled by a uniform-distribution of control poison, the quantity of which, of course, varies during the lifetime in order to make the poisoned core criticality factor, C_w , equal to one, or at least sufficiently close to one so that the resulting flux shape is essentially that of the steady-state flux, see IV. A. 2. 5. This model of the poisoning would be strictly true for control with soluble poison in the moderator, but is an approximation also to one reasonable method of programming control rods so as to reduce flux distortions. This occurs when the reactor has a large number of control rods, so that the rods can be divided into local groups and criticality can be maintained by the complete withdrawal or insertion of combinations of rods in each group with the required reactivity worth.

The reactivity, flux shape, and composition changes that occur during the core life are calculated stepwise from the uniform loaded

condition. Flux-time steps are specified for that portion of the fuel which is in the central core region. These steps are uniform until the overall criticality factor, C , becomes less than unity, after which appropriate sized steps are calculated to converge to the condition $C=1$. The flux-time steps for the fuel in other regions are calculated from the central step and the latest flux distribution assuming no change in flux shape during a step. The nuclear properties required for the criticality calculation can then be obtained at each step for each region since they depend only on the cumulative flux-time experienced by the fuel, see IV. A. 3.

The batch method of irradiation is generally very wasteful of neutrons, and so results in a lower fuel burnup than is necessary. An additional disadvantage of the batch method results from the large variation in power density throughout the core and, even more important, the change in shape of the power density distribution during the life history of the core. These characteristics make the heat transfer design difficult and inefficient for the batch-operated reactor. Methods of fuel movement which improve over Batch in neutron economy and/or heat transfer properties are considered in the next three subsections. The main advantage of Batch irradiation as compared to these other methods is that it involves either fewer reactor shutdowns for recharging the fuel, or less elaborate fuel handling equipment.

In considering the reactor power output, it is assumed in this study that the heat transfer characteristics of the core, as characterized by the power density distribution, are not the limiting characteristic, but rather that the limitation is on the total power output. The latter would

be the case if the generating equipment or heat transfer equipment external to the core were the limiting factor. However, regional power densities and the ratio of maximum to average power densities, i. e., the hot-spot factor, are calculated and can be used to adjust the results for different limitations, for instance for constant maximum power density. Fuel cycle costs for low burnups are primarily flux-time dependent so there will be little change for operation at different flux levels. The only variables affected by the magnitude of the flux are the "on stream" time that the fuel spends in the reactor, t_R , and the Xenon poisoning. The flux level is of considerable importance, however, for fuel cycle costs at high burnups and for the "capital charge" part of the power cost, which is inversely proportional to the power level.

2.2 Progressive Radial Fuel Movement from Inside to Outside.

To avoid wasting neutrons in control poisons fuel elements can be charged to, and discharged from, the core periodically during the life of any one fuel element. The reactivity of the discharged fuel is then allowed to become sufficiently negative before discharge to just balance the positive reactivity of the fresh fuel. The "Inout" fuel movement method increases the efficiency of the neutron usage even further by charging the fresh fuel elements, which act as a neutron source for the rest of the core, near the radial center of the reactor where the probability of leakage is low, and therefore the importance high. The fuel is then moved stepwise to outer positions as new fuel is charged and fuel elements are discharged from the radial edge of the core. As the number of fuel element positions and the frequency of charging increases, the fuel spends less time at any given point in the core so the nuclear

properties at any point tend to become nearly constant with time. In the limit this approaches the steady-state model of continuous fuel feed and discharge with the reactor always just critical. This idealized steady-state condition is used here for the Inout movement as well as for Outin and Graded, which are to be discussed in Section 2.3 and 2.4.

For fuel elements of a specified composition, the steady-state condition that just maintains criticality must be calculated by a double iteration involving initial guesses both for the flux distribution and for the irradiation level of the discharged fuel that will just make the reactor critical.

The double-iteration procedure for Inout will now be described.

An initial estimate is made of the flux-time, θ_c , received by the central portion of each fuel element at the time of discharge. An initial estimate is made of the spatial flux distribution. From these initial estimates, the spatial distributions of nuclear properties is computed. From this spatial distribution, the overall criticality factor and a new flux distribution are computed. With this new flux distribution and the original estimate of θ_c , a second calculation is made of the spatial distribution of flux-time, and nuclear properties, and from them of the overall criticality factor and flux distribution. The procedure is repeated until the criticality factor and flux distribution converge to limiting values for the initial estimate of θ_c .

This procedure has been called the "criticality iteration", since its purpose is to generate the criticality factor for a given θ_c . The criticality iteration is then carried out again for a second estimate of θ_c . After this, new estimates of θ_c are generated by a linear interpolation

between criticality factors for the last two θ_c values until the criticality factor converges to unity. The converged flux-time distribution is then used to calculate the final nuclide concentrations.

The procedure for computing the flux-time which a fuel element leaving a particular (r, z) region of the reactor has received will now be described. It is assumed that azimuthal symmetry is maintained during fuel movement.

The flux in region (r, z) is to be denoted by $\phi_{r, z}$ and the volume of the region by V_r . With steady movement of fuel, the time t_r that a fuel element spends in region (r, z) is proportional to its volume V_r :

$$t_r = t_v V_r \quad (4.146A)$$

The constant of proportionality t_v may be evaluated from the axial central flux-time, θ_c , received by fuel at time of discharge and the flux distribution $\phi_{r, 1}$ and region volume distribution V_r at the value of z for the axial central flux distribution, ($z=1$):

$$\theta_c = \sum_{r=1}^{r_2} \phi_{r, 1} t_v V_r \quad (4.146B)$$

from which,

$$t_v = \frac{\theta_c}{\sum_{r=1}^{r_2} \phi_{r, 1} V_r} \quad (4.147)$$

The flux-time of the fuel leaving region (r, z) , $\theta_{r, z, L}$ is obtained from the flux-time of fuel leaving the next inner region $\theta_{r-1, z, L}$ and

the increment of flux-time $t_v \phi_{r,z} V_r$ received in the region (r, z) ;

$$\theta_{r,z,L} = \theta_{r-1,z,L} + t_v \phi_{r,z} V_r, \quad r \neq 1 \quad (4.148)$$

when $r=1$, the flux-time of fuel entering the region is zero so that

$$\theta_{1,z,L} = t_v \phi_{1,z} V_1 \quad (4.149)$$

The average flux-time within the region (r, z) , $\theta_{r,z}$, needed to obtain the nuclear properties of the region, is obtained as the arithmetic average of the flux-time of fuel entering and leaving the region:

$$\theta_{r,z} = \frac{\theta_{r,z,L} + \theta_{r-1,z,L}}{2}, \quad r \neq 1 \quad (4.150)$$

When $r=1$, $\theta_{r-1,z,L}$ is zero, so that

$$\theta_{1,z} = \frac{\theta_{1,z,L}}{2} \quad (4.150A)$$

In some cases during criticality iterations successive values for estimates that are generated from Eq (4.150) and (4.150A) tend to oscillate about the true value instead of converging. To eliminate this these equations are modified as follows, introducing a damping factor, f_d ,

$$\theta_{r,z}^{(i)} = f_d [\theta_{r,z}^{(i)}] + (1 - f_d) [\theta_{r,z}^{(i-1)}] \quad (4.151)$$

where $\theta_{r,z}^{(i)}$ refers to the initial estimate from Eq. (4.150) or (4.150A) and the index i is the loop count for passes through the criticality iteration. For the first time through the iteration, ($i=1$), f_d is set equal to one which gives no damping; since in this case there are no values

for $\theta_{1,z}^{(i-1)}$ corresponding to the new θ_c . For remaining iterations, ($i > 1$), f_d is empirically set to a value which gives good convergence. It has been found that $f_d = .5$ is usually a good choice.

Because of its efficient use of neutrons, the Inout method gives the highest burnup of the four methods studied. The power density distribution, however, is the most non-uniform of the four methods due to providing more excess reactivity towards the center. Although the non-uniform Inout power density distribution would not vary with time, it is still disadvantageous since the rate of power generation from a given size of core would be less for this method of feeding than for any other method studied.

In light of this, the fuel scheduling method discussed in the next subsection is of interest in attaining a more nearly constant power density distribution, and thus permitting a higher total power output for a given maximum power density.

2.3 Progressive Radial Fuel Movement from Outside to Inside.

This scheme is the same as the previous one except that the fuel moves in the opposite direction, being charged near the radial edge of the core and discharged near the radial center. Considerably better burnup than for Batch irradiation can be expected due to no control poison wastage but less than for Inout since the fuel is charged in regions of low importance and its reactivity becomes negative in regions of high importance. Due to this reactivity distribution, however, the flux is considerably flattened, producing less variation in power densities for the Outin method than for any of the other four.

The solution procedure for Outin is analogous to that for Inout. The

time constant, t_v , is calculated from Eq. (4.147). For the flux-time estimates for the fuel leaving region r, z we have

$$\theta_{r, z, L} = \theta_{r+1, z, L} + t_v \phi_{r, z} V_{r, z}, \quad r \neq r_L \quad (4.152)$$

and

$$\theta_{r_L, z, L} = t_v \phi_{r_L, z} V_{r_L, z} \quad (4.153)$$

The regional flux times for estimating nuclear properties are given by:

$$\theta_{r, z}^{(i)} = f_d \left(\frac{\theta_{r+1, z, L}^{(i)} + \theta_{r, z, L}^{(i)}}{2} \right) + (1 - f_d) \theta_{r, z}^{(i-1)}, \quad r \neq r_L \quad (4.154)$$

and

$$\theta_{r_L, z}^{(i)} = f_d \left(\frac{\theta_{r_L, z, L}^{(i)}}{2} \right) + (1 - f_d) \theta_{r_L, z}^{(i-1)} \quad (4.155)$$

A fuel scheduling method that is intermediate between Inout and Outin, both with regards to burnup and to power density distribution, is presented in the next subsection.

2.4 Graded Irradiation. As for Inout and Outin, fuel elements for Graded are assumed to extend the full length of the core and are charged and discharged periodically. However, in this method the fuel elements are divided into a number of local groups. The most irradiated fuel element in each local group is periodically replaced by a fresh fuel element. The rate of replacement is varied from group to group so that the central part of every discharged fuel element has received the same irradiation. It is assumed that a local group is

radially small enough so that its effect in the core at any axial point is given by averaging the nuclear properties of the different elements within the group at that axial point. In addition it is assumed that there are sufficient elements within the group so that the replacement rate is rapid and, therefore, the average properties of the group at any axial point are essentially constant with time. Thus the average nuclear properties representative of the group of elements, $\bar{f}(\theta)$, are given by,

$$\bar{f}(\theta) = \frac{\int_0^\theta f(\theta') d\theta'}{\theta} \quad (4.156)$$

where θ is the flux time of the most exposed fuel element of the group at the specified axial position, and $f(\theta)$ represents one of the seven nuclear properties required for the spatial solution, as listed in IV. A. 3; ($\Sigma_f(\theta)$, for example). Having calculated the flux-time of the average properties, from Eq. (4.156), a double iteration procedure similar to that of Inout and Outin is used to converge to the correct steady-state condition with a criticality factor of unity. Taking θ_c as the flux-time at the axial center of the discharged fuel elements, which is the same value for all the discharged fuel, the regional flux times for evaluating the nuclear properties are given by,

$$\theta_{r,z}^{(i)} = f_d \theta_c \frac{\phi_{r,z}^{(i)}}{\phi_{r,1}^{(i)}} + (1 - f_d) \theta_{r,z}^{(i-1)} \quad \begin{array}{l} 1 \leq r \leq r_L \\ 1 \leq z \leq z_L \end{array} \quad (4.157)$$

where f_d is the damping factor, as before, and is set equal to unity the first time through each criticality iteration.

Graded irradiation would be expected to give burnups and maximum to average power density ratios intermediate between Inout and Outin since positive reactivity is added and negative reactivity removed throughout the core rather than at specific radial locations as in the other two methods.

3. Solution Procedure

An understanding of how the previously developed theory is put together to form the code FUELCYC is best obtained by reference to flow charts, or computer logic diagrams. Fig. 4.7 is such a diagram for the main control program, called MAIN, for the four fuel movement methods discussed in Section IV.C.2. Fig. 4.6 explains the symbols used in this and subsequent flow charts. This MAIN flow chart essentially gives the order of entry to the various subprograms that are required. In turn some of the subprograms indicated require additional subprograms not shown in Fig. 4.7.

However, the overall logic of FUELCYC can be gleaned from this single simplified flow chart since comments are included to explain the purpose of the various subroutines entered. Flow charts and descriptions for the 32 subroutines of FUELCYC, plus a few other clerical subroutines, are provided in Appendix C. Note that in the triangles of Fig. 4.7 denoting transfer to a subroutine, the number of the section of Appendix C which describes the subroutine is given. The steps on the flow charts are numbered for easy reference. The source language was Fortran II in all cases, so the corresponding Fortran statement numbers are tabulated for the benefit of those readers who have a listing of the source program. The manner of presentation generally follows that approved by the American Institute of Chemical Engineers, A16.

To condense the basic logic flow even further, the following overall purposes of the indicated groups of steps in Fig. 4.7 can be stated:

1. Steps 1-17, initialization.

2. Steps 18-31, calculation of the initial criticality of the uniform loaded reactor: a) with no Xe and "Sm group" poisoning; and b) with saturated amounts of this poison. The average fast to thermal non-leakage probability, P_1 , calculated in b) is used in the solution for the nuclide concentrations as functions of flux time.
3. Steps 32-41, calculation of nuclide concentrations and required space properties as functions of flux time.
4. Steps 42-47, calculation of criticality, nuclide concentrations present, maximum to average power density, and other fuel cycle parameters throughout the life history of the fuel. This is a stepwise calculation for Batch irradiation, and an iteration to converge to the steady-state condition for Inout, Outin and Graded. These subroutines contain the bulk of the calculations of FUELCYC and are described in Appendices C.30. -C.33.
5. Steps 48-49, calculation of burnup and time spent in the reactor, using the final average concentrations from 4.
6. Steps 50-51, calculation of the fuel cycle costs.
7. Steps 52-73, looping and initialization for the next problem, if any.

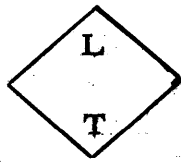
Information on input data preparation and other operational details is given in Appendix D.



Input (read), output (write), calculations.



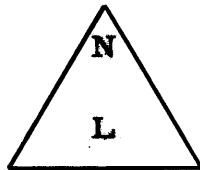
Decisions and branches.



Stops: L gives the absolute octal location of the stop, T gives the type of stop.



Identifying decisions where D is the designator: Y means yes; N, no; 1, branch 1, etc.



Transfer and return from subprogram L, which is described, with flow chart, in Appendix C.N.



Connector for sections of logic: transfer is from or to Step N.

Fig. 4.6 Symbol key for FUELCYC flow charts.

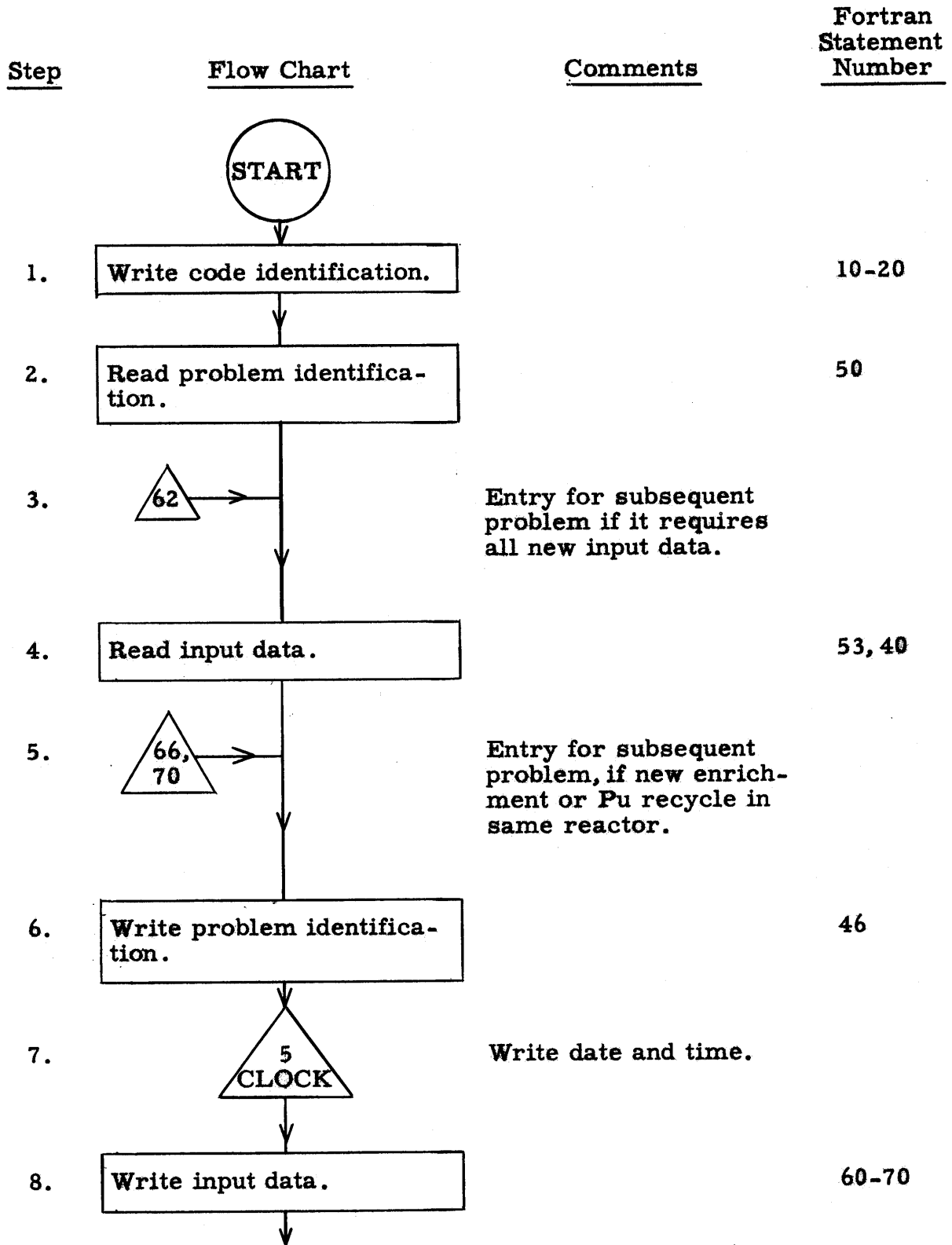


Fig. 4.7 Flow chart for the MAIN control program in FUELCYC.

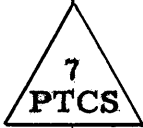

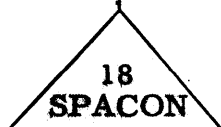
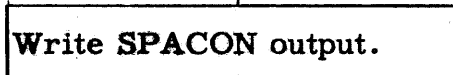
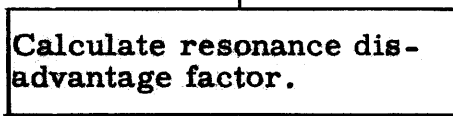
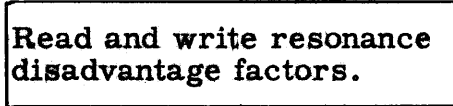
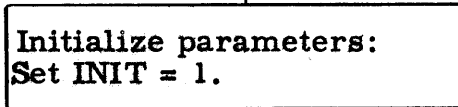

<u>Step</u>	<u>Flow Chart</u>	<u>Comments</u>	<u>Fortran Statement Number</u>
9.		Calculate microscopic cross sections vs. velocity.	100
10.		Tabulate constant nuclear data, v 's, etc.	
11.		Calculate spatial constants, h , g , etc.	
12.		This print-out is usually bypassed.	120-125
13.		$\psi_{1,m} = 1.$ $m \neq 8, 10.$	130-150
14.		Alternate if factors other than the above are desired, usually bypassed.	
15.		INIT is branching variable in later logic.	127
16.		Calculate resonance escape probabilities.	

Fig. 4.7 (cont.)

<u>Step</u>	<u>Flow Chart</u>	<u>Comments</u>	<u>Fortran Statement Number</u>
17.		Calculate average thermal microscopic cross sections. No hardening due to moderator.	
17.5			
18.		Cross sections with moderator hardening included.	128
19.		Initially INIT = 1 .	
20.			
21.		The purpose of Steps 18-31 is to calculate initial criticality with and without Xe and Sm group poisoning.	215-225
22.		Write the time.	
23.		Calculate criticality flux shape, leakage, power density, etc.	230

Fig. 4.7 (cont.)

<u>Step</u>	<u>Flow Chart</u>	<u>Comments</u>	<u>Fortran Statement Number</u>
24.			
25.		Stop for no reactivity.	235
26.			240
27.			
28.			245-250
29.			

Fig. 4.7 (cont.)

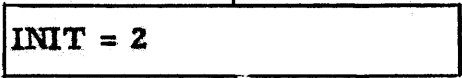


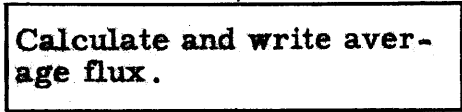
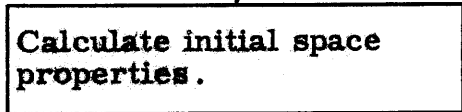


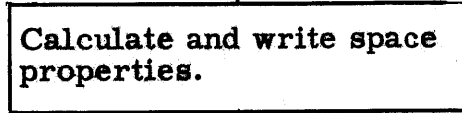
<u>Step</u>	<u>Flow Chart</u>	<u>Comments</u>	<u>Fortran Statement Number</u>
30.			260
31.			
32.		Calculation of initial criticality completed.	
33.		For use in (36.) Fast nonleakage probability from (23.) used in (36.).	300-310
34.		These are the space properties discussed in IV. A. 3.	320-330
35.			
36.		Calculate fuel nuclide concentrations at new flux time step.	
37.		See IV. A. 3.	335-360

Fig. 4.7 (cont.)


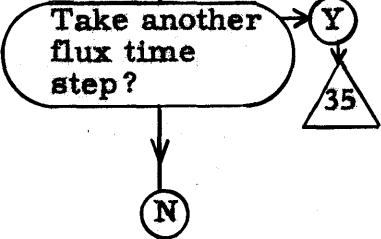
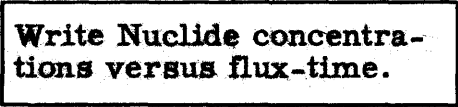
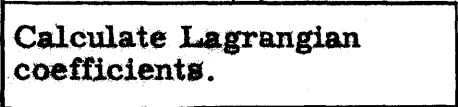

<u>Step</u>	<u>Flow Chart</u>	<u>Comments</u>	<u>Fortran Statement Number</u>
38.		Calculate new microscopic cross sections.	
39.			370
40.			380
41.		For polynomial fit of nuclide concentrations and space properties.	385-400
42.		Entry for next problem if new fuel movement.	

Fig. 4.7 (cont.)

<u>Step</u>	<u>Flow Chart</u>	<u>Comments</u>	<u>Fortran Statement Number</u>
43.		Selection of fuel scheduling procedure from input index IMOVE.	410
44.		Material fuel cycle calculations such as criticality factors, flux shapes, and power densities, made during life history of fuel with Batch fuel scheduling. See Appendix C. 30.	420
45.		Inout fuel scheduling. See Appendix C. 31.	430
46.		Outin fuel scheduling. See Appendix C. 32	440
47.		Graded fuel scheduling. See Appendix C. 33.	450
47.5		Space for new fuel movements.	460-490
48.			500-540

Fig. 4.7 (cont.)

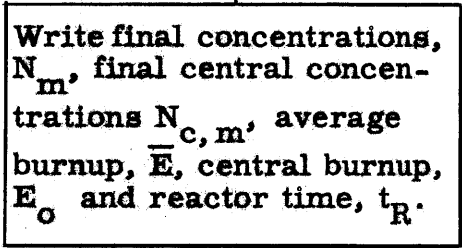
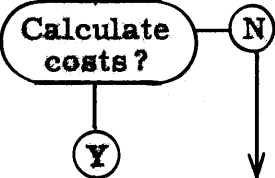

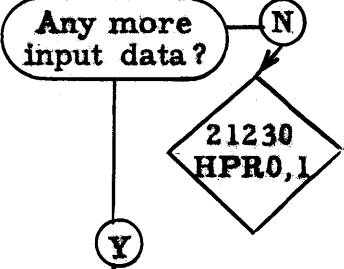
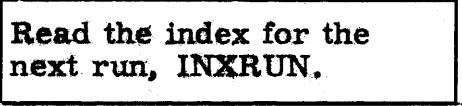
Step	Flow Chart	Comments	Fortran Statement Number
49.			510-550
50.		<p>COSTT = 0: Y COSTT ≠ 0: N</p>	
51.		Calculate costs.	560
52.		<p>Normal stop in read routine for no input cards in hopper.</p>	
53.		<p>To control the initialization and reentry for the next run.</p>	580

Fig. 4.7 (cont.)

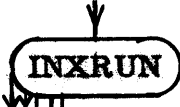
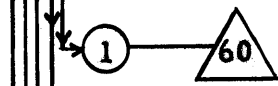
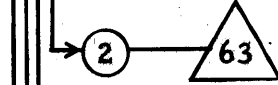
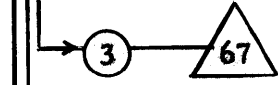
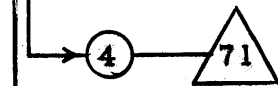


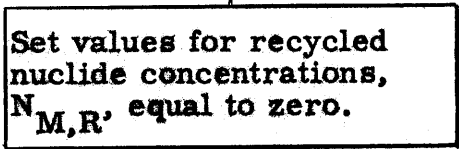


Step	Flow Chart	Comments	Fortran Statement Number
54.			
55.			
56.			
57.			
58.			
59.		For future modifications.	680
60.		When the next run requires reading all new input data.	
61.			590-600
62.			
63.			

Fig. 4.7 (cont.)

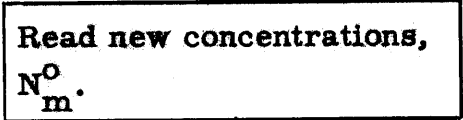
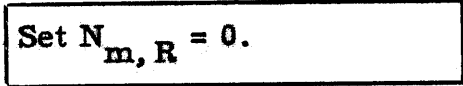


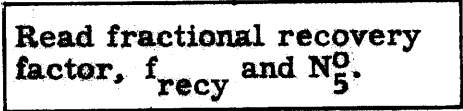
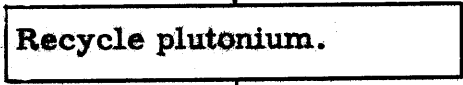




<u>Step</u>	<u>Flow Chart</u>	<u>Comments</u>	<u>Fortran Statement Number</u>
64.		For a new set of initial fuel concentrations in same reactor.	610-620
65.		As before.	630
66.			
67.		For Pu recycle.	
68.			640-650
69.		$N_m^0 = f_{recy} N_m$ $m = 9-12$	660
70.			
71.		For a new fuel movement method in the same reactor.	
72.		Read the new value for IMOVE.	670
73.		The code stops when there are no more input data cards, see (52.).	

Fig. 4.7 (cont.)

4. Machine and Time Requirements

The code requires a 32,768 word IBM 704 computer and one or two tape units. The space actually used in octal units is: (0-64011)₈ and (65032-77777)₈. Output is on Tape 2 and the binary information can be read in from the card reader or can be loaded on to Tape 4 and subsequently read in from there. Problem input data is provided via the card reader. If the "real time" prints are used, a clock must be connected to the computer.

The following equation gives an estimate of the computer time required for one problem,

$$t(\text{minutes}) = sn_L \left\{ \left[\frac{\text{SPACE 2}}{.001 \delta_1 + .004 \left(\frac{j}{3}\right)^4} \right] + \left[\frac{\text{SPPROP}}{.001 \delta_2 + .001 \left(\frac{f}{5}\right)^{1.3}} \right] \right\} \\ + m \left\{ \frac{\text{NUCON}}{.01 + i_L} \left[\frac{\text{AVGCS2}}{.001 \delta_3 + .0004} \right] \right\} + .3 + r \quad (4.158)$$

where,

s = number of passes through the spatial subroutines.

n_L = number of mesh points, $n_L = r_L z_L$.

j = loop count of the average number of iterations for flux convergence in the SPACFX subroutine (for spatial flux shape).

f = number of fit points used for the polynomial fit of space

properties versus flux time, $f = \left(1 + \frac{n_\zeta - 1}{n_{sp}} \right)$.

m = number of passes through NUCON (for a flux time step in the nuclide concentration equation solution or through AVCGS2

(calculation of average cross sections), $m \sim n_\zeta$.

i_L = number of velocity points for calculation of the thermal flux

energy distribution (and for averaging the thermal cross sections).

r = "read in" time for the binary information.

δ_i , $i=1, 2, 3$ are print options, $\delta_i = 1$ for print, $\delta_i = 0$ for no print.

The values of the above variables depend on the problem being solved and upon the accuracy desired; however, for simplification Eq. (4. 158) will be reduced to the more approximate Eq. (4. 159) using average values for the parameters used in past runs. r is approximately 4 minutes if the binary information is on cards, but is negligible if it is on tape and is zero for problems after the first. Tape input was used for essentially all of the runs of this work, so r will be taken as zero. The three values of .001 in Eq. (4. 158) are for secondary printouts: the first two are for space functions at each mesh point and are generally bypassed; the third is for the thermal energy spectrum of the flux, and is often used. Therefore, δ_1 and δ_2 will be taken as zero and $\delta_3 = 1$. Average values for other terms are: $s = 10$, $j=3$, $f=5$, $i_L = 25$. An average value of m is 10 for the first fuel movement of a given reactor but for subsequent fuel movements $m=0$. In the simplified equation m is taken as 5. These substitutions give the considerably simplified equation:

$$t \sim .5 + .05 n_L, \text{ min.} \quad (4. 159)$$

The smallest value for the number of mesh points, n_L , that has been used is 9 and the largest 100, which would give a time range of from 1 to 6 minutes per problem.

Due to the large number of assumptions made in Eq. (4. 159), the time estimate might be appreciably in error for a specific problem; however, if control variables are chosen carefully, it should give a reasonable estimate of the average behavior. Since the solution converges for a

mesh as coarse as 3×3 and the answers are good enough for first approximations (costs might be expected to be 10% off), it is usually conservative of time to make an initial survey series of runs at this mesh spacing, and later a more accurate set at a finer mesh for increased accuracy. The first set serves to eliminate unnecessary runs, to give good estimates for parameters that have a strong effect on the time required such as final steady-state flux-time guesses, and in general to allow desired changes to be made with a minimum of computer time.

V. REACTOR DESIGN DATA

A. PRESSURIZED LIGHT WATER REACTOR

1. General Description

Most of the calculations for this study have been made for a pressurized light-water reactor that is structurally similar to the Yankee Atomic Electric Company reactor designed by Westinghouse Electric Corporation. An early version of this design is described in Reference Y1 and later design data were obtained from Dr. W. H. Arnold of Westinghouse.

The reference design for the reactor of this report is fueled with 51420 lbs. of UO_2 of 3.4 w/o U^{235} and is cooled and moderated by light water at a pressure of 2000 psi and a temperature of 516°F . The reflector consists of a one-half inch steel baffle with an effective infinite amount of water beyond. The reactor produces 480 Mev of heat and generates 134 Mev of electric power. The load factor has been taken as 0.8.

The fuel elements consist of UO_2 pellets, 0.29 inches in diameter loaded into 20 mil thick stainless steel tubes. The tubes are placed on a 0.42 in. square pitch in a cylindrical core 3.1 ft. in radius and 7.7 ft. in height. More exact values for some of these dimensions and additional design data are listed in Table 5.1.

Fuel cycle calculations, i. e. fuel cycle costs, nuclide inventories, burnups, flux and power density distribution, etc., have been made for this reference design and for variations to it with different U^{235} enrichments. For these enrichment variations all the input data parameters, of Table D1., were assumed to have the same value as for the reference

design reactor except for the initial inventory of U235. The fuel cycle calculations have been made for the four fuel scheduling methods described in Section IV. C. 2. These results are presented in Section VI.

Table 5.1 Reference Design Data for Pressurized Light Water Reactor.*

Inventories

<u>Item</u>	<u>Volume (in)³</u>	<u>Weight (lbs.)</u>	<u>References</u>
UO ₂ (w/o U235 = 3.4)	141,091.	51,420.	A10
Stainless Steel (Type 348)	48,025.	13,520.	A10
H ₂ O	208,330.	5,881.	A10
Zirconium	12,137.	2,850.	A10
Void	5,421.	---	A10
Total	415,004.	73,671.	---

Core Dimensions (in)

Equivalent Diameter	75.68	A10
Total Active Length	92.257	A10
<u>Temperature, mean, T_{md}, (°F)</u>	516.	A10

Power, (Mw)

Thermal	480.	Y1
Net Electric	134.	Y1

Nuclear Properties

Initial resonance escape probability for U238, p _g	0.738	A10
Initial resonance escape probability for structural materials and coolant, p _c	0.942	A10

* All values are for the mean temperature of 516°F.

Table 5.1 (Cont.)

<u>Nuclear Properties</u>		<u>Reference</u>
Fast fission factor, ϵ	1.0584	A10
Fermi age, τ , (cm^2)	51.5	A10
Thermal disadvantage factor, ψ	1.141	A10
Reflector savings, $\delta_R = \delta_H$, (cm)	7.5	A10
Microscopic 2200 m/s absorption cross section for H_2O , (b)	0.575	W8
Microscopic transport cross section for H_2O , (b)	70.	W8
Microscopic slowing down power for H_2O , $(\xi\sigma_s)_{\text{H}_2\text{O}}$, (b)	41.2	W8
Microscopic 2200 m/s absorption cross section for Type 348 stainless steel, (b)	3.206	H29 (calculated)
Atomic weight of Type 348 stainless steel	55.63	H29 (calculated)

2. Calculation of FUELCYC Nuclear Input Data for the Pressurized Light-Water Reactor

Values of the required nuclear input data for FUELCYC, as specified in Table D1., can be calculated for the pressurized light-water reactor from the basic reference design data of Table 5.1. These calculated values are listed in Table 5.2. The calculation procedure is straightforward for most of the nuclear parameters but will be described below when it differs from standard techniques. Recommended settings for the spacing parameters of the various numerical methods, μ_v , i_L , ζ , n_ζ , n_{sp} , r_L , z_L , ζ_2 , θ_1 , θ_2 , are listed and discussed in Appendix E.

Since we have an experimental value for p_8 , $\psi_{1,8}$ was calculated from,

$$\psi_{1,8} = - \frac{C_1 N_8 I_8^\infty}{\ln p_8} \quad (5.1)$$

The initial estimate for the fast non-leakage probability, P_1 , was calculated from the relationship for the one fast group diffusion model, see Section IV.A.2.2, for a uniformly loaded core,

$$P_1 = \frac{1}{1 + B_g^2 \tau} \quad (5.2)$$

where B_g is the geometric buckling and τ is given by Table 5.1.

Correspondingly, the initial estimate for $(-D\nabla^2)$ was DB_g^2 .

For the calculation of Σ_{md} and σ_{Xe} , the initial energy spectrum of the flux in the fuel was required. This is because the fuel flux increased

Table 5.2 FUELCYC Nuclear Input Data for the Pressurized Light-Water Reactor.*

Item	Value	Units
N_5^0	0.0008785	$\frac{\text{atoms}}{\text{b cm (of fuel)}}$
N_8^0	0.02465	"
$N_6^0, N_{FP}^0, N_9^0 - N_{12}^0$	0.	"
$\xi \Sigma_s$	0.8181	cm^{-1} (of mod.)
$(T_o/T_{md})^{1/2}$	0.7359	-
$\psi_{1,8}$	14.76	-
C_1	0.6297	cm (of fuel)
ϵ	1.0584	-
P_1^0	0.9654	-
$(-D\nabla^2)^0$	0.000192	cm^{-1}
R	96.11	cm
H	234.33	cm
δ_R	7.5	cm
δ_H	7.5	cm
D	0.2755	cm
τ	51.5	cm^2
Σ_{md}	0.0542	cm^{-1} (of mod.)
σ_{Xe}	1.35 E6	b
σ_{FP}	31.9	b
ψ	1.141	-
P_d	70.57	kw/liter
V_{fl}	0.3400	-
$\Sigma_{s, fl}$	0.4271	cm^{-1} (of fuel)

* For definitions and further description see Table D1. For the spacing parameters for the numerical solution methods see Appendix E.

by the disadvantage factor is used in calculating the moderator reaction rate rather than the moderator flux. To be compatible with this procedure the moderator cross section, Σ_{md} , must have been evaluated for the fuel flux-energy distribution. * As discussed in Section IV. A. 1. 2, the assumption was made that the distribution of fuel flux with respect to energy was equivalent to that of a hardened Maxwell-Boltzmann distribution in which the neutron temperature was given by,

$$T_{\text{neutron}} = T_{\text{md}} (1 + 0.46 \Delta), \quad (^{\circ}\text{K}) \quad (5.3)$$

where Δ is evaluated at T_{md} from,

$$\Delta = \frac{4\Sigma}{\xi \Sigma_s V_{\text{md}}} \quad (5.4)$$

and the initial macroscopic absorption cross section at kT_{md} , Σ , was given by the homogenized average for the initial loading,

$$\begin{aligned} \Sigma \text{ (cm}^{-1}\text{)} = & (N_5 \sigma_5 + N_8 \sigma_8) V_{fl} + (N_{ss} \sigma_{ss} + N_{\text{H}_2\text{O}} \sigma_{\text{H}_2\text{O}} \\ & + N_{\text{Zr}} \sigma_{\text{Zr}}) V_{\text{md}} \psi \end{aligned} \quad (5.5)$$

where the σ 's are values at T_{md} , and $V_{\text{md}} = (1 - V_{fl})$.

*The core average reaction rate density is calculated by FUELCYC for fuel materials as $N_{fl} V_{fl} \sigma_{fl} n_{fl} \bar{v}_{fl}$; for the slowing down power, as $(\xi \Sigma_s) V_{\text{md}} n_{fl} \bar{v}_{fl}$; for the moderator (plus other materials with constant microscopic cross sections) by, $\Sigma_{\text{md}} V_{\text{md}} \psi_{fl} \bar{v}_{fl}$. In these expressions \bar{v}_{fl} is the average velocity for the neutron distribution in the fuel, and the moderator volume fraction, V_{md} , is taken as $1 - V_{fl}$.

For the reference design reactor this calculation gave $\Delta = 1.45$ and therefore from (5.3), $T_{\text{neutron}} = 908^\circ\text{K}$.

Using this value of T_{neutron} , the microscopic absorption cross section of Xenon, σ_{Xe} , was calculated from,

$$\sigma_{\text{Xe}} = \sigma_{\text{Xe}}^0 g_{\text{Xe}} \sqrt{\frac{\pi T_0}{4 T_{\text{neutron}}}} \quad (5.6)$$

where σ_{Xe}^0 and g were taken from the Bernstein, $g^* = 5/8$, values listed in Reference W11.

An effective thermal value of Σ_{md} was calculated as the sum of the real thermal contribution plus a resonance contribution. The thermal part was calculated as a Maxwellian average at T_{neutron} . This gave for Σ_{md} ,

$$\Sigma_{\text{md}} = \Sigma_{\text{md}}^0 \sqrt{\frac{\pi T_0}{4 T_{\text{neutron}}}} + \frac{q}{\phi} \frac{P_1}{V_{\text{md}} \psi} (1 - p_c) \quad (5.7)$$

where it was assumed that the structural and coolant resonance occurred prior to those of the fuel materials. Initially $\frac{q}{\phi}$ is given by

$$\frac{q}{\phi} = \frac{\epsilon N_5 \sigma_{5,f} v_{5,f} V_{f1}}{1 - \epsilon P_1 (1-p) \eta} \quad (5.8)$$

$\sigma_{5,f}$ was calculated from W11 (analogous to σ_{Xe}) using the relationship,

$$\sigma_{5,f} = \sigma_{5,f}^0 g_{5,f} \sqrt{\frac{\pi T_0}{4 T_{\text{neutron}}}} \quad (5.9)$$

The initial resonance production term in Eq. (5.8) is given by,

$$(1-p)\eta = \frac{N_5 I_5^\infty \eta_5}{N_5 I_5 + \frac{N_8 I_8}{\psi_{1,8}}} \left(1 - p_8 e^{-C_1 N_5 I_5} \right) \quad (5.10)$$

This calculation gave $\frac{q}{\phi} = 0.288 \text{ cm}^{-1}$, resulting in a resonance contribution to Σ_{md} that was nearly as large as the thermal contribution (0.0244 for resonance versus 0.0298 for thermal).

σ_{FP}^0 was taken from Reference S3, with the assumption that: (1) 75% of the fissions were from U235, which burns out exponentially, (2) 25% of the fissions were from Pu239, which builds up exponentially, (3) the thermal flux was 10^{13} n/cm² sec, (4) the final flux-time was 1 n/kb, (5) that fission products with unknown cross sections have the same average cross section as the known low-cross-section group. σ_{FP} was then calculated from

$$\sigma_{\text{FP}} = \sigma_{\text{FP}}^0 \sqrt{\frac{\pi T_0}{4 T_{\text{neutron}}}} \quad (5.11)$$

B. NRX REACTOR AND THE GLEEP

1. Long Term Irradiations in the NRX Reactor

In general there is little experimental information for checking long term irradiation calculations, and the available information is difficult to interpret analytically due to the large number of variables present. In the case of the NRX reactor, however, a substantial experimental program in long-term changes in composition and reactivity has been carried out and significant results have been published.* These data have been used for comparison with the FUELCYC analytical calculations.

NRX is a natural-uranium-fueled, heavy-water-moderated, light-water-cooled, graphite-reflected, research reactor at Chalk River, Ontario, Canada. It produces 40 Mw of heat, while operating at a mean temperature of 38°C and at atmospheric pressure. There are 175 fuel rods, 3.45 cm. in diameter on a $6\frac{13}{16}$ in. triangular pitch. The active dimensions of the core are 8.75 ft. in diameter and 10.5 ft. in height. The principle core structural material is aluminum.**

Natural uranium has been irradiated in the NRX reactor to beyond 6000 MWD/ton. Chemical and isotopic analyses have been performed at Chalk River and at Argonne National Laboratory for samples of various degrees of irradiation, mostly taken from NRX rod No. 683, see Reference H20. Reactivity measurements were made for additional NRX samples. As explained in Reference C11, the "reactivity samples"

*The best summary of the results is given in Reference C11, and additional information is in H15, H20, H28, K11, L5, L23, and L24.

**See Reference H15 for further description of the NRX reactor.

were cut from standard NRX metal rods and were 15.2 cm in length, 3.45 cm in diameter, and were clad with aluminum tubing. Sixteen of these samples were placed in an aluminum tube to form an assembly geometrically similar to an NRX rod and were irradiated near the center of the NRX lattice. Following irradiation the reactivity of these samples was measured by the pile oscillator method in the GLEEP at A. E. R. E., Harwell, England.

The GLEEP is a natural-uranium and UO_2 -fueled, (U metal to a radius of 1.75 m, UO_2 in outer region), graphite-moderated and reflected, and air-cooled research reactor, which has been in operation since August, 1947. The fuel elements consist of U rods 0.9 in. in diameter or UO_2 pellets 1.62 in. in diameter and 2 in. in length. In both cases the cladding is aluminum and the fuel element is 12 in. in height (6 UO_2 pellets per fuel element). The active core dimensions are 5.72 meters in diameter and 5.2 meters in length with the fuel elements set in a $7\frac{1}{4}$ in. square lattice. The GLEEP produces a thermal neutron flux between $10^6 - 10^8$ n/cm² sec, C18.

For the FUELCYC analytical calculations to compare with these experimental results, design data was required for both the NRX reactor, to calculate composition changes with irradiation, and for the GLEEP, to calculate the reactivity of the irradiated samples in the GLEEP. The input data for NRX calculations will be considered in the next section, and the GLEEP calculational information in the section following that.

2. Calculation of FUELCYC Nuclear Input Data for the NRX Reactor.

The purpose of the NRX calculation is to compute the isotopic composition and cross sections of the fuel nuclides at different degrees of irradiation. These results can then be compared with the experimentally determined values and can also be used as a basis for the reactivity calculations (as measured in the GLEEP) described in the next section.

These experimental cross sections and compositions are for small samples and not reactor averages. For this reason, and because local values of these parameters are essentially only flux-time dependent, see Section IV. A. 3, the spatial computation parts of FUELCYC were not required (i. e., calculation of flux distribution, reactor criticality, etc.). Therefore, these parts of the code were bypassed for the NRX calculations (by octal correction cards) and the abridged input data as listed in Table 5.4 was used. The basic design data used to derive these input values are listed in Table 5.3 along with their source.

To facilitate the comparison with experimental data the Canadian system of normalization to the initial amount of fissile material has been adopted. In this system, cell average nuclide concentrations are divided by the initial concentration of U235 giving them units of "atoms per initial fissile atom," or aifa. If microscopic cross sections are in barns then macroscopic cross sections have the units of "barns per initial fissile atom" or bifa.

Table 5.3 Reference Design Data for NRX

Item	Value	Units	Reference
Volume ratio of moderator to fuel, V_{md}/V_{fl}	27	-	C11, p.18
Natural uranium fuel	-	-	C11, 1
Density of uranium fuel	18.9	g/cm^3	H28, p.16
Slowing down power for H_2O , D_2O mixture	0.195	cm^{-1}	K11, p.18
Moderator temperature	38	$^{\circ}C$	C11, p.30
Fast fission factor	1.036	-	C11, p.30
2200 m/s flux, $\phi_0 = nv_0$	2×10^{13}	$n/cm^2 \text{ sec}$	C11, p.30
Inverse of fast non-leakage probability, $(1 + B^2\tau)$	1.05	-	L5, p.6
Initial conversion ratio, icr	0.77	-	C11, p.20

Table 5.4 FUELCYC Nuclear Input Data for NRX*

Item	Values	Units
N_5^0	1.	aifa
N_8^0	139.06	aifa
$\xi\Sigma_s$	15400.	bifa
$(T_0/T_{md})^{1/2}$	0.971	-
$\psi_{1,8}$	21.5	-
C_1	6.49 E-5	$(bifa)^{-1}$
ϵ	1.036	-
P_1^0	.9542	-
Σ_{md}	0.	bifa
σ_{Xe}	2.39 E6	barns
σ_{FP}	51.6	barns
V_{fl} (pseudo value)	0.5	-
$\Sigma_{s, fl}$	1160. or .230	bifa

*In addition to this normal FUELCYC input data, C_5 was taken as 0.727.

For the volume fraction of fuel, V_{ff} , and moderator, $V_{md} = (1 - V_{ff})$, equal pseudo values of 0.5 have been used, because cross sections for fuel and moderator are on the same basis of one atom of initial fissile material.

The value of $(\xi\sigma_g)$ listed in Table 5.3 represents the average recommended by Kushneriuk, K11, for the proportions of H_2O and D_2O in the NRX reactor. The magnitude of Σ_{md} is not needed for the reactivity calculations of the next section assuming it is a constant since reactivity changes from that of the initial fuel are reported and as a result it drops out. It only appears in the calculations of the macroscopic cell absorption cross section for the thermal energy spectrum of the flux. Since the moderator is composed mainly of D_2O and aluminum, its cross section is very small compared to the fuel cross section, so was taken here as zero.

The spectrum parameter, Δ , was then calculated as in Section IV. A. 2. Its value was 0.256 which gave a neutron temperature of 348°K. σ_{Xe} and σ_{FP} were then calculated by the method explained in Section IV. A. 2.

The proper resonance escape probability, for U238 was calculated from the measured initial conversion ratio, and then $\psi_{1,8}$ (the required input data item) was calculated from it. *

*The value for p_8 of 0.91 listed in Reference C11 was not used since this accounts for only those resonance absorptions in excess of the $1/v$ contributions whereas FUELCYC uses the total resonance absorption. To clarify this, in the Westcott expression for the effective 2200 m/s cross section, $\sigma = \sigma_0 (g + rs)$, p_8 of 0.91 would account for the $\sigma_0 rs$ contribution. The total resonance contribution is equivalent to $(\sigma_0 n_e/n) (g + s/b)$, or $\sigma_0 (brg + rs)$, or approximately $\sigma_0 r(g+s)$ (since $b \sim 1$ for a

The expression for the initial conversion ratio is:

$$\text{icr} = \frac{N_8 \sigma_8 + \frac{q}{\phi} \left[P_1 \langle 1 - p_8 \rangle + \frac{a_8}{(1 + a_8)} \frac{(\epsilon - 1)}{\epsilon (n_8 - 1)} \right]}{N_5 \sigma_5 + \frac{q}{\phi} P_1 \langle 1 - p_5 \rangle} \quad (5.12)$$

where,

$$\frac{q}{\phi} = \frac{N_5 \sigma_5 f \nu_5}{1 - \epsilon P_1 \langle 1 - p_5 \rangle n_5} \quad (5.13)$$

$$\langle 1 - p_m \rangle = \frac{\ln p_m}{\ln p_5 + \ln p_8} (1 - p_5 p_8), \quad \text{for } m=5 \text{ or } 8 \quad (5.14)$$

If Eqs. (5.13) and (5.14) are substituted in Eq. (5.12), the only unknown is p_8 . The σ 's for Eqs. (5.12) and (5.13) were calculated as Maxwell-Boltzmann averages at T_{neutron} . The proper value of p_8 was determined by a trial and error solution of Eq. (5.12) to give $\text{icr} = 0.77$. The value obtained was $p_8 = 0.886$, which was then used to calculate the input disadvantage factor $\psi_{1,8}$.

For the NRX reactor an extra input parameter was required, namely $C_5 = \sigma_{\text{Xe}} \phi / (\sigma_{\text{Xe}} \phi + \lambda_{\text{Xe}})$, which is normally evaluated by FUELCYC as the core average. In this case a mean value of C_5 for the NRX samples was

D_2O lattice). The total Westcott cross section separated into the sum of thermal and resonance parts, then has the form: $\sigma = \sigma_0 \left[\left(\frac{n_{\text{th}}}{n} \right) g + \left(\frac{n_e}{n} \right) (g + s/b) \right]$ or $\sigma_0 \left[(1 - br)g + (brg + rs) \right]$.

desired. This was derived from the 2200 m/s flux given in Reference C11, $\phi_0 = 2 \times 10^{13}$ n/cm² sec. The relationship between the FUELCYC thermal flux, ϕ , and ϕ_0 is

$$\phi = \phi_0 \frac{n_{th}}{n} \frac{\bar{v}_{th}}{v_0} \quad (5.15)$$

The mean velocity of the thermal group is taken, as before, as the mean Maxwell-Boltzmann velocity at $T_{neutron}$ giving,

$$\frac{\bar{v}_{th}}{v_0} = \sqrt{\frac{4 T_{neutron}}{\pi T_0}} \quad (5.16)$$

The assumption of a 1/E epithermal flux (defined here as including all energies above the thermal cutoff) for a mean slowing down density of qP_1 gives the relationship for the ratio of epithermal to thermal neutron densities as,

$$\frac{n_e}{n_{th}} = 2 \sqrt{\frac{E_0}{E_1}} \frac{\bar{v}_{th}}{v_0} \frac{P_1}{\xi \Sigma_s} \frac{q}{\phi} \quad (5.17)$$

where E_1 represents the thermal cutoff energy, which was 0.45 ev in all cases. This calculation gave $n_e/n_{th} = 0.044$ initially, and the resulting value for ϕ of 2.35×10^{13} , from Eq. (5.15).

The calculated value for $\Sigma_{s,fl}$ was 1160 bifa. Runs were made using this value and also with a value of 230, which gave better agreement for the Pu240 disadvantage factor. This is discussed in Section VI.

3. Calculation of the Reactivity of the NRX Samples as Measured in the GLEEP.

The macroscopic neutron absorption cross sections of the NRX samples were determined by pile oscillator measurements in GLEEP calibrated by "standard boron". In this method the amplitude of the relative change in neutron density, due to the periodic insertion of the sample in the reactor, is taken to be proportional to the macroscopic absorption cross section of the sample. The proportionality constant is determined by oscillation tests with a boron sample, for which it is assumed that the macroscopic cross section is accurately known (from velocity-selector measurements). The cross section value so obtained is an apparent value, being the true cross section for $1/v$ absorbers, an effective or pile cross section for non- $1/v$ absorbers and the pile absorption cross section less the "neutron production" cross section for fissionable materials. This technique is described by Littler in Reference L23.

The apparent cross section of the unirradiated sample, $\Sigma_{app, s}^o$, is related to the equivalent cross section of the standard boron, $\Sigma_{app, B}$, by,

$$\Sigma_{app, s}^o = \frac{F_o \Sigma_{app, B}}{F} \quad (5.18)$$

where, *

* For convenience the nomenclature used by Craig et. al., C11, will be adopted for this section and for Section VI.B.2, which is in general different from that used in the rest of this text. Therefore, these symbols will be defined in this section only (and not in Appendix G on Nomenclature).

F_o = the average neutron flux in the boron sample (equivalent to the flux at the empty sample position).

F = the average neutron flux in the unirradiated sample

The experimental value reported for the GLEEP measurements is the change in the apparent cross section for the irradiated sample from that of the unirradiated sample, based on the flux, F , in the unirradiated sample. The negative of this value is the change in the production of excess neutrons. This term will be called R ,

$$R \equiv \frac{-F_o X}{F} \quad (5.19)$$

where

$$X \equiv \delta\Sigma_{app, B}$$

$$R \equiv \delta\Sigma_{app, s}$$

For the unirradiated NRX samples in GLEEP, F_o/F was experimentally found to have the value 2.13 which was used in equation (5.19) along with the measured value X for different samples to give the experimental values for R .

For the calculation of R from basic atomic compositions knowledge of the macroscopic cross sections of the sample, the flux in the sample, and (on a two group basis) the importance of a fast neutron at the sample position is required. This involves, of course, consideration of the neutron physics of the GLEEP as well as the properties of the sample. Craig et al., C11, have given a relationship for R based on a series of experimental measurements on various samples with known compositions. This expression for R , in units of bifa, is,

$$R = (1 + \frac{\Delta F}{F}) (0.878 \hat{\Sigma}_f \nu - \hat{\Sigma}) + 0.159 A \frac{\Delta F}{F} \quad (5.20)$$

A is the cross section of the unirradiated uranium, excluding resonance captures in U238 in excess of $1/\nu$ captures, and is given by,

$$A = \hat{\sigma}_5 + \frac{N_8}{N_5} \sigma_8^0 \quad (5.21)$$

Craig et al. also state that the relative change in flux is given by

$$\frac{\Delta F}{F} = \frac{1}{A} [-0.66 \hat{\Sigma} + 0.13 \hat{\Sigma}_f \nu + 0.04 \hat{\Sigma}_9 + 0.22 \hat{\Sigma}_{10}] \quad (5.22)$$

The symbols $\hat{\Sigma}$, $\hat{\Sigma}_f \nu$, $\hat{\Sigma}_9$, and $\hat{\Sigma}_{10}$ represent the change in the indicated cross section for the irradiated sample from the unirradiated sample, for 2200 m/sec neutrons. There are macroscopic cross sections with units of bifa.

The flux change for different NRX samples is so small that negligible error is introduced in Eq. (5.20) by considering the term $(1 + \frac{\Delta F}{F})$ to be constant. A value of 0.97 is representative for the samples considered and permits the rewriting of Eq. (5.20) as follows.

$$R = 0.872 \hat{\Sigma}_f \nu - 1.075 \hat{\Sigma} + 0.006 \hat{\Sigma}_9 + 0.035 \hat{\Sigma}_{10} \quad (5.23)$$

Therefore R can be calculated from Eq. (5.23) for the NRX samples if the macroscopic cross sections for the samples are known. The nuclide compositions for a sample of a specified irradiation were given by the NRX calculation and the macroscopic cross sections must be calculated for the GLEEP spectrum. This calculation is discussed in Section VI. B.

C. THE SIMPLER MODEL

Additional calculations were made for the 3.44 a/o U235, pressurized light-water reactor for Batch and Graded fuel scheduling by a simpler method than that employed in FUELCYC. The result of these calculations as compared to those of FUELCYC are discussed in Section VI.C. in light of the differences in the theoretical models.

The "simpler" method used was that described by Pigford et al. in Reference P3. This model assumes that the energy and spatial distribution of the flux is constant and employs effective thermal absorption cross sections for all nuclides except for U238, for which a resonance capture term is provided. Spatial non-uniformity of flux is considered by perturbation methods, taking the statistical weight at any point as the square of the thermal flux. Nuclide concentrations and the "excess reactivity cross section" are fitted versus flux-time and the fit coefficients are weighted by appropriate factors (generated using chopped-cos and chopped- J_0 flux distributions in the perturbation calculation) to convert central properties to reactor average properties for the fuel scheduling method specified. This latter method is explained, and additional details on the general calculation procedure are given, in Reference P3.

The initial effective thermal cross sections were calculated by Westcott's method, W11, at a neutron temperature of 908°K, except for Pu240 for which the effective average cross section in the FUELCYC calculation was used, and for U236 for which only a rough approximation to the effective cross section was made since this nuclide has essentially

no effect on the reactivity. The same cross section was used for the low cross-section fission products as in FUELCYC.

The resonance escape probability for U238 was then chosen to give the same initial conversion ratio as in the FUELCYC calculation. The value specified for the concentration of U235 to make the reactor just critical, N_5^* , was chosen to give the same initial criticality factor as for the corresponding FUELCYC calculation, using the FUELCYC fast fission factor and fast non-leakage probability. This N_5^* factor accounts for the consumption terms which are assumed constant in the "simplified" model: namely, the thermal absorptions in U238, those of the moderator and structural materials, the xenon and Samarium group absorptions, and the thermal leakage. Finally, appropriate averages of nuclide concentrations and reactivity were taken over the core of the reactor with its assumed flux distribution by the procedure described in Reference P3. The calculation was performed on an I. B. M. 704 computer and the nuclear parameters that were used are listed in Table 5.5.

Table 5.5 Nuclear Parameters for the Simpler Model

Nuclide	Initial Conc. (a/b cm)	Effective values for,		
		α	η	σ_a (b)
U235	8.785E-4	0.253	1.97	515.
U236				100.
N_{FP}				31.9
U238	2.465E-2	0.0687*	2.44*	1.365†
Pu239		0.600	1.81	1690.
Pu240				1870.
Pu241		0.3765	2.225	1590.
Pu242				570.
Neutron temperature, °K				908.
Westcott r factor				0.34
Just critical concentration of U235, a/b cm				7.15E-4
Resonance escape probability for U238				0.758
Fast fission factor				1.0584
Fast non-leakage probability				0.9654

* Fast fission value.

† Thermal contributions only.

VI. DISCUSSION OF RESULTS

A. PRESSURIZED-LIGHT WATER REACTOR

Results are presented for the study of different methods of fuel scheduling along with variations in the initial U235 enrichment in the pressurized light-water reactor. Results are presented first for those material properties which are only functions of initial enrichment and flux-time; next, for the material properties that depend on the fuel-scheduling method, and finally, for the fuel-cycle cost results.

1. Material Properties of the Fuel Depending on Initial Enrichment and Flux-Time.

The variation in the energy distribution of the thermal flux in the fuel during its life history is shown in Fig. 6.1, for an initial enrichment of 3.44 a/o U235 (which will be henceforth referred to as the reference-design enrichment). The property that is plotted is the flux per unit velocity times velocity, which was chosen since on this basis a $1/E$ flux per unit energy appears as a horizontal line. The final curve is for a flux-time of 2.2 n/kb which would be attained in Inout fuel scheduling. Besides the hardening effect there is a pronounced flux depression in the vicinity of 0.29 ev (or approximately at velocity step 19) for the final curve, which is due primarily to the build-up of Pu239 with its large absorption resonance at this energy. For comparison, a Maxwell-Boltzmann distribution is shown at the moderator temperature and a $1/E$ flux per unit energy is shown as the epithermal flux which appears as a horizontal line in the units of Fig. 6.1 (velocity times the flux per unit velocity).

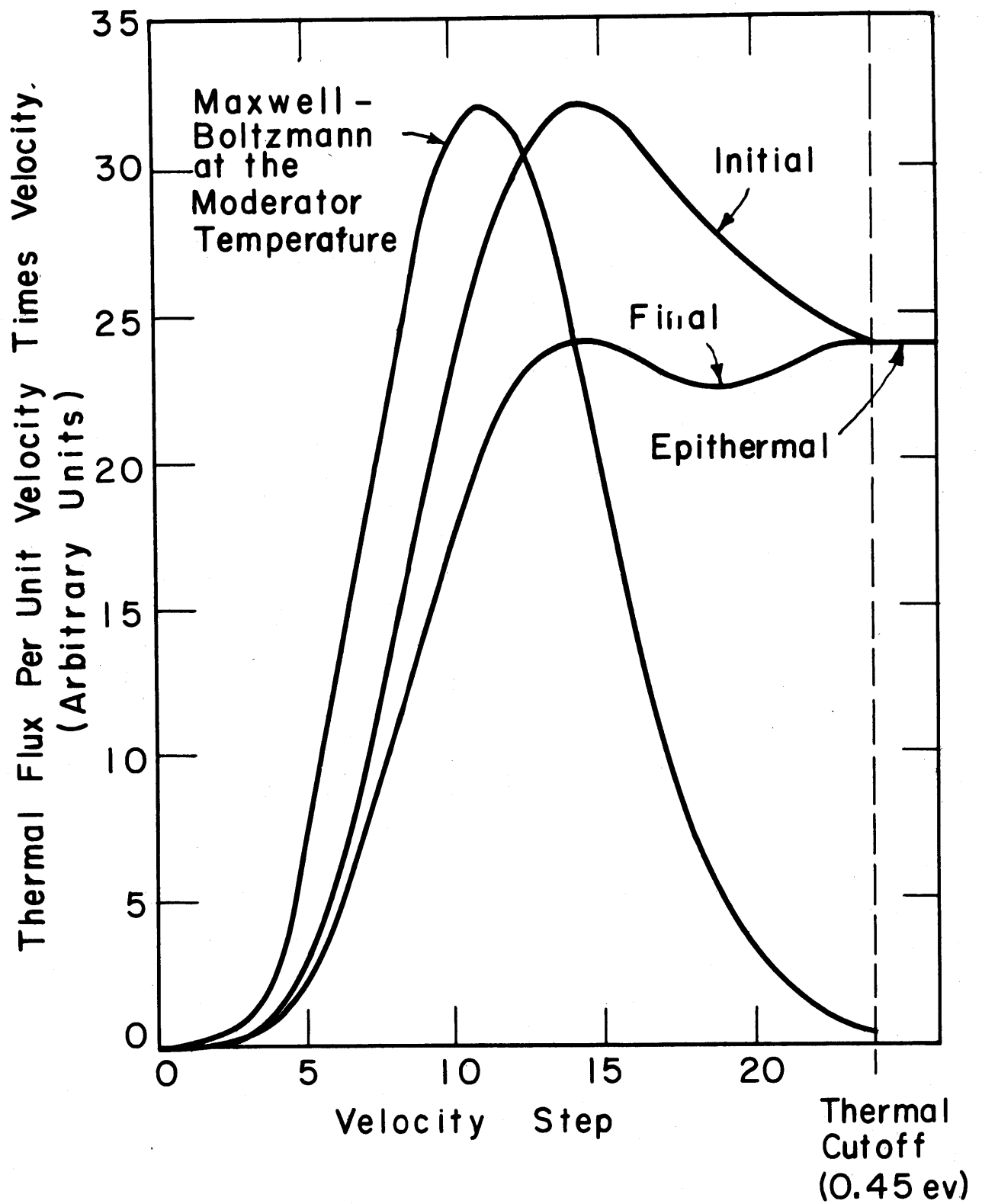


FIG. 6.1 THERMAL FLUX SPECTRUM AS A FUNCTION OF VELOCITY, INITIAL ENRICHMENT OF 3.44 a/o U235.

The effect of these changes on the calculation of the average thermal absorption cross sections is shown in Fig. 6.2 for the reference-design case. The initial values are calculated with an equilibrium amount of xenon and Samarium group poisoning. The maximum change for any of the cross sections for this case was approximately 2%. This may at first seem to be an insignificant variation, but is actually quite significant in the prediction of reactivity changes for low flux-times as will be shown in Section VI.B.2. In particular, the ratio of cross sections of Pu239 to U235 is important, and this varies by as much as 4% for the typical case shown in Fig. 6.2. A major factor in the behavior of the curves of Fig. 6.2 is the progressive increase in the gross absorption cross section with flux-time for the left hand side of the graph followed by a progressive decrease for the right hand side, which tends to harden or soften the spectrum, respectively. The asymmetry of the curves, about the vertical line through the maximum and minimum points or as compared to the $1/v$ behavior of the U238 curve, is due to the progressive flattening of the spectrum which tends to raise the Pu239 and Pu240 cross sections as flux-time progresses, and to the deepening of the 0.29 ev flux dip with increased flux-time which dominates in the case of Pu241 and continues to drive its cross section downward. (Were the base neutron temperature lower, the Pu240 curve would fall below the Pu241 curve.) Fission cross sections are not shown in Fig. 6.2 but the relative changes in these values fall within 0.002 of the absorption cross sections. The fission cross sections are listed in Table 6.1, for the reference-design reactor.

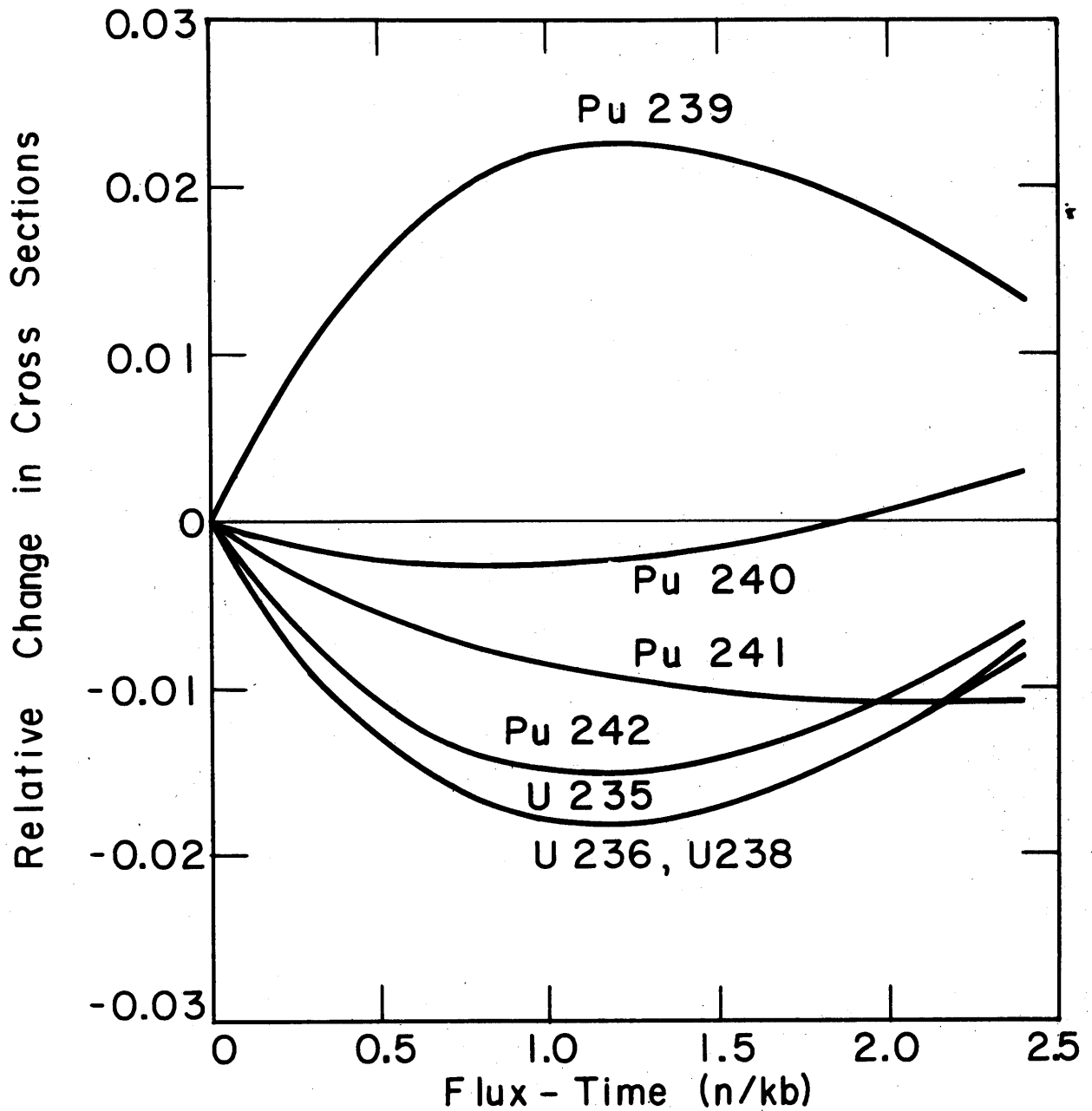


FIG. 6.2 RELATIVE CHANGE IN THE AVERAGE THERMAL MICROSCOPIC ABSORPTION CROSS SECTIONS FOR FUEL NUCLIDES, INITIAL ENRICHMENT OF 3.44 a/o U235

These results show that at any specified time the correct thermal cross sections depend on the relative amounts of the different fuel nuclides present, and, therefore, that the concept of a single effective neutron temperature for a Maxwell Boltzmann distribution is not applicable. The effective neutron temperature can, of course, be specified for a $1/v$ absorber in a particular combination of fuel nuclides. The temperature is derived from the U238 cross section from,

$$T_{\text{neutron}} = \frac{\pi}{4} \left(\frac{\sigma_8^0}{\sigma_8} \right)^2 T_0 \quad (6.1)$$

where $\sigma_8^0 = 2.71$ barns and $T_0 = 293.6^\circ\text{K}$. For the pressurized water reactor where $T_{\text{mod}}/T_0 = 1.82$, the ratio of neutron temperature to moderator temperature is given by,

$$\frac{T_{\text{neutron}}}{T_{\text{mod}}} = \frac{3.17}{\sigma_8^2} \quad (6.2)$$

From Table 6.1 for the initial fuel of the reference-design enrichment σ_8 is seen to be 1.342 barns which gives $T_{\text{neutron}}/T_{\text{mod}} = 1.75$ ($T_{\text{neutron}} = 935^\circ\text{K}$). The value of Δ at a particular velocity can be calculated as $4x$ times the values of the inverse moderating ratio ($A_i = \Sigma_i/\xi\Sigma_s$) which are tabulated for five different velocities in Table 6.1. The value for x is given by $0.129 i$ where i is the step number, so $\Delta = 0.516iA_i$. The value of Δ varies so greatly over the spectrum after Pu239 builds up that it is impossible to relate T_{neutron} (for $1/v$ absorbers) to this quantity as has been done by Cohen, C6, and others for $1/v$ absorbers. For example, for the reference design reactor Δ varies from 1.6 to 6.5

Table 6.1 Local Properties of Fuel Dependent on Initial Enrichment and Flux-Time

Initial Enrichment: 3.441 a/o U235

Runs No. 1

Property	Flux-Time (n/kb)					
	0	0*	0.6	1.2	1.8	2.4
Cross Sections (b)						
$\sigma_{5,f}$	261.1	257.9	253.9	253.0	254.0	255.9
$\sigma_{9,f}$	901.2	911.2	925.6	929.7	927.9	922.7
$\sigma_{11,f}$	839.9	840.3	834.8	832.2	831.2	831.2
σ_5	313.2	309.4	304.7	303.7	304.8	307.1
σ_6	3.467	3.427	3.376	3.365	3.376	3.399
σ_8	1.342	1.327	1.307	1.303	1.307	1.316
σ_9	1461.	1480.	1507.	1514.	1510.	1500.
σ_{10}	188.5	187.6	187.2	187.2	187.6	188.2
σ_{11}	1156.	1157.	1149.	1146.	1144.	1144.
σ_{12}	15.69	15.54	15.34	15.30	15.35	15.44
Atoms/b cm (of fuel)						
N_5	8.785 E-4	8.785 E-4	6.613 E-4	4.937 E-4	3.686 E-4	2.765 E-4
N_6	0	0	4.258 E-5	7.326 E-5	9.366 E-5	1.064 E-4
N_{FP}	0	0	2.294 E-4	4.713 E-4	7.056 E-4	9.222 E-4
N_8	2.465 E-2	2.465 E-2	2.448 E-2	2.430 E-2	2.411 E-2	2.394 E-2
N_9	0	0	9.486 E-5	1.340 E-4	1.464 E-4	1.464 E-4

*With equilibrium Xenon and "Samarium Group" poison.

Table 6.1 (Cont.)

Property	Flux-Time (n/kb)					
	0	0*	0.6	1.2	1.8	2.4
N_{10}	0	0	1.245 E-5	2.874 E-5	4.176 E-5	5.124 E-5
N_{11}	0	0	6.609 E-6	2.297 E-5	3.713 E-5	4.590 E-5
N_{12}	0	0	4.738 E-7	3.714 E-6	9.773 E-6	1.707 E-5
Space Properties						
$\Sigma_{Xe, max}$, cm^{-1} (fuel)	0	0.02244	0.02433	0.02379	0.02211	0.01995
$(\Sigma_{fl} - \Sigma_{Xe})$, cm^{-1} (fuel)	0.3082	0.3108	0.4030	0.4414	0.4485	0.4381
$\Sigma_f V_{fl}$, cm^{-1}	0.07799	0.07702	0.08890	0.09131	0.08851	0.08298
$v\Sigma_f V_{fl}$, cm^{-1}	0.1926	0.1902	0.2335	0.2476	0.2447	0.2324
$(1-p)/(1+\alpha)$	0.1175	0.1175	0.1063	0.09542	0.08520	0.07571
$(1-p)\eta$	0.2902	0.2902	0.2700	0.2487	0.2269	0.2051
p	0.6013	0.6013	0.5769	0.5594	0.5534	0.5527
Inverse Mod. Ratio, $\frac{\Sigma}{\xi\Sigma_S}$						
Velocity Step,** 4	0.8327	0.8817	0.8636	0.8320	0.7946	0.7556
9	0.3371	0.3589	0.3659	0.3621	0.3521	0.3390
14	0.2033	0.2173	0.2521	0.2667	0.2689	0.2640
19	0.1887	0.1990	0.4843	0.6113	0.6552	0.6556
24	0.1010	0.1092	0.1298	0.1374	0.1382	0.1357

*With equilibrium Xenon and "Samarium Group" poison.

**The step number is proportional to velocity where step 24 corresponds to an energy of 0.45 ev.

at a flux-time of 2.4 n/kb.

Fig. 6.3 illustrates the variation in the concentration of the fuel nuclides with flux-time, and Fig. 6.4 shows the variation in the "space properties" with flux-time. The buildup of Pu239 causes an initial increase in the thermal fission, Σ_f , and thermal production, $\Sigma_f \nu$, cross sections; however, the burnout of U235 dominates in the resonance region and causes a decrease in the corresponding resonance terms, $(1-p)/(1+a)$ and $(1-p)\eta$.

These flux-time-dependent properties, cross sections, nuclide concentrations, "space properties", and inverse moderating ratios, are listed in Table 6.1 for the reference design case. The same flux-time-dependent properties are tabulated in Appendix F for the six other enrichments studied, which varied from 2.876 to 6.452 a/o U235.

2. Material Properties of the Fuel for Different Fuel Scheduling Methods.

In this section various properties of interest are presented and discussed in comparison between the different fuel scheduling methods which were described in Section IV:C.2.

Fig. 6.5 shows the variation with enrichment of the average burnup which is one of the most important variables in fuel cycle calculations. For any given enrichment the average burnup increases going from Batch to Outin, to Graded, to Inout Fuel Scheduling. The greatest increase is found in the step from Batch to Outin, which is the first of the three steady-state methods of fuel movement. This behavior is as would be expected and is due to the increased efficiency of neutron utilization as

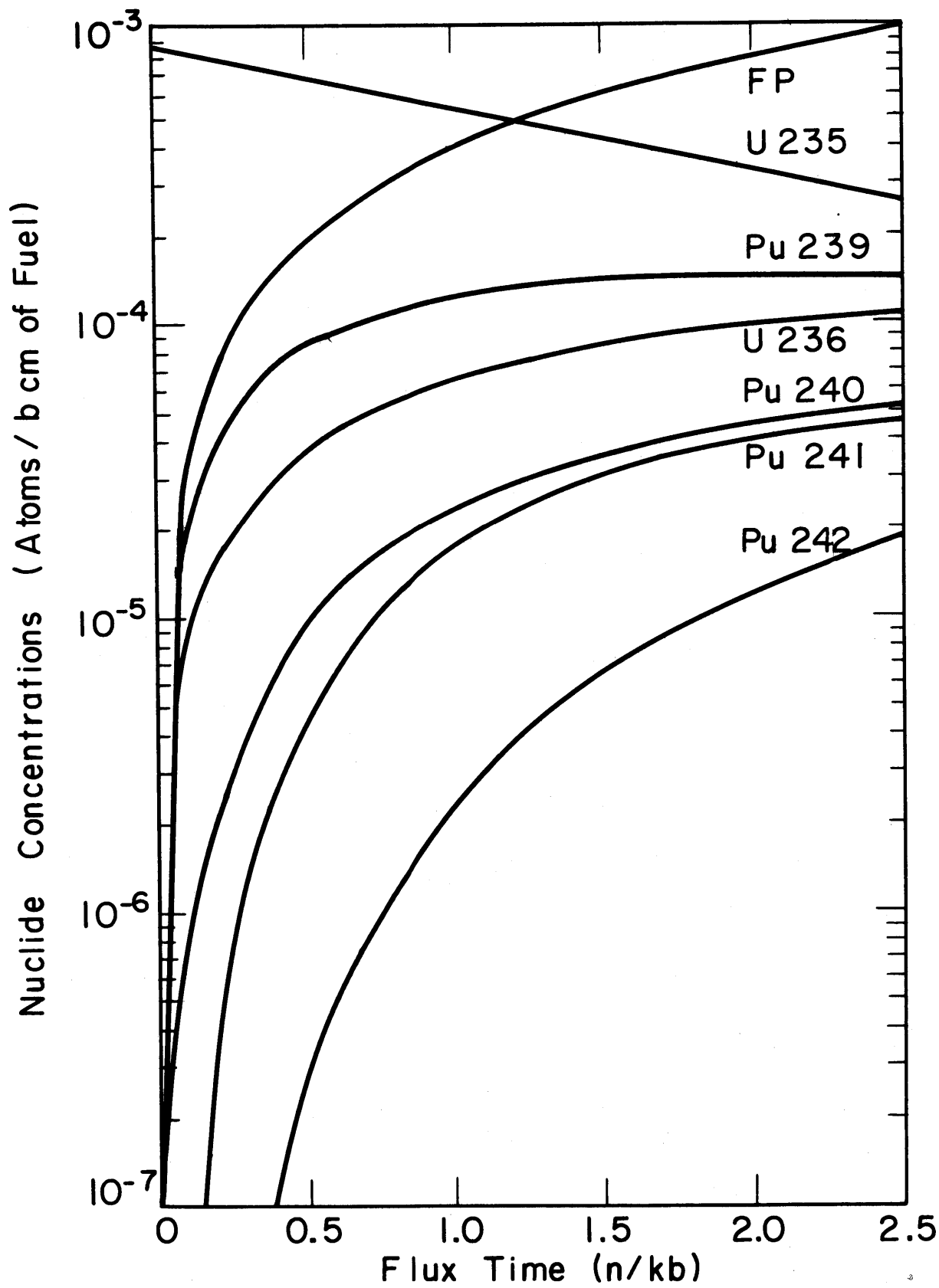


FIG. 6.3 CHANGES IN FUEL COMPOSITIONS WITH FLUX-TIME, INITIAL ENRICHMENT OF 3.44 a/o U235 (INITIAL CONCENTRATION OF U238 WAS 0.02465 a/b cm)

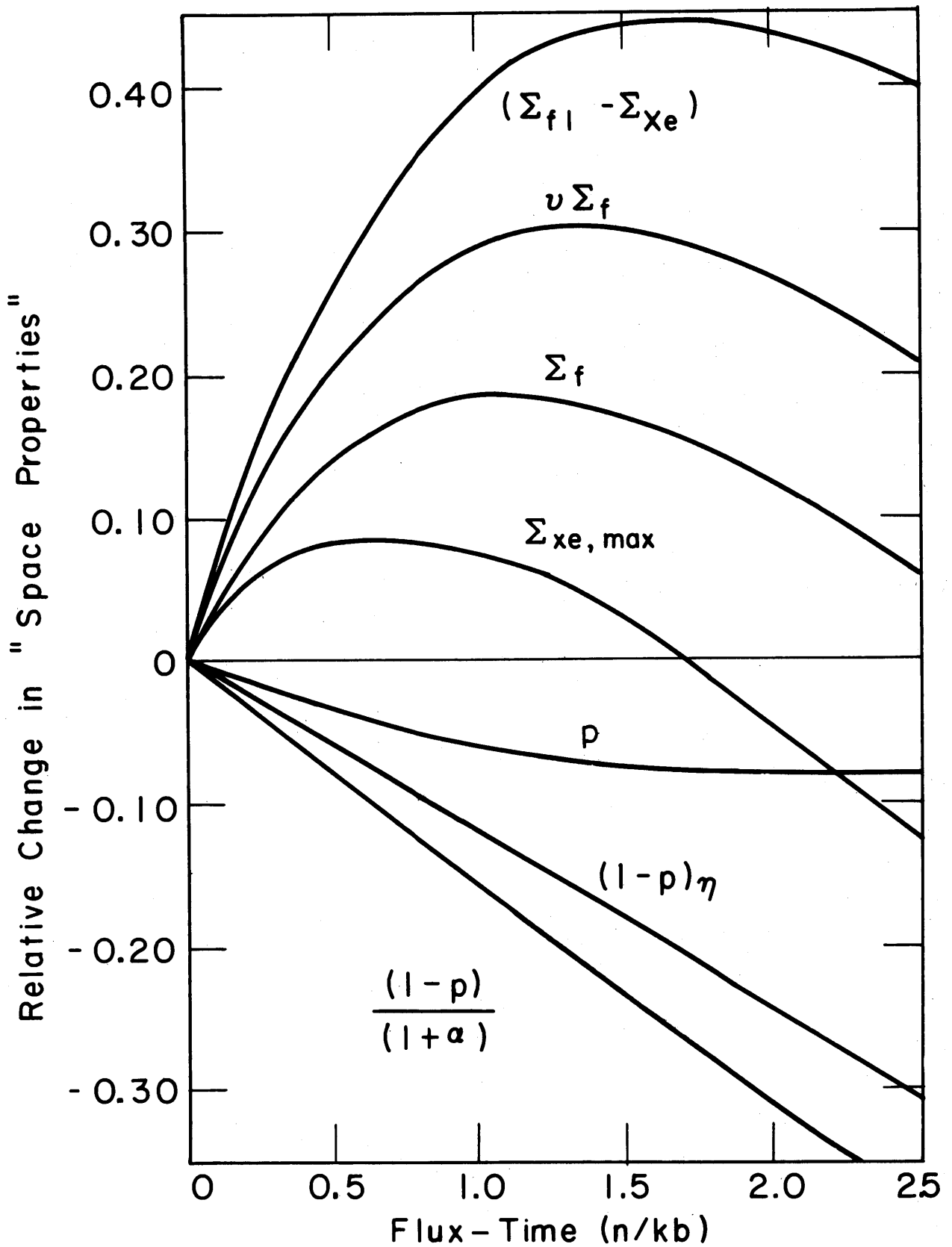


FIG. 6.4 RELATIVE CHANGE IN "SPACE PROPERTIES" WITH FLUX-TIME; INITIAL ENRICHMENT OF 3.44 a/o U235.

one moves from left to right in the fuel scheduling methods of Fig. 6.5.

An additional benefit of the steady-state methods of fuel movement is illustrated by Fig. 6.6, which shows the relation between maximum local burnup and average burnup. This Figure shows that if radiation damage limited the burnup which could be accepted in any local spot in the fuel, then the average burnup attainable would be considerably higher for the steady-state methods of fuel scheduling than for Batch, which, of course, means that more power can be obtained from a given charge of fuel in the steady-state methods. This desirable trend is being carried even further by Dr. W. B. Lewis's group at Chalk River, L19, who propose to move short fuel slugs steadily through the reactor in such a manner that the maximum and average burnup would be essentially the same. It is interesting to note from Fig. 6.6 that the maximum versus average burnup curve is substantially the same for all the steady state fuel methods. This results from the fact that the axial spatial flux-distribution is essentially identical for these cases.

Fig. 6.7 is presented for convenience in determining the "on-stream" time that the reactor would operate if run at a constant thermal power of 480 MW until the specified average burnup had been obtained. It is merely the graphical plot of the linear relationship obtained by combining Eqs. (4.79) and (4.80).

Inout fuel scheduling achieved the highest average burnup for a given enrichment only at the expense of an extremely disadvantageous power density distribution as is illustrated by Fig. 6.8. This figure shows the ratio of peak to average power density, as a function of flux-time.

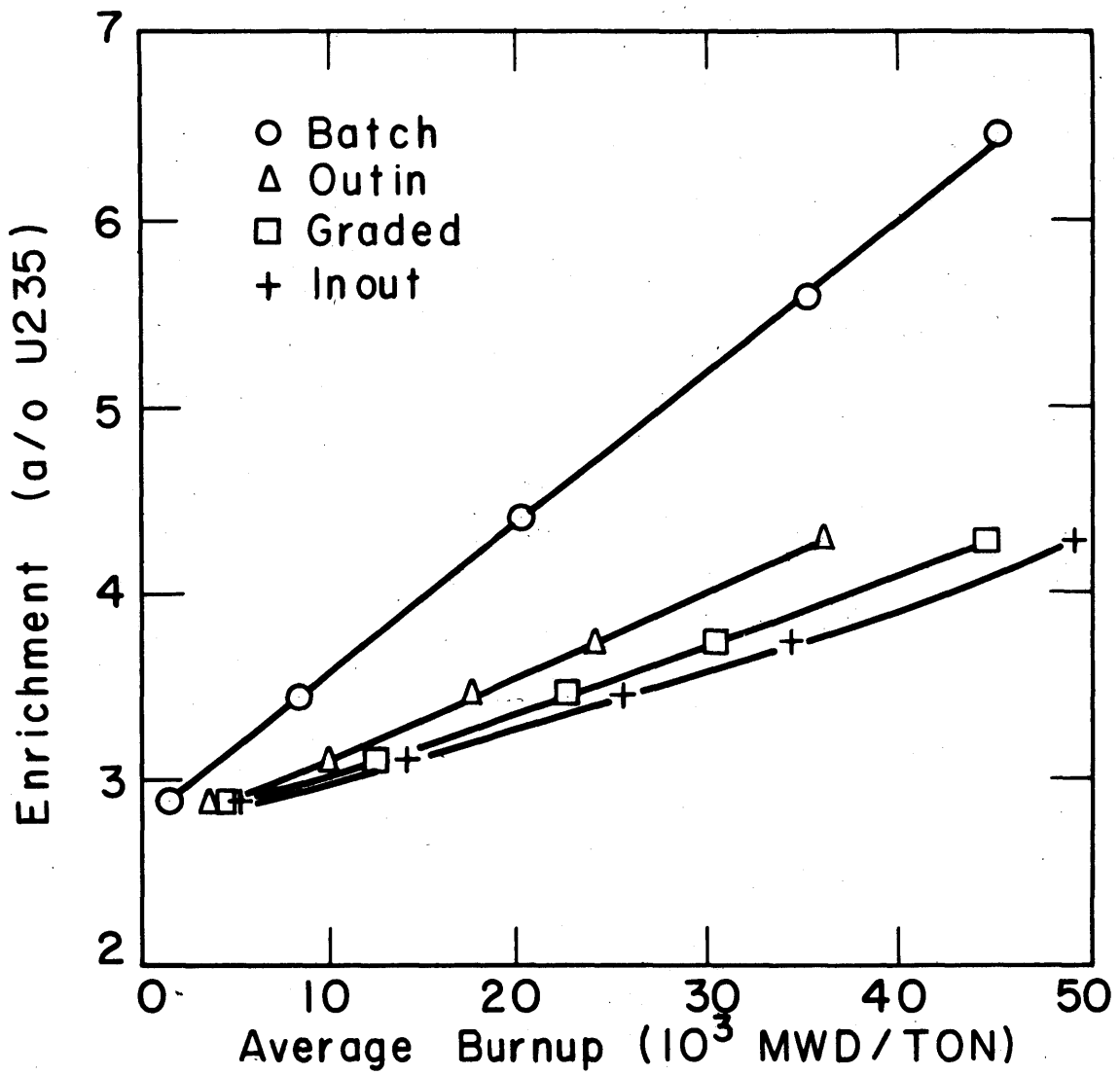


FIG. 6.5 INITIAL ENRICHMENT AS A FUNCTION OF AVERAGE BURNUP

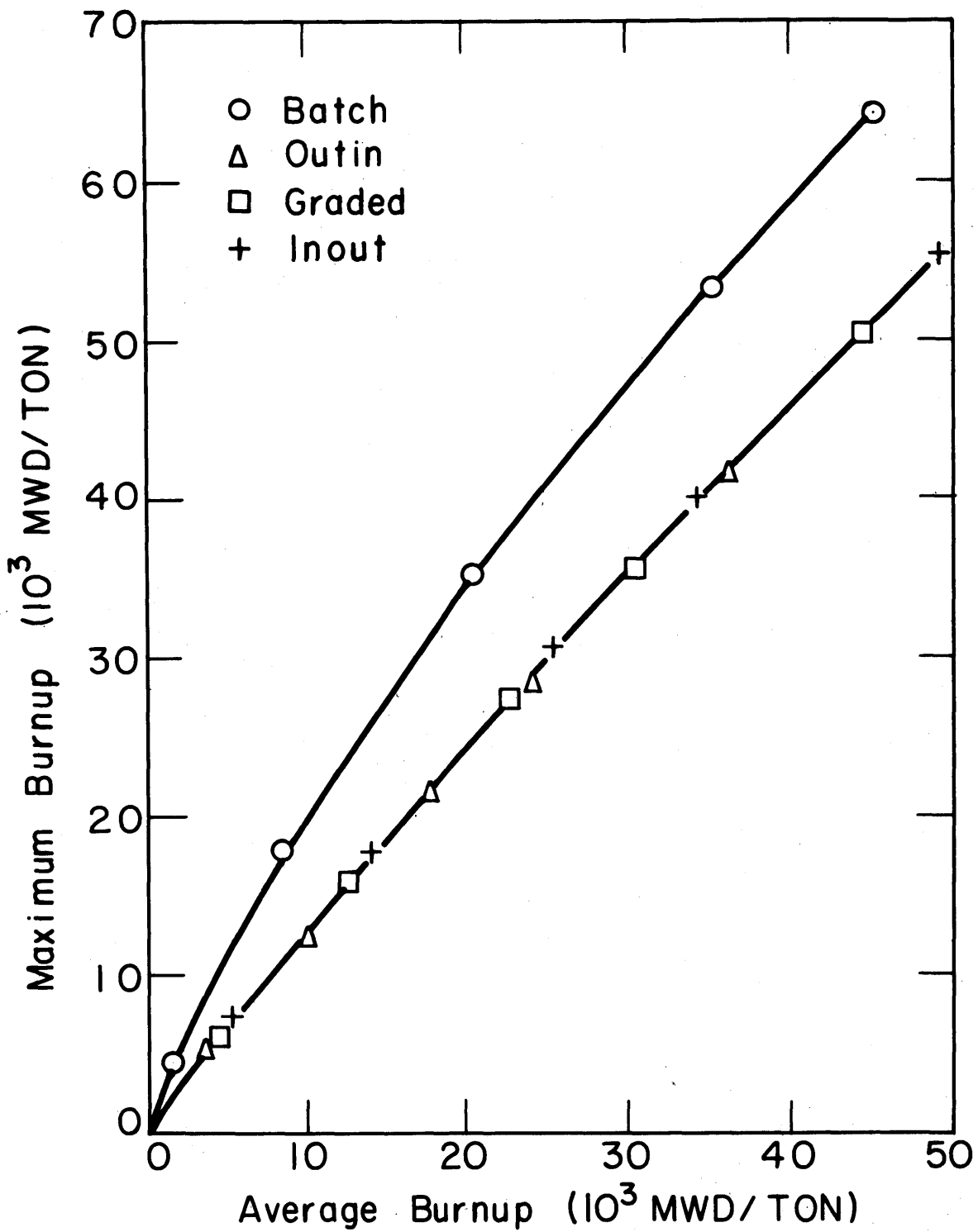


FIG. 6.6 MAXIMUM BURNUP AS A FUNCTION OF AVERAGE BURNUP

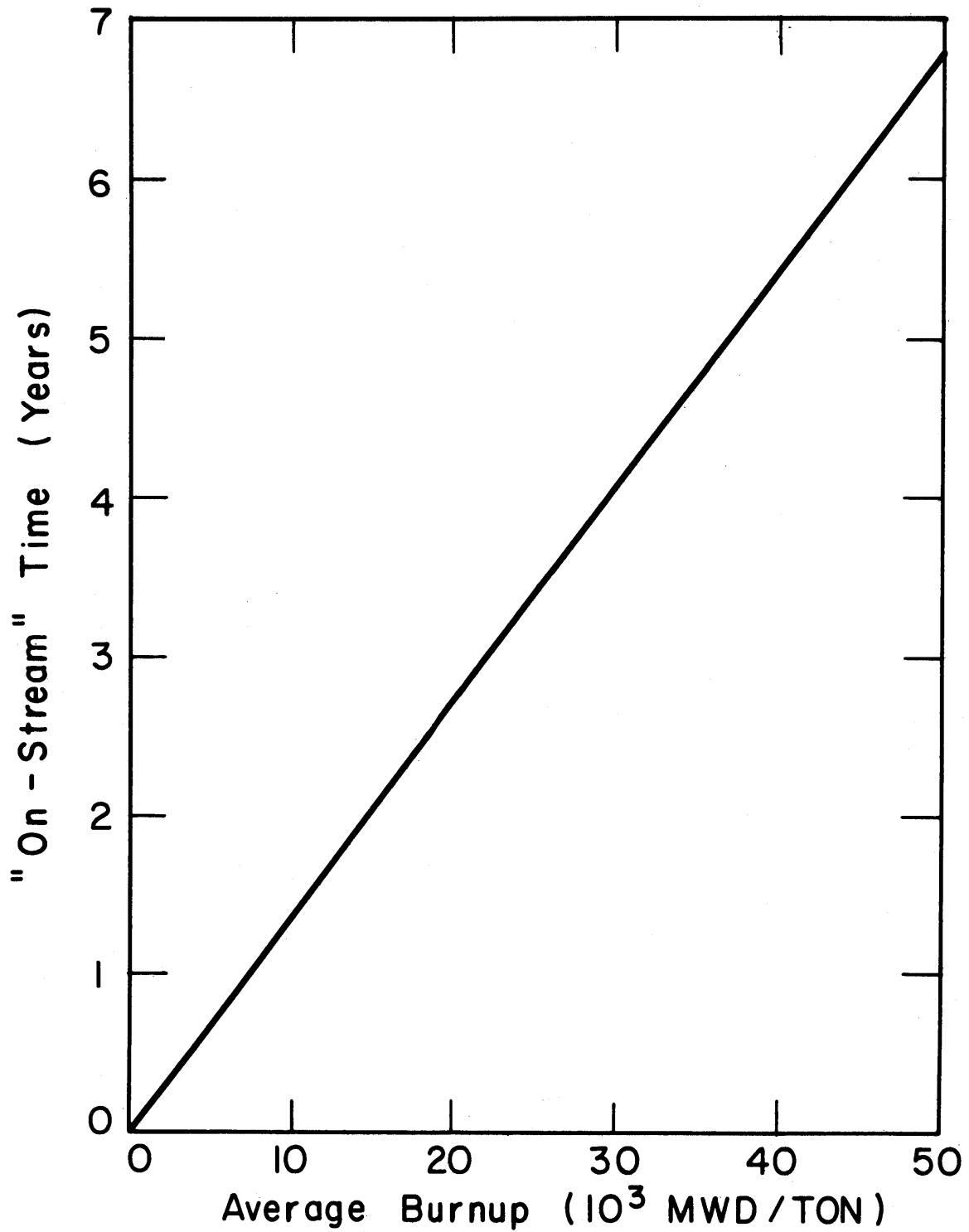


FIG. 6.7 VARIATION OF "ON-STREAM" TIME THAT THE FUEL SPENDS IN THE REACTOR WITH AVERAGE BURNUP

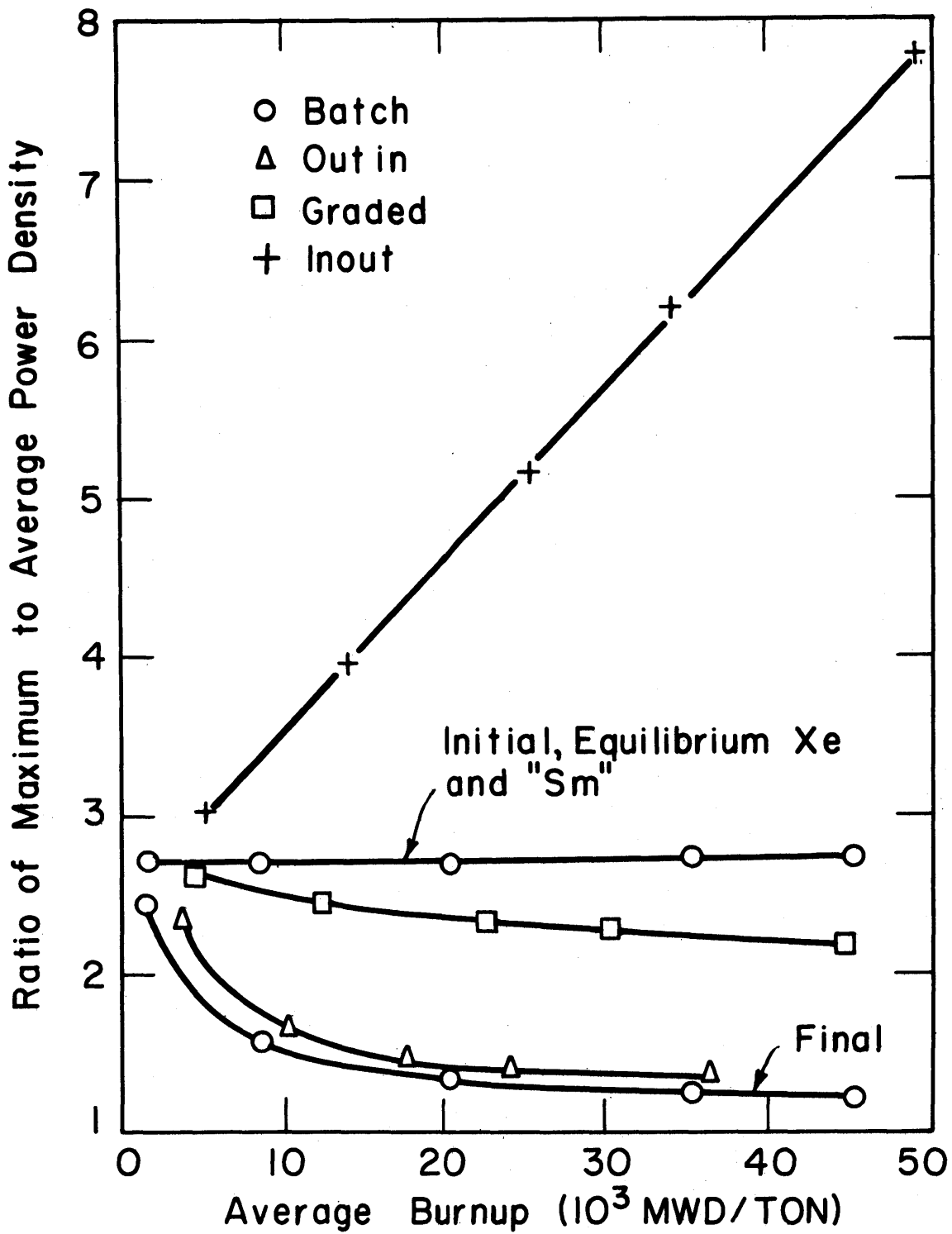


FIG. 6.8 VARIATION OF MAXIMUM TO AVERAGE POWER DENSITY RATIO WITH AVERAGE BURNUP.

The power-density distribution associated with Inout fuel movement probably would not permit operation of the reactor at rated power, owing to heat-transfer and control difficulties. The ratio of peak-to-average power density in the graded case is only slightly lower than that of the initial ratio in the Batch case but is considerably more favorable than that of the Batch case, since the Graded distribution is time-invariant whereas that of Batch varies during the fuel lifetime, as shown in Fig. 6.9. It is seen that the Outin method of fuel scheduling has a very favorable power-density ratio.

Fig. 6.10 is presented to indicate the variation in the average value of the fast non-leakage probability as compared to that of the initial uniformly-loaded reactor with equilibrium xenon and Samarium poisoning. The latter value was used as the non-leakage probability estimate in the solution of the nuclide concentration equations versus flux-time. The greatest deviation is seen to occur for Outin fuel scheduling but the resulting error in the average burnup is small even here, being over-estimated by an amount varying from zero at low burnups to less than two percent at high values. *

The initial criticality factor for Batch irradiation increases linearly with average burnup as shown in Fig. 6.11. This linearity is due in part to the "amplification term", $C_2 = 1/[1-\epsilon(1-p)\eta]$, in the

*This was checked using a slightly reduced value of C_1 , in Outin Run 5.3 so as to give the correct average resonance absorption rate in U238.

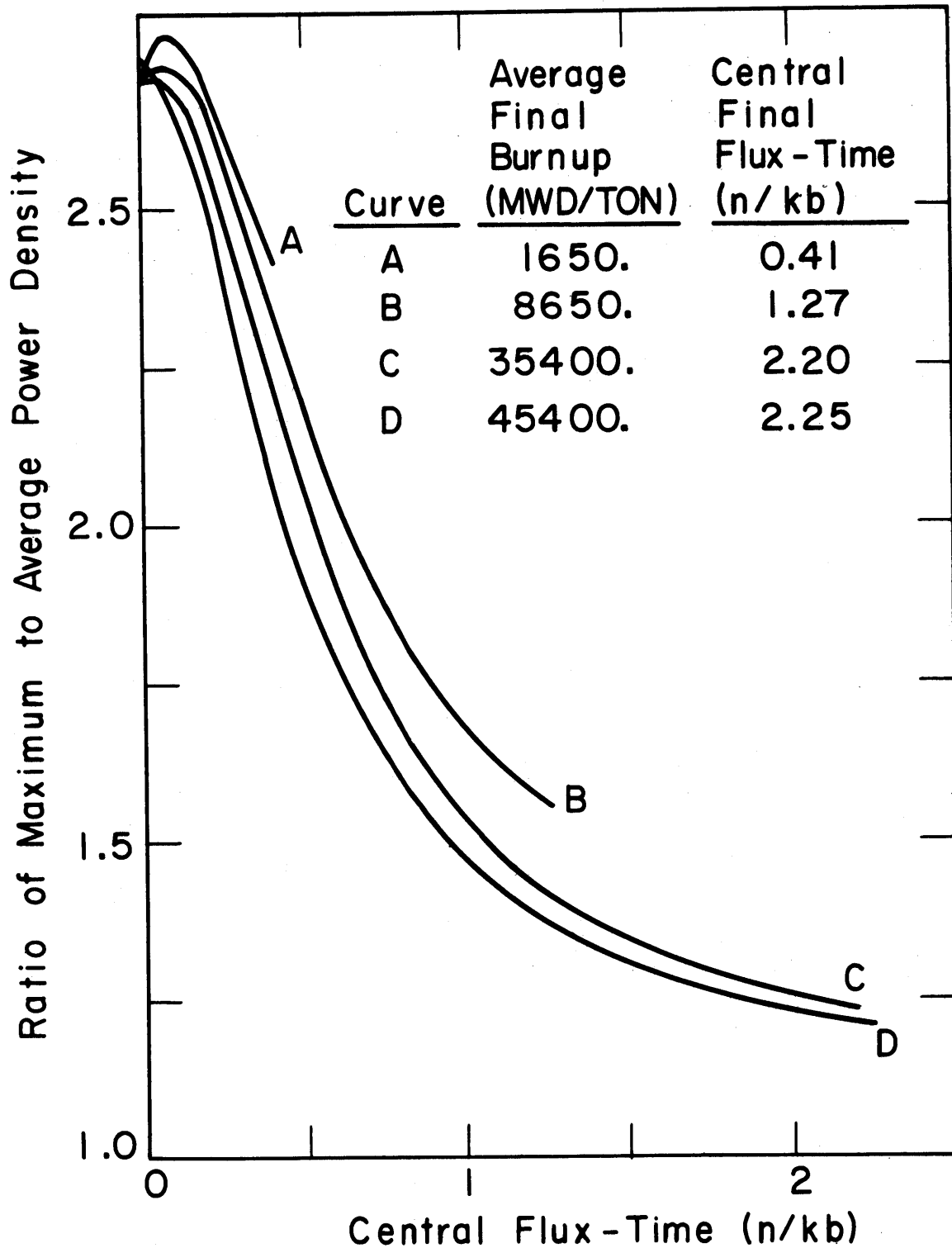


FIG. 6.9 VARIATION OF THE MAXIMUM TO AVERAGE POWER DENSITY RATIO DURING A BATCH IRRADIATION

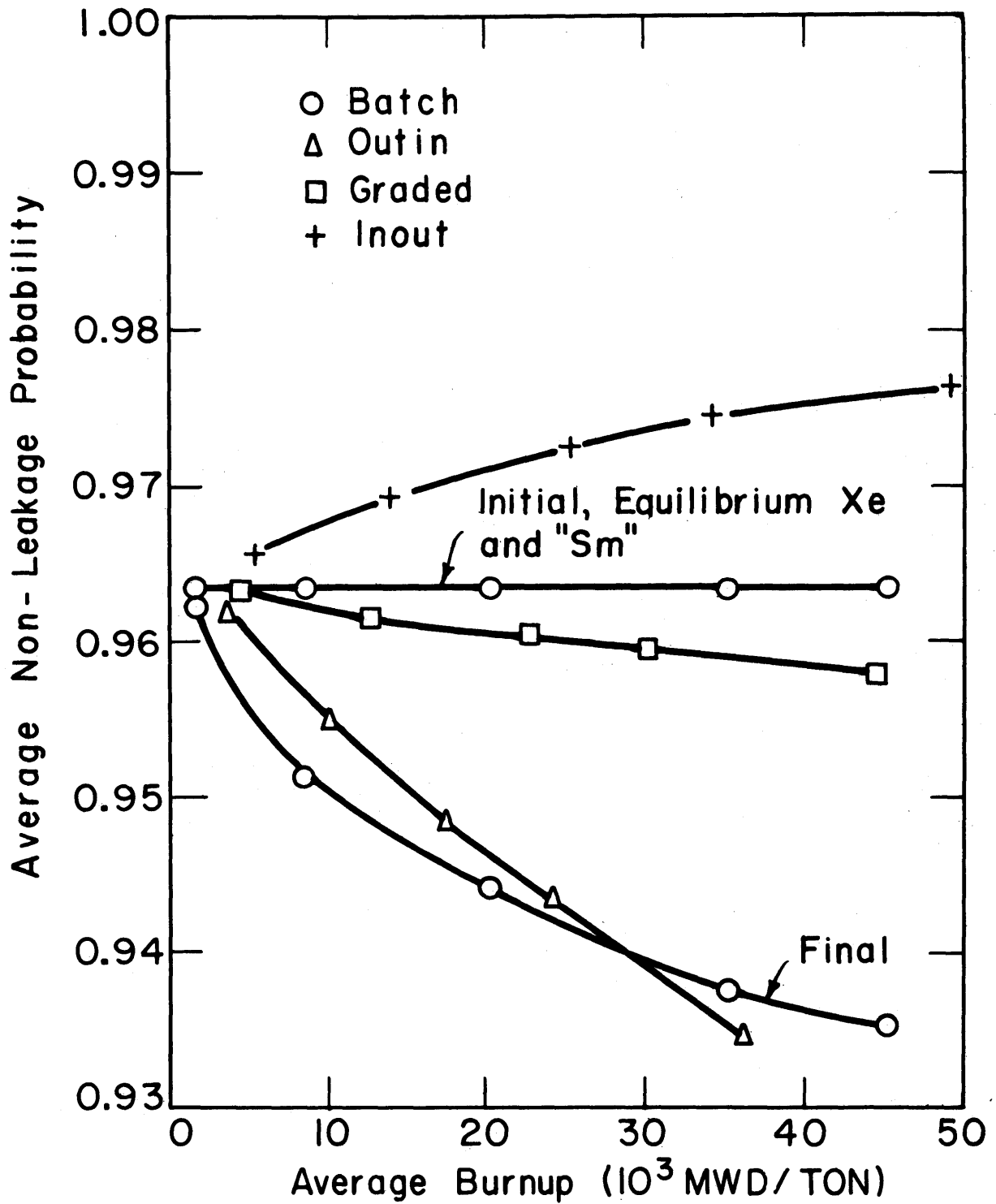


FIG. 6.10 VARIATION OF THE AVERAGE NON-LEAKAGE PROBABILITY FOR THE FAST GROUP WITH AVERAGE BURNUP

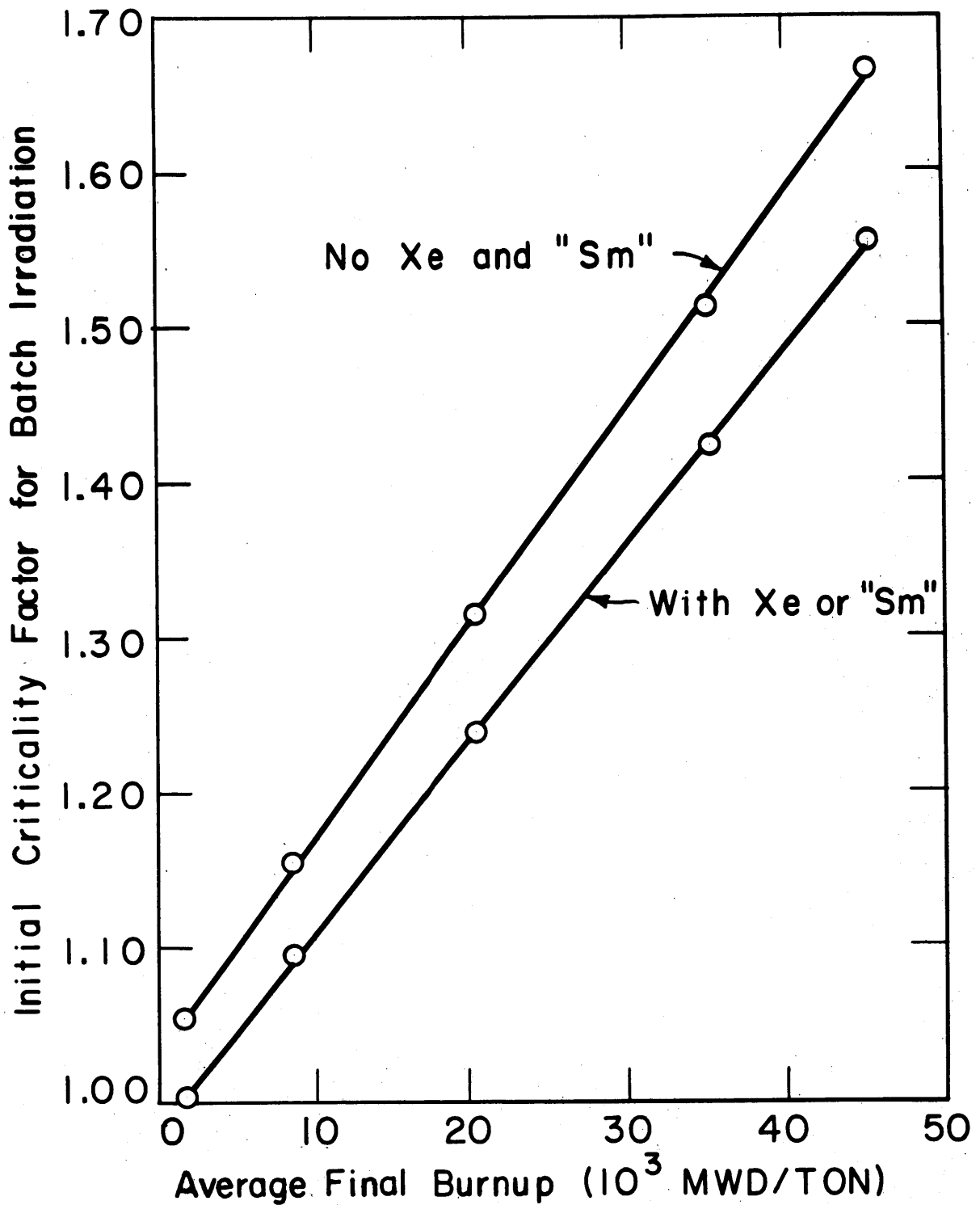


FIG. 6.II INITIAL CRITICALITY FACTOR WITH AND WITHOUT EQUILIBRIUM XENON AND "SAMARIUM GROUP" POISONING FOR BATCH IRRADIATION.

criticality equation (see Eq. 4.30) which results when resonance fissions are considered. The variation of the criticality factor during a Batch irradiation is indicated in Fig. 6.12, for different initial enrichments.

Fig. 6.13, gives the final central flux-time plotted as a function of the initial concentrations of U235.

The remaining illustrations, Figs. 6.14 to 6.20, show the variation in the thermal flux and in the local power density throughout the core for the different fuel-scheduling methods. The lines plotted are from Runs: No. 9.1, for Batch; No. 1.2, for Inout; No. 6.3, for Outin; and No. 1.4, for Graded. These runs were chosen to give final burnups that were approximately the same. The burnup value of approximately 23,000 MWD/TON was taken because this is large enough to give fuel cycle costs near the minimum values (see Fig. 6.21) and yet is attainable for UO_2 fuel without excessive radiation damage.

Fig. 6.14 shows the magnitude of the thermal flux (for a total thermal power output of 480 Mw), proceeding radially outward from the core axis along a plane perpendicular to the axis at the core center. The flux curves of this figure clearly explain the maximum to average power density behavior, as plotted in Fig. 6.8. The Inout fueling has the effect of compacting the effective critical part of the core into a tight region along the axis while the outer core regions are being used only as a sort of reflector. The Graded radial flux distribution is the same as that of the initial distribution in Batch irradiation since in both cases the fuel composition is uniform radially (except for the Xe-135 concentration).

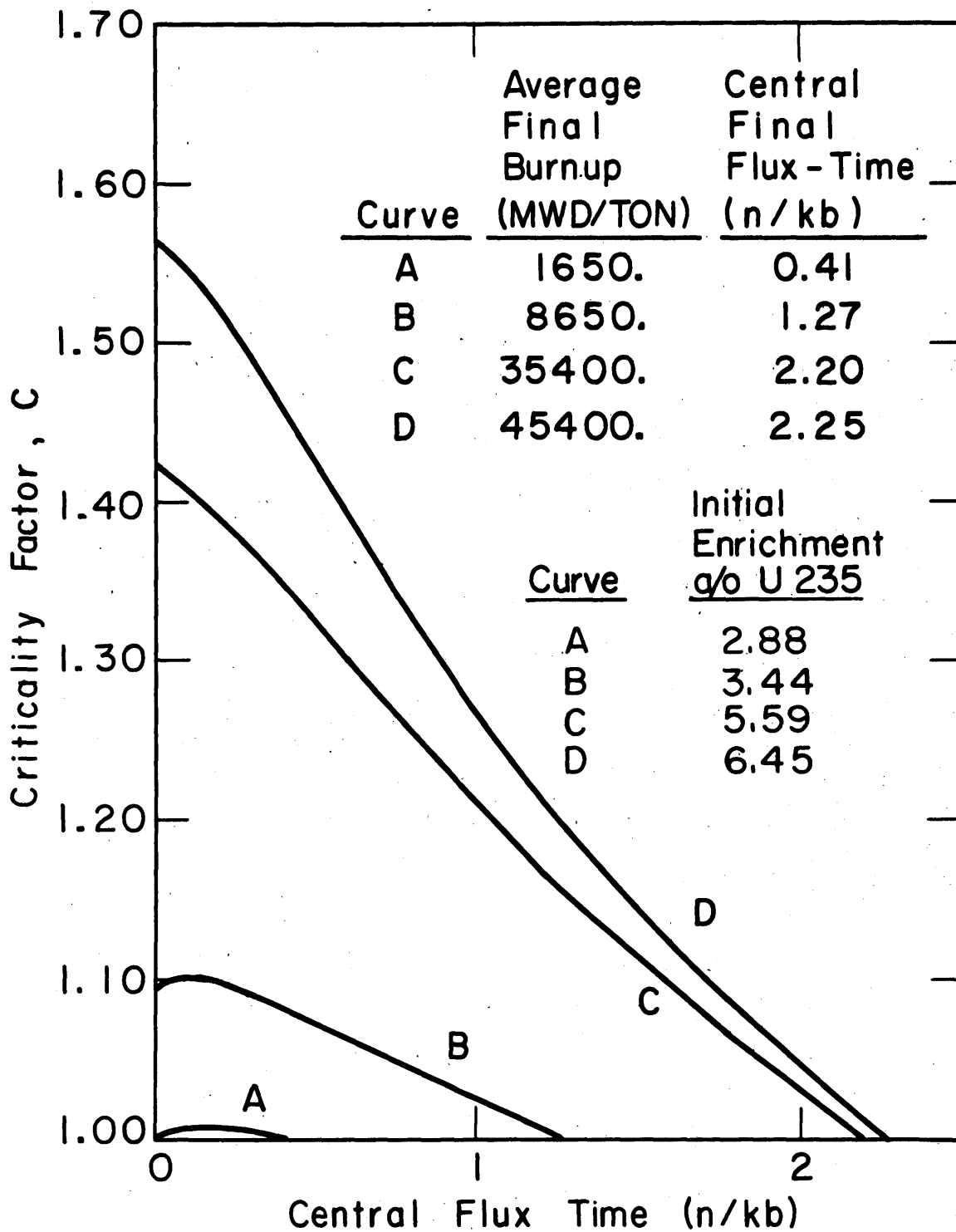


FIG. 6.12 VARIATION OF THE CRITICALITY FACTOR DURING A BATCH IRRADIATION

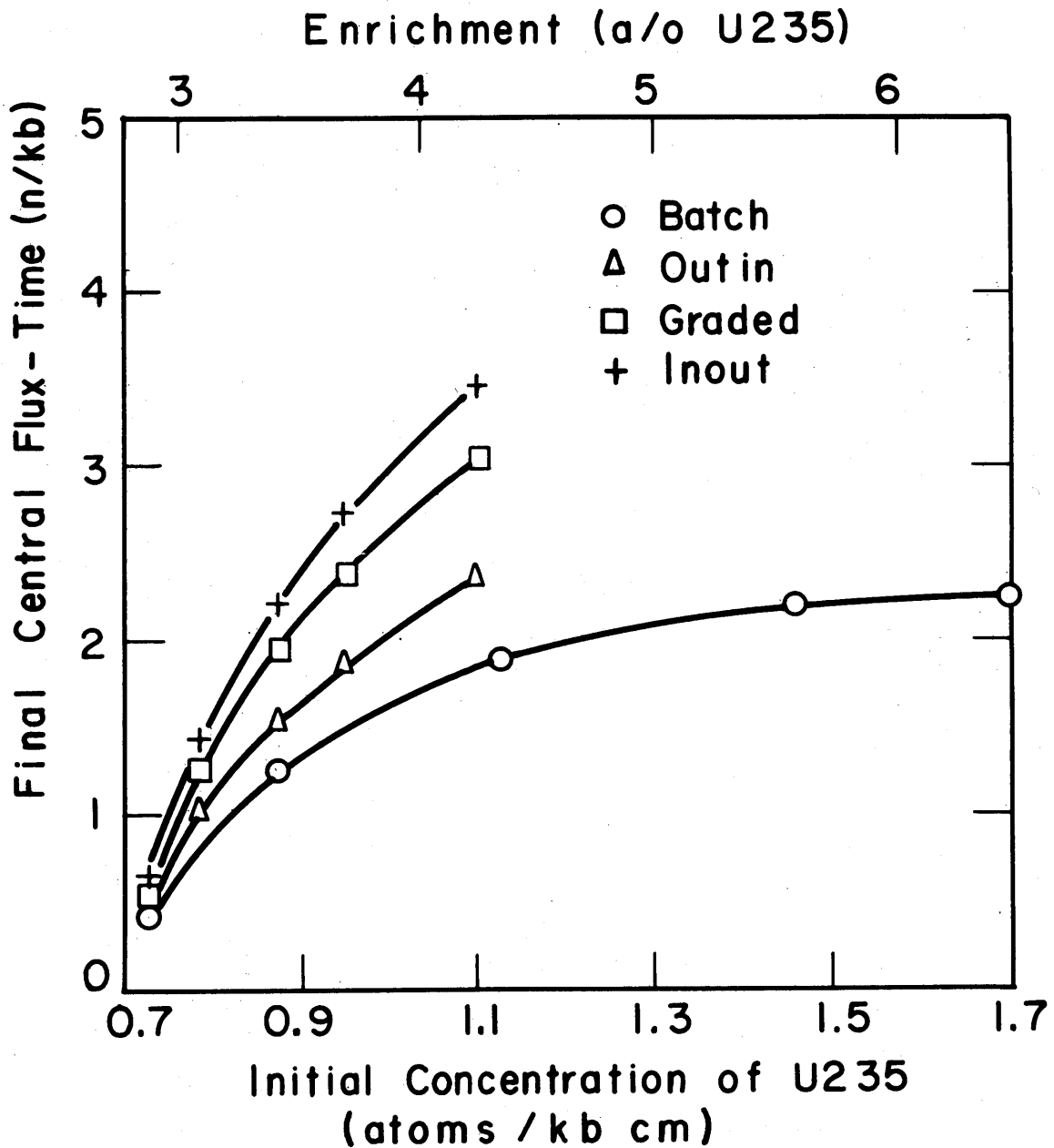


FIG. 6.13 VARIATION OF THE FINAL FLUX-TIME AT THE CENTER OF THE DISCHARGED FUEL WITH THE INITIAL CONCENTRATION OF U235 ($N_8 = 0.02465$ atoms / b cm)

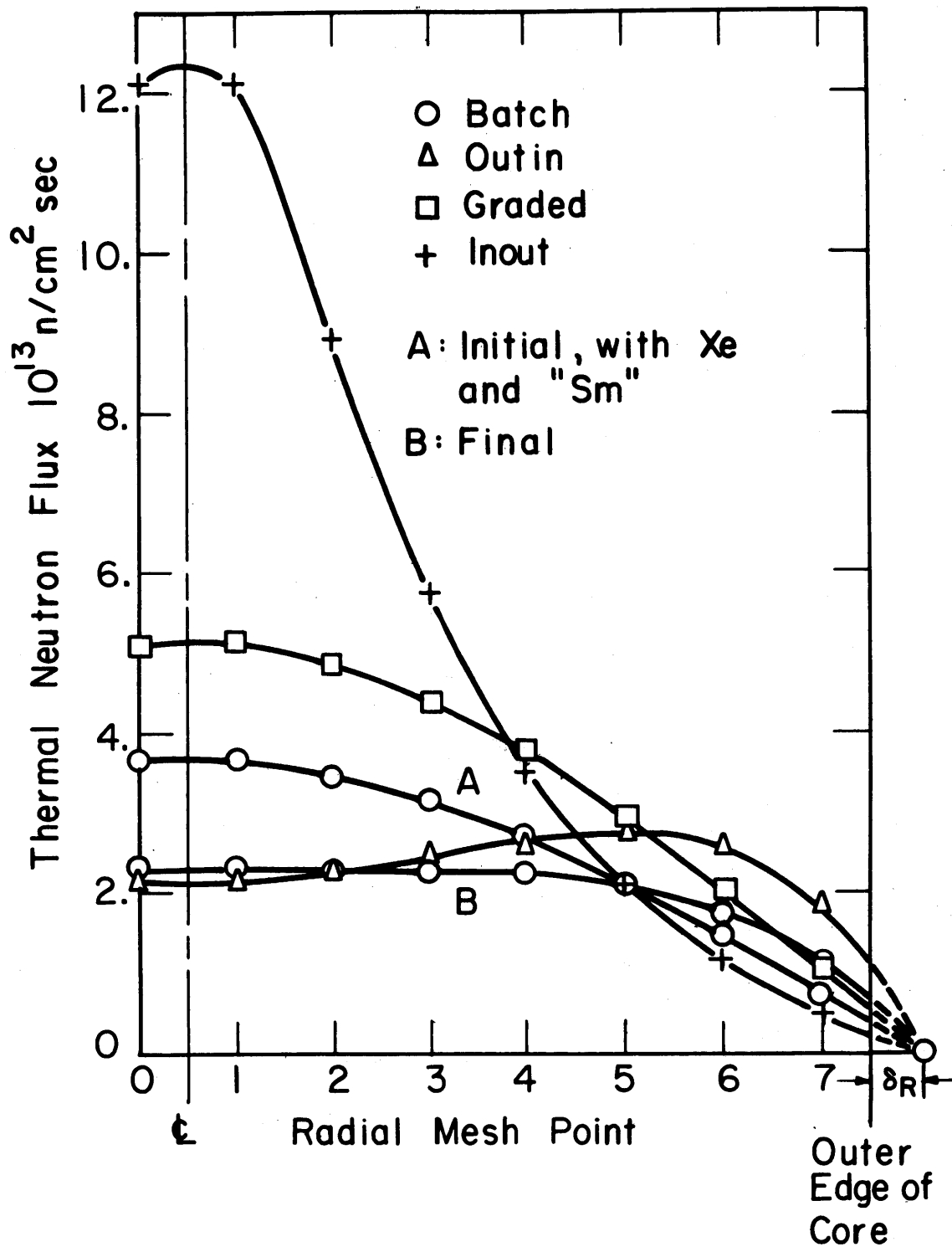


FIG. 6.14 THERMAL NEUTRON FLUX AS A FUNCTION OF RADIUS AT THE AXIAL CENTER PLANE OF THE CORE, AVERAGE BURNUP OF APX. 23,000 MWD/TON.

In the Graded case the uniformity is the result of averaging the properties of a local group of fuel rod sections which individually have different compositions; the average, however, is kept the same on the central plane by appropriately varying the recharging rate for the different local rod groupings. The average concentration of fissionable nuclides is lower in the Graded case than in Batch irradiation so the flux magnitude must be higher than that of Batch to achieve the same power output. Both the final Batch flux distribution and the steady-state Outin distribution are considerably flattened over the other methods and in both cases the flux shape is grossly different from that of the uniformly loaded, chopped- J_0 distribution.

Fig. 6.15 shows the relative thermal flux magnitude along an axial cut in the vicinity of the most exposed fuel element at the time of discharge. Since the fuel was not shuffled in the axial direction there is less variation among the curves of this plot than among those of Fig. 6.14. The axial flux distribution is identical in the vicinity of the discharged fuel for Inout and Outin fuel scheduling. During its life-time this radially-shuffled fuel is exposed to axial flux-shapes that progressively change from that of Curve A to that of the discharge curve for Inout and Outin. The average is approximately the same as that for the Graded curve in Fig. 6.15 and therefore gives essentially the same ratio of maximum to average burnup for these three cases, as was shown in Fig. 6.6.

The complete picture of the flux-distribution and, what is more important, the power density distribution is presented in Figs. 6.16 to 6.20. These are two-dimensioned (r, z) plots of the relative magnitudes of

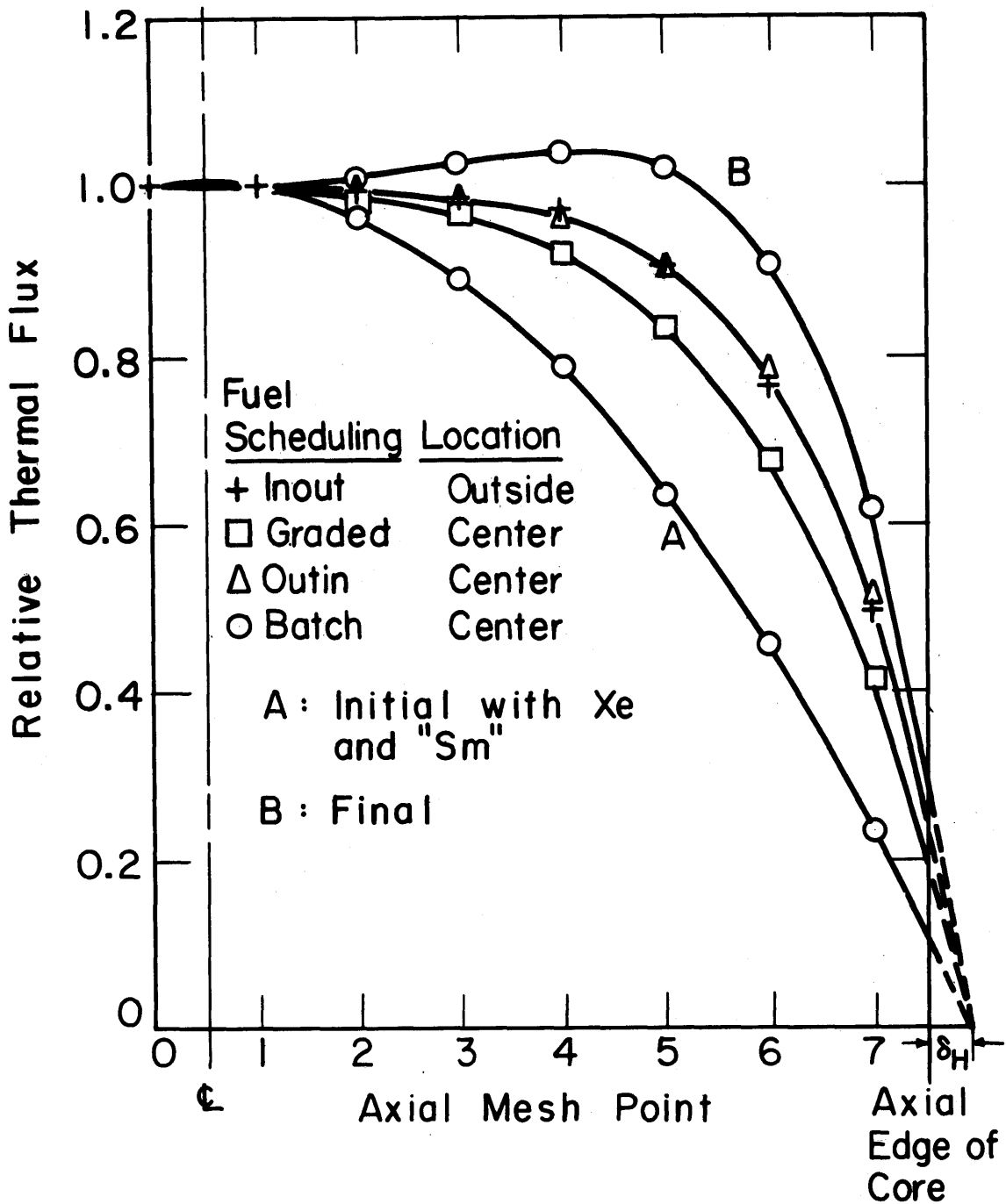


FIG.6.15 RATIO OF THERMAL NEUTRON FLUX IN FUEL TO FLUX AT MIDPLANE OF REACTOR, AVERAGE FINAL BURNUP OF APX. 23,000 MWD/TON

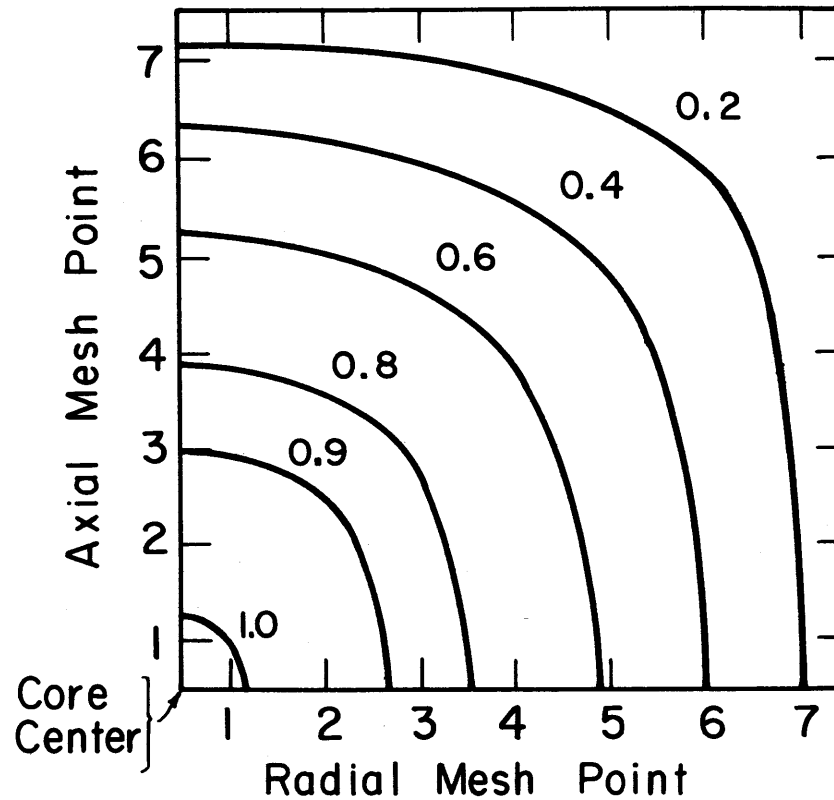


FIG. 6.16 TWO-DIMENSIONAL CONTOUR PLOT OF THE INITIAL SPATIAL DISTRIBUTION OF THE RELATIVE THERMAL FLUX OR THE POWER DENSITY FOR BATCH IRRADIATION, WITH EQUILIBRIUM Xe AND Sm (ONE QUADRANT OF THE CORE IS SHOWN)

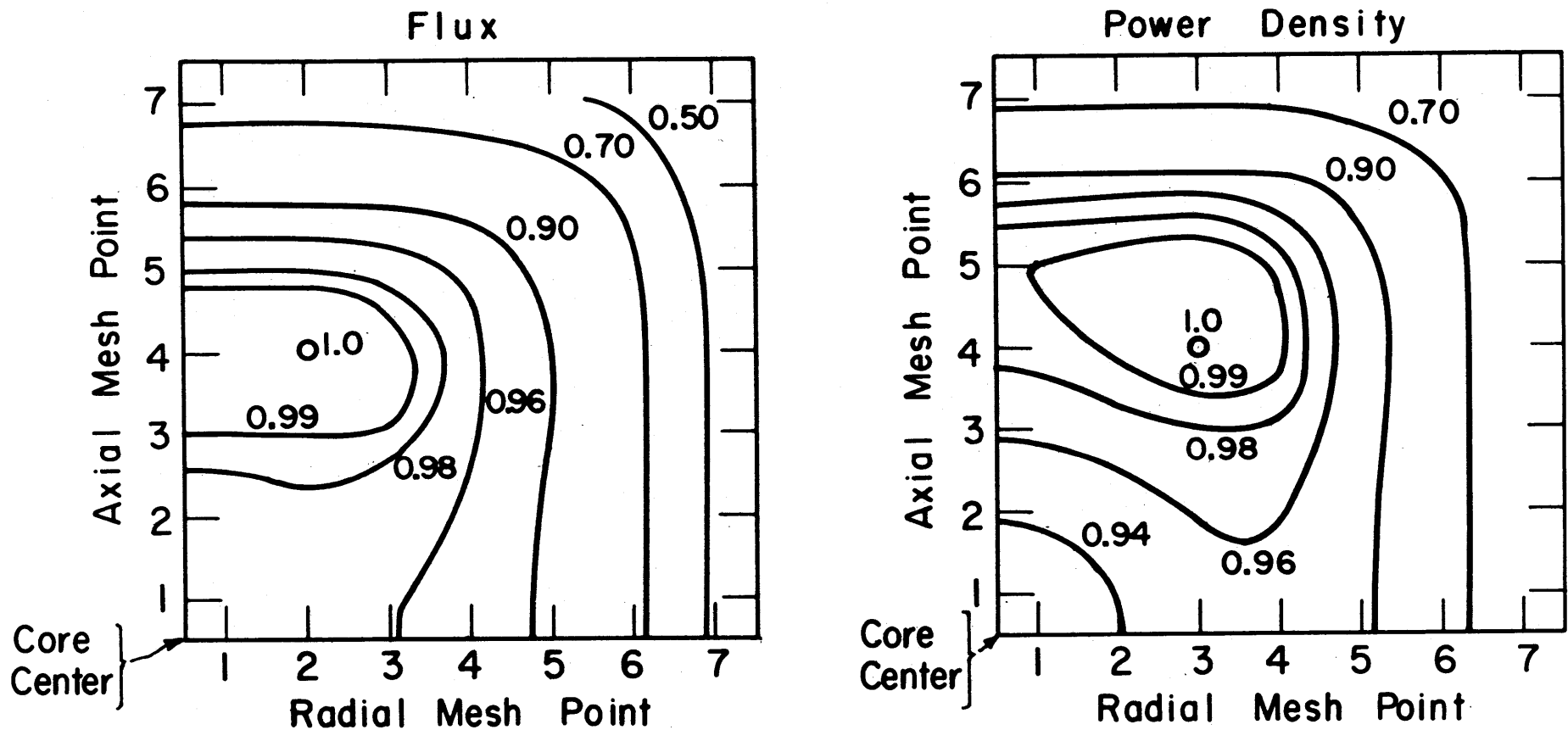


FIG. 6.17 TWO-DIMENSIONAL CONTOUR PLOTS OF THE FINAL SPATIAL DISTRIBUTIONS OF THE RELATIVE THERMAL FLUX AND THE POWER DENSITY, FOR BATCH FUEL SCHEDULING, AVERAGE BURNUP OF APX. 23,000 MWD/TON (ONE QUADRANT OF THE CORE IS SHOWN)

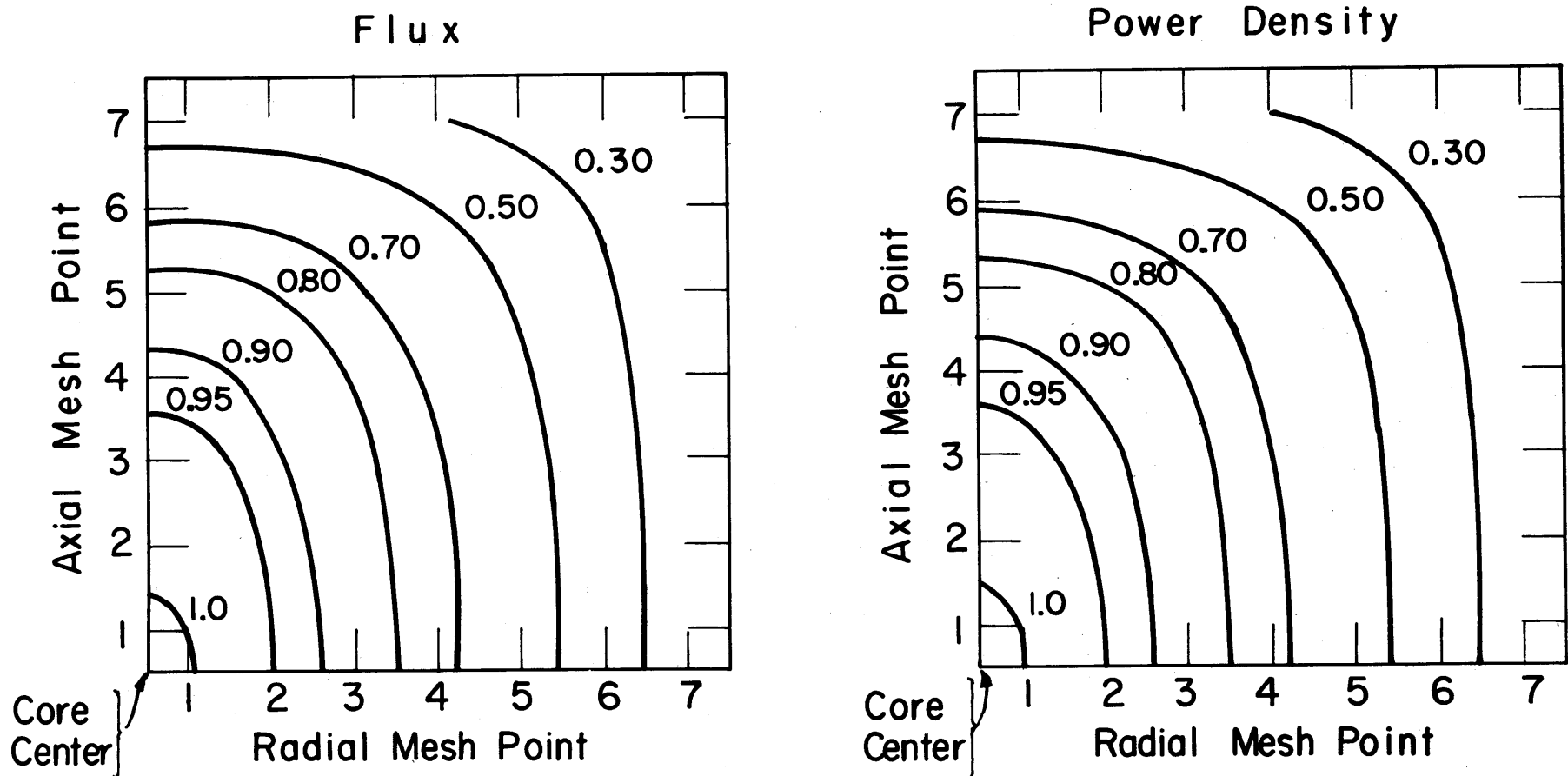


FIG. 6.18 TWO-DIMENSIONAL CONTOUR PLOTS OF THE SPATIAL DISTRIBUTIONS OF THE RELATIVE THERMAL FLUX AND THE RELATIVE POWER DENSITY FOR GRADED FUEL SCHEDULING, AVERAGE BURNUP OF APX. 23,000 MWD/TON (ONE QUADRANT OF THE CORE IS SHOWN)

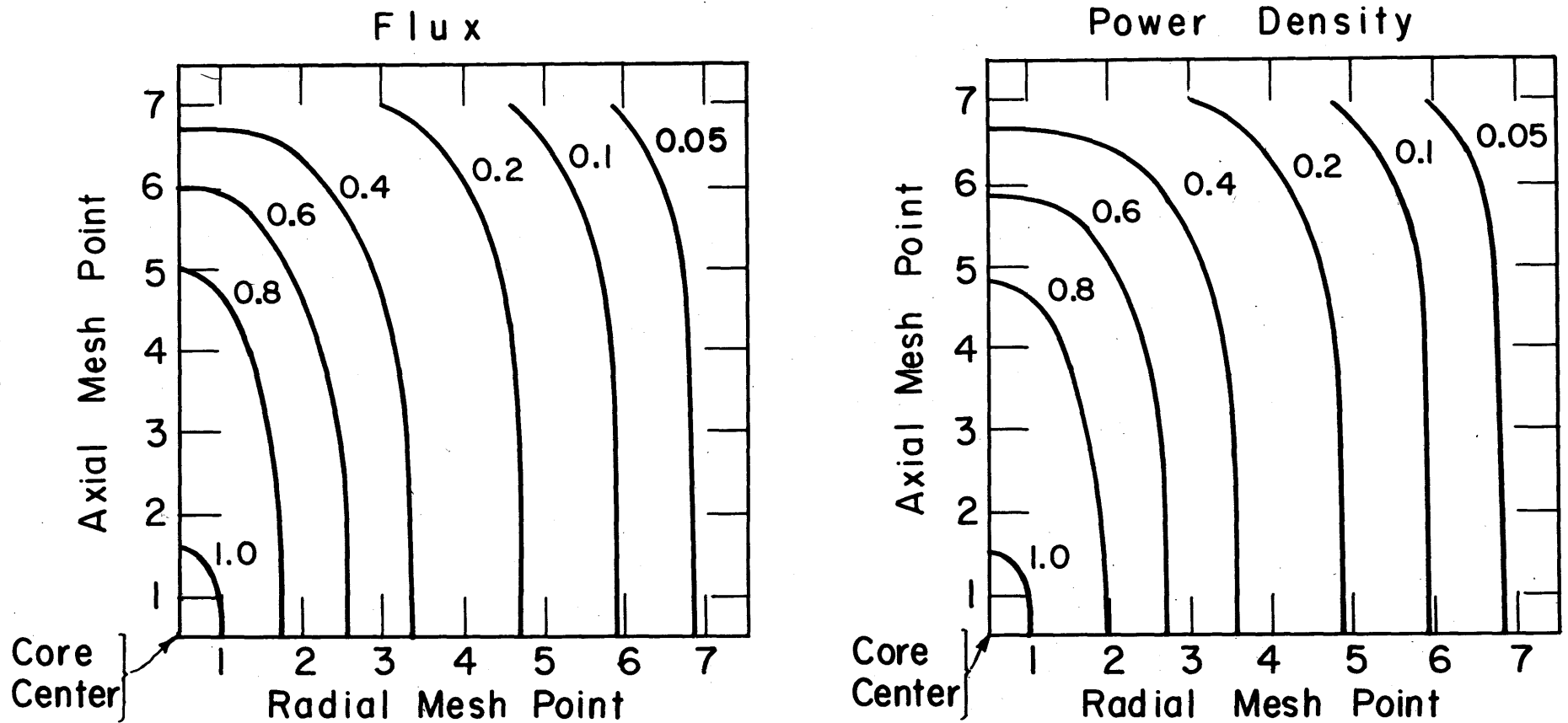


FIG. 6.19 TWO-DIMENSIONAL CONTOUR PLOTS OF THE SPATIAL DISTRIBUTIONS OF THE RELATIVE THERMAL FLUX AND THE RELATIVE POWER DENSITY FOR INOUT FUEL SCHEDULING, AVERAGE BURNUP OF APX. 23,000 MWD/TON (ONE QUADRANT OF THE CORE IS SHOWN)

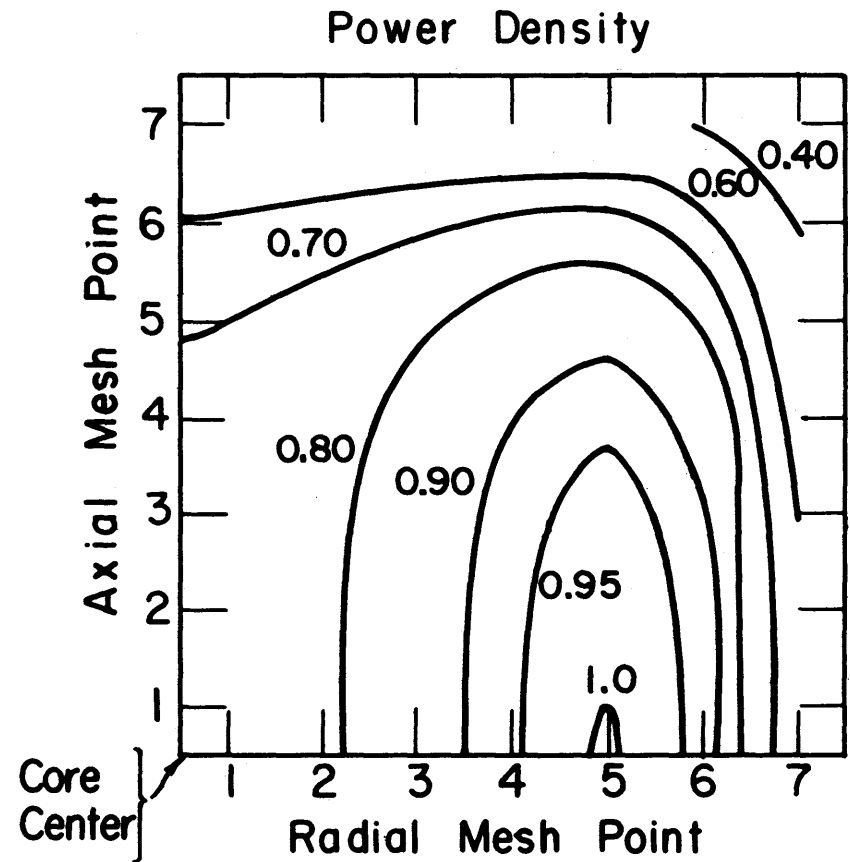
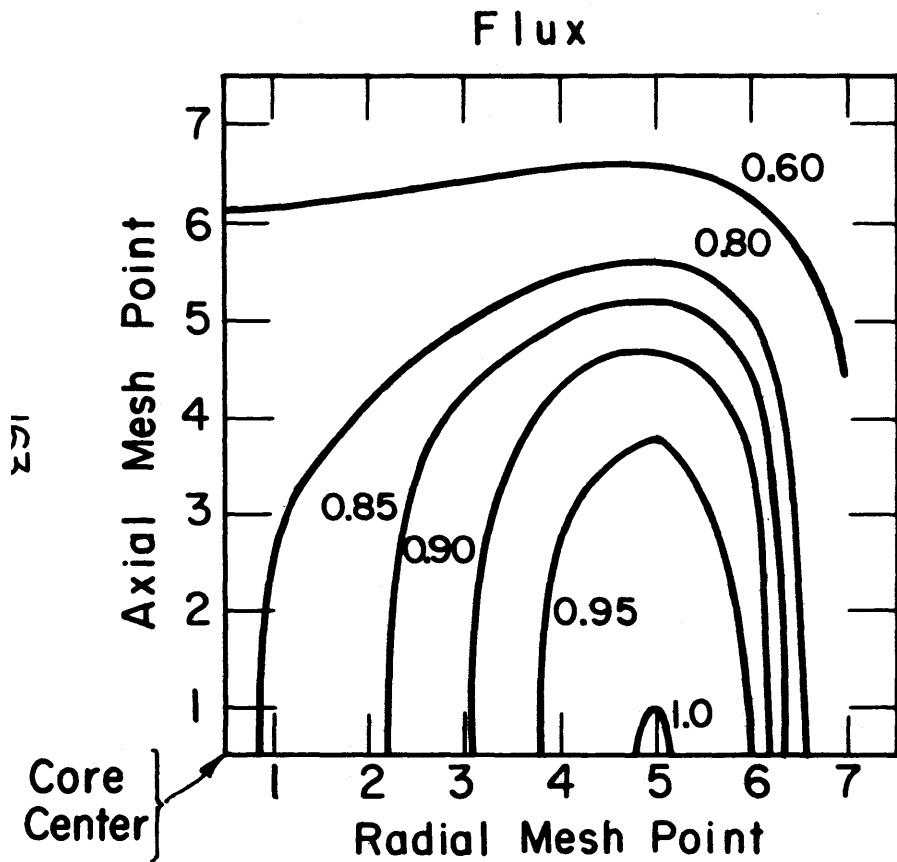


FIG. 6.20 TWO-DIMENSIONAL CONTOUR PLOTS OF THE SPATIAL DISTRIBUTIONS OF THE RELATIVE THERMAL FLUX AND THE RELATIVE POWER DENSITY FOR OUTIN FUEL SCHEDULING, AVERAGE BURNUP OF APX. 23,000 MWD/TON (ONE QUADRANT OF THE CORE IS SHOWN)

these quantities normalized to unity near the maximum points. Since the core is symmetric about the axial and radial center lines only one quadrant need be shown. In these plots the axial direction is taken as the vertical axis and the radial direction as the horizontal axis.

The power density distribution is the same as the flux distributions for the initial distributions for Batch fuel scheduling because the fuel composition is uniform for this case. The two-dimensional variation of both these properties is shown in the single plot, Fig. 6.16. This distribution is slightly more flattened than that of a chopped-cos, chopped- J_0 flux due to the higher concentration of Xe-135 towards the center of the core.

Fig. 6.17 shows the radical change that has occurred to these distributions by the end of the irradiation. The maximum flux point has shifted off the center both radially and axially and the maximum power density, or hot-spot, has shifted even further in the radial direction. This small hot-spot area that appears as a circle in Fig. 6.17 is actually, of course, a "doughnut" shape about the core axis, and, due to axial symmetry, there would be an identical hot-spot "doughnut" on the other side of the central plane.

Fig. 6.18 is a similar plot for the Graded case. Distributions of flux and power density are similar to the initial Batch distributions except they are more flattened axially. The Inout distributions, given in Fig. 6.19, are similar to Graded axially but undergo a much steeper drop radially. The Outin distributions are plotted in Fig. 6.20 and show the hot-spot remaining on the axial central plane but shifted far

but radially. However, the changes in the magnitude of the flux or power density are small across the core for Outin fuel scheduling.

Results of runs useful in computing material properties and fuel cycle costs have been recorded for the four different fuel scheduling methods in Tables 6.2 to 6.5. These listings include final nuclide inventories, burnups, flux-times, and maximum to average power density ratios. The results are given for five different enrichments for each fuel scheduling method.

Table 6.2 Results of Runs Dependent on Initial Enrichment for Batch Fuel Scheduling Method.

Feed:	a/o, U235	2.876	3.441	4.383	5.592	6.452
Atomic Conc.* a/bcm	, U235	7.300 E-4	8.785 E-4	1.130 E-3	1.460 E-3	1.700 E-3
	a/bcm, U238	2.465 E-2	2.465 E-2	2.465 E-2	2.465 E-2	2.465 E-2
Run No.		4.1	1.1	9.1	8.1	3.1
Maximum Flux-time (n/kb)		0.4143	1.268	1.889	2.200	2.250
Burnup (MWD/TON), Maximum		4.507 E3	1.791 E4	3.504 E4	5.331 E4	6.445 E4
	Average	1.654 E3	8.648 E3	2.051 E4	3.538 E4	4.542 E4
kwhe/kg of total fuel charge		1.108 E4	5.793 E4	1.374 E5	2.370 E5	3.042 E5
Fuel on-stream time (years)		0.2188	1.151	2.757	4.817	6.240
Spent Fuel:	a/o, U235	2.641	2.622	2.625	2.704	2.786
Atomic Conc.* a/bcm	, U235	6.682 E-4	6.600 E-4	6.560 E-4	6.701 E-4	6.867 E-4
	, U236	9.310 E-6	4.249 E-5	9.187 E-5	1.514 E-4	1.927 E-4
	, FP	4.576 E-5	2.407 E-4	5.765 E-4	1.007 E-3	1.305 E-3
	, U238	2.462 E-2	2.447 E-2	2.424 E-2	2.396 E-2	2.377 E-2
	, Pu239	2.646 E-5	9.044 E-5	1.467 E-4	1.907 E-4	2.146 E-4
	, Pu240	1.470 E-6	1.330 E-5	2.971 E-5	4.457 E-5	5.280 E-5
	, Pu241	3.096 E-7	8.383 E-6	2.667 E-5	4.603 E-5	5.660 E-5
	, Pu242	9.334 E-9	9.571 E-7	5.376 E-6	1.245 E-5	1.701 E-5
Max. to Avg. Power Density Ratio, Initial †		2.703	2.694	2.683	2.710	2.732
	Final	2.420	1.561	1.331	1.237	1.207

*To obtain inventories in kgram atoms, multiply these concentrations, in atoms/barn cm (of fuel), by 3385.

†With equilibrium Xe and Sm Group poisoning. Initial maximum to average power density without these poisons is 2.932 for all enrichments.

Table 6.3 Results of Runs Dependent on Initial Enrichment for Inout Fuel Scheduling Method.

Feed:	a/o, U235	2.876	3.105	3.441	3.711	4.272
Atomic Conc.* a/bcm	, U235	7.300 E-4	7.900 E-4	8.785 E-4	9.500 E-4	1.100 E-3
	a/bcm , U238	2.465 E-2	2.465 E-2	2.465 E-2	2.465 E-2	2.465 E-2
Run No.		4.2	7.2	1.2	6.2	5.2
Maximum Flux-time (n/kb)		0.6490	1.411	2.200	2.710	3.450
Burnup (MWD/TON), Maximum		7.224 E3	1.773 E4	3.062 E4	3.986 E4	5.550 E4
	Average	5.326 E3	1.409 E4	2.558 E4	3.442 E4	4.932 E4
kwhe/kg of total fuel charge		3.568 E4	9.438 E4	1.713 E5	2.306 E5	3.304 E5
Fuel on-stream time (years)		0.7048	1.869	3.405	4.595	6.662
Spent Fuel:	a/o, U235	2.342	1.899	1.516	1.295	1.053
Atomic Conc.* a/bcm	, U235	5.891 E-4	4.724 E-4	3.726 E-4	3.152 E-4	2.528 E-4
	, U236	2.706 E-5	5.986 E-5	9.228 E-5	1.126 E-4	1.431 E-4
	, FP	1.474 E-4	3.908 E-4	7.122 E-4	9.610 E-4	1.385 E-3
	, U238	2.454 E-2	2.435 E-2	2.411 E-2	2.392 E-2	2.361 E-2
	, Pu239	6.825 E-5	1.174 E-4	1.428 E-4	1.501 E-4	1.532 E-4
	, Pu240	8.096 E-6	2.485 E-5	4.135 E-5	5.074 E-5	6.197 E-5
	, Pu241	3.451 E-6	1.838 E-5	3.633 E-5	4.596 E-5	5.559 E-5
	, Pu242	2.228 E-7	3.032 E-6	1.052 E-5	1.750 E-5	2.897 E-5
Max. to Avg. Power Density Ratio		3.014	3.970	5.156	6.195	7.762

*To obtain inventories in kgram atoms, multiply these concentrations, in atoms/barn cm (of fuel), by 3385.

Table 6.4 Results of Runs Dependent on Initial Enrichment for Outin Fuel Scheduling Method.

Feed:	a/o, U235	2.876	3.105	3.441	3.711	4.272
Atomic Conc.* a/bcm	, U235	7.300 E-4	7.900 E-4	8.785 E-4	9.500 E-4	1.100 E-3
	a/bcm , U238	2.465 E-2	2.465 E-2	2.465 E-2	2.465 E-2	2.465 E-2
Run No.		4.3	7.3	1.3	6.3	5.3
Maximum Flux-time (n/kb)		0.4771	1.016	1.521	1.854	2.355
Burnup (MWD/TON), Maximum		5.226 E3	1.265 E4	2.149 E4	2.839 E4	4.124 E4
	Average	3.817 E3	1.001 E4	1.780 E4	2.412 E4	3.618 E4
kwhe/kg of total fuel charge		2.557 E4	6.705 E4	1.192 E5	1.616 E5	2.423 E5
Fuel on-stream time (years)		0.5051	1.328	2.369	3.219	4.857
Spent Fuel:	a/o, U235	2.477	2.181	1.950	1.800	1.602
Atomic Conc.* a/bcm	, U235	6.247 E-4	5.459 E-4	4.843 E-4	4.445 E-4	3.911 E-4
	, U236	2.029 E-5	4.673 E-5	7.449 E-5	9.424 E-5	1.285 E-4
	, FP	1.057 E-4	2.778 E-4	4.956 E-4	6.732 E-4	1.016 E-3
	, U238	2.457 E-2	2.444 E-2	2.428 E-2	2.415 E-2	2.390 E-2
	, Pu239	5.390 E-5	1.011 E-4	1.327 E-4	1.479 E-4	1.651 E-4
	, Pu240	5.020 E-6	1.706 E-5	2.985 E-5	3.827 E-5	5.078 E-5
	, Pu241	1.650 E-6	1.075 E-5	2.443 E-5	3.429 E-5	4.884 E-5
	, Pu242	7.549 E-8	1.213 E-6	4.619 E-6	8.438 E-6	1.668 E-5
Max. to Avg. Power Density Ratio		2.320	1.662	1.442	1.397	1.367

*To obtain inventories in kgram atoms, multiply these concentrations, in atoms/barn cm (of fuel), by 3385.

Table 6.5 Results of Runs Dependent on Initial Enrichment for Graded Fuel Scheduling Method.

Feed:	a/o, U235	2.876	3.105	3.441	3.711	4.272
Atomic Conc.* a/bcm	, U235	7.300 E-4	7.900 E-4	8.785 E-4	9.500 E-4	1.100 E-3
	a/bcm , U238	2.465 E-2	2.456 E-2	2.465 E-2	2.465 E-2	2.465 E-2
Run No.		4.4	7.4	1.4	6.4	5.4
Maximum Flux-time (n/kb)		0.5459	1.262	1.953	2.379	3.029
Burnup (MWD/TON), Maximum		6.021 E3	1.583 E4	2.739 E4	3.564 E4	5.044 E4
	Average	4.420 E3	1.256 E4	2.282 E4	3.045 E4	4.472 E4
kwhe/kg of total fuel charge		2.961 E4	8.413 E4	1.529 E5	2.040 E5	2.996 E5
Fuel on-stream time (years)		0.5850	1.667	3.038	4.065	6.004
Spent Fuel:	a/o, U235	2.422	2.000	1.660	1.476	1.227
Atomic Conc.* a/bcm	, U235	6.101 E-4	4.986 E-4	4.094 E-4	3.613 E-4	2.965 E-4
	, U236	2.307 E-5	5.526 E-5	8.670 E-5	1.065 E-4	1.393 E-4
	, FP	1.223 E-4	3.486 E-4	6.353 E-4	8.501 E-4	1.256 E-3
	, U238	2.456 E-2	2.438 E-2	2.417 E-2	2.401 E-2	2.372 E-2
	, Pu239	6.000 E-5	1.123 E-4	1.407 E-4	1.508 E-4	1.588 E-4
	, Pu240	6.224 E-6	2.202 E-5	3.756 E-5	4.635 E-5	5.863 E-5
	, Pu241	2.300 E-6	1.553 E-5	3.254 E-5	4.226 E-5	5.434 E-5
	, Pu242	1.223 E-7	2.250 E-6	8.219 E-6	1.381 E-5	2.460 E-5
Max. to Avg. Power Density Ratio		2.636	2.441	2.313	2.248	2.163

*To obtain inventories in kgram atoms, multiply these concentrations, in atoms/barn cm (of fuel), by 3385.

3. Cost Results

Cost results have been tabulated for each run for the four different sets of cost input data given in Table 4.2. Table 6.6 is a typical cost tabulation for Batch fuel scheduling with an initial enrichment of 3.44 a/o U235. Cost results for other enrichments and other fuel scheduling methods are located in Appendix F, Tables F8 through F25. The unit prices and other cost parameters were listed in Table 4.2.

In addition to these tabulations a few graphs have been provided to indicate the important trends in the cost behavior. Fig. 6.21 shows the net fuel cycle cost for the current, the highest, and the lowest price sets as a function of average burnup and for the four different fuel scheduling methods that were studied. The main trend in all cases is the initial sharp decrease in fuel cycle costs as the average burnup increases (the cost is approximately inversely proportional to burnup in the region of very low burnups), followed by a minimum point (although this is beyond the range of the abscissa in some cases), and an increase in the net cost as average burnup increases for high burnups.

Table 6.6 Partial and Net Fuel Cycle Costs, in mills/kwhe, Depending on Enrichment, Fuel Scheduling Procedure, and Unit Price Basis.

Enrichment: 3.441 a/o U235
Average Burnup: 8648. (MWD/ton)

Fuel Scheduling Method: Batch
Run No. 1.1

Fuel Cycle Step		Unit Price Set No.			
No.	Process	1	2	3	4
2	UF ₆ from A. E. C., mills/kwhe	7.71	*	5.15	6.11
6	UF ₆ → UO ₂	0.39	0.78	*	*
8	Physical Fabrication	1.55	*	0.52	0.78
9	Shipping	0.16	*	0.09	*
10	Solvent Extraction	0.37	*	*	*
11	UO ₂ (NO ₃) ₂ → UF ₆	0.09	*	*	*
12	Pu(NO ₃) ₄ → Pu	0.11	*	*	*
13	UF ₆ to A. E. C.	-5.23	*	-3.49	-4.08
14	Pu to A. E. C.	-0.91	*	-2.28	*
16	UF ₆ Lease Charge	0.96	2.88	0.64	0.76
17	Working Capital Charge	0.21	0.25	0.10	0.12
	Net Fuel Cycle Cost	5.39	7.74	1.66	3.87

* An asterisk means same value as given for Cost Set No. 1

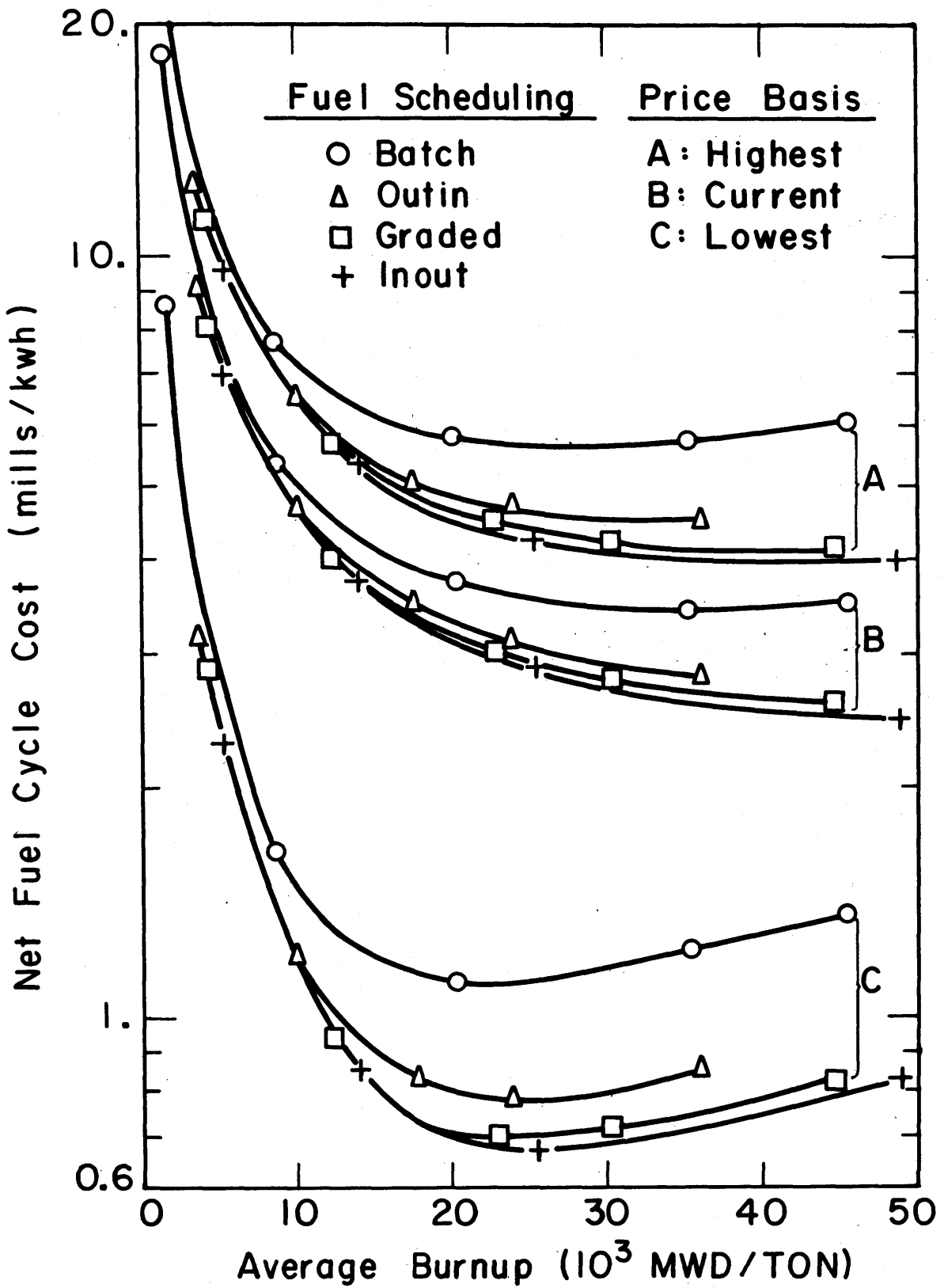


FIG. 6.21 NET FUEL-CYCLE COST AS A FUNCTION OF THE AVERAGE BURNUP OF THE DISCHARGED FUEL

For any chosen price set and any specified average burnup it is seen that Inout fuel scheduling produces the lowest fuel-cycle costs followed by Graded, Outin, and Batch, although there is less difference between the steady-state fuel scheduling methods than between Batch and Outin. The main cause of the increase of the "highest price" set of curves over that of the current set is the assumption of a UF_6 lease charge of 12% rather than 4%. The major causes of the difference between the lowest and the current curves is a reduction in the price of UF_6 and an increase in Pu credit value (from \$12/gm for current to \$30/gm for lowest). The UF_6 charge and the Pu credit value are the two factors which tend to raise the costs curve for high burnups. The former is the dominant factor for Price Set A where the value of UF_6 is the highest, and the latter is the dominant factor for Price Set B where the credit for Pu is high. Here the reduction in the average production rate of Pu as burnup increases tends to lower the credit per unit power. The cost curves for current prices, having a lower lease charge rate and a lower Pu credit value, tend to reach the minimum point at higher burnups than the curves for either the lower or higher price basis. For Batch fuel scheduling the minimum cost occurs at an average burnup of approximately 35,000 MWD/TON. The minima for the steady state methods with current prices are beyond the burnup range shown.

Since radiation damage rather than loss of reactivity often limits the maximum attainable burnup it is of interest to plot the net fuel cycle cost versus the maximum local burnup in the discharged fuel. This has been done in Fig. 6.22 which generally shows a greater cost reduction

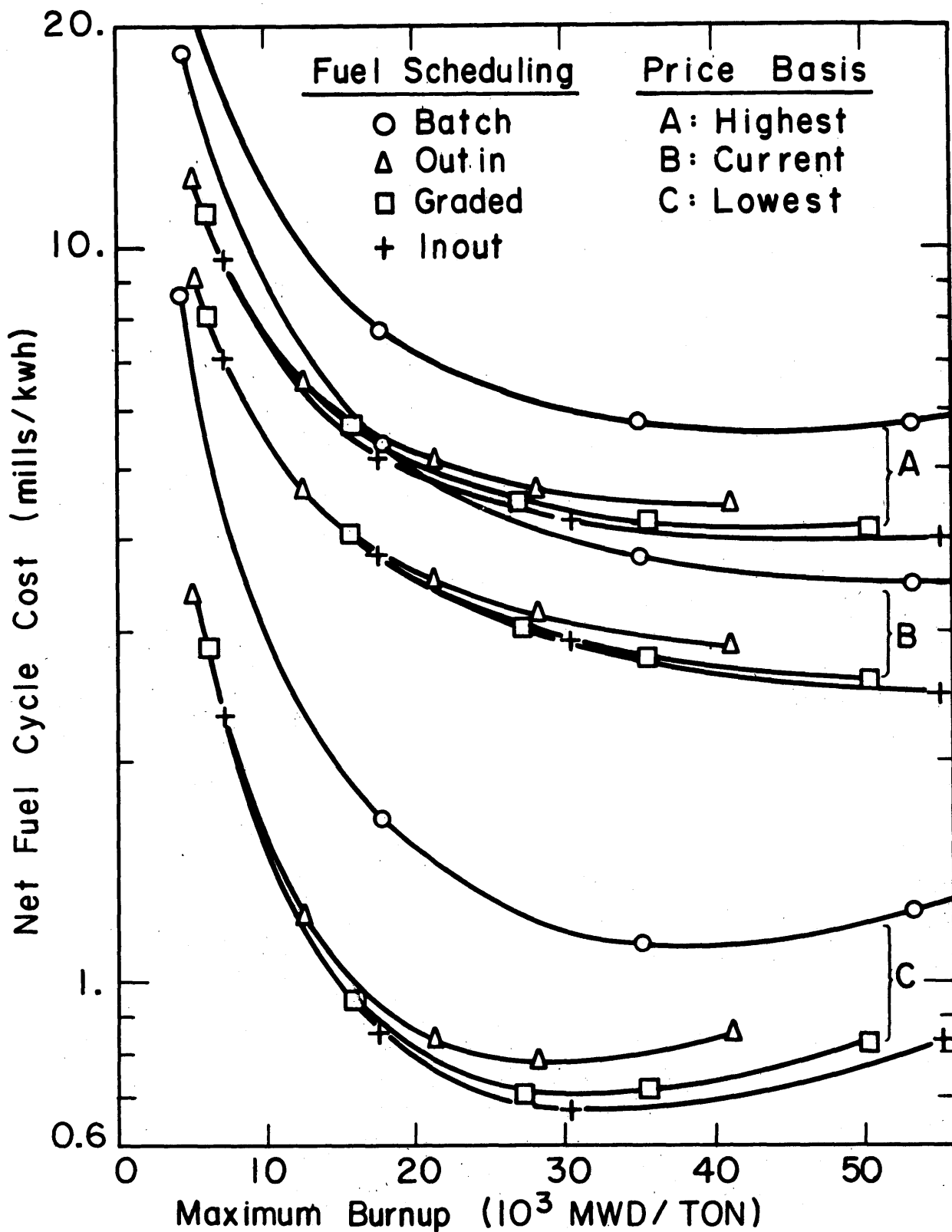


FIG. 6.22 NET FUEL-CYCLE COST AS A FUNCTION OF THE MAXIMUM BURNUP OF THE DISCHARGED FUEL.

in going from Batch to a steady-state type of fuel movement, for a specified maximum local burnup, than did Fig. 6.21.

In Figs. 6.23 to 6.25 the net fuel cycle cost for current prices is broken down into the partial costs: material, fabrication, reprocessing, UF_6 lease charge, and the working capital charge, as described in Section IV:B. and illustrated in Fig. 4.5. The fabrication and reprocessing costs are essentially straight lines on a log-log plot for all of the fuel scheduling methods. The decrease of these costs with increasing burnup is slightly less than that of a cost inversely proportional to burnup (which would have a -45° slope) due to the enrichment dependence of the conversion cost for UF_6 and to the dependence of the $Pu(NO_3)_4$ conversion cost on the quantity of Pu produced.

The material cost charge decreases initially due to the increase in the amount of energy obtained from Pu239 and finally increases due to the increased price for the more highly enriched UF_6 that is required.

The UF_6 lease charge follows the same trend as the UF_6 part of the material charge. In addition, this charge tends to drop initially, as does the working capital charge, as the ratio of non-productive holdup time to reactor time decreases.

Finally, a bar graph, Fig. 6.26, is presented to show the combined effects of the partial fuel cycle costs as burnup increases. The last bar on this graph shows that the minimum fuel cost is due essentially to the material cost and the UF_6 lease charge and, therefore, primarily due to the price of the feed UF_6 .

The fuel cycle costs are further broken down in Table 6.6 of this chapter and Tables F8 through F25 of Appendix F for all the pressurized light-water reactor runs.

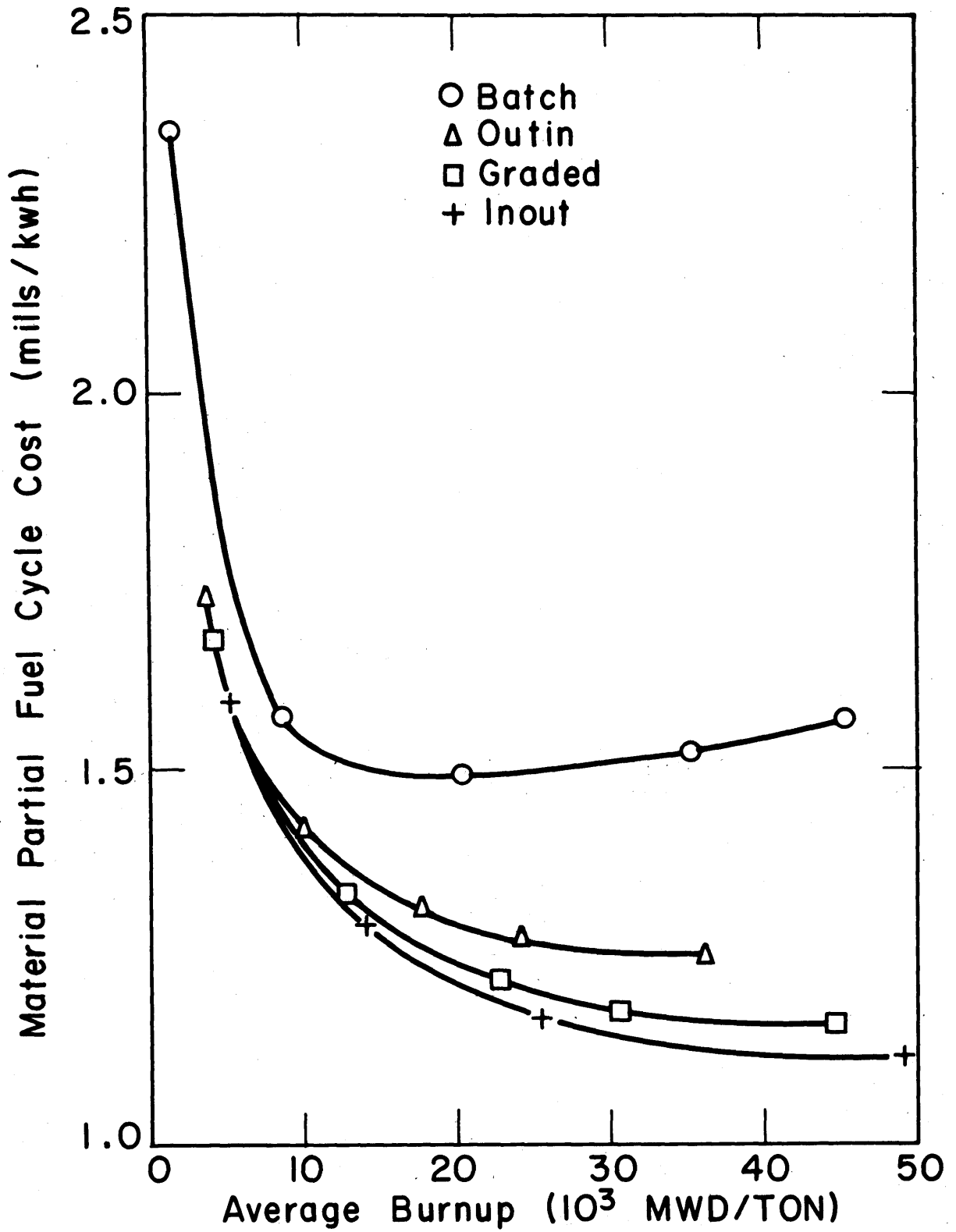


FIG. 6.23 MATERIAL COST AS A FUNCTION OF BURNUP, USING CURRENT PRICES

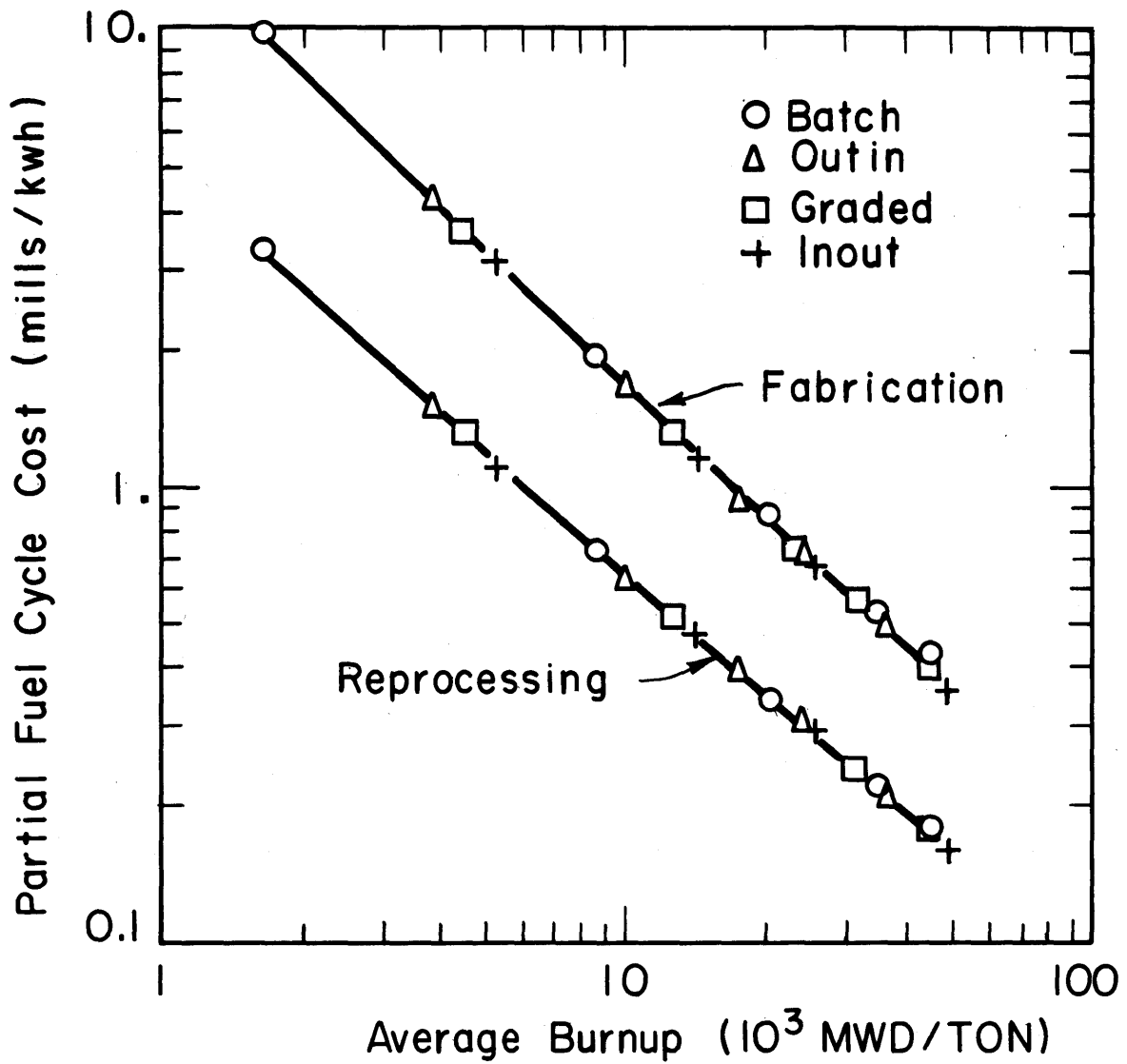


FIG. 6.24 FABRICATION AND REPROCESSING COSTS AS FUNCTIONS OF AVERAGE BURNUP, USING CURRENT PRICES.

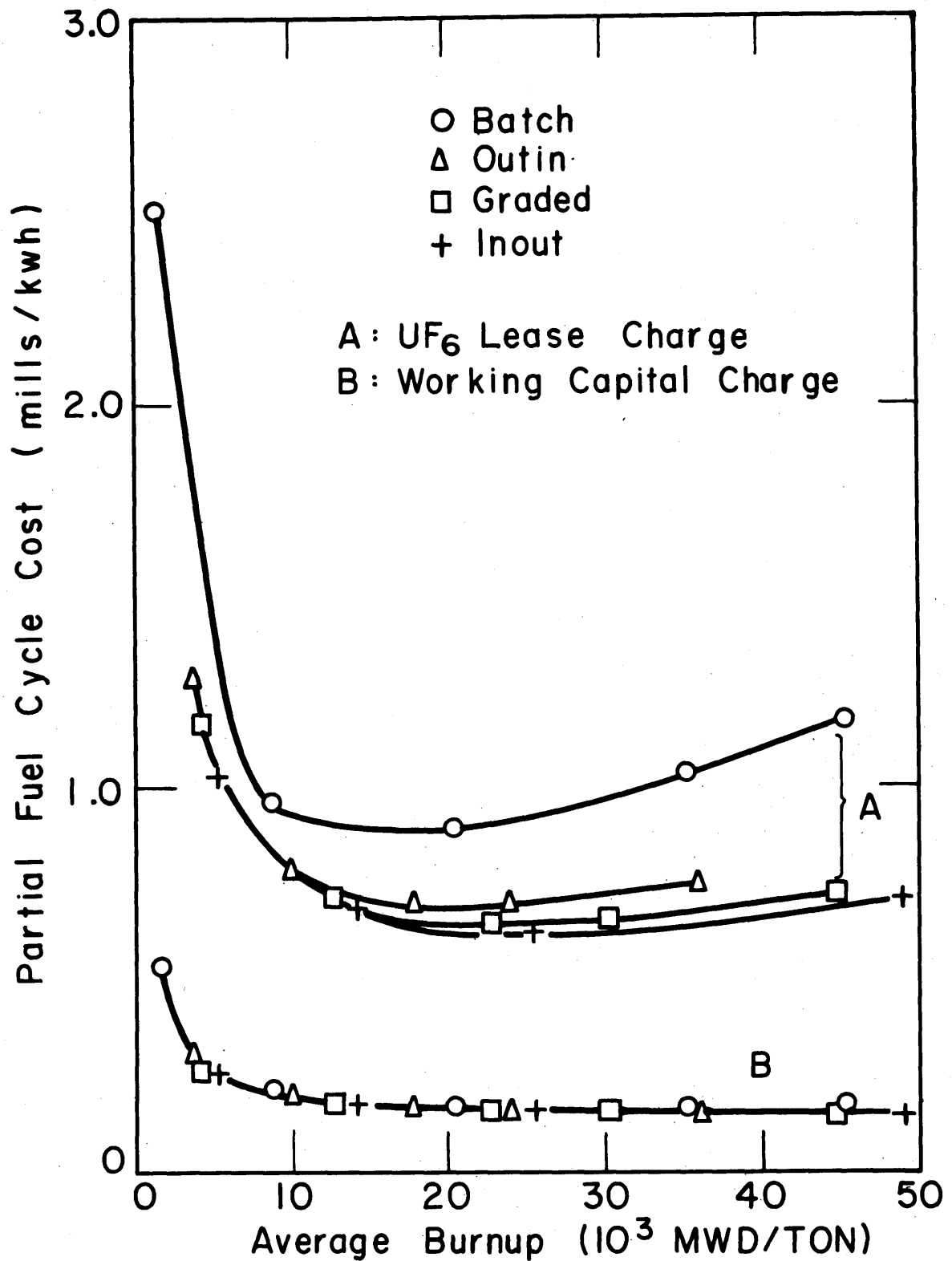


FIG. 6.25 INTEREST CHARGES AS FUNCTIONS OF BURNUP, USING CURRENT PRICES

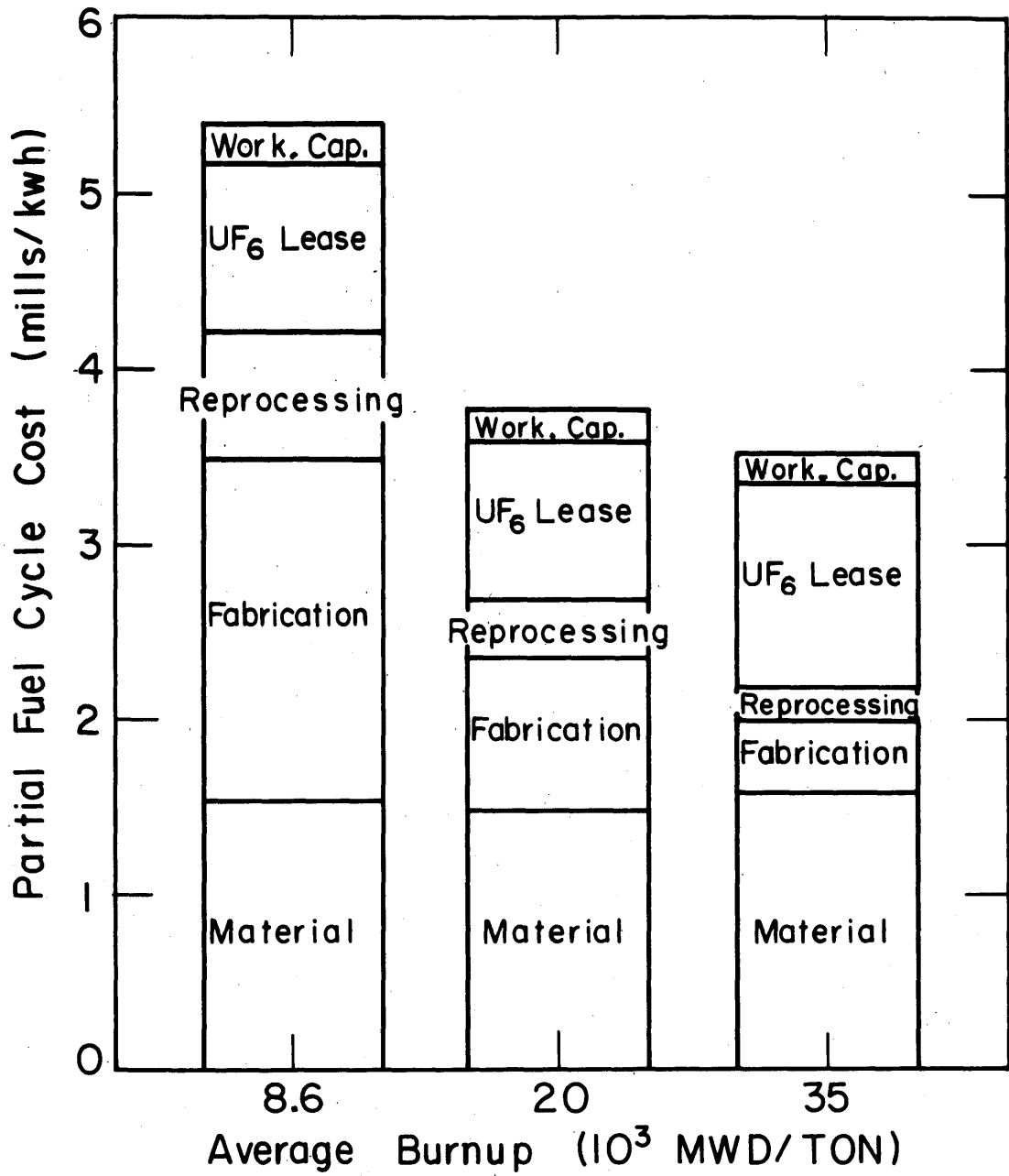


FIG. 6.26 BREAKDOWN OF FUEL-CYCLE COST FOR DIFFERENT VALUES OF AVERAGE BURNUP, FOR BATCH FUEL SCHEDULING, USING CURRENT PRICES

For the previous results it was assumed that the reactor was capable of operation on an 80% load factor at design power regardless of the ratio of maximum to average power density. Actually, if the ratio of maximum to average power density for one method of fuel scheduling differs from that for which the reactor has been designed, the power level in this method of fuel scheduling may differ from the design level. The maximum power at which a reactor can be operated may be set by a maximum temperature allowable in some material, by a maximum permissible thermal stress in some part or by a maximum permissible heat flux or maximum permissible power density. No matter which of these conditions determines the maximum permissible power, if a particular method of fuel scheduling produces a ratio of maximum to average power density less than at design conditions it should be possible to operate the reactor at a power level above the design value without exceeding the maximum allowable temperature, thermal stress, heat flux, or power density. If, at the same time, there is spare capacity in the steam boiler and turbogenerator, it should be possible to increase the electric power output when the ratio of maximum to average power density is less than design. On the other hand, if a method of fuel scheduling produces a ratio of maximum to average power density greater than design, and if the power level is limited by some maximum allowable reactor temperature, thermal stress, heat flux, or power density (rather than by the capacity of the steam boiler or turbogenerator) the electric power output will be less than the design value.

The greatest possible effect of a change in the ratio of maximum to average power density would be to change the electric power output in

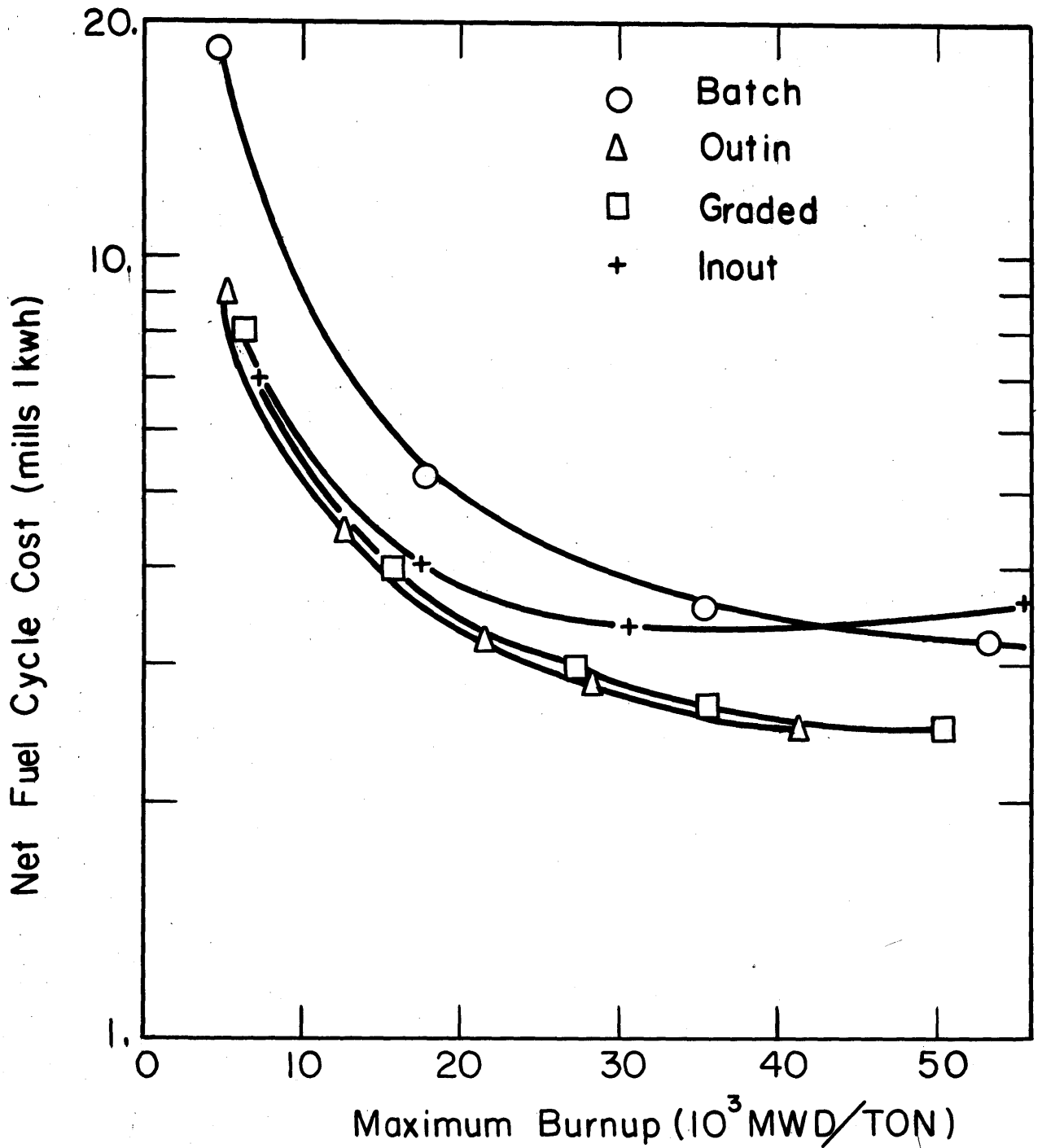


FIG. 6.27 NET FUEL-CYCLE COST AS A FUNCTION OF THE MAXIMUM BURNUP OF THE FUEL, FOR CURRENT PRICES, OPERATION WITH CONSTANT MAXIMUM POWER DENSITY.

inverse proportion to the ratio of maximum to average power density, as would be the case if the maximum power density could be kept constant. Figure 6.27 shows how fuel-cycle costs would vary with maximum burnup if the maximum local power density were kept constant rather than the electric power output. Current prices have been used in computing these costs, and it has been assumed that the reactor has been designed for a ratio of maximum to average power of 2.7, the value for Batch fuel scheduling at the beginning of the cycle when xenon and the Samarium group of fission products have reached equilibrium. Comparison of Fig. 6.27 with Fig. 6.22 shows that the Outin method of fuel scheduling now produces the lowest fuel-cycle costs rather than Inout, and that at high burnup, the Inout method has the highest fuel-cycle cost of all methods. This is because the high ratio of maximum to average power density in Inout scheduling greatly reduces the reactor power level under the present assumption, stretches out the time the fuel is left in the reactor, and increases the charges for working capital and UF_6 rental.

In the Batch curve of Fig. 6.27 the time-average ratio of maximum to average power density has been taken as the arithmetic mean of the values of this ratio at the beginning and end of the batch cycle.

The overall cost of nuclear power is the sum of fuel-cycle costs, capital charges and operating costs. Changes in the power level at which a reactor may be operated occasioned by changes in the ratio of maximum to average power density from the design value will affect the capital and operating components of nuclear power cost as well as the fuel-cycle component discussed above. In an extreme case in which the electric power output is inversely proportional to the ratio of maximum to average

power density, and total reactor capital charges and operating costs are independent of power level, the capital component due to the reactor and the operating component of nuclear power cost would be directly proportional to the ratio of maximum to average power density. Thus, the Outin and Graded methods of fuel scheduling have cost advantages in addition to the reduction in fuel-cycle costs shown in Fig. 6.27.

An upper bound for the effect of the maximum to average power-density ratio on the capital component of power cost may be obtained as follows. The component C_{cp} of power cost due to capital investment in the reactor is given by

$$C_{cp} = \frac{10^3}{8760L} F_I I \quad (6.3)$$

where,

I = unit capital investment in reactor, \$/installed ekw

F_I = fractional yearly charge on capital investment

L = load factor

In the extreme case, by decreasing the maximum to average power-density ratio from the design value of M_0 to M , it would be possible to increase the power output by a factor of M_0/M , and to reduce the capital component of power cost by the factor M/M_0 . With representative values for a UO_2 light-water reactor of $I = 250\$/ekw$ (for reactor exclusive of steam boiler and turbogenerator) $F_I = 0.14/yr$ and $L = 0.8$, the extreme effect on the component of power cost due to capital investment in the reactor would be given by

$$C_{cp} = 5.0M/M_0 \text{ mills/kwhe} \quad (6.4)$$

The maximum savings in the capital component of power cost that might be realized with various fuel scheduling methods may be estimated with the aid of Eq. (6.4) and Fig. 6.8. For example, if the reactor had been designed for a maximum to average power-density ratio of $M_0 = 2.7$, as at the beginning of a batch irradiation cycle and it was later decided to operate with Outin fuel movement at an average burnup of 20,000 MWD/ton, with $M = 1.4$, the capital component of power cost due to investment in the reactor would be decreased from 5.0 mills/kwhe to $5.0 \times 1.4/2.7 = 2.6$ mills/kwhe. This assumes that the capacity of the steam boiler and turbogenerator would be increased to permit production of 2.7/1.4 times as much electric power and that the unit capital cost of these items, in terms of \$/installed ekw would not change. Additions to operating costs associated with radial movement of fuel are neglected. Correspondingly, the capital component of the power cost due to investment in the reactor, in mills/kwhe, would be decreased to 4.4 for Graded, and increased to 8.5 for Inout for average burnups of 20,000 MWD/ton.

The above estimates are upper bounds for the effect; more accurate estimates would call for detailed thermal analysis of the reactor, which is beyond the scope of this report.

B. COMPARISON WITH EXPERIMENTAL DATA

Results are presented in this section to compare the FUELCYC calculations with experimental data for the NRX reactor. The NRX reactor, the GLEEP, and the FUELCYC input data for these reactors were discussed in Section V.B. and the special nomenclature was there defined.

1. Buildup of Plutonium Nuclides

Craig et al., C11, report measured values for the isotopic composition of the plutonium in one NRX sample which was irradiated to a 2200 m/s flux-time of 0.633 n/kb. The 2200 m/s flux-time will be denoted by θ^0 and is related to the true thermal flux-time, θ , by

$$\theta = \theta^0 \frac{n_{th}}{n} \frac{\bar{v}_{th}}{v_0} \quad (6.5)$$

For the NRX irradiations $n_{th} \bar{v}_{th} / n v_0$ was essentially constant, having the value 1.217, so the corresponding FUELCYC flux-time for this irradiation was 0.770 n/kb. The experimental values, values calculated by FUELCYC, and values calculated by Kushneriuk, C11, K11, are presented in Table 6.7. Kushneriuk's cross sections were calculated using a "Blackness" method for a Maxwellian (38° C) incurrent plus a 1/E component, which enabled calculation of the variation in the effective cross sections as a function of position in the fuel rod. The average value over the fuel rod for each nuclide was used in Kushneriuk's calculations of nuclide concentrations. These results are labeled under "Blackness Calculations" in Table 6.7. The FUELCYC cross sections are homogenized values, and are therefore less refined than those of

Kushneriuk with regards to local spatial considerations, but are more refined with regard to the average energy distribution of the thermal flux.

Table 6.7 Isotopic Composition of Plutonium in an Irradiated NRX Sample ($\theta^0 = 0.633 \text{ n/kb}$)

Isotope	Measured (Mass Spectrometer)	Isotopic Composition, %		Blackness Calculations
		Calculated		
		FUELCYC Run NRX1*	Run NRX2**	
Pu 239	87.117 ± 0.052	87.22	87.30	87.281
Pu 240	11.244 ± 0.051	11.19	10.72	11.083
Pu 241	1.521 ± 0.010	1.47	1.84	1.518
Pu 242	0.118 ± 0.005	0.12	0.14	(0.118)

Two values were used for $\Sigma_{s,fl}$ in the FUELCYC runs to give different magnitudes for the disadvantage factor for Pu240, which is calculated from $\Sigma_{s,fl}$ according to Eq. (4.13). When the true scattering cross section of the fuel was used, 1160 bifa, the disadvantage factor for Pu240 was 1.2 at the final flux time. As shown in Table 6.7, Run NRX2, the resulting Pu240 concentration was lower, and that of Pu241 was higher, than those measured. Both the experimental data and Kusherniuk's theoretical calculations, K11, indicated that the disadvantage factor should have a value of approximately 2.0 at this flux time. The correct Pu240 disadvantage factor for a particular flux-time, $\psi_{1,10}$, can be reproduced by FUELCYC since the input data parameter $\Sigma_{s,fl}$ is only used in computing

* $\Sigma_{s,fl} = 230. \text{ bifa}$

** $\Sigma_{s,fl} = 1160. \text{ bifa}$

this factor. (For a given concentration of Pu240, $(\psi_1, 10^{-1})$ is inversely proportional to $\Sigma_{s,fl}$). Therefore in the other run $\Sigma_{s,fl}$ was set at 230. bifa which gave $\psi_1, 10$ the value 2.0 at a flux-time of 0.633 n/kb. This calculation, Run NRX1, gave excellent agreement with experimental data for the composition of all plutonium isotopes, which is an indication that the Crowther and Weil relationship, Eq. (4.8A), gives reasonably accurate results for the time dependence of the change in the Pu240 resonance absorptions for uranium metal fuel elements if normalized to the correct value near the end of the irradiation (by an appropriate pseudo value for $\Sigma_{s,fl}$). Despite the better agreement with experimental results for uranium metal obtained by using a pseudo value for $\Sigma_{s,fl}$, it is felt that the true value of $\Sigma_{s,fl}$ should still be used for UO₂ fuel elements (until experimental long term irradiation data is available for UO₂) since Crowther and Weil, C13, checked this relationship for UO₂ fuel elements and found it compared well with calculations by the more accurate method of G. M. Roe, R9.

The calculated nuclide concentrations for Runs NRX1 and NRX2 are listed in Table 6.8 for different flux times. Except for Pu240, Pu241, and Pu242 the concentrations were the same for Run NRX2 as for NRX1.

2. The Reactivity of the NRX Samples

In this section a comparison is made between experimental and calculated values for the reactivity change of a uranium metal rod which had been irradiated in the NRX reactor and tested for reactivity in the GLEEP. R has been defined in Section V.B.3. In order to calculate values for R from Eq. (5.23) the macroscopic cross sections must be

Table 6.8A Nuclide Concentrations in Units of Atoms per Initial Fissile Atom for an NRX Sample Depending on the Flux-Time, Values the Same for Runs NRX1 and NRX2

True Flux-Time (n/kb)	U235	U236	Fission Products	U238	Pu239
0	1.	0.	0.	1.391E+2	0.
0.1	9.465E-1	8.820E-3	4.893E-2	1.390E+2	4.042E-2
0.2	8.958E-1	1.715E-2	9.835E-2	1.390E+2	7.692E-2
0.3	8.478E-1	2.502E-2	1.481E-1	1.389E+2	1.098E-1
0.4	8.024E-1	3.245E-2	1.981E-1	1.389E+2	1.395E-1
0.5	7.595E-1	3.947E-2	2.483E-1	1.388E+2	1.662E-1
0.6	7.189E-1	4.609E-2	2.984E-1	1.388E+2	1.902E-1
0.7	6.804E-1	5.233E-2	3.486E-1	1.387E+2	2.118E-1
0.8	6.440E-1	5.822E-2	3.986E-1	1.387E+2	2.311E-1
0.9	6.096E-1	6.377E-2	4.485E-1	1.387E+2	2.485E-1
1.0	5.770E-1	6.901E-2	4.981E-1	1.386E+2	2.640E-1

Table 6.8B Nuclide Concentrations in units of Atoms per Initial Fissile Atom for an NRX Sample Depending on the Flux-time, values different for Runs NRX1 and NRX2

True Flux-time (n/kb)	Pu 240		Pu 241		Pu 242	
	NRX1	NRX2	NRX1	NRX2	NRX1	NRX2
0.	0	0	0	0	0.	0
0.1	6.816E-4	6.814E-4	1.792E-5	1.808E-5	1.720E-7	1.728E-7
0.2	2.575E-3	2.571E-3	1.305E-4	1.347E-4	2.409E-6	2.461E-6
0.3	5.484E-3	5.456E-3	3.944E-4	4.202E-4	1.114E-5	1.163E-5
0.4	9.251E-3	9.155E-3	8.304E-4	9.171E-4	3.207E-5	3.440E-5
0.5	1.375E-2	1.352E-2	1.435E-3	1.645E-3	7.115E-5	7.846E-5
0.6	1.889E-2	1.841E-2	2.194E-3	2.605E-3	1.339E-4	1.518E-4
0.7	2.456E-2	2.372E-2	3.088E-3	3.787E-3	2.252E-4	2.622E-4
0.8	3.071E-2	2.937E-2	4.096E-3	5.171E-3	3.492E-4	4.169E-4
0.9	3.725E-2	3.528E-2	5.200E-3	6.735E-3	5.093E-4	6.220E-4
1.0	4.413E-2	4.139E-2	6.385E-3	8.452E-3	7.081E-4	8.830E-4

calculated for the sample in the GLEEP spectrum. It is instructive to first calculate these cross sections and the corresponding R values assuming the spectrum to be that of the sample surrounded by natural uranium in the NRX reactor. The results are then in a tractable form which clearly shows the individual effect of the different terms and which can easily be modified to give the R values for the true GLEEP spectrum. In addition the effect of spectrum changes between the NRX reactor and the GLEEP is obtained.

The effective change in the cross section of nuclide m at a flux time, θ , was calculated from,

$$\Sigma_{m,\theta} \equiv (N_m \sigma_m)_\theta - (N_m \sigma_m)_o + \frac{q}{\phi} P_1 \left[\langle 1 - p_m \rangle_\theta - \langle 1 - p_m \rangle_o \right] \quad (6.6)$$

where qP_1/ϕ was taken as 1119.5 bifa which was the value obtained in the NRX calculations, for natural-uranium, with equilibrium xenon and Samarium group poison. The values for N_m , σ_m , and $\langle 1 - p_m \rangle$ were obtained from Run NRXI for the specified flux-times since this run gave the better agreement with measured isotopic compositions. The resulting values of Σ_m are listed in Table 6.9; their thermal components, $\Sigma^{th} \equiv \delta N \sigma$, in Table 6.10; and their resonance components, $\Sigma^r \equiv \delta \frac{q}{\phi} P_1 \langle 1 - p_m \rangle$, in Table 6.11. It is obvious from these tabulated values that the reactivity changes for the NRX fuel are primarily due to the thermal energy region (zero to 0.45 ev). Values of the 2200 m/s macroscopic cross section changes for use in Eq. (5.23) were calculated from

$$\Delta \Sigma_m = 1.217 \Sigma_m \quad (6.7)$$

Table 6.9 Effective Macroscopic Cross Section Changes for the NRX Reactor, in bifa*

Cross Section Change	True Thermal Flux-time (n/kb)				
	0.1	0.2	0.3	0.5	0.7
Σ_5	-30.0	-58.3	-84.9	-133.9	-177.5
Σ_6	0.2	0.4	0.5	0.9	1.1
Σ_8	-0.4	-0.8	-1.2	-1.8	-2.2
Σ_9	43.5	82.9	118.5	179.5	229.1
Σ_{10}	.5	1.9	3.9	8.4	13.1
Σ_{11}	0.0	0.2	0.5	1.9	4.0
Σ_{FP}	2.7	5.0	7.0	12.9	16.3
Σ_{Sm}	9.0	9.5	10.0	10.7	11.3
Σ	25.5	40.8	54.3	78.6	95.2
Σ_{5, f^v_5}	-61.9	-120.2	-175.2	-276.3	-366.2
Σ_{9, f^v_9}	86.3	164.2	234.7	355.4	453.3
$\Sigma_{11, f^v_{11}}$	0.0	0.4	1.1	4.1	8.8
Σ_{f^v}	24.4	44.4	60.6	83.2	95.9

* $\Sigma_{12} = 0.0$ for all flux times; $\Sigma_{sm} = 8.4$ at $\theta = 0$

Table 6.10 Effective Thermal Macroscopic Cross Section Changes for the NRX Reactor, in bifa*

Cross Section Change	True Thermal Flux-time (n/kb)				
	0.1	0.2	0.3	0.5	0.7
Σ_5^{th}	-28.7	-55.7	-81.1	-127.9	169.5
Σ_6^{th}	0.0	0.1	0.1	0.6	0.3
Σ_8^{th}	-0.4	-0.7	-1.1	-1.6	-2.0
Σ_9^{th}	42.2	80.4	115.0	174.1	222.3
Σ_{10}^{th}	0.2	0.6	1.4	3.4	6.1
Σ_{11}^{th}	0.0	0.2	0.5	1.8	3.8
Σ_{FP}^{th}	2.7	5.0	7.0	12.9	16.3
Σ_{Sm}^{th}	9.0	9.5	10.0	10.7	11.3
Σ^{th}	25.0	39.4	51.8	74.0	88.6
$\Sigma_{5,f^v_5}^{th}$	-59.5	-115.5	-168.4	-265.3	-351.8
$\Sigma_{9,f^v_9}^{th}$	83.7	159.4	227.8	345.0	440.0
$\Sigma_{11,f^v_{11}}^{th}$	0.0	0.4	1.1	3.9	8.5
Σ_f^{th}	24.2	44.3	60.5	83.6	96.7

* $\Sigma_{12}^{th} = 0.0$ for all flux times; $\Sigma_{sm}^{th} = 8.4$ at $\theta = 0$

Table 6.11 Effective Resonance Macroscopic Cross Section Changes for the NRX Reactor, in bifa*

Cross Section Change	True Thermal Flux-time (n/kb)				
	0.1	0.2	0.3	0.5	0.7
Σ_5^r	-1.3	-2.6	-3.8	-6.0	-8.0
Σ_6^r	0.1	0.3	0.4	0.2	0.8
Σ_9^r	1.3	2.5	3.6	5.4	6.9
Σ_{10}^r	0.4	1.3	2.5	5.0	7.0
Σ_8^r	0.0	-0.1	-0.1	-0.2	-0.2
Σ_{11}^r	0.0	0.0	0.0	0.1	0.2
Σ^r	0.5	1.4	2.6	4.5	6.7
Σ_{5,f^v}^r	-2.4	-4.7	-6.9	-11.0	-14.4
Σ_{9,f^v}^r	2.5	4.8	6.9	10.4	13.3
Σ_{11,f^v}^r	0.0	0.0	0.0	0.2	0.4
$\Sigma_{f^v}^r$	0.1	0.1	0.0	-0.4	-0.7

* $\Sigma_{12}^r = 0.0$ for all flux times

and the 2200 m/s flux-time from,

$$\theta^0 = \frac{\theta}{1.217} \quad (6.8)$$

The microscopic gross cross section of the fission products with cross sections less than 10,000 barns was evaluated by the method of Reference S3 for each flux-time step, taking into consideration the number of fissions from Pu239 relative to those from U235, considering that Pu239 was building up exponentially as it produced the fission products and that U235 was decaying exponentially, and increasing the resulting cross-sections by the ratio of the total yield of known plus unknown fission products to the known products. The resulting σ_{FP} varied from 55.8 b at 0.1 n/kb to 47 b at 0.7 n/kb. This calculation indicates that the input data value of 51.6 was a reasonable one. (This value was used in the NRX calculation only in computing the effect of fission product absorptions on the flux spectrum.)

Values of R were calculated for the NRX spectrum using Eq. (5.23) and Table 6.8. For small modifications to this spectrum or to basic physics parameters the changes in these base values of R were calculated from the following simplification of Eq. (5.23),

$$\delta R = 0.872 \delta(\hat{\Sigma}_f \nu) - 1.075 \delta \hat{\Sigma} \quad (6.9)$$

or for the true-flux cross sections,

$$\delta R = 1.06 \delta(\Sigma_f \nu) - 1.31 \delta \Sigma \quad (6.10)$$

Changes involved in the last two terms of Eq. (5.23) are negligible.

Results of these calculations are listed in Table 6.12.

Craig et. al., C11, p. 23, have used the same moderator temperature

(38°C) for the GLEEP spectrum as for the NRX reactor but assume that the epithermal proportion of neutrons to be 11/7 times that of the NRX reactor. The changes in the R values for the GLEEP from that of the NRX reactor were calculated using this information. The changes were only significant for U235, Pu239, and Pu240. The change in Σ_{10} was taken as

$$\delta\Sigma_{10} = \frac{4}{7} \Sigma_{10}^r \quad (6.11)$$

where Σ_{10}^r is given in Table 6.11. A different method was used for Pu239 and U235 since the 0.3 ev resonance absorptions in these nuclides are included in Σ^{th} . For well moderated reactors such as GLEEP the relative change in cross section can be derived from the Westcott factors, W11, where $\sigma = \sigma^0(g + rs)$

$$\frac{\delta\Sigma}{\Sigma} = \frac{\delta\sigma}{\sigma} = \frac{\delta rs}{g + rs} = \frac{\frac{\delta r}{r}}{1 + \frac{g}{rs}} \quad (6.12)$$

Evaluating these terms at $T_{\text{neutron}} = 60^\circ\text{C}$ and for $r = 0.042$ gives

$$\text{a) } \frac{\delta\Sigma_9}{\Sigma_9} = 0.082 \frac{\delta r}{r} \quad (6.13)$$

$$\text{b) } \frac{\delta\Sigma_{f,9}}{\Sigma_{f,9}} = 0.066 \frac{\delta r}{r} \quad (6.14)$$

$$\text{c) } \frac{\delta\Sigma_5}{\Sigma_5} = 2.8 \times 10^{-3} \frac{\delta r}{r} \quad (6.15)$$

$$\text{d) } \frac{\delta\Sigma_{f,5}}{\Sigma_{f,5}} = 1.2 \times 10^{-3} \frac{\delta r}{r} \quad (6.16)$$

The combination of changes c) and d) for U235 was found to give a negligible change in R values from those of the NRX reactor. The changes to R due to Pu240 and Pu239 were calculated from Eqs. (6.10), (6.11), (6.13) and (6.14) taking $\delta r/r = 4/7$.

Table 6.12 and Figure 6.28 provide a comparison between values of R determined experimentally in the GLEEP with those computed in different ways. Results computed as described in the previous paragraph are listed as Case 2) in Table 6.12 and are plotted as Curve B in Fig. 6.28. The experimental curve for the reactivity term R, from Reference C11, is shown as Curve A. Craig et al, C11, have corrected the experimental results for flux-dependent effects (mainly due to Pm149 and Np239 holdup) so that Curve A effectively gives the R values for NRX samples irradiated in a very low flux. The curves apparently extrapolate to points below zero because measurements were not given, nor calculations made, for flux-times below 0.05 n/kb where the Samarium group of fission products undergoes rapid buildup. Curve B, as calculated by FUELCYC intersects the ordinate at -11 bifa which is the value of R due to a saturated amount of the Samarium group. Curve C in Fig. 6.28 or Case 3) in Table 6.12 was calculated from Curve B taking into account the buildup of each member of this group according to,

$$\Sigma(\theta) = \Sigma_{\max} (1 - e^{-\sigma \theta}) \quad (6.17)$$

where the microscopic cross sections and the U235 fission yields recommended by Craig, C11, p.22, were used. These values are

Table 6.12 Reactivity Change Term, R, for the NRX Samples for Different Assumptions for Basic Parameters. (R in units of bifa for a 2200 m/s flux.)

Source of Data	Curve in Fig. 6.28	2200 m/s Flux-Time (n/kb)					
		0	0.0822	0.164	0.246	0.411	0.575
Experimental	A	0	0.0	3.1	2.6	- 4.3	-15.4
Calculated							
1) NRX Spectrum		-11.0	-7.2	-5.6	-5.6	-13.0	-20.6
2) GLEEP Spectrum	B	-11.0	-6.8	-5.1	-5.4	-13.5	-21.7
3) GLEEP Spectrum corrected for delayed buildup of Sm group	C	0	-5.5	-4.7	-5.2	-13.5	-21.7
4) Case 3), with "World Average Values"	D	0	-4.1	-2.0	-1.3	-7.4	-13.7
5) Case 3), with correction for Sm-149 yield	E	0	-3.5	-2.7	-3.2	-11.5	-19.7
6) Case 5), plus an increase in R. c. r. of 6% at low flux times, decreasing to 2% at $\theta^0 = 0.575$	A	0	0.0	3.1	2.6	- 4.3	-15.4

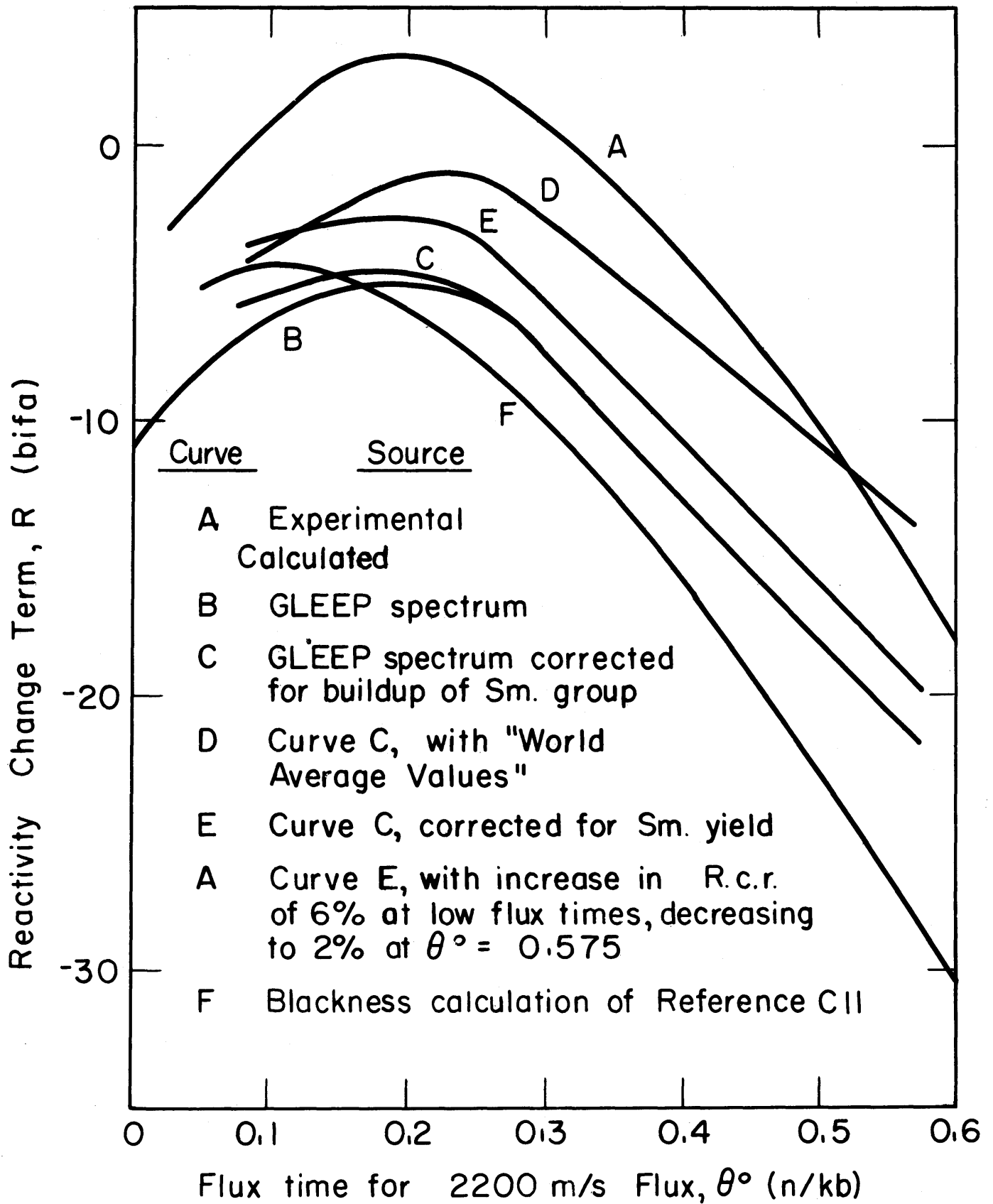


FIG. 6.28 VARIATION OF R FOR NRX FUEL AS MEASURED IN GLEEP

Table 6.13 The Samarium Group of Fission Products (with cross sections > 10,000 b)

Nuclide	Cross Section (barns)	U235 Fission Yield
Sm149	75,500	1.15
Sm151	12,000	0.45
Cd113	25,000	0.011
Eu155	14,000	0.031
Gd157	160,000	0.0074

given in Table 6.13. Curve C should agree with Curve A but is lower by 5 to 10 bifa, or roughly 0.003 to 0.006 in reactivity.*

It is interesting to note the sensitivity of this curve to small changes in the basic physics constants, a fact which has been pointed out both by Littler, L23, and by Craig, C11. For example, Curve D would have been generated by FUELCYC rather than Curve C had the "World Average Values" been used for σ_5 , σ_9 , $\sigma_{f,9}$, ν_5 , and ν_9 rather than the "World Consistent Values" which are now used in FUELCYC. Curve D gives fair agreement with the experimental data. Curve F is that calculated by Craig et al., C11, using Kushneriuk's cross sections and the "World Average Values" for nuclear parameters. Eq. (6.10) shows that a change in production cross section, $\Sigma_f \nu$, has an effect on R that is roughly the same in magnitude but opposite in sign to that of an absorption cross section. Table 6.9 shows that the effect of U235 on

*The reactivity can be estimated from R using the expression

$$\rho \sim \frac{R}{1600}$$

R is approximately equal but opposite to that of Pu239, and that these two nuclides have the greatest effect on R. For these reasons the following ratio is useful in the prediction of reactivity changes, and will be designated R. c. r. for "Reactivity change ratio,"

$$\text{R. c. r.} \equiv - \frac{\delta N_9 \sigma_9 (\eta_9 - 1)}{\delta N_5 \sigma_5 (\eta_5 - 1)} \quad (6.18)$$

For the FUELCYC calculations the R. c. r. varied from 1.34 at a flux-time (θ) of 0.1 to 1.18 at a flux-time of 0.7.

The 2200 m/s values for the σ 's and the η 's in Eq. (6.18) have standard deviations of approximately 1% according to BNL-325, which gives at 2% deviation in $(\eta-1)$ terms, and a total standard deviation in the R. c. r. of 6% if only these microscopic terms are considered. ($\sigma_f v$ has been replaced by $\sigma \eta$ in Eq. (6.18) however it should be noted that in the case of "World Average Values" it makes considerable difference which term is actually used.) This would allow an additional change to curve D of three times that change made in going from C to D, which is easily sufficient to force a considerably better fit to Curve A.

On the one hand this indicates that better values are needed for these constants before accurate long term reactivity calculations can be made, when starting with basic data. On the other hand, the combination of the theoretical calculations that have been made plus the experimental isotopic analysis and reactivity measurements for the NRX samples permit the recommendation of particular values for some of these parameters, within the standard deviations of the more basic

measurements. Let us proceed along the latter tack accepting Curve A as the true behavior. (The standard deviations of the experimental values for R were not indicated.)

Sm-149, has, effectively reached its saturation value at a flux-time (θ^0) of 0.05 n/kb so the "R" curves of Fig. 6.27 are smooth above this value. The intercept on the R axis should be the same for these curves if they are extrapolated back to zero flux-time from the point $\theta^0 = 0.05$. The initial value of R so obtained is essentially due to Sm-149. It is seen that the FUELCYC Curves C and D as well as the Canadian Curve E, intersect the axis at approximately -7 bifa. This is as it should be since the Samarium group of fission products, including yield values, was the same for both calculation ($y_{Sm,5} = 0.01649$, $y_{Sm,8} = 0.03154$). The experimental curve, however, has a higher intercept at a value of R of approximately -5. This suggests a value of 0.008 for the yield of Sm-149 rather than the value of 0.0115 which was used both in this paper and in the Canadian paper, C11. This reduction would give a Samarium group yield of $y_{Sm,5} = 0.0130$. It is recognized that the curve extrapolation is only rough; however, support for this Sm-149 yield value is given by the measurement of Littler, L23, of 0.009 ± 0.002 . Normalizing to the same extrapolated value of initial poisoning changes Curve C to Curve E as shown in Fig. 6.28. This curve is still considerably lower than the measured curve.

In the initial portion of the curve higher plutonium isotopes than Pu239 and the low cross section fission products have negligible effect, and the discrepancy must be due to a wrong value for the R.c.r. of Eq. (6.18). Since the calculational value used for the i.c.r. ($-\delta N_9 / \delta N_5$) agreed with

experimental data, C11, p. 20, it appears that the ratio of $\sigma_9(\eta_9 - 1)/\sigma_5(\eta_5 - 1)$ is in error. The error here could be due either to the basic point cross section data or to an error in the neutron temperature. The magnitude of the latter effect can be estimated by again referring to the Westcott parameters, W11, at approximately 60° C (and taking $r \sim 0.07$). A 20° C increase in temperature would produce: a 2% increase in σ_9 , a 1% decrease in $(\eta_9 - 1)$, a 0.5% decrease in σ_5 , and no change in $(\eta_5 - 1)$. The combined change in the R. c. r. would be a 1.5% increase for each 20° C increase in the neutron temperature, which would give an increase in R of approximately 0.7 bifa at a flux-time (θ) of 0.1 n/kb; and 3.9 bifa, at 0.7 n/kb. To fit the initial part of the curve would require an increase in the R. c. r. of approximately 6%, or a 80° C neutron temperature rise, if due to this factor alone. As pointed out in the Canadian report, C11, p. 28, later measurements by Tattersall et al, T8, indicate an additional 30° C temperature rise (T_{mod} for GLEEP of 70° C rather than 38° C). The additional increase in the R. c. r. required to match experimental data then appears to require changes to the 2200 m/s values for σ 's and η 's. The Canadian paper, C11, p. 26, suggests a 3% increase in the ratio $\sigma_{f,9}/\sigma_{f,5}$ over that of the "World Average Values" (which would be a 3.5% increase over the "World Consistent Values," and between a 3.5 to 7% increase in the R. c. r.) based on the recent measurements of Bigham et al, B24. This increase is sufficient to bring the FUELCYC results into agreement with the experimental results in the range from zero to 0.2 n/kb.

However, the above increase in the R. c. r. of 6% to fit the initial part of the curve results in an excess of about 10 bifa over the experimental curve at a flux-time (θ) of 0.7 n/kb ($\theta = 0.575$). Therefore consider the factors which would leave the initial part of the R curve unchanged but which would lower the curve at higher flux-times. These factors are:

1.) A decrease in the Pu239 cross section with flux-time. Such a decrease is indicated by the "blackness" calculations of Kushneriuk, C11, K11, due to self shielding in the 0.3 ev resonance. Kushneriuk's value for the average Pu239 cross section in the fuel rod decreases by 5% from zero to 0.6 n/kb ($\theta = 0$) while the FUELCYC cross section is approximately constant. A decrease in σ_0 of 4% at a flux-time (θ) of 0.7 n/kb gives a decrease in R of approximately 11 bifa.

2) An initial increase in the Pu239 cross section relative to that of U235, due to spectral hardening of the thermal flux, followed by a softening at higher flux-times, similar to the behavior of the pressurized light-water reactor. This would have been observed had the moderating ratio been lower, but would tend to peak the Pu239 cross section at a higher flux-time than indicated for the NRX results.

3) A decrease in the Pu240 disadvantage factor or an increase in the epithermal to thermal flux ratio. Run NRX2 would have given a decrease in R of approximately 12 bifa at a flux-time (θ) of 0.7 n/kb. This is the net change due in part to different concentrations of Pu240 and Pu241 but mainly reflects the change in disadvantage factors between these two runs: 1.2 for NRX2 versus 2.0 for NRX1 at a flux-time (θ) of 0.7 n/kb. (Errors in the Pu240 cross section produce their greatest effect in this flux-time range.)

4.) An increase in the cross section assumed for the unknown fission products. Doubling their cross section would decrease R by approximately 5 bifa at a flux-time (θ) of 0.7 n/kb.

It is thought that of the above possibilities the most probable is that the Pu239 cross section, and therefore the R. c. r., did indeed decrease a few percent during the irradiation, which is sufficient to bring the right hand side of the curve into agreement with the experimental results. It should be noted however that the cross sections calculated for Pu239 in FUELCYC gave excellent agreement with the isotopic analysis which indicates that the average absorption cross section for Pu239, as calculated by FUELCYC, was correct.

In summary, the most reasonable variations to bring the FUELCYC calculations into agreement with the experimental data for the NRX samples are:

1.) A change in the U235 fission yield of Sm 149 from 1.15% to 0.8%.

2.) An increase in the ratio $\sigma_9(\eta_9 - 1)/\sigma_5(\eta_5 - 1)$ of 6% at low flux-times, mainly due to changes in the point values of these terms versus energy. (This would increase the R. c. r. to 1.42 from 1.34)

3.) A progressive reduction of the increase in the above ratio until the increase is only 2% at a flux-time (θ) of 0.7 n/kb, where this reduction is primarily due to a drop in the value of σ_9 because of self-shielding. (This would give an R. c. r. of 1.20 instead of 1.18.)

3. Effect of Changes on Pressurized Light-Water Reactor Results

The question arises: what effect would the changes discussed in

Section VI.B.1 and VI.B.2 have on the results for the pressurized-light water reactor. The answer is that the effect would be small, due primarily to the longer irradiations considered for the latter cases. The effect of using different values for the Sm 149 yield, for the Pu240 disadvantage factor, and for the R.c.r. will be discussed in the following paragraphs.

A few approximate relationships have been derived from the NRX results and the pressurized light-water reactor results which will be useful in making the comparison. Eq. (6.19) relates changes in the true reactivity, $\rho = \delta k/k$, to changes in the reactivity change term R and in the cross sections for the NRX samples,

$$\delta\rho \sim \frac{\delta R}{1600} \sim \frac{\delta(\Sigma_f v - \Sigma)}{1200} \quad (6.9)$$

where R and Σ 's are in units of bifa. Table 6.14 gives values of different dimensionless ratios for the end of batch irradiations in the pressurized light-water reactor.

Table 6.14 Approximate Values of Different Scaling Ratios for the Pressurized Light-Water Reactor; Final Values for Batch Irradiation.

Ratio	Average Burnup (MWD/ton)		
	10,000	20,000	40,000
Fractional change in burnup per unit change in reactivity ($\delta E/E\delta\rho$)	7.8	4.5	2.9
Atoms of Pu239 per atom of fission product pairs (N_9/N_{FP})	0.25	0.18	0.12
Fraction of production cross section due to Pu239 ($\Sigma_9\eta_9/\Sigma\eta$)	0.55	0.62	0.70

A change in Sm 149 yield of U235 from the value 0.0115 to 0.008 would initially represent a cross section change of approximately -1.8 bifa in the NRX samples or, from Eq. (6.19), a reactivity change of 0.0015. (This would become less as U235 burned out.) From the ratio of $\delta E/E\delta\rho$ in Table 6.14 it can be seen that a reactivity change of 0.0015 in the pressurized light-water runs would give an error in average burnup (or in costs) of 1% or less.

As mentioned before it is thought that the method used by FUELCYC for the calculation of the Pu240 disadvantage factor is satisfactory for UO₂ fuel (due to the theoretical comparison made in Reference C13), even though it needed adjustment for uranium metal. Also, errors in the Pu240 cross section become of less importance at higher irradiations (1 n/kb and up) due to the compensating effect of Pu241. Both Reference C11 and Reference C13 show that the effect of errors in the Pu240 cross section reduces to zero within the burnup range of 10,000 to 15,000 MWD/ton. For these reasons it is estimated that errors in the Pu240 disadvantage factor for the pressurized light-water runs caused negligible error in the average burnup, and in cost values, for burnups of 10,000 MWD/ton or greater. (Had the error been as large (12 bifa in R) as that for run NRX2, the reactivity change would have been -0.007 and the relative burnup or cost change would have been a maximum of 5% .)

Consider R. c. r. changes as caused by a change in σ_9 . The required 2% increase in the R. c. r. for the most highly irradiated samples, would require a 2% increase in σ_9 . For the burnups of Table 6.14, Pu239 is near its saturated value. Also, small changes in the amounts of the

higher plutonium isotopes have little effect on the neutron balance due to the cancelling effect of Pu240 and Pu241 in this burnup range. For these reasons the only effect of a change in the Pu239 cross section (at a given flux-time after Pu239 has saturated) is an equal but opposite change in the number of atoms of Pu239. The neutron balance is unchanged. Therefore a 2% increase in σ_0 would cause a 2% decrease in N_0 . Since approximately two-thirds of Pu239 is destroyed by fission this represents an increase in the number of fissions, δN_{FP} , of $.013N_0$. Using the maximum value (0.25) of the ratio of N_0/N_{FP} from Table 6.14, the maximum relative change in the number of fissions, $\delta N_{FP}/N_{FP}$, is found to have the value 0.003. Therefore the change in average burnup and in costs would be less than 0.3% due to this effect.

Were the indicated 2% R. c. r. change due to a change in η_0 a 1% increase would be required. From Table 6.14 it is seen that a 1% increase in η_0 would give a 0.55% change in $\Sigma\eta$ at 10,000 MWD/ton which would also produce an increase in reactivity of 0.0055. This would produce a 4% increase in the average burnup at 10,000 MWD/ton but less at higher burnups.

This analysis has shown, that results presented for the pressurized water reactor are valid if the errors in the input data parameters are no larger than those indicated by the NRX experiments.

C. COMPARISON OF THE FUELCYC CALCULATIONS WITH THOSE OF A SIMPLER CODE

The results of calculations for the simpler model, as described in Section V.C., are presented here. A Batch fuel scheduling run and a Graded run were made with this model; both for the 3.44 a/o U235 enriched, pressurized-water reactor. The variations in the nuclide concentrations with irradiation are compared with those calculated by FUELCYC in Fig. 6.29. The good agreement is due to the choice of the resonance escape probability for U238 so that the initial conversion ratio would agree with that of FUELCYC and 2), the choice of the Pu240 cross section to agree with the average effective cross section in FUELCYC. Minor differences between the two codes are due to: 1) the more refined treatment of resonance captures in FUELCYC; and 2), the recalculation of thermal cross sections in FUELCYC as opposed to the assumption of constant values in the simpler method.

Table 6.15 compares the maximum and average burnups calculated by the present code for the above two runs with those calculated by the simpler code for a chopped $\cos-J_0$ flux and a spatially uniform flux.

The simpler code applied to the chopped $\cos-J_0$ flux does remarkably well in predicting the maximum burnup but the agreement is much poorer for the average burnup. The main error is introduced in the averaging of the properties over a chopped $\cos-J_0$ flux rather than over the true flux distribution, which is considerably more flattened. This error in the average burnup is on the order of 25% for the two cases studied. Results for spatially uniform flux are worse than for the $\cos-J_0$ results

for Batch Irradiation, as would be expected, but are actually better than the $\cos-J_0$ results for the average burnup in Graded fuel scheduling.

Table 6.15 Values for the Maximum and Average Burnup, in MWD/ton, Predicted by Different Physical Models.

Fuel Sch'd.	Type of Burnup	FUELCYC	"Simpler" Code			
			Chopped-Cos, Chopped- J_0 Flux	Rel. Error	Constant Flux	Rel. Error
Batch	Maximum	17900.	18400.	-3%	11600.	35%
Batch	Average	8650.	6110.	29%	11600.	-34%
Graded	Maximum	27400.	26200.	4%	22500.	18%
Graded	Average	22800.	17700.	22%	22500.	-1%

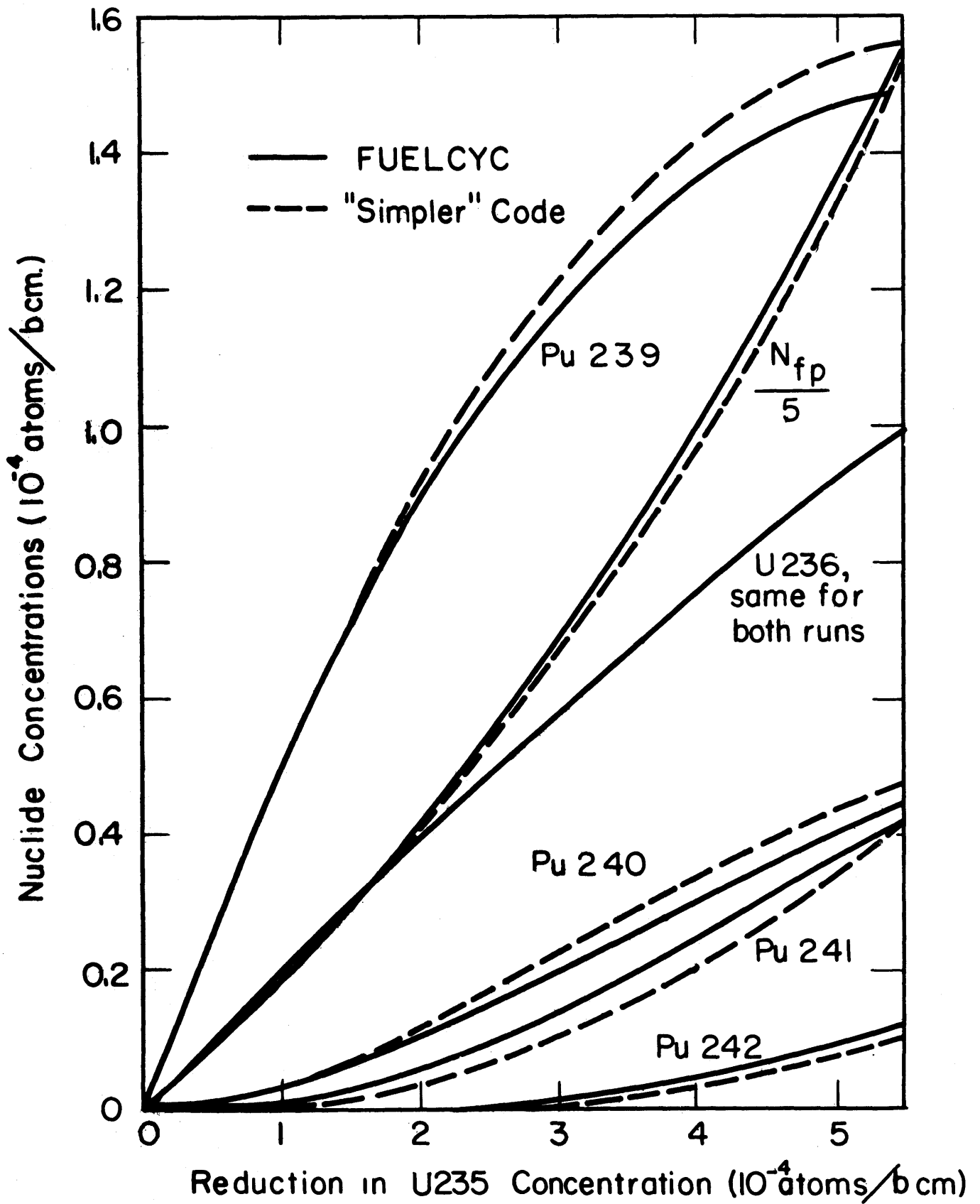


FIG. 6.29 COMPARISON OF NUCLIDE CONCENTRATIONS: THE "SIMPLER CODE" VERSUS FUELCYC.

VII. CONCLUSIONS

A. COMPARISON OF FUELCYC CALCULATIONS WITH EXPERIMENT

The only experimental results available for this work which could be compared with the predictions of FUELCYC are on the irradiation of uranium metal rods in the NRX reactor at relatively low flux-times (up to 0.63 n/kb) (Reference C11). The isotopic content of plutonium observed in this irradiated metal is in fair agreement (0.5%) with the prediction of FUELCYC; excellent agreement (0.1%) can be secured by adjusting $\Sigma_{s,fl}$, the input parameter of the code used to compute the Pu240 resonance disadvantage factor. For UO₂ fuel, however, it is believed that no adjustment is needed, since good agreement was obtained with a more refined theoretical model (Reference C13) for this fuel material.

The reactivity of fuel irradiated in the NRX reactor has been measured in the GLEEP. The reactivity predicted by FUELCYC is in fair agreement with that observed in GLEEP, falling within 9 barns per initial fissile atom, or 0.6% of the observed reactivity. The discrepancy can be eliminated by: (1) decreasing the yield of Sm149 in the fission of U235 from 1.15% to 0.8%, (2) adjusting the parameter $\sigma_9(\eta_9-1)/\sigma_5(\eta_5-1)$ for 2200 m/s properties of Pu239 (subscript 9) and U235 (subscript 5) by amounts which fall within the standard deviations assigned to measured values of cross sections (σ) and neutron yields (η). An increase of 6% in this parameter is needed at low flux-times and 2% at a flux-time of 0.7 n/kb. At the higher flux-times of interest for power-reactor irradiations, the reactivity is less sensitive to changes in these

parameters, and FUELCYC with its present input properties is deemed capable of giving results of sufficient precision for practical fuel cycle analysis.

B. PERFORMANCE OF CODE

A thorough set of debugging runs have been made for the FUELCYC code. The results of these runs and the runs made for this study indicate that the code is performing correctly. The convergence methods used have been found to be reliable and rapid.

The entire set of twenty runs (each using fifty mesh points) for the pressurized light-water reactor required a total computer time of only 70 minutes. This performance shows that FUELCYC can be used for extensive fuel-cycle studies without excessive use of computer time.

Since FUELCYC generates most of the parameters required for its calculation (such as values for cross sections, α 's, and η 's) the input data preparation is minimal. The code is divided into many subroutines and as a result is particularly easy to modify for the addition of new methods of fuel scheduling or for new techniques of programming control rods.

It is intended to make FUELCYC binary decks available for distribution. Further information may be obtained from R. T. Shanstrom.

C. STUDY OF ALTERNATE FUELING METHODS

Of the four fueling methods studied, batch irradiation leads to highest fuel costs for a specified burnup. The three other methods lead to costs that are lower by from 0 to 1 mill/kwh, depending on the

burnup. Movement of fuel from outside to inside leads to the flattest distribution of flux and power density, and is the most advantageous fueling method for this reason and because of its lower fuel cost.

D. FUEL CYCLE COSTS IN PRESSURIZED WATER REACTOR

Because of the marked decrease in fuel-cycle costs as the average burnup is increased there is a strong economic incentive in this pressurized-water reactor to develop fuel elements capable of withstanding average burnups of 20-25,000 MWD/ton and maximum burnups of 30-40,000 MWD/ton and to use a fueling method and feed enrichments which give enough excess reactivity to permit attainment of these average burnups in reactor operation. If burnups of this order of magnitude can be obtained, fuel-cycle costs in this pressurized light-water reactor can be reduced to 3.5 mills/kwh for simple Batch irradiation and 2.5 mills/kwh for the Graded or Outin fuel scheduling methods, based on present AEC prices.

At these high burnups, rental and burnup charges for U235 and the fuel fabrication costs are the most important components in the fuel cycle cost. The most important single factor is the initial price of the enriched UF_6 . The charge for the production of UF_6 from the spent fuel that is now made by the AEC, approximately \$25/kgm U for this reactor adds only 0.2 mills/kwh to the fuel cycle cost at a maximum burnup of 30,000 MWD/ton, and is not important even at lower burnups.

Changes in the rental charge for UF_6 , the price scale for UF_6 and the credit for plutonium would have a pronounced effect on the

fuel-cycle cost. For example, an increase in the UF_6 rental charge from 4% to 12% per year would add about 2 mills/kwh to the overall cost. A reduction of 33% in UF_6 price scale would reduce fuel cycle costs by about 1 mill/kwh. Increase in plutonium credit from \$12 to \$30 per gm would decrease fuel cycle costs by 1.5 mills/kwh at low burnup and about half this at high burnup.

VIII. RECOMMENDATIONS FOR FUTURE WORK

A. USE OF FUELCYC

It is recommended that the current version of the FUELCYC code be used for fuel-cycle analyses in large uranium-fueled power reactors, which have azimuthal symmetry, and in which most of the reactions occur at thermal energies. S. L. Amberg of M. I. T. is currently using FUELCYC for the analysis of a 150 eMw organic-moderated reactor and N.B. McLeod is undertaking the study of a 200 eMw heavy-water-moderated, natural-uranium-fueled reactor.

B. EXTENSION OF FUELCYC

The library of FUELCYC fuel-scheduling and control-rod programming subroutines should be extended. A fuel-scheduling method of particular interest is the bi-directed axial flow (of short fuel slugs) method proposed by Dr. Lewis, L19, since essentially uniform fuel burnup is achieved. This technique has already been coded by P. Steranka of M. I. T. and is now being debugged. Another fuel scheduling method of interest is the axial inversion technique. In this method fuel rods of half (or less) the core length are periodically inverted to give a more uniform burnup. This inversion technique could perhaps be combined with Outin radial motion to give flux-flattening along with more uniform burnup.

Non-uniform initial loadings could be studied. These cases are of interest in breeder reactors, in flux-flattening, and in the approach to steady state operation.

For non-steady state operation the method in which control poison is inserted has a strong effect on the flux shape. For example, there will be some program of control rod motion, which gives preference to the removal of outer control rods with respect to inner rods as irradiation progresses, that will flatten the flux radially without causing severe peaks where the rods are removed. P. Steranka also has a control-rod programming subroutine in the debugging stage as a first step in this investigation. Studies of burnable poisons are of interest; either homogeneous poisons or heterogeneous poisons, shaped in a manner to give the desired changes in reactivity worth as irradiation progresses.

Studies of recycling and of other fuel mixtures are also of interest. In this area another M. I. T. student, J. M. Neill, is currently undertaking a modification of FUELCYC to allow study of thorium fuel.

C. OPERATIONS ANALYSIS STUDY

A complete analysis of the effects of the fuel cycle on power production cost for a specific reactor would be of considerable interest. Items not included in the present study which should be considered are:

- 1) the effect of a finite number of fuel elements on the degree to which steady-state fueling could be approached
- 2) the effect of a finite number of control rods on techniques for programming control of the reactor
- 3) the reactor start-up period and approach to the final-state of fuel scheduling
- 4) the effect of different fuel scheduling methods on the operating costs of the reactor and on the fraction of the time it is in operation.
- 5) the effect of variations in the maximum to average power

density ratio on the capital charges, taking into consideration all of the equipment required for power production (i. e., turbines, generators, and heat exchangers, as well as the reactor).

The ultimate purpose of this study would be to determine the optimum methods of fueling and controlling the chosen reactor.

D. COMPARISON WITH EXPERIMENTAL DATA

Additional comparison of the calculations of FUELCYC with experimental data is recommended as these data become available. Parts B and C of Reference W17, when issued, will give additional information on the NRX irradiations of natural uranium metal.

There is an obvious need, however, for experimental data on the behavior of UO_2 fuel during irradiation. Measurements of interest which should be taken at intervals as the irradiation progresses are: nuclide compositions, both average values and values as a function of position in the fuel element; reactivity measurements; and the flux history of the irradiation, with values for the flux (and flux-time) as a function of position in the fuel element.

E. EXPERIMENTAL WORK IN THE M. I. T. REACTOR

As pointed out in Section VI. B., the reactivity of the fuel for all degrees of irradiation are of interest. The very low region, 0.05 n/kb and less, is of interest in studying the buildup of the Samarium group of high cross section fission products. The range from 0.05 to approximately 2 n/kb is of interest in tying down values for the initial conversion ratio and the reactivity change ratio. Longer irradiations give information on the effect of higher plutonium isotopes. The feasibility of initiating an experimental program of irradiation and reactivity

measurement in the M. I. T. reactor should be investigated, to study the low irradiation range. (0.05 n/kb could be achieved in approximately 100 days of operation at a flux of 5×10^{12} n/cm² sec.)

F. FURTHER THEORETICAL INVESTIGATION

If further theoretical refinements are undertaken for the FUELCYC calculational method, it is suggested that the local spatial properties of the fuel be investigated. This could be directed towards more exact techniques for the calculation of disadvantage factors and for consideration of the uneven buildup of higher isotopes in the fuel element as irradiation progresses.

IX. APPENDIX

A. NUMERICAL SOLUTION OF THE WILKINS EQUATION

The Wilkins Equation is the second order differential equation

$$x^2 \frac{d^2 Y}{dx^2} + (2x^3 - 3x) \frac{dY}{dx} + (2x^2 - 4x^2 A(x) + 3) Y = 0 \quad (1)$$

where,

$$Y = \frac{d\phi}{dx} \quad (2)$$

and x is the dimensionless velocity variable normalized to the velocity corresponding to kT_{md} , (see H 21). Since (1) is a linear equation, Y can be replaced by a new function, y , which will eliminate the first derivative. This is convenient since we aren't concerned with the values of Y' . The proper function is,

$$y = Yx^{-3/2} e^{x^2/2} \quad (3)$$

which, when substituted for Y in Eq. (1), gives the working form of the Wilkins Equation,

$$4x^2 \frac{d^2 y}{dx^2} - [4x^4 - 16x^2 + 16x^2 A(x) + 3] y = 0 \quad (4)$$

Equation (4) is then solved numerically by a fifth-order Milne method, H27, p. 223, where the relationship,

$$y_i^{(0)} = y_i + y_{i-2} - y_{i-3} + \frac{\mu^2}{4} (5y_i'' + 2y_{i-1}'' - 5y_{i-2}'') + O(\mu^6) \quad (5)$$

is used for prediction, in which μ is the constant spacing in normalized velocity, $\mu = \delta x$, and the relationship,

$$y_{i+1} = 2y_i - y_{i-1} + \frac{\mu^2}{12}(y_{i+1}'' + 10y_i'' + y_{i-1}'') + O(\mu^6) \quad (6)$$

is used for revision of the initial estimate for y_{i+1} given by (5). The y_i are then generated step by step from Eqs. (5) and (6) using Eq. (4) to calculate the required values of y_i'' . It is seen that information is required four velocity steps back or, in particular, to calculate y_4 from Eqs. (5) and (6) we need previous values for: $y_0, y_1, y_2, y_3, y_1'', y_2''$, and y_3'' . The method used is to start at $x = 0$ and obtain the required terms by a series solution of Eq. (4) assuming $1/v$ cross sectional behavior in this initial region. With this assumption Eq. (4) can be rewritten for startup in terms of $\Delta = 4xA(x)$ which is a constant. The variable s where,

$$s^2 \equiv x \quad (6)$$

is substituted for x to eliminate the exponents of order $1/2$ which are required. This requirement can be anticipated by the form of y for a Maxwell-Boltzmann flux, namely

$$y_{M.B} = (\text{const.}) x^{3/2} e^{-x^2/2} \quad (6.4)$$

since,

$$Y_{M.B} = (\text{const.}) s^3 e^{-x^2} \quad (6.6)$$

This changes Eq. (4) to,

$$s^2 \frac{d^2 y}{ds^2} - s \frac{dy}{ds} - (4s^8 - 16s^4 + 4s^2 \Delta + 3)y = 0 \quad (7)$$

A solution is assumed in the form,

$$y = \sum_{k=0}^{\infty} a_k s^k \quad (8)$$

which yields the requirement,

$$\sum_{k=0}^{\infty} a_k \{ [-3+k(k-2)] s^k - 4\Delta s^{k+2} + 16s^{k+4} - 4s^{k+8} \} = 0 \quad (9)$$

Or, equivalently,

$$\sum_{k=0}^{\infty} \{ [-3+k(k-2)] a_k - 4\Delta a_{k-2} + 16a_{k-4} - 4a_{k-8} \} s^k = 0 \quad (10)$$

if the a's with negative subscripts are understood to be zero. Setting the successive coefficients equal to zero gives,

$$a_k = 0, \quad \text{for } k \text{ negative or even} \quad (11)$$

$$a_1 = 0 \quad (12)$$

$$a_3 = 1, \quad \text{can be chosen arbitrarily} \quad (13)$$

$$a_5 = \frac{\Delta}{3} \quad (14)$$

$$a_7 = -\frac{1}{2} + \frac{\Delta^2}{24} \quad (15)$$

$$a_9 = -\frac{11\Delta}{90} + \frac{\Delta^3}{360} \quad (16)$$

or in general,

$$a_k = \frac{4[a_{k-8} - 4a_{k-4} + \Delta a_{k-2}]}{k(k-2) - 3}, \quad \text{for odd } k \quad (17)$$

The value of Δ at $x = 2\mu$ is used for the startup constant.

$$\Delta = 4x_2 A_2 = 8\mu A_2 \quad (18)$$

Eq. (8) can now be written in terms of x and a more convenient set

of coefficients, b_j :

$$y = x^{1/2} \sum_{j=1}^{\infty} b_j x^j \quad (19)$$

where,

$$b_j \equiv a(2j+1) \quad (20)$$

and in general,

$$b_j = \frac{4[b_{j-4} - 4b_{j-2} + \Delta b_{j-1}]}{(2j+1)(2j-1) - 3} \quad (21)$$

Startup values of y_i are calculated from Eq. (18), truncating when the magnitude of the last calculated term becomes less than 10^{-6} times the sum of the preceding terms. After the first four points, Eqs. (5) and (6) are used to generate the y_i . Values for Y_i are obtained from the y_i by applying Eq. (3). An estimate of the truncation error in the i^{th} step after startup is given by,

$$F_{T,i} \sim - \frac{Y_i}{18} \quad (22)$$

where

$$Y_i = y_i - y_i^{(0)} \quad (23)$$

The cumulative truncation error for the Milne solution up to step i is then roughly estimated from,

$$F_{\text{cum},i} = \sum_{k=5}^i F_{T,k} \quad (24)$$

B. A CONDENSED CROUT REDUCTION THAT MINIMIZED THE STORAGE AND TIME REQUIREMENTS

The Gauss reduction is a well known method of solving sets of linear algebraic equations, and the Crout reduction is a modification of this technique which reduces the storage of intermediate data, see H-27, Chap. 10. Nevertheless, for the solution of a set of n_L equations in n_L unknowns, the complete Crout reduction requires the calculation and storage of a $n_L \times n_L$ auxiliary matrix. For n_L equal to approximately 180 this equals the entire fast memory capacity of the full IBM-704 computer. (Core memory is 32,768 words.) In many cases, however, such as the reactor problems of this work, advantage can be taken of the many zero elements in the matrix to effect a considerable reduction in the storage requirement, as well as in the computer time requirement.

The equations of this appendix illustrate the method for the two-dimensional, five-point-difference, spatial flux-shape problem described in IV. A. 2. The subscript notation is in general different from the normal matrix notation so that the equations can be coded directly, in a system such as Fortran for the IBM-704, without wasting storage space. The method described here requires less than $(2r_L + 1) n_L$ storage spaces for the auxiliary matrix, where $n_L = r_L z_L$. For $r_L = z_L$ this gives a reduction in storage space by a factor of approximately $n_L/2$ from that required by the standard Crout reduction.

Consider the set of linear equations of Chap. IV, Eq. (4.59),

$$d\phi = c \tag{1}$$

where d is the coefficient matrix, c is the constant column matrix, corresponding to the assumed source term $\gamma e \phi$ in Eq. (4.59), and ϕ , in Eq. (1), is the column matrix of the unknown fluxes, $\phi_{r,z}$.

The radial index, r , and axial index, z , can be replaced by the single row index, n , which is defined by,

$$n \equiv r + (z-1) r_L \quad (2)$$

where,

$$1 \leq n \leq n_L$$

and,

$$n_L \equiv r_L z_L \quad (3)$$

So here the $\phi_{r,z}$ of IV. A.2 will be written ϕ_n ; the $d_{r,z,u}$ as $d_{n,u}$ etc.

The coefficient matrix d has the form illustrated in Fig. B1., where the non zero elements fall on five diagonals: the principal diagonal, those on each side of it, and the diagonals r_L units away from the principal diagonal. This causes the Crout coefficient auxiliary matrix to have only zero terms outside of the diagonals r_L units away from the principal diagonal, so there is no need to include these terms in the calculational procedure or to save computer core space for them. The nomenclature for the terms in this auxiliary matrix is illustrated in Fig. B2. The purpose of the indexing system is merely to give consecutive numbers to the non-zero terms so as to exclude the storage of zero terms. It is seen from Figs. B1. and B2, that the first index is the row index and the second is a diagonal index.

The following equations define the method of calculation of this reduced Crout coefficient auxiliary matrix.

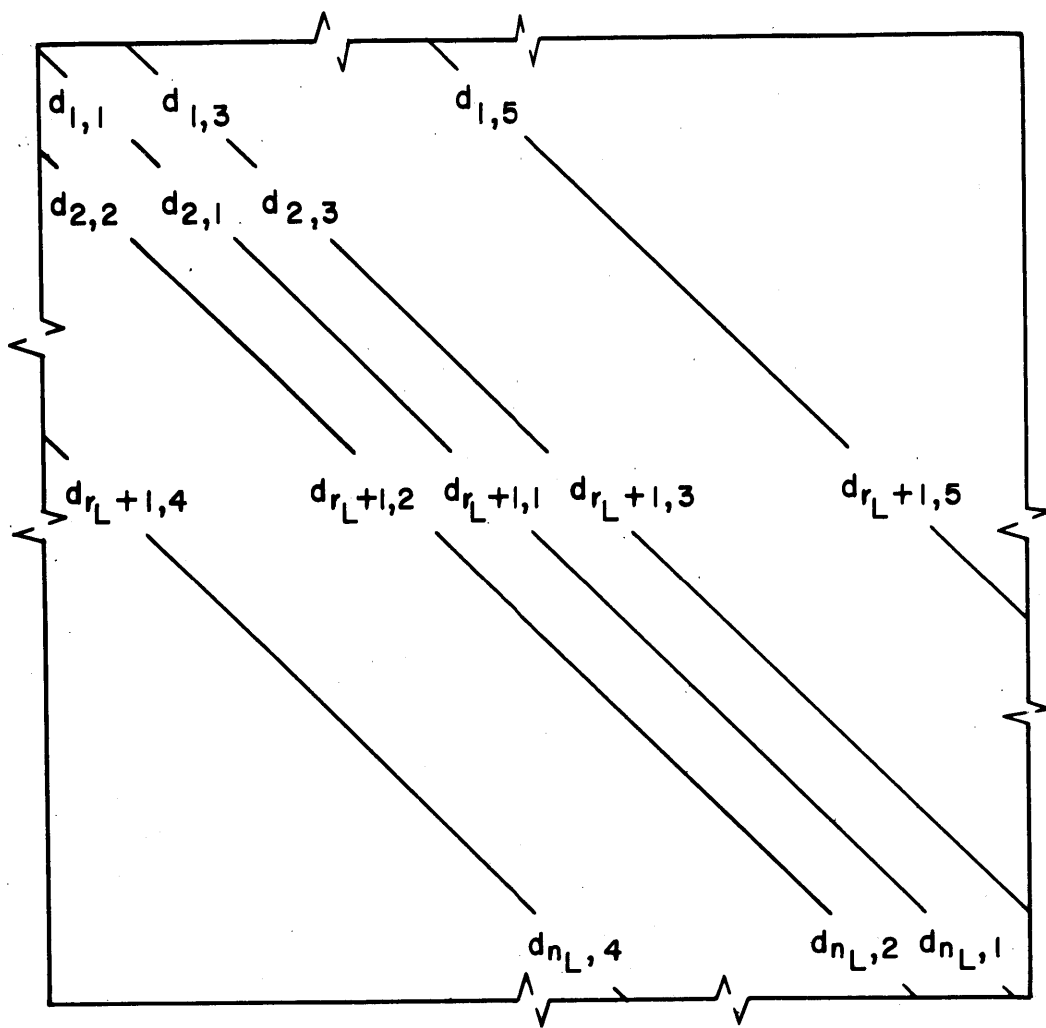


FIG. B1. SCHEMATIC DIAGRAM OF THE COEFFICIENT MATRIX FOR THE SPATIAL FLUX SHAPE

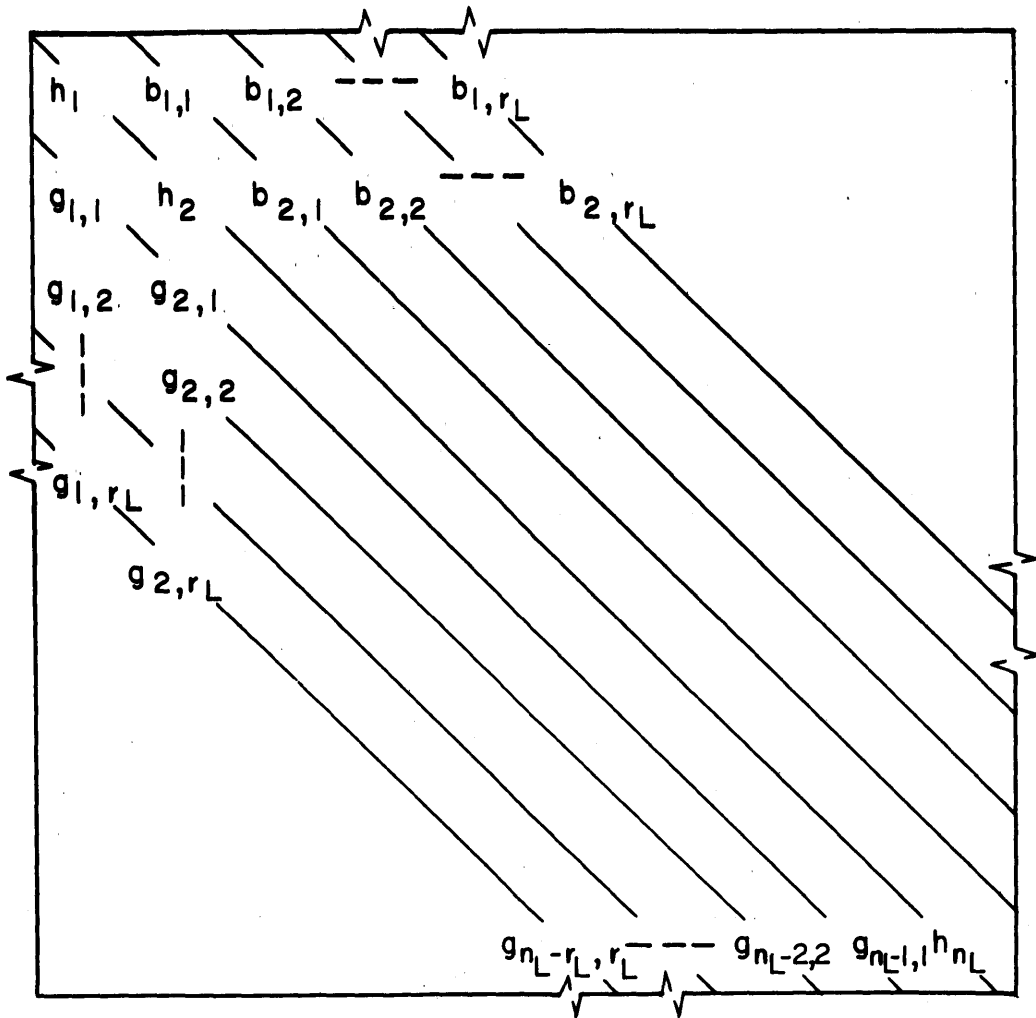


FIG. B2. SCHEMATIC DIAGRAM OF THE CROUT COEFFICIENT AUXILIARY MATRIX

$$h_1 = d_{1,1} \quad (4)$$

$$g_{1,1} = d_{2,2} \quad (5)$$

$$g_{1,r_L} = d_{r_L+1,4} \quad (6)$$

$$b_{1,1} = d_{1,3}/h_1 \quad (7)$$

$$b_{1,r_L} = d_{1,5}/h_1 \quad (8)$$

$$g_{1,k} = b_{1,k} = 0 \quad , \quad 2 \leq k \leq r_L - 1 \quad (9)$$

The remainder of the auxiliary matrix is obtained by repeating the sequential calculations of Eq. (10) through Eq. (14), starting with $n = 2$ and increasing n by 1 each loop until $n = n_L$. When $n > (n_L - r_L)$ Eqs. (13) and (14) are omitted and when $n = n_L$ only Eq. (10) is calculated.

$$h_n = d_{n,1} - \sum_{i=m}^{n-1} g_{i,n-i} b_{i,n-i} \quad (10)$$

where

$$m = 1 \quad , \quad n \leq r_L$$

$$m = n - r_L \quad , \quad n > r_L$$

Equation (11) and Eq. (12) are repeated for the same value of n , starting with $k = 1$ and increasing by one until $k = k_L$ where,

$$k_L = r_L - 1 \quad , \quad n \leq n_L - r_L$$

$$k_L = n_L - n \quad , \quad n > n_L - r_L$$

$$g_{n,k} = \sum_{i=m_2}^{n-1} g_{i,n+k-i} b_{i,n-i} + \delta(k) d_{n+1,2} \quad (11)$$

where,

$$m_2 = 1 \quad n \leq r_L - k$$

$$m_2 = n + k - r_L \quad n > r_L - k$$

$$\delta(k) = 1 \quad k = 1$$

$$\delta(k) = 0 \quad k \neq 1$$

$$b_{n,k} = \frac{1}{h_n} \left[- \sum_{i=m_2}^{n-1} b_{i,n+k-i} g_{i,n-i} + \delta(k) d_{n,3} \right] \quad (12)$$

$$g_{n,r_L} = d_{n+r_L,4} \quad (13)$$

$$b_{n,r_L} = \frac{d_{n,5}}{h_n} \quad (14)$$

Having calculated the coefficient auxiliary matrix one now proceeds to calculate the constant auxiliary matrix. The terms of the c matrix of Eq. (1) are known. These values would have been calculated from the last estimate for the fluxes, Eq. (4.59),

$$c = \gamma e \phi \quad (15)$$

The constant auxiliary column matrix composed of f_n terms, is then formed according to Eqs. (16) and (17).

$$f_1 = \frac{c_1}{h_1} \quad (16)$$

Equation (17) is repeated starting with $n = 2$ and increasing by one until $n = n_L$.

$$f_n = \frac{1}{h_n} \left[c_n - \sum_{i=m_3}^{n-1} f_i g_{i,n-i} \right] \quad (17)$$

where,

$$m_3 = 1 \quad n \leq r_L$$

$$m_3 = n - r_L \quad n > r_L$$

The solution matrix, containing the new values for the fluxes, ϕ_n , is then obtained according to Eqs. (18) and (19),

$$\phi_{n_L} = f_{n_L} \quad (18)$$

Equation (19) is the repeated starting with $n = n_L - 1$ and decreasing by one each time until $n = 1$.

$$\phi_n = f_n - \sum_{i=1}^{m_4} b_{n,i} \phi_{n+i} \quad (19)$$

where,

$$m_4 = n_L - n \quad n > n_L - r_L$$

$$m_4 = r_L \quad n \leq n_L - r_L$$

The new flux values are then normalized if desired (to $\phi_1 = 1$ in this work), and the procedure of Eq. (15) to Eq. (19) is repeated until successive values of ϕ_n converge. (The criterion used here for convergence is that

$$\frac{\phi_n^{(i+1)} - \phi_n^{(i)}}{\phi_n^{(i+1)}} \leq .01 \text{ for all values of } n)$$

The iterations are rapid since they do not require recalculation of the auxiliary coefficient matrix.

C. FUELCYC SUBPROGRAMS

Each section of this appendix describes one of the subprograms which were developed for FUELCYC. The standard Fortran II subprograms that are required are listed but not described. A discussion of the MAIN program has been given in Section IV. C.3., and Fig. 4.6 explains the flow chart symbols that are used. The current absolute locations are indicated under "Space required.", however, these are not fixed positions since all subprograms are relocatable. The symbolic meaning of the subprogram's name is given in parenthesis in the Purpose statement when not obvious. Many of the indicated print steps were primarily for debugging purposes and have now been bypassed by octal correction cards, as indicated on the flow charts. If desired, these print outs can be reactivated merely by the removal of the appropriate correction card. "Input arguments" and "Output parameters" are listed to show the required flow of information between subprograms. Additional information for running FUELCYC is given in Appendix D.

1. LOADER

Purpose: to load and relocate binary cards, BCD identification cards, and octal correction cards.

Subprograms called: The MIT subprograms WOT, NOLOAD, OCTOFF, STPRNT, WOTF (these subprograms will not be discussed here).

Space required: 641, $(30-1230)_8$

Discussion: The symbol table is written off-line by STPRNT and octal correction cards are written off-line by OCTOFF, NOLOAD gives an on-line diagnostic print if the cards fail to load. Octal correction cards are discussed in Appendix D. 2.

2. MAIN

Space required: 8000, $(1231-20730)_8$

Discussion: The flow chart and discussion of MAIN is given in Section IV. C. 3.

3. READ-PRINT

Purpose: to read cards, read or write tapes, and to print on line.

Subprograms called: The standard Fortran II read-print subroutines: DBC, CSH, SPH, FIL, BDC, STH, RTN, and LEV.

Space required: 2427, $(20731-23357)_8$

4. TIMECK

Purpose: to write the time and identify the location in the program (for timing different parts of the code). (Time check)


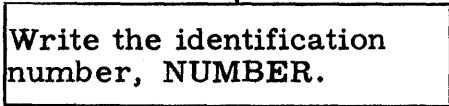

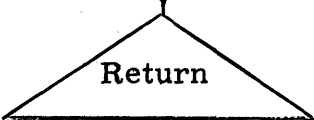
Input arguments: NUMBER

Output parameters: none

Subprograms called: TIME, PRINT

Space required: 42, (23360-23431)₈

Discussion: A "real time" clock must be connected.

<u>Step</u>	<u>Flow Chart</u>	<u>Comments</u>	<u>Fortran Statement Number</u>
1.			
2.			10
3.		Write the time.	
4.			

5. TIME - CLOCK

Purpose: to write the time and/or date.

Input arguments: i

Space required: 148, (23432-23655)₈

Discussion: This is an MIT subprogram. Transfer to TIME causes the time to be written on tape i; transfer to CLOCK causes the date and time to be written on tape i. A clock must be connected.

6. CONST

Purpose; to tabulate the nuclear constants which are invariant for all cases. (Constants)

Input arguments: none

Output parameters: $\nu_m, \alpha_m, \eta_m, Y_{Xe, m}, Y_{Sm, m}$ for $m = 5, 8, 9, 11$

λ_{Xe}, I_m^∞ for $m = 5, 6, 8-12$

Subprograms called: PRINT

Space required: 290, (23656-24317)₈

Discussion: The value of λ_{11} is tabulated in NUCON. η 's and α 's are averages for the resonance region, except for U238 for which they are fast fission terms. The values used for these parameters have been listed in Table 4.1.

<u>Step</u>	<u>Flow Chart</u>	<u>Comments</u>	<u>Fortran Statement Number</u>
1.	<pre> graph TD A[6 CONST] --> B[Tabulate nuclear constants.] B --> C[Write nuclear constants.] C --> D[Return] </pre>		
2.			10-30
3.			40-90
4.			

7. PTCS

Purpose: to calculate and tabulate the microscopic cross sections of the fuel nuclides at different velocities in the thermal range. (Point cross sections)

Input arguments: i_L, μ_v

Output parameters: $\sigma_{i,m}$ for $1 \leq i \leq i_L$

$m = 5; 6; 8 \text{ to } 12; f, 5; f, 9; f, 11$

Subprograms called: PRINT

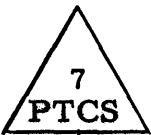
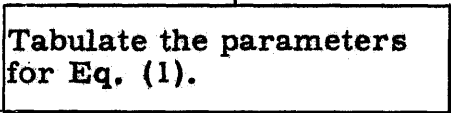
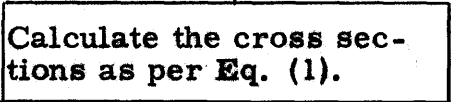
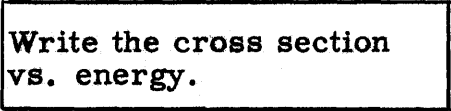

Space required: 634+530 common, (24320-25511)_g, (76441-77462)_g

Discussion: The cross sections are calculated at the velocities $i\mu_v v_0$, where μ_v is the spacing normalized to v_0 , and i takes values from unity to i_L . (i_L must be odd and less than 100.)

The method used is to calculate the cross sections at each velocity point using the equations given by Westcott, W11. The fit equation is:

$$\sigma(E) = E^{-1/2} a + \sum_{j=1}^n \frac{C_j}{b_j + (E - e_j)^2} \quad (1)$$

The parameters a , b_j , c_j , and e_j are tabulated in W11 for the nuclides required. These terms are the resolved resonance parameters for energies near resonances and are chosen so that the sum of "resonance type" terms fits the BNL-325 curves in regions away from the resonances. Normalization values for the cross sections have been listed in Table 4.1.

<u>Step</u>	<u>Flow Chart</u>	<u>Comments</u>	<u>Fortran Statement Number</u>
1.			
2.			10-160
3.		Taking velocity steps of $\mu_v v_0$.	170-300
4.		Normally bypassed.	310-320
5.			

8. AVGCS2

Purpose: to calculate average thermal cross sections for the fuel nuclides
(Average cross sections, 2nd revision).

Input arguments: $T, \sigma_{i,m}, \xi \Sigma_s, N_m, N_{8p}, \Sigma_{md}, \psi, V_{fl}, \mu_v, i_L$

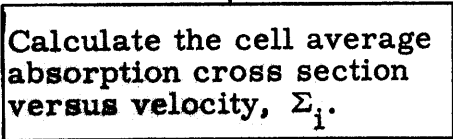
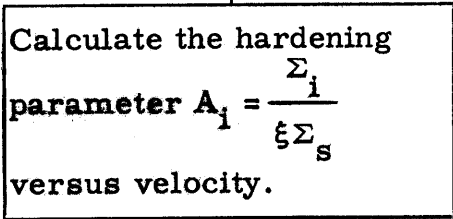



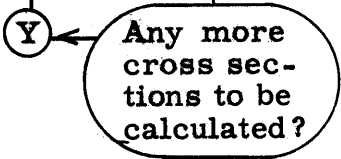
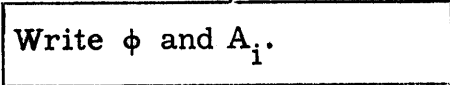
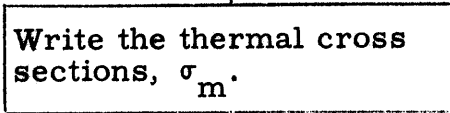
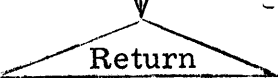
Output parameters: σ_m , for $m = 5; 6; 8$ to $12; f, 5; f, 9; f, 11$

Subprograms called: WILK2, FLF2, CSF2, PRINT

Space required: 450, (25512-26413)₈

Discussion: N_{8p} is a term proportional to the concentration of fission products which when multiplied by the microscopic cross section of U238 will give the proper effect of fission products in hardening the thermal neutron spectrum. The reason for treating fission products in this way is that the cross sections of fission products, like U238, are assumed to be inversely proportional to velocity, and the $1/v$ dependence of the U238 cross section is available to this subprogram.

<u>Step</u>	<u>Flow Chart</u>	<u>Comments</u>	<u>Fortran Statement Number</u>
1.	<pre> graph TD A[8 AVGCS2] --> B[Calculate the equivalent additional pseudo amount of U-238 to give Σ_{md} a 1/v behavior (energy wise).] </pre>		
2.	<div style="border: 1px solid black; padding: 5px; width: fit-content;"> Calculate the equivalent additional pseudo amount of U-238 to give Σ_{md} a $1/v$ behavior (energy wise). </div>	Requires an estimate of σ_8 .	10-30

<u>Step</u>	<u>Flow Chart</u>	<u>Comments</u>	<u>Fortran Statement Number</u>
3.		i is the velocity step index.	10-30
4.			10-30
5.		Calculate the energy spectrum.	
6.		Calculate the integrated flux, φ.	
7.		Calculate the cross sections, σ _m .	46
8.			50
9.		Normally bypassed.	60
10.			70
11.			

9. WILK2

Purpose: to solve for the energy distribution of the thermal flux according to Wilkins equation. (Wilkins)

Input arguments: T, i_L, μ_v, A_i

Output parameters: $Y_i = \frac{d\phi}{dx}$

Subprograms called: PRINT, EXP, SQRT

Space required: 517 + 519 common, (26414-27420)₈, (76454-77462)₈

Discussion: The equations used to generate the Wilkins spectrum are given in Appendix A.

<u>Step</u>	<u>Flow Chart</u>	<u>Comments</u>	<u>Fortran Statement Number</u>
1.			
2.			
3.		Eqs. (3), (4) and (19) from Appendix A.	10-50
4.			

<u>Step</u>	<u>Flow Chart</u>	<u>Comments</u>	<u>Fortran Statement Number</u>
	(N)		
5.	Write "no convergence in Wilkins startup," list the last term in the series and the sum of terms.		35
6.	26667 HPR7		
7.	4		
8.	Have we completed the four startup calculations?		
	(Y)		
9.	Calculate Y_i for $i = 5$ to i_L by the Milne method: also calculate y_i' , y_i'' , the truncation error estimate, and the cumulative truncation error estimate.	Eqs. (3), (4), (5), (6), and (22) from Appendix A.	60-80
10.	Write the flux per unit velocity, Y_i , the truncation error, F_T , and the cumulative truncation error, F_{cum} , versus energy.		90-100
11.	Return		

10. FLF2

Purpose: to integrate the flux per unit velocity, Y_i , giving the magnitude of the flux (i. e., the integrated weighting function for averaging thermal cross sections). (Flux function, 2nd revision)

Input arguments: $i_L, \mu_v, Y_i, (T_o/T_{md})^{1/2}$

Output parameters: ϕ

Space required: 97, (27421-27561)₈


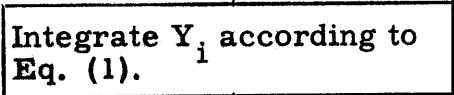

Discussion: The parabolic rule is used for integration of Y .

$$\phi = \int_0^{x_{\max}} Y(x) dx = \frac{\mu}{3} (Y_1 + 4Y_2 + 2Y_3 + 4Y_4 + \dots + 4Y_{i_L-1} + Y_{i_L}) + O(\mu^5) \quad (1)$$

where μ is the spacing in x , given by,

$$\mu = \mu_v (T_o/T_{md})^{1/2} \quad (2)$$

Since the parabolic rule is used, i_L must be odd (and < 100).

<u>Step</u>	<u>Flow Chart</u>	<u>Comments</u>	<u>Fortran Statement Number</u>
1.			
2.			10-30
3.			

11. CSF2

Purpose: to calculate the average thermal cross section for nuclide m, given Y_i and ϕ . (Cross section function, 2nd revision)

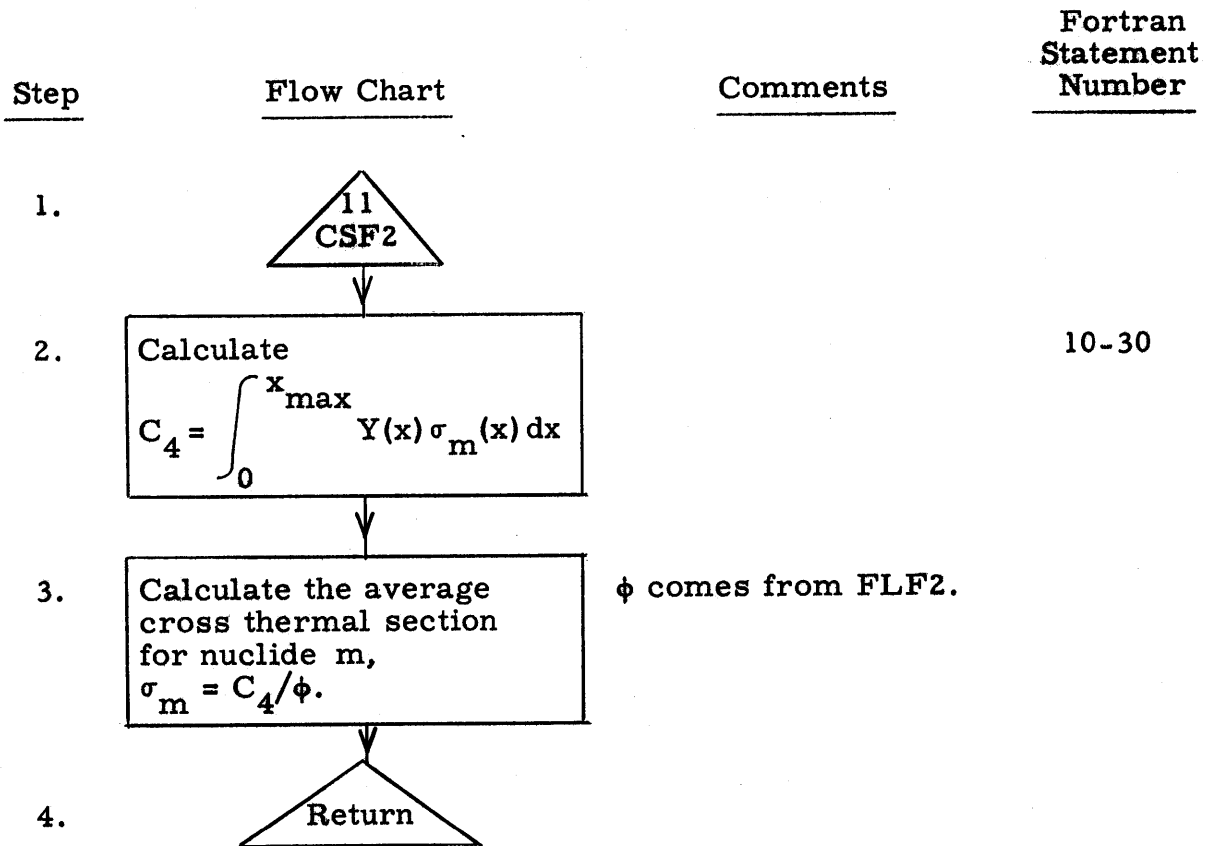
Input arguments: m, ϕ , i_L , μ_v , Y_i , $\sigma_{i,m}$, $(T_o/T_{md})^{1/2}$

Output parameters: σ_m , for given input value of m

Space required: 175, (27562-30040)₈

Discussion: The parabolic rule is used for the integration,

$$\sigma_m = \frac{1}{\phi} \int_0^{x_{\max}} \sigma_m(x) Y(x) dx = \frac{\mu}{3\phi} \left[\sigma_{1,m} Y_1 + 4\sigma_{2,m} Y_2 + \dots + \sigma_{i_L,m} Y_{i_L} \right] + O(\mu^5) \quad (1)$$



12. SQRT

Purpose: to calculate the square root of a given floating point number; a standard Fortran II subprogram.

Space required: 45, (30041-30115)₈

13. EXP

Purpose: to calculate e^x , given the floating point number x ; a standard Fortran II subprogram.

Space required: 62, (30116-30214)₈

14. NUCON

Purpose: to solve for the nuclide concentrations one flux time step, ζ , advanced from the known values, to calculate resonance escape probabilities, macroscopic S_m group cross section and the average macroscopic Xe cross section. (Nuclide concentrations)

Input arguments: $N_{m,\theta}$, σ_m , $\langle 1-p \rangle_m$, $C_5 = \frac{\sigma_{Xe} \bar{\phi}}{\sigma_{Xe} \bar{\phi} + \lambda}$

\bar{P}_1 , ϵ , v_m , a_m , η_m , $y_{Xe,m}$, $y_{Sm,m}$

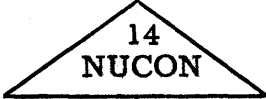
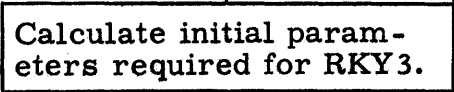
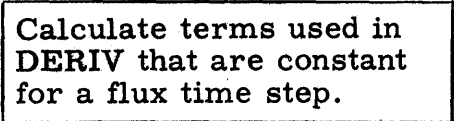


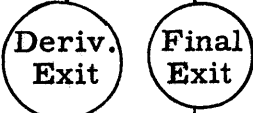


$\zeta = \delta\theta$, I_m^∞ , $\psi_{1,m}$, $C_1 = \frac{V_{fl}}{\xi \Sigma_s V_{md}}$, $\Sigma_{s,fl}$

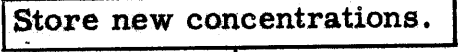

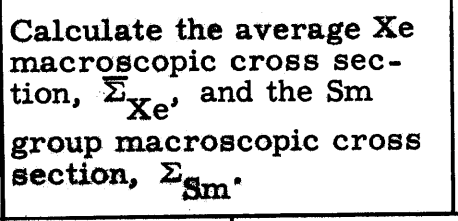
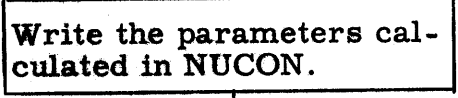
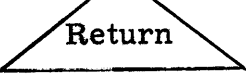
Output parameters: $N_{m,\theta+\zeta}$, Σ_{Xe} , Σ_{Sm} , p_m , p

Subprograms called: RKY3, DERIV, RESPRB, PRINT, (RETRKY)

Space required: 507 + 32 common, (30215-31207)_g, (77423-77462)_g

Discussion: NUCON is coded in a manner to preserve the relocable features of its subprograms, while allowing a SAP subprogram, RKY3, to be used for the numerical integrations. The numerical integration is by a fourth order Runge-Kutta method, as modified by Gill. The entry to DERIV for the derivative calculation is via the entry point called **DERIV1** in NUCON. Return after the derivative calculation is to the entry point in RKY3 called **RETRKY**.

Step	Flow Chart	Comments	Fortran Statement Number
1.			
2.		$N_{m, \theta} \rightarrow \text{XRKY3}$ $N_{m, \theta} \rightarrow \text{YRKY3}$ $0 \rightarrow \text{QRKY3}$	10-20
3.		$(a_m), (e_m)$ $(\sigma_{f,v})_m$	30-35
4.		2^{nd} entry point for RKY3.	
5.		Numerical solution of the nuclide concentration differential equations.	
6.		There are four derivative exits for each final exit.	
7.		2^{nd} entry point of Nucon, provides input data for DERIV.	
8.		Calculate derivatives.	40

<u>Step</u>	<u>Flow Chart</u>	<u>Comments</u>	<u>Fortran Statement Number</u>
9.		XRKY3 → $N_{m, \theta+\zeta}$	
10.		Calculate resonance escape probabilities using the new concen- trations.	
11.			80-100
12.		Normally bypassed.	
13.			

15. RKY3

Purpose: to solve numerically the set of first order differential equations for the nuclide concentrations one flux time advanced from the last values.
(Runge-Kutta)

Input parameters: ζ (flux time step) (also needs initial values of XRKY3, YRKY3, and QRKY3 which were stored in common by NUCON and $\frac{dN_m}{d\theta}$, or YRKY3, stored in common by DERIV)

Output parameters: $N_{m, \theta+\zeta}$ (XRKY3 in SAP)

Subprograms called: DERIV (via DERIV1 in NUCON)

Space required: 151 + 32 common (31210-31436)_g, (77423-77462)_g

Discussion: This is a standard SAP subprogram only modified to make it compatible with the connected relocatable Fortran programs. The method used is a fourth order Runge-Kutta process as modified by Gill, see G2.

16. DERIV

Purpose: to calculate the flux time derivatives of the nuclide concentrations. (Derivatives)

Input arguments: $\eta_m, I_m^\infty, \psi_{1,m}, C_1, \Sigma_{s,fl}, a_m, e_m, (\sigma_{fv})_m, \sigma_m, N_m$ (XRKY3)

Output parameters: $\frac{dN_m}{d\theta}$ (VRKY3) ("pseudo" values at partial flux time steps are also stored for $N_m, p_m, <1 - p_m>$, and p for the RKY3 Runge-Kutta solution)

Subroutines called: RESPRB, PRINT

Space required: 318 + 16 common, (31437-32134)₈, (77443-77462)₈

Discussion: Equations for the derivatives have been given in Section IV. A. 3. Combinations of terms in these equations that are considered constant for a flux time step are combined in NUCON, into the term $a_m, e_m,$ and $(\sigma_{fv})_m,$ prior to entry into RKY3 and DERIV.

<u>Step</u>	<u>Flow Chart</u>	<u>Comments</u>	<u>Fortran Statement Number</u>
1.			
2.		XRKY3 → N_m	10-20
3.		Calculate the real or pseudo p_m for use in the derivative equations.	

<u>Step</u>	<u>Flow Chart</u>	<u>Comments</u>	<u>Fortran Statement Number</u>
4.		$\frac{dN_m}{d\theta} \rightarrow$ VRKY3.	30-90
5.		Normally bypassed.	95
6.			

17. RESPRB

Purpose: to calculate resonance escape probabilities for the fuel nuclides.

Input arguments: $N_m, I_m^\infty, \psi_{1,m}, C_1, \Sigma_{s,fl}$


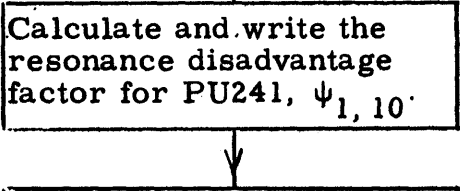
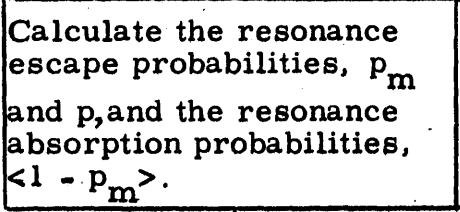
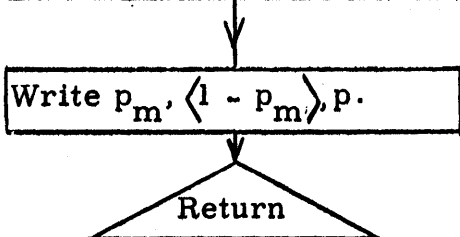
Output parameters: $p_m, \langle 1 - p_m \rangle, p$

$m = 5$ to 12 except 7

Subprograms called: EXP, PRINT

Space required: 319, (32135-32634)₈

Discussion: Equations for the resonance escape probabilities are given in Section IV. A. 1. 3.

<u>Step</u>	<u>Flow Chart</u>	<u>Comments</u>	<u>Fortran Statement Number</u>
1.			
2.		See Section IV. A. 1. 3.	
3.			10-40
4.			50-60

18. SPACON

Purpose: to calculate the parameters for the spatial subprogram (SPACE 2), which are constant for a given problem. (Space constants)

Input arguments: R, H, δ_R , δ_H , D, τ , Z_{sym} , r_L (IFIN), z_L (JFIN)

Output parameters: $V_r = C_{13}$; the constants for the thermal diffusion terms, C15's; the constants for fast diffusion terms, C17's.

Space required: 621, (32634-34010)₈

Discussion: The terms calculated here are merely combinations of the time-invariant terms in Eq. (4.39). For example, $C_{17} = -\frac{\tau}{h^2}$

<u>Step</u>	<u>Flow Chart</u>	<u>Comments</u>	<u>Fortran Statement Number</u>
1.			
2.			90
3.			10-140
4.			

19. SPACE 2

Purpose: to calculate the criticality factor, C, the spatial flux distribution, the power densities, and other spatial parameters.

Input arguments: $\Sigma_{Xe, \max, r, z}$, $(\Sigma_{ff} - \Sigma_{Xe})_{r, z}$, $\Sigma_{f, r, z} = C53$,

$(\nu\Sigma_f)_{r, z} = C10$, $\left(\frac{1-p}{1+a}\right)_{r, z} = C54$, $[(1-p)\eta]_{r, z} = C11$, $p_{r, z} = PL$, $\phi_{r, z} =$

PHIS, $\frac{\phi_{r, z}}{\phi_{1, 1}} = PHISN$, $V_r \phi_{r, z} = C28$, $(-D\nabla^2)_{r, z} = C36$, $P_{1, r, z}$ (the

preceding five terms provide initial estimates for the iteration),

$\frac{\Sigma_{w, r, z}}{\Sigma_{w, 1, 1}}$, Σ_{md} , σ_{Xe} , ϵ , λ_{Xe} , V_{ff} , α_1 , η_1 , $V_r = C13$, $C15$'s, $C17$'s, P_d ,

r_L , z_L

Output parameters: $\phi_{r, z}$, $\frac{\phi_{r, z}}{\phi_{1, 1}}$, $V_r \phi_{r, z}$, $(D\nabla^2)_{r, z}$, $P_{1, r, z}$ (the new



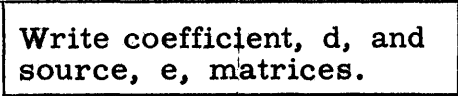
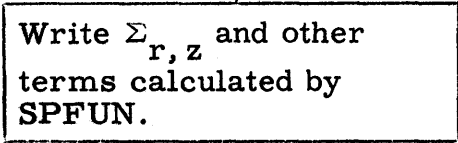
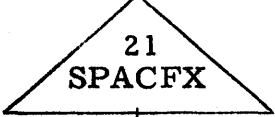
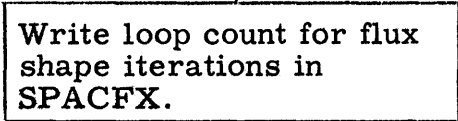


values of these preceding five terms replace those of the input data),

$$C, \bar{P}_1, \frac{\sigma_{Xe} \bar{\phi}}{\sigma_{Xe} \bar{\phi} + \lambda_{Xe}}$$

Subprograms called: SPFUN, SPACFX, SPFUN2, PRINT

Space required: 2593, (34011-41621)₈

Discussion: This is a control program to connect the spatial subprograms.

<u>Step</u>	<u>Flow Chart</u>	<u>Comments</u>	<u>Fortran Statement Number</u>
1.			
2.		Calculate d and e matrices of Eq. (4.59).	
3.		Normally bypassed.	10
4.		Normally bypassed.	20
5.		Calculate spatial flux distribution.	
6.			30
7.		Calculate criticality and other spatial parameters at each mesh point, and core average values.	
8.			

20. SPFUN

Purpose: to calculate the coefficient matrix, d , and the source matrix, e , for SPACFX. (Space functions)

Input arguments: $(\Sigma_{fl} - \Sigma_{Xe})_{r,z}$, V_{fl} , ψ , Σ_{md} , $\Sigma_{Xe, max, rx}$, σ_{Xe} , λ_{Xe} ,

$(\nu\Sigma_f)_{r,z}$, $p_{r,z}$, $[(1-p)\eta]_{r,z}$, $\phi_{r,z}$, $P_{1,r,z}$, $(-D\nabla^2)_{r,z}$, $(V_r\phi_{r,z})$, C15's,

C17's, $\frac{\Sigma_{w,r,z}}{\Sigma_{w,1,1}}$, ϵ , r_L , z_L

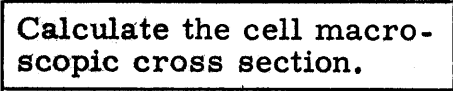
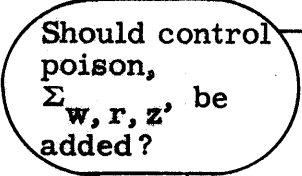
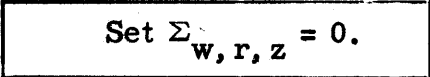
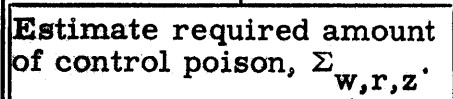
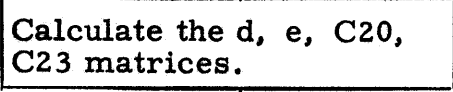

Output parameters: $d_{r,z,u}$, $e_{r,z}$, $(\Sigma_{r,z} + \Sigma_{w,r,z}) = C20_{r,z}$

$$C_{23,r,z} = \left({}^n C_{17}^u \left(\frac{C_{20}}{p} \right)_{rz} \right)$$

Space required: $476 + 800_{common}$, (41622-42555)₈

Discussion: The $d_{r,z,u}$ and $e_{r,z}$ are as defined in Eq. (4.39). (The $C_{2,r,z}$ in Fortran differs from the $C_{2,r,z}$ of this text by the factor $p_{r,z}$.)

<u>Step</u>	<u>Flow Chart</u>	<u>Comments</u>	<u>Fortran Statement Number</u>
1.	<pre> graph TD A[20 SPFUN] --> B[Calculate the macroscopic Xe cross section at each mesh point.] </pre>		
2.	<div style="border: 1px solid black; padding: 5px; width: fit-content; margin: auto;"> Calculate the macroscopic Xe cross section at each mesh point. </div>		10-20

Step	Flow Chart	Comments	Fortran Statement Number
3.		$\Sigma_{r,z} = (\Sigma_{fl,r,z}) V_{fl} + \psi \Sigma_{md}(1 - V_{fl})$	10-20
4.			
5.			28
6.			22-25
7.		See Eq. (4.39).	29-200
8.			

21. SPACFX

Purpose: to calculate the spatial flux distribution. (Space flux)


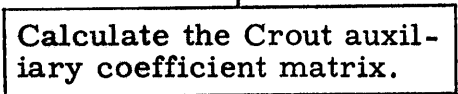
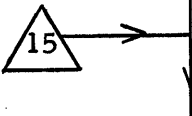
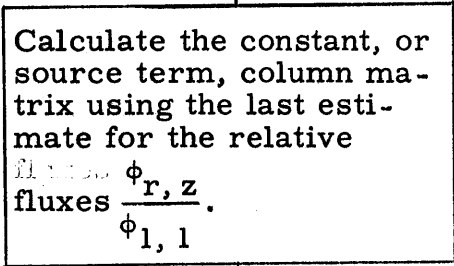

Input arguments: $d_{r,z,u}$, $e_{r,z}$, $r_L (=i_L)$, $z_L (=j_L)$

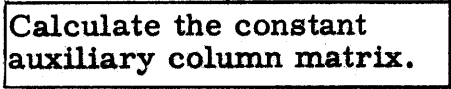
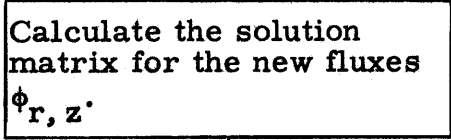
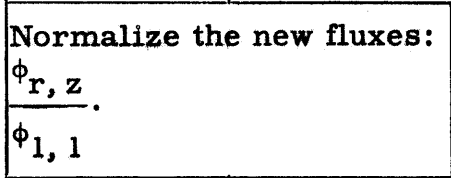
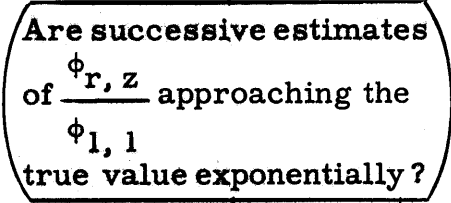
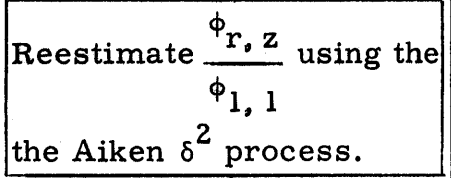
Output parameters: $\phi_{r,z}$, COUNT (loop count of the number of iterations
 $\phi_{1,1}$
 required for the flux convergence)

Subprograms called: PRINT

Space required: 999 + 5400 common, (42556-44524)₈, (5033-77462)₈

Discussion: The iteration method has been discussed in Section IV. A. 2.5-2.6. Equations for the modified Crout reduction method used for the generation of new flux values has been discussed in Appendix B.

<u>Step</u>	<u>Flow Chart</u>	<u>Comments</u>	<u>Fortran Statement Number</u>
1.			
2.			10-211
3.		Entry for iteration loop.	215
4.		C(N)	215-220
			253

<u>Step</u>	<u>Flow Chart</u>	<u>Comments</u>	<u>Fortran Statement Number</u>
5.	 <pre> graph TD Start(()) --> Step5[Calculate the constant auxiliary column matrix.] Step5 --> Step6[Calculate the solution matrix for the new fluxes φ_{r,z}.] Step6 --> Step7[Normalize the new fluxes: φ_{r,z} / φ_{1,1}.] Step7 --> Step8{Are successive estimates of φ_{r,z} / φ_{1,1} approaching the true value exponentially?} Step8 -- Y --> Step9[Reestimate φ_{r,z} / φ_{1,1} using the Aiken δ² process.] Step8 -- N --> Step9 Step9 --> End(()) </pre>	F(N)	230-270
6.			280-320
7.			330
8.			
9.			340-360

Step	Flow Chart	Comments	Fortran Statement Number
10.		Convergence assumed when successive flux values change less than 1% at every mesh point.	370-390
11.			
12.			400
13.		Unconditional stop for no convergence.	410
14.		Normally bypassed.	405-406
15.		Loop for new flux calculation.	
16.			
17.		Converged values of $\phi_{r,z}$. $\phi_{1,1}$	420-430
18.			440

22. SPFUN2

Purpose: to calculate the following properties at each mesh point and also the core average values: the criticality factor, C; the fast non-leakage probability, P_1 ; the thermal production term, $(q/\phi)P_1p$; the thermal macroscopic cross section, Σ ; the thermal leakage term $(-D\nabla^2)$; and the power densities. In addition the reactor criticality factor with control poison, C_w , is calculated, the Xe poisoning factor, C_5 , the flux magnitudes, $\phi_{r,z}$, and the maximum to average power density ratio. (Space functions 2)

Input arguments: $\frac{\phi_{r,z}}{\phi_{1,1}}, V_r, C_{15's}, C_{23,r,z}, (\nu\Sigma_f)_{r,z}, [(1-p)\eta]_{r,z}$

$C_{20,r,z}, \Sigma_{f,r,z}, \left(\frac{1-p}{1+\alpha}\right)_{r,z}, \epsilon, p_{r,z}, \Sigma_{r,z}, P, \alpha_1, \eta_1, \lambda_{Xe}, \sigma_{Xe}, r_L,$
 z_L

Output parameters: $\phi_{r,z}, V_r\phi_{r,z} = C_{28,r,z}, (-D\nabla^2)_{r,z} = C_{36,r,z}$

$$P_{1,r,z}, C, \bar{P}_1, C_5 = \frac{\sigma_{Xe}\bar{\phi}}{\sigma_{Xe}\bar{\phi} + \lambda_{Xe}}$$

Subprograms called: PRINT

Space required: 854 + 2260 common, (44525-46252)₈, (75203-77462)₈

Discussion: The core averaging method has been discussed in Section IV.A.2.7. The value of C_5 calculated here, with the core average flux, is used only in the average cross section calculation for estimating Xenon's effect on the energy spectrum of the flux. The true

values of the flux at each mesh point are used for calculating the Xenon poisoning for the spatial flux shape calculations.

<u>Step</u>	<u>Flow Chart</u>	<u>Comments</u>	<u>Fortran Statement Number</u>
1.			
2.			625-710
3.			10-50
4.		Often bypassed when only interested in core average values.	70
5.			80
6.		Calculated so as to give the specified power output.	90-110
7.			120-140

<u>Step</u>	<u>Flow Chart</u>	<u>Comments</u>	<u>Fortran Statement Number</u>
8.	<pre> graph TD Start(()) --> Step8[Write the maximum to average power density ratio.] style Start fill:none,stroke:none </pre>		150
9.	<pre> graph TD Step8[Write the maximum to average power density ratio.] --> Step9[/Return/] </pre>		

23. SPPROP

Purpose: to calculate the seven space properties required by SPACFX at each mesh point: $\Sigma_{Xe, \max}$, $(\Sigma_{fl} - \Sigma_{Xe})$, Σ_f , $v\Sigma_f$, $\left(\frac{1-p}{1+a}\right)$, $(1-p)\eta$, p .
(Space properties)

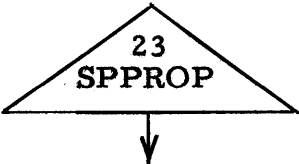
Input arguments: r_L , z_L , n_z , n_{sp} , a_{Lag} (Denominator terms in the Lagrangian coefficients), the values of flux-time at which the fit was made (TH), the values of the seven space properties at these flux times, and the value of flux-time at each mesh point, $\theta_{r, z}$ (THETA).

Output parameters: a_{Lag2} (the set of Lagrangian fit coefficients), and the values for the seven space properties at each mesh point.

Subprograms called: PRINT

Space required: 311, (46253-46741)₈

Discussion: The fit is made by the Lagrangian method of polynomial approximation. Up to 20 Lagrangian coefficients can be used in the fit, which is equivalent to a 19th degree polynomial fit at maximum. Only enough points to give the required accuracy should be used, however, to conserve computer time (see Appendix E. for recommendations).

<u>Step</u>	<u>Flow Chart</u>	<u>Comments</u>	<u>Fortran Statement Number</u>
1.			

<u>Step</u>	<u>Flow Chart</u>	<u>Comments</u>	<u>Fortran Statement Number</u>
2.		The denominators for these terms were calculated in MAIN.	420-440
3.			440-450
4.		Normally bypassed.	460
5.			

24. NCGTHV

Purpose: to calculate the nuclide concentrations at a specified flux time.

(Nuclide concentrations given a theta value)


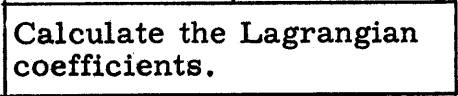
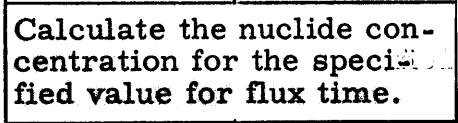
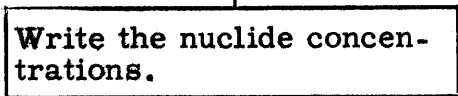
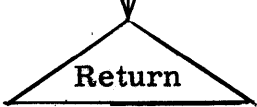
Input arguments: n_v , n_{sp} , θ_v (the value of flux time), TH values (see SPPROP), a_{Lag} , $N_{m,\theta}$ (values of the nuclide concentrations at the flux times TH)

Output parameters: a_{Lag2} , N_{m,θ_v} (the values at θ_v) for $m = 5$ to 12

Subprograms called: PRINT

Space required: 210, (46742-47263)₈

Discussion: This subroutine is analagous to SPPROP

<u>Step</u>	<u>Flow Chart</u>	<u>Comments</u>	<u>Fortran Statement Number</u>
1.			
2.			10-40
3.			50-60
4.		Normally bypassed.	70
5.			

25. NEWIMV


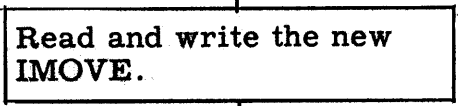

Purpose: to read a new value for IMOVE, the index governing the type of fuel movement.

Input arguments: none

Output parameters: IMOVE

Subprograms called: PRINT

Space required: 56, (47264-47353)₈

<u>Step</u>	<u>Flow Chart</u>	<u>Comments</u>	<u>Fortran Statement Number</u>
1.			
2.			10-30
3.			

26. AVGFTH

Purpose: to calculate integral flux time averages of the seven space properties discussed in SPPROP. (Average functions of theta)

Input arguments: fitted flux value (TH), the seven nuclear properties at the TH points (see SPPROP), a_{Lag} , n_{ζ} , n_{sp}

Output parameters: the seven average properties at fit flux time points, TH, for the most irradiated fuel

Subprograms called: PRINT

Space required: 846, (47354-51071)₈

Discussion: Let $f(\theta)$ represent one of the seven properties at the flux time θ , and $\bar{f}(\theta)$ the average value of that property when the maximum flux time is θ . Then

$$\bar{f} = \frac{I(\theta)}{\theta} \quad (1)$$

when

$$I(\theta) \equiv \int_0^{\theta} f(\theta') d\theta' \quad (2)$$

and Simpson's rule is used for the numerical integration of (2), giving







$$\bar{f}(\theta_i) = \frac{1}{\theta_i} \left\{ I(\theta_{i-2}) + \frac{h}{3} [f(\theta_{i-2}) + 4f(\theta_{i-1}) + f(\theta_i)] + O(h^5) \right\} \quad (3)$$

where

$$h = \delta\theta$$

The $\bar{f}(\theta_i)$ are calculated for even values of i and these $\bar{f}(\theta_i)$ are then used

rather than the $f(\theta_i)$ in calculating the spatial properties for GRADED.

Step	Flow Chart	Comments	Fortran Statement Number
1.			
2.	 <div data-bbox="350 638 781 737" style="border: 1px solid black; padding: 5px;"> Tabulate the $f(\theta_i)$ for even i. </div>	These are the values that were calculated in the NUCON loop of MAIN.	10-20
3.	 <div data-bbox="350 852 781 963" style="border: 1px solid black; padding: 5px;"> Calculate the $f(\theta_i)$ for odd i. </div>	By the Lagrangian method.	20-60
4.	 <div data-bbox="350 1010 781 1129" style="border: 1px solid black; padding: 5px;"> Calculate the $\bar{f}(\theta_i)$ and tabulate for even i. </div>	The even θ_i values are the original fit points for $f(\theta)$.	60-70
5.	 <div data-bbox="350 1220 781 1354" style="border: 1px solid black; padding: 5px;"> Write the seven average space properties, \bar{f}, at the flux time fit points. </div>		70-80
6.	 <div data-bbox="444 1398 708 1497" style="border: 1px solid black; padding: 5px; text-align: center;"> Return </div>		

27. COST

Purpose: to calculate the fuel cycle costs using up to eight different sets of cost parameters.

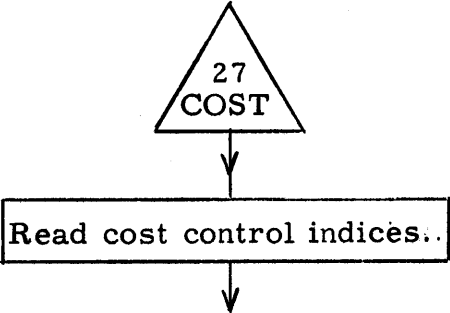
Input arguments: values of the nuclide concentrations for the fuel entering the reactor, N_m^0 ; values for the discharged fuel, N_m ; the contribution to N_m^0 from recycled fuel, $N_{R,m}$; the "on-stream" reactor time, t_R ; and the average burnup, \bar{E} .

Output parameters: none (all the costs are printed out, not transferred)

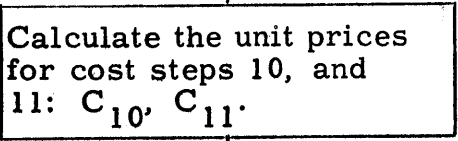

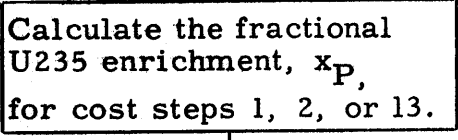
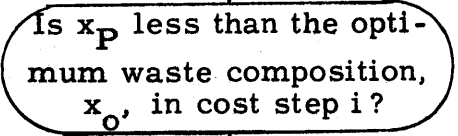
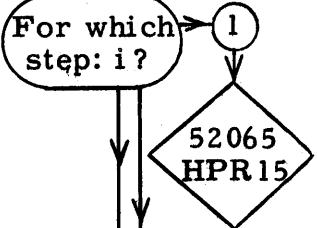
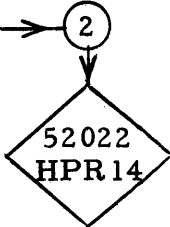
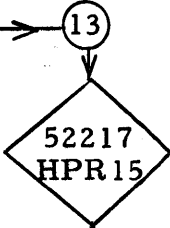
Subprograms called: READ-PRINT; CPF

Space required: 1772, (51072-54445)₈

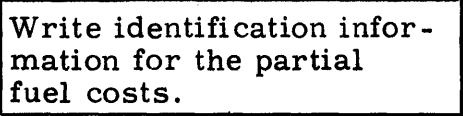
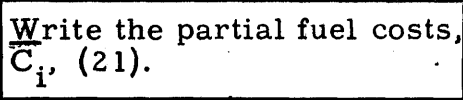
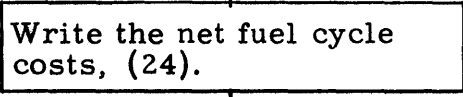
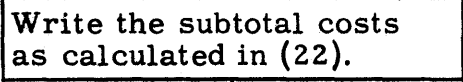
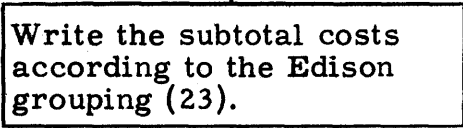

Discussion: The equations given in IV.B.2 are evaluated by this subprogram. The external cost input data listed in Table D3. is read in via the card reader (see Appendix D.1).

<u>Step</u>	<u>Flow Chart</u>	<u>Comments</u>	<u>Fortran Statement Number</u>
1.	 <pre> graph TD A[27 COST] --> B[Read cost control indices..] </pre>		
2.		INPCST and JCOSTL, see Table D3.	10

Step	Flow Chart	Comments	Fortran Statement Number
3.		JCOSTL > 8	
4.		Stop for too many cost sets specified.	
5.		INPCST = 0: Y INPCST ≠ 0: N Cost input data is preserved from the preceding run.	10
6.		See Appendix D. 1 and Table D3.	19-20
7.			22-27
8.			35-50
9.		Entry point for new set of cost input data.	60-18
10.			

Step	Flow Chart	Comments	Fortran Statement Number
11.			210-310
12.			
13.		See Fig. 4.5.	150, 100, 210
14.			
15.			160
16.			110
17.			350

Step	Flow Chart	Comments	Fortran Statement Number
18.		Calculate the unit price of enriched uranium.	
19.			200, 120, 360
20.			
21.			370-390
22.			390-400
23.			400-405
24.			410
25.			410

<u>Step</u>	<u>Flow Chart</u>	<u>Comments</u>	<u>Fortran Statement Number</u>
26.	 <pre> graph TD Start(()) --> S26[Write identification information for the partial fuel costs.] S26 --> S27[Write the partial fuel costs, C_i, (21).] S27 --> S28[Write the net fuel cycle costs, (24).] S28 --> S29[Write the subtotal costs as calculated in (22).] S29 --> S30[Write the subtotal costs according to the Edison grouping (23).] S30 --> S31[/Return/] </pre>		415-417
27.			
28.			430
29.		Normally bypassed.	440
30.			445-450
31.			


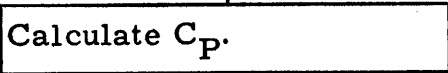
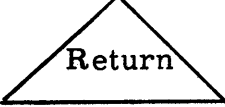
28. CPF

Purpose: to calculate the unit price of UF_6 (C_P function).

Input arguments: fractional enrichment, x_P ; optimum waste composition, x_0 ; and the unit price of natural UF_6 , C_E .

Output parameters: the unit price of UF_6 , C_P

Space required: 91, (54446-54600)₈

<u>Step</u>	<u>Flow Chart</u>	<u>Comments</u>	<u>Fortran Statement Number</u>
1.			
2.		Equations given in Section IV.B.2.	
3.			

29. LOG

Purpose: to calculate the natural logarithm of a given floating point number; a standard Fortran II subprogram.

Space required: 154, (54601-55032)₈

30. BATCH

Purpose: to make the material fuel cycle calculations: flux shape, criticality factor, power density, etc., stepwise through the life history of the fuel when the core is irradiated batchwise.

Input arguments: $V_r \phi_{r,z} = C_{28,r,z}, r_L, z_L, \tau, \theta, n_{\zeta}, n_{sp}, a_{Lag}, a_{Lag2}, TH, N_{m,\theta}, \Sigma_{Xe,max,\theta}, (\Sigma_{fl} - \Sigma_{Xe})_{\theta}, \Sigma_f, \theta, (v\Sigma_f)_{\theta}, \left(\frac{1-p}{1+a}\right)_{\theta}, [(1-p)\eta]_{\theta}, p_{\theta}, \phi_{r,z}, \frac{\phi_{r,z}}{\phi_{1,1}}, (-D\nabla^2)_{r,z}, P_{1,r,z}, \frac{\Sigma_{w,r,z}}{\Sigma_{w,1,1}}, \Sigma_{md}, \sigma_{Xe}, \epsilon, \lambda_{Xe}, \psi, V_{fl}, a_1, \eta_1, V_r = C_{13}, C_{15}, C_{17}, P_d.$

Output parameters: $C, \bar{P}_1, C_5, \bar{N}_m, N_{c,m}$


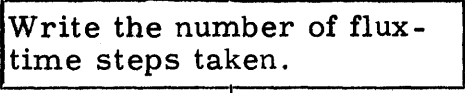

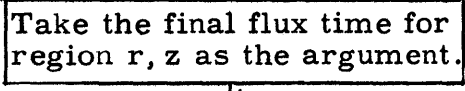
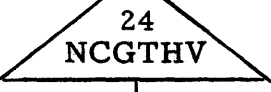
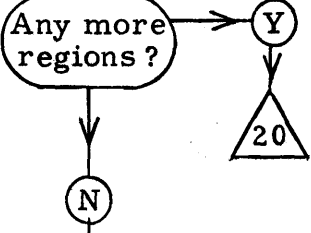
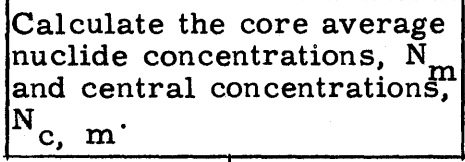


Subprograms called: READ-PRINT; TIMECK; SPPROP; SPACE2; NCGTHV

Space required: 571, (55033-56125)₈

Discussion: This is a control program for ordering the entry and directing the flow of information to the major subprogram groups of FUELCYC for batch irradiation fuel movement. This fuel movement method has been discussed in Section IV.C.2.1. The external input card "B" of Table D2. is read from the card reader.

<u>Step</u>	<u>Flow Chart</u>	<u>Comments</u>	<u>Fortran Statement Number</u>
1.			
2.			5
3.		Card "B" in Table D2.	6-7
4.			10-15
5.		Loop entry point for new flux time step	20
6.		n now set at 30	
7.		Unconditional stop for reactivity too high	30
8.		Write the time at location No. 6	40
9.			50

Step	Flow Chart	Comments	Fortran Statement Number
10.			25
11.		Calculate "Space Properties".	
12.			
13.		Calculate flux shape criticality, etc.	
14.			60-70
15.		$C = 1 \pm m?$ m now set at .001.	80
16.		by linear interpolation in flux time.	90
17.			

<u>Step</u>	<u>Flow Chart</u>	<u>Comments</u>	<u>Fortran Statement Number</u>
18.			100
19.			100-110
20.			
21.			
22.		Calculate the final nuclide concentrations, N_m , in region r, z.	120-130
23.			
24.			140
25.			
26.			

31. INOUT or 32. OUTIN

Purpose: to make the material fuel cycle calculations for Inout or Outin fuel scheduling.

Input arguments: Same as BATCH.

Output parameters: same as BATCH.

Subprograms called: same as BATCH.

Space required: 820, (56126-57611)₈, INOUT
850, (57612-61333)₈, OUTIN

Discussion: See Sections IV. C.2.2 and IV. C.2.3. The logical flow and Fortran statement numbers are the same for these two subprograms, so only one flow diagram is required. The external input data card IOG is read from the card reader.

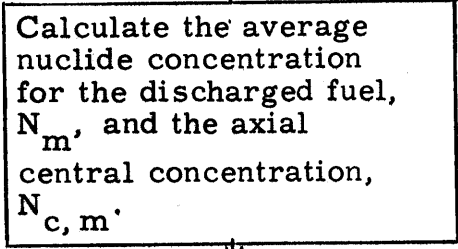
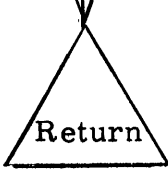
<u>Step</u>	<u>Flow Chart</u>	<u>Comments</u>	<u>Fortran Statement Number</u>
1.			
2.			5
3.		Card "IOG" of Table D2.	6-7

<u>Step</u>	<u>Flow Chart</u>	<u>Comments</u>	<u>Fortran Statement Number</u>
4.	Initialize: set $\theta_c = \theta_1$.	Initial flux-time estimate.	10
5.	23, 27	Flux-time iteration entry point.	
6.	Write the number of flux-time iterations and the last estimate for θ_c .		21
7.	Have n flux time iterations been made?	n now set at 15.	
8.	56515 or 60177 HPR151	INOUT OR OUTIN unconditional stop for no convergence.	22
9.	16, 19	Criticality iteration entry point.	
10.	Calculate flux time of fuel when leaving each region, $\theta_{r,z,L}$ using latest θ_c .		23-50
11.	Calculate average flux time of the fuel in each region, $\theta_{r,z}$.		23-50

<u>Step</u>	<u>Flow Chart</u>	<u>Comments</u>	<u>Fortran Statement Number</u>
12.			
13.		Calculate "Space Prop- erties."	
14.			
15.		Calculate flux shape criticality, etc.	
16.			
17.		Convergence if frac- tional change in last iteration was less than m_1 . m_1 now set at 0.001.	

<u>Step</u>	<u>Flow Chart</u>	<u>Comments</u>	<u>Fortran Statement Number</u>
18.	<pre> graph TD Start(()) --> D1{Have m2 criticality iterations been made?} D1 -- Y --> C20((20)) D1 -- N --> C9((9)) </pre>	For no convergence in criticality iteration; m_2 now set at 10.	54
19.	<pre> graph TD C9((9)) --> P9(9) </pre>	Loop for new criticality calculation.	55
20.	<pre> graph TD C17_18(17, 18) --> P17_18(17, 18) </pre>		59
21.	<pre> graph TD Start(()) --> D2{Is this the 1st flux-time estimate?} D2 -- Y --> C5((5)) D2 -- N --> C24((24)) </pre>		
22.	<pre> graph TD C5((5)) --> P22[Set theta_c = theta_2.] </pre>	2^{nd} flux-time estimate.	
23.	<pre> graph TD C21((21)) --> P23(5) </pre>		
24.	<pre> graph TD C24((24)) --> P24(21) </pre>		

Step	Flow Chart	Comments	Fortran Statement Number
25.	<pre> graph TD Start(()) --> Q25{Is the reactivity approximately zero?} Q25 -- Y --> C28((28)) Q25 -- N --> P26[] </pre>	$C = 1 \pm m_3$ m_3 now .001.	
26.	<pre> graph TD P26[Estimate new theta_c to make C = 1.] --> C27((5)) </pre>	Linear interpolation.	80
27.			
28.			
29.			
30.	<pre> graph TD P30[Take the final flux time for a section of discharged fuel as the argument.] --> C31((24)) </pre>		
31.		Calculate final nuclide concentrations in each portion of the discharged fuel element.	90-140
32.	<pre> graph TD Q32{Any more fuel sections?} Q32 -- Y --> C29((29)) Q32 -- N --> End(()) </pre>		

<u>Step</u>	<u>Flow Chart</u>	<u>Comments</u>	<u>Fortran Statement Number</u>
33;	 <p>Calculate the average nuclide concentration for the discharged fuel, $N_{m'}$, and the axial central concentration, $N_{c, m'}$.</p>		140
34.	 <p>Return</p>		

33. GRADED

Purpose: to make the fuel cycle calculations for "Graded" fuel movement.

Input arguments: same as BATCH.



Output parameters: same as BATCH.

Subprograms called: those of BATCH plus AVGFTH.

Space required: 1209, (61334-63624)₈

Discussion: See Section IV.C.2.4. The flow diagram is the same as in Appendix C.31 and C.32 for INOUT and OUTIN (including statement numbers) except for the below listed changes. The actual calculation procedure represented by Steps 10, 11, 30, and 33 are, of course, different for these three fuel movements. The external input data card IOG is read from the card reader.

Changes to the Flow Chart of Appendix C.31 and 32

<u>Change</u>	<u>Step</u>	<u>Flow Chart</u>	<u>Comments</u>	<u>Fortran Statement Number</u>
Insert	4.5		Calculate the average "space properties."	10
Change stop to	8.			
Omit	10.			
Insert comment	13.		The average "Space Properties" are used as arguments for SPPROP.	

34. (WTPE)

Purpose: to load the contents of the core on Tape 4

Space required: 34

Discussion: When the WTPE subprogram is encountered during the loading of the object program, it is loaded into memory, logical tape 4 is rewound, the entire core memory is written onto tape 4, tape 4 is rewound, and control is passed to the BSS loader so that the loading of cards may continue.

Subsequently if the original tape is mounted as logical tape 4, a single card, GETTPE 04, is used to replace all the original deck that preceded the WTPE program, including the BSS loader.

A check sum is made on the record read from tape 4 and if there is disagreement the error stop HTR 17_8 occurs in location 16_8 .

This is an M.I.T. subprogram and is further described in M.I.T. Computation Center Memo 127.

35. MI CPM2

Purpose: to print identification data on the on-line printer.

Discussion: This is a one card self loading program that:

- a) restores the printer
- b) prints columns 1-72 of Hollerith cards with a 9 punch in column 2 (i. e. 9, I, R, Z)
- c) executes a "load card" sequence after the last Hollerith card has been printed

See M.I. T. Computation Center Memo 63 for further information.

The only on-line print out in FUELCYC is by the NOLOAD diagnostic routine (see 1. LOADER) if the problem fails to load, so normally the on-line identification as provided by this subroutine is not needed.

36. MI CTH2

Purpose: to write identification information on tape.

Discussion: Writes Hollerith information in BCD on the logical tape specified by the punch in column 1 of the Hollerith card. In addition a 9 punch must appear in column 2. Information written in columns 3-72 is written on the specified tape and a "load cards" sequence is executed after the last Hollerith card is written. See M.I. T. CC-63 for further information. This routine is used if more identification is required than the 72 Hollerith characters allowed in the MAIN identification card, see Appendix D. 1, and for identification of octal correction cards and the symbol table which are written on tape 2 prior to the MAIN identification card.

D. OPERATIONAL INFORMATION FOR FUELCYC

1. Input Data Preparation

Input data for FUELCYC is written in one of three conversion forms:

1, Hollerith, H; 2, floating point, E; 3, integer, I.

Tables D1., D2. and D3. list the input data required with the card number and column field assignment indicated for each item. No decimal points should appear in integer data and, since blanks are equivalent to zero, all numbers should be moved to the right hand side of the field. There are several ways that the floating point numbers can be punched in the E-conversion and these are listed in the Fortran II manual. The method usually used by the author is to punch the decimal point in floating point numbers so they can appear anywhere in the assigned field and to use the E designation if exponents are necessary. The exponent field must be moved to the far right when used. For example, the following forms give the value 1.2, assuming a field width of 8:

<u>1</u>	<u>2</u>	<u>3</u>	<u>4</u>	<u>5</u>	<u>6</u>	<u>7</u>	<u>8</u>
					1	.	2
			1	.	2		
		.	1	2		E	1
	.	1	2		E	+	0 1
		1	2	.	E	-	1

Hollerith data consists of English letters, Arabic numerals, and other characters that appear on the keypunch machine.

Table D1. lists the 9 cards of input data required for MAIN. Following these cards and depending upon the fuel scheduling method either the card B (for Batch) or IOG (for Inout, Outin, or Graded) must appear. The content of these cards is given in Table D2.

Next comes the set of Cost input cards if the cost calculation is desired, i. e. if $COSTT = 0$. For $COSTT \neq 0$ the cost input cards are omitted. The cost input cards are designated by the letter C and are listed in Table D3. The eight cards C2 through C9 constitute a cost set. If more than one cost calculation is desired the cost sets are stacked consecutively.

For problems after the first, considerable reduction in the subsequent input data is usually possible. The identification card is first read, Card 1, in Table D1. Following this, the problem index card is read, designated by R (for rerun), see Table D2. If the rerun index is given the value unity, $i_{run} = 1$, then new values for all of the MAIN input data of Table 1 are read except for Card 1 (which was already read in). If $i_{run} = 2$, for an enrichment change in the same reactor, the single "2R" card of Table D2. is required instead of the cards of Table D1. For Pu recycle in the same reactor, $i_{run} = 3$, the single "3R" card replaces those of Table D1. Finally, for a new method of fuel movement, $i_{run} = 4$, the Table D1. data is again not needed and Card "4R" is read.

Following this, input cards are stacked in the normal logical order of the program. For example, after one of the "iR" cards should appear either a B or an IOG card. Note that the reading of the cost input sets C2-C9 can be bypassed on runs after the first, if there is no change in the cost input data. This is effected by setting i_{cst} to a value other than zero on Card C1.

Table D4. is a print out of the input data for a sample set of two runs to further illustrate the input data order and form. The order of the cards in Table D4. is:

Run 1	1	, identification run 1, (a Batch run)
	2-9	, initial MAIN input
	B	, BATCH input
	C1	, COST input designator
	C2-C9	, 1 st set COST input
	C2-C9	, 2 nd set COST input
Run 2	1	, identification run 2, an Inout run for the same reactor
	R	, index for second run, i_{run}
	4R	, new value for i_{move}
	IOG	, INOUT input
	C1	, COST input designator, (for same cost input data as before)

The last input data card should be the last card in the deck, since the normal program stop occurs for no cards in the card reader hopper.

Table D1. Input Data Required by MAIN.

Card No.	Column No.	Input Form	Item	Symbol		Compatible Units
				Text	FUELCYC Printout	
1	1-72	H	Identification data.	—	—	—
2	1-14	E	Initial concentration, U235.	N_5^0	N(5)	$\frac{\text{atoms}}{\text{barn cm (of fuel)}}$
2	15-28	E	Initial concentration, U236.	N_6^0	N(6)	$\frac{\text{atoms}}{\text{barn cm (of fuel)}}$
2	29-42	E	Initial concentration, low cross section fission products.	N_{FP}^0	N(7)	$\frac{\text{atoms}}{\text{barn cm (of fuel)}}$
2	43-56	E	Initial concentration, U238.	N_8^0	N(8)	$\frac{\text{atoms}}{\text{barn cm (of fuel)}}$
2	57-70	E	Initial concentration, Pu239.	N_9^0	N(9)	$\frac{\text{atoms}}{\text{barn cm (of fuel)}}$
3	1-14	E	Initial concentration, Pu240.	N_{10}^0	N(10)	$\frac{\text{atoms}}{\text{barn cm (of fuel)}}$
3	15-28	E	Initial concentration, Pu241.	N_{11}^0	N(11)	$\frac{\text{atoms}}{\text{barn cm (of fuel)}}$
3	29-42	E	Initial concentration, Pu242.	N_{12}^0	N(12)	$\frac{\text{atoms}}{\text{barn cm (of fuel)}}$
3	43-56	E	Normalized velocity spacing for Wilkins equation solution, $\frac{\delta v}{2200\text{m/s}}$	μ_V	AMUV	—

Table D1. (Con't)

Card No.	Column No.	Input Form	Item	Symbol		Compatible Units
				Text	FUELCYC Printout	
3	57-70	E	Slowing down power.	$\xi \Sigma_s$	SDP	cm ⁻¹ (of moderator)
4	1-14	E	Normalized moderator temperature variable, $\left(\frac{293.6^\circ\text{K}}{T_{\text{md}}}\right)^{1/2}$	$\left(\frac{T_o}{T_{\text{md}}}\right)^{1/2}$	T	—
4	15-28	E	Resonance disadvantage factor for U238.	$\psi_{1,8}$	PSI1 (8)	—
4	29-42	E	Constant terms in resonance integral, $\frac{V_{\text{fl}}}{\xi \Sigma_s V_{\text{md}}}$	C_1	C1	cm (of fuel)
4	43-56	E	Fast fission factor.	ϵ	EPSI	—
4	57-70	E	Initial Estimate of non-leakage probability.	P_1^0	P1IN	—
5	1-14	E	Initial Estimate of $\frac{-D\nabla^2 \phi}{\phi}$.	$(-D\nabla^2)^0$	C36IN	cm ⁻¹
5	15-28	E	Radius of core.	R	R	cm
5	29-42	E	Height of core.	H	H	cm

Table D1. (Con't.)

Card No.	Column No.	Input Form	Item	Symbol		Compatible Units
				Text	FUELCYC Printout	
5	43-56	E	Radial extrapolation distance to zero flux (reflector savings).	δ_R	DELR	cm
5	57-70	E	Axial extrapolation distance to zero flux (reflector savings).	δ_H	DELH	cm
6	1-14	E	Thermal diffusion coefficient.	D	D	cm
6	15-28	E	Fermi age.	τ	TAU	cm ²
6	29-42	E	Macroscopic absorption cross section for the moderation region.	Σ_{md}	SIGMOD	cm ⁻¹ (of moderator)
6	43-56	E	Microscopic Xe cross section.	σ_{Xe}	SIGXE	barns
6	57-70	E	Microscopic cross section per fission product pair, (or per fission), for the low cross section fission products.	σ_{FP}	SIG (7)	barns
7	1-14	E	Flux time spacing for solution of nuclide concentration equations, $\delta\theta$.	ζ	ZETA	(barns) ⁻¹

Table D1. (Con't.)

Card No.	Column No.	Input Form	Item	Symbol		Compatible Units
				Text	FUELCYC Printout	
7	15-28	E	Thermal disadvantage factor (only used as multiple of Σ_{md}).	ψ	PSI	—
7	29-42	E	Power density.	P_d	POWERD	$\frac{\text{Kilowatts}}{\text{liter}}$
7	43-56	E	Designator for axial symmetry: $Z_{sym} = 0$, axial symmetry $Z_{sym} = \text{non-zero}$, no axial symmetry.	Z_{sym}	ZSYM	—
7	57-70	E	Volume fraction of fuel in core.	V_{fl}	VFL	—
8	1-14	E	Macroscopic scattering cross section of the fuel.	$\Sigma_{s, fl}$	SGMSFL	cm^{-1} (of fuel)
8	15-28	E	Designator for calculation of costs: COSTT=0, do cost calculation COSTT=non-zero, omit cost calculation.	COSTT	COSTT	—

Table D1. (Con't.)

Card No.	Column No.	Input Form	Item	Symbol		Compatible Units
				Text	FUELCYC Printout	
9	1-10	I	Number of velocity points for Wilkins equation solution (or one plus number of steps) (must be odd and < 100).	i_L	IL	—
9	11-20	I	Number of flux-time points for solution of nuclide concentration equations (one plus number of steps).	n_ζ	NUMPOZ	—
9	21-30	I	Number of nuclide concentration solution points (n_ζ points) included in spacing for flux time fit. Degree of fit polynomial = $\frac{n_\zeta - 1}{n_{sp}}$, (the degree must be an integer ≤ 19).	n_{sp}	NUMSPA	—
9	31-40	I	Number of radial mesh points.	r_L	RL	—

Table D1. (Con't.)

Card No.	Column No.	Input Form	Item	Symbol		Compatible Units
				Text	FUELCYC Printout	
9	41-50	I	Number of axial mesh points.	z_L	ZL	—
9	51-60	I	Designator for type of fuel movement. IMOVE = 1 = Batch IMOVE = 2 = Inout IMOVE = 3 = Outin IMOVE = 4 = Graded.	i_{move}	IMOVE	—

Table D2. Input Data Required by Fuel Movement Subprograms
and for Initialization for a New Run.

Card Designation	Column No.	Input Form	Item	Symbol		Compatible Units
				Text	FUELCYC Printout	
B	1-14	E	Central flux time step for Batch fuel scheduling.	ζ_2	ZET2	(barns) ⁻¹
IOG	1-14	E	1 st estimate, final central flux time, for Inout, Outin or Graded fuel scheduling.	θ_1	THETA1	(barns) ⁻¹
IOG	15-28	E	2 nd estimate, final central flux time.	θ_2	THETA2	(barns) ⁻¹
R	14	I	Index for the next run $i_{run}=1$: complete new input. $i_{run}=2$: enrichment change (follow by 2R card). $i_{run}=3$: Pu recycle (follow by 3R card). $i_{run}=4$: new fuel movement method (follow by 4R card).	i_{run}	INXRUN	—
2R	1-14	E	New U235 concentration.	N_5^0	N(5)	$\frac{\text{atoms}}{\text{barn cm}^2(\text{of fuel})}$

Table D2. (con't.)

Card Designation	Column No.	Input Form	Item	Symbol		Compatible Units
				Text	FUELCYC Printout	
3R	1-14	E	Fractional recovery of Pu.	f_{recy}	FRECY	—
3R	15-28	E	New U235 concentration.	N_5^0	N(5)	$\frac{\text{atoms}}{\text{barn cm (of fuel)}}$
4R	2	I	New value for IMOVE (See Table 1, Card 9, Column 51-60).	i_{move}	IMOVE	—

Table D3. Cost Input Data.

Card Designation	Column No.	Input Form	Item	Symbol		Compatible Units
				Text	FUELCYC Printout	
C1	14	I	Designator for reading cost input; $i_{cst} = 0$, read cost input; $i_{cst} \neq 0$, don't read input (in this case the input data from the last run is used).	i_{cst}	INPCST	—
C1	28	I	Number of cost sets to be calculated, and, for $i_{cst} = 0$, number of sets to be read. (Each cost set consists of the cards C2-C9) ($j_{cst, L} \leq 8$).	$j_{cst, L}$	JCOSTL	—
C2	1-14	E	Material adjustment factor, Cost Step 1 (see Fig. 4.5).	f_1	F(1)	—
C2	15-28	E	Material adjustment factor, Cost Step 2.	f_2	F(2)	—
C2	29-42	E	Material adjustment factor, Cost Step 3.	f_3	F(3)	—
C2	43-56	E	Material adjustment factor, Cost Step 4.	f_4	F(4)	—

Table D3. (Con't.)

Card Designation	Column No.	Input Form	Item	Symbol		Compatible Units
				Text	FUELCYC Printout	
C2	57-70	E	Material adjustment factor, Cost Step 5.	f_5	F(5)	—
C3	1-14	E	Material adjustment factor, Cost Step 6.	f_6	F(6)	—
C3	15-28	E	Material adjustment factor, Cost Step 7.	f_7	F(7)	—
C3	29-42	E	Material adjustment factor, Cost Step 8.	f_8	F(8)	—
C3	43-56	E	Material adjustment factor, Cost Step 9.	f_9	F(9)	—
C3	57-70	E	Material adjustment factor, Cost Step 10.	f_{10}	F(10)	—
C4	1-14	E	Material adjustment factor, Cost Step 11.	f_{11}	F(11)	—
C4	15-28	E	Material adjustment factor, Cost Step 12.	f_{12}	F(12)	—
C4	29-42	E	Material adjustment factor, Cost Step 13.	f_{13}	F(13)	—
C4	43-56	E	Material adjustment factor, Cost Step 14.	f_{14}	F(14)	—

Table D3. (Con't.)

Card Designation	Column No.	Input Form	Item	Symbol		Compatible Units
				Text	FUELCYC Printout	
C4	57-70	E	Material adjustment factor, Cost Step 15.	f_{15}	F(15)	—
C5	1-14	E	Fraction of non-recycled U235 from natural U.	f_{nat}	FNAT	—
C5	15-28	E	Unit price for Cost Step 3 (for price basis see Fig. 4.5).	C_3	C(3)	\$/kg U
C5	29-42	E	Unit price for Cost Step 4.	C_4	C(4)	\$/kg Pu
C5	43-56	E	Unit price for Cost Step 5.	C_5	C(5)	\$/kg U235
C5	57-70	E	Unit price for Cost Step 6.	C_6	C(6)	\$/kg U235
C6	1-14	E	Unit price for Cost Step 7.	C_7	C(7)	\$/kg Pu
C6	15-28	E	Unit price for Cost Step 8.	C_8	C(8)	\$/kg fuel
C6	29-42	E	Unit price for Cost Step 9.	C_9	C(9)	\$/kg fuel
C6	43-56	E	Unit price for Cost Step 12.	C_{12}	C(12)	\$/kg Pu
C6	57-70	E	Unit price for Cost Step 14.	C_{14}	C(14)	\$/kg Pu

Table D3. (Con't.)

Card Designation	Column No.	Input Form	Item	Symbol		Compatible Units
				Text	FUELCYC Printout	
C7	1-14	E	Unit price for Cost Step 15.	C_{15}	C(15)	\$/kg fuel
C7	15-28	E	Daily reprocessing charge.	d_{10}	D10	\$/day
C7	29-42	E	Unit price Cost Step 11, Alternate 1.	$d_{11,1}$	D111	\$/kg U
C7	43-56	E	Unit price Cost Step 11, Alternate 2.	$d_{11,2}$	D112	\$/kg U
C7	57-70	E	Unit price of separative work.	C_E	CE	\$/kg U
C8	1-14	E	Optimum weight fraction U235 for diffusion cascade waste.	x_o	XO	—
C8	15-28	E	Net thermal efficiency	γ	GAMMA	—
C8	29-42	E	UF ₆ fractional yearly lease charge.	F_N	FN	<u>fraction of initial cost</u> year
C8	43-56	E	Working Capital fractional yearly charge.	F_W	FW	<u>fraction of working capital</u> year
C8	57-70	E	Lease charge time excluding reactor time.	t_L	TL	years

Table D3. (Con't.)

Card Designation	Column No.	Input Form	Item	Symbol		Compatible Units
				Text	FUELCYC Printout	
C9	1-14	E	Working Capital charge time excluding reactor time.	t_w	TW	years
C9	15-28	E	Load factor.	L	FLOAD	—
C9	29-42	E	Weight of fuel charged to the reactor.	W_{fl}	WTF	kg.

TABLE D4. SAMPLE INPUT DATA FOR FUELCYC

0 SAMPLE RUN NO. 1, WITH BATCH FUEL SCHEDULING					
.0008785	0	0	.02465		0
0	0	0	.17573		.8181
.7359	14.76	.6297	1.0584		.9654
.000192	96.11	234.33	7.5		7.5
.2755	51.5	.0542	1.35		E+0631.9
.0002	1.141	70.57	0.		.3400
.4271					
	25	13	1	7	7
.0001					1
	0	2			
	1.02				
1.01		1.	1.		.99
.99	.99	.99	.99		
	40.				660.
	90.	9.	1500.		12000.
0.	15300.	5.6	32.		37.286
.0022138	.2791	.04	.09		1.67
.458	.8	24395.			
	1.02				
1.01		1.	1.		.99
.99	.99	.99	.99		
	40.				1320.
	90.	9.	1500.		12000.
0.	15300.	5.6	32.		37.286
.0022138	.2791	.12	.09		1.67
.458	.8	24395.			
0 SAMPLE RUN NO. 2, WITH INOUT FUEL SCHEDULING					
	4				
2					
.002	.0022				
	1	2			

2. Octal Correction Cards

For changes to the program other than in the input data, such as bypassing printouts or resetting convergence parameters, use can be made of octal correction cards. These cards will be read by the loader and listed on Tape 2. The preparation of these cards is described fully in the M.I.T. Computation Center Memo CC-119, but for convenience this information will be summarized here.

An octal correction card is needed for each word and a blank or a zero have equivalent values. The format of the correction card is as follows:

<u>Columns</u>	<u>Contents</u>
1-2	both must contain 9 punches
3	blank
4-8	nominal octal address if relocatable card, true octal address if absolute card
9	blank
10-11	a) if even, the relocation number which corresponds to the first two octal digits of the 8L word of an equivalent one-word relocatable binary card. For example: 00 would mean decrement absolute, address absolute; 20 would mean decre- ment absolute, address relative (to be relocated in lower memory or stored in upper memory, common, depending upon the magnitude of the address relative to the program break.)

10-11	b) if odd, it is an absolute card (usually 77 is used.)
12	blank
13-24	nominal octal word if relocatable card, true octal word if absolute card.
25-72	arbitrary comment field, ignored by loader (but will be listed on Tape 2).

3. Program Stops in FUELCYC

Table D5. lists program stops for FUELCYC. Except for the normal stop, HPR 0, 1 in 21230_g, program stops are not given for the standard Fortran II Subprograms. Such stops can be identified from local write-ups of these subprograms, where the relative stop location can be obtained from the absolute location by referring to the subprogram entry points given in Appendix C.

Table D5. Program Stops in FUELCYC.

Program	Fortran Statement Number	Relative Location (Octal)	Absolute Location (Octal)	Octal Address Display	Reason for Stop
GETTPY 4	—	—	16	17	Check sum error in reading Tape 4.
MAIN	235	1132	2363	373	Initial Criticality Factor less than unity.
MAIN	460	2331	3562	6	IMOVE = 5
MAIN	470	2333	3564	7	IMOVE = 6
MAIN	480	2335	3566	11	IMOVE = 7
MAIN	490	2337	3570	12	IMOVE = 8
MAIN	680	2655	4106	2	INXRUN = 5
READ-PRINT	—	277	21230	0, 1	Normal, no cards in hopper.
WILK2	—	253	26667	7	No convergence of Wilkins Equation in startup.
SPACON	90	371	33225	21	$r_L < 1$
SPACFX	410	1412	44170	71	No convergence in spatial flux-shape iteration.
COST	15	134	51226	111	More than 8 cost sets.
COST	110	730	52022	14	$x_p < x_o$, Cost Step 2.
COST	160	773	52065	15	$x_p < x_o$, Cost Step 1.
COST	350	1125	52217	15	$x_p < x_o$, Cost Step 13.
BATCH	30	370	55423	717	C didn't go to 1 in 30 steps.
INOUT	22	366	56514	151	No convergence in flux-time iteration.
OUTIN	22	365	60177	151	No convergence in flux-time iteration.
GRADED	22	425	61761	555	No convergence in flux-time iteration.

E. ERROR ESTIMATION FOR THE NUMERICAL METHODS

This section considers the magnitude of the errors involved in various mathematical approximations employed in FUELCYC. The relationship of different truncation errors to various input data spacing parameters is also discussed. In all cases the price of an increase in the accuracy of the results is a corresponding increase in the computer time required for the solution. Methods for estimating the errors are given and, in addition, values for the spacing parameters are listed which were used for the pressurized light-water reactor calculations of this study.

Settings for the normalized velocity spacing (μ_v) and for the number of points for calculation of the velocity distribution of the thermal flux (i_L) are considered in Section 1 of this Appendix; the flux-time spacing for the step-wise solution of the nuclide concentration equations (ζ) is considered in Section 2.1; the total number of these solution points (n_ζ) and the number of ζ steps per flux-time fit point (n_{sp}) are considered in Section 2.1; the number of radial and axial mesh points (r_L and z_L) is discussed in Sections 3.3 and 3.4; the flux-time step for Batch irradiation (ζ_2) and initial estimates for the final flux time for steady-state fuel scheduling (θ_1 and θ_2) are considered in Section 3.5. Eq. (4.158) gives an estimate of the time requirement, as a function of these parameters, which can be used along with the discussion of this section to pick efficient settings.

1. Truncation Errors in Computing Average Cross Sections.

There are two sources of error in the numerical methods used for averaging microscopic cross sections over a Wilkins spectrum, assuming the microscopic point cross sections to be correct.* These occur in the numerical solution of Wilkins equation for the flux per unit energy, $Y(x)$, and in the numerical integration of the point cross sections weighted by Y .

The startup of the Wilkins equation solution is by a truncated Taylor series. Here the values for Y are small and enough terms are retained in the series to reduce the relative truncation error to negligible size (1×10^{-6}). The majority of the solution values are then generated by 2nd difference, 5th order Milne formulas, see Appendix A. The error term in the prediction formula for each step is,

$$y - y^{(0)} \approx \frac{17\mu^6}{240} y^{VI} [\xi^{(0)}] \quad (1)$$

where ξ is some value of x within the range of the x values being used for the step, y is the true value, and μ is the spacing in x . The error term in the revision formula is approximately,

$$y - y^{(1)} \sim -\frac{1}{240}\mu^6 y^{VI} [\xi^{(1)}] \quad (2)$$

*The equations used to generate point cross sections are discussed in Section IV.A.4. and in Appendix C.7. Westcott, W11, states that in the cases when these equations were designed to fit the BNL-325 curves the accuracy was 1/4% or better below 0.2 ev, 1% or better between 0.2 and 0.4 ev, and with less accuracy above 0.4 ev. BNL-325 reports standard deviations for 2200 m/s values of σ_{abs} for the nuclides used in this study, of approximately 1% for U235, U238, and Pu239; 7% for Pu240, Pu241, and Pu242; and 30% for U236.

Assuming $y^{VI} [\xi^{(0)}] \sim y^{VI} [\xi^{(1)}]$, Eqs. (1) and (2) give the truncation error estimate of

$$F_T = y - y^{(1)} \sim \frac{(y^{(1)} - y^{(0)})}{18} \quad (3)$$

The summation of the truncation error estimates for past steps gives some indication of the cumulative truncation error to that point. Both the step and the cumulative error values are printed out by the WILK2 subroutine, see Appendix C.9., so this information can be used to control the accuracy in this part of the code. A reduction in the magnitude of the WILK2 spacing parameter, μ , should produce a corresponding reduction in this truncation error. If no reduction occurs it is an indication that the accuracy is as good as can be obtained and that the errors are not due to the spacing (but rather to "noise" in the input parameter A (x)).

The average cross sections are then calculated by integrating the point values over x with the weighting function Y(x). This integration is achieved with the parabolic rule, where the truncation error is proportional to $n\mu^5$, n being the number of steps. No error estimate is available for a single calculation but if a second calculation, $\sigma^{(2)}$, is made with half the spacing (therefore requiring 2n steps), the ratio of truncation errors can be estimated as,

$$\frac{\sigma - \sigma^{(1)}}{\sigma - \sigma^{(2)}} \sim \frac{n\mu^5}{2n(\mu/2)^5} \quad (4)$$

This can be solved for the estimate for the true cross section value as,

$$\sigma \sim \sigma^{(2)} + \frac{\sigma^{(2)} - \sigma^{(1)}}{15} \quad (5)$$

This is a standard technique, H27, p. 238, for error estimates in initial-value problems and will also be referred to in other sections of this Appendix. The general form of Eq. (5) for the true value of a parameter, z , given by an equation of order r (i.e., the error term is of degree $r + 1$ in the spacing) is seen to be,

$$z \sim z^{(2)} - \frac{z^{(2)} - z^{(1)}}{2^r - 1} \quad (6)$$

where $z^{(2)}$ is calculated at half the spacing used for $z^{(1)}$.

The Wilkins equation spacing parameter, μ , is related to the input parameter, μ_V , according to,

$$\mu = \mu_V \sqrt{\frac{T_0}{T_{md}}} \quad (7)$$

so higher values of μ_V can be specified as T_{md} increases.

The energy distribution of the flux is more severe (i.e., there is greater variation in the higher order derivatives) in well-moderated lattices than for poorly moderated ones, so the well-moderated cases require a smaller value of μ .

μ_V is related to the number of steps, $i_L - 1$, by

$$\mu_V = \frac{1}{(i_L - 1)} \sqrt{\frac{T_1}{T_0}} \quad (8)$$

where the thermal cutoff energy is kT_1 , and T_0 is 293.6°K.

For the pressurized-light water reactor, with $kT_1 = 0.45$ ev and $(T_0/T_{md})^{1/2} = 0.7359$, a value of 25 was used for i_L (the fractional differences between calculated cross sections for this value and for $i_L = 49$ were less than .02%). For the NRX heavy water moderated

cases, with $kT_1 = 0.45$ eV and $(T_o/T_{md})^{1/2} = 0.971$, a value for i_L of 49 was used. In testing the WILK2 subroutine a Maxwell-Boltzmann flux was reproduced, with $kT_1 = 0.2488$ and $T_{md} = T_o$, and here i_L was taken as 99.* In this calculation the estimated cumulative truncation error in the flux was quite conservative for high velocities, being too large by a factor of approximately 10 for the final point. (Since this estimate is a cumulative sum of successive step error estimates starting from zero velocity, it would not be expected to be accurate after a large number of steps.)

Normally the value of 25 should be sufficient for i_L for power reactor calculations.

2. Truncation Errors in Computing Nuclide Concentrations as Functions of Flux-Time

2.1 Solution of the Nuclide Concentration Equations. Since a Runge-Kutta method is used for solution of the first order differential equations for the nuclide concentrations, no error estimate is available for a single calculation. The halved spacing method described in the previous section, Eq. (6), was used for error estimation. The method is fourth order which gives the estimate for the fractional error in the value for a nuclide concentration of,

$$\frac{N-N^{(2)}}{N^{(2)}} \sim - \frac{N^{(2)} - N^{(1)}}{15 N^{(2)}} \quad (9)$$

This test was made for the concentration equation solution using initial values typical of the pressurized light-water reactor. In Eq. (9),

* i_L must be odd and less than 100.

$N^{(2)}$ was calculated for a constant flux time spacing, ζ , of 0.1 n/kb and $N^{(1)}$ for a constant spacing of 0.2 n/kb. This gave values for the fractional difference, $[N^{(2)} - N^{(1)}]/N^{(2)}$, which were 0.003 or less at 0.5 n/kb and were 0.001 or less at 1 n/kb.* From Eq. (9) it is seen that $N^{(2)} \sim N$ so the above values can be taken as the relative truncation errors in the nuclide concentrations using a flux time spacing of 0.2 n/kb. Fractional errors of approximately 15 times this would be anticipated for a spacing of 0.4 n/kb.

For these reasons the value 0.2 n/kb (0.0002 n/b using input data units) was normally used for ζ . The parameter n_ζ is the number plus one of steps and should be chosen so that the product $(n_\zeta - 1)\zeta$ is larger than the maximum expected flux-time.

2.2 Polynomial Fit of the Nuclide Concentrations and the "Space Properties" Versus Flux-Time. For low enrichments in the uranium fueled, batch irradiated, pressurized-water reactor studied here the criticality factor usually had a peak in the vicinity of 0.1 n/kb. From this it might be expected that the spacing for the fit of the spatial properties would have to be no greater than this value. Fortunately this is not true since the peak is produced by a combination of space properties which individually are much smoother functions.

The Lagrangian interpolation polynomial, H27, p. 62, is used to calculate the value of the various functions. This is a convenient way to calculate these values but has the disadvantage that it is difficult to

*It is generally true, due to the exponential nature of the solution, that the accuracy improves as flux-time increases.

estimate the truncation error.

A comparison was made, however, for a typical pressurized light-water reactor enrichment using spacings of 0.2 n/kb and 0.1 n/kb between flux-time fit points. The relative difference between values for the criticality factor at 0.1 n/kb was less than 0.05% and became better at higher flux-times. In an analogous manner the spacing of 0.2 n/kb was also found to be adequate for the calculation of the final average nuclide concentrations, so was generally used for the flux-time spacing. For long irradiations a close fit to the properties at low flux-times is less important and a larger value can be used for the spacing. The rule used for the pressurized water reactor was to take a spacing of 0.2 n/kb unless the degree of the flux-time fit polynomial became greater than ten; for which case a spacing of 0.4 n/kb was used.

The fractional changes in concentrations and space properties, for a flux-time spacing, $\delta\theta$, are related to the product $\sigma(\delta\theta)$ or to

$$(\delta\theta) \sigma_0 \sqrt{\frac{\pi T_0}{4 T_{\text{neutron}}}} \text{ for } 1/v \text{ cross sectional behavior. This relation-}$$

ship can be used to revise the above estimates for the flux-time spacing, for reactors with different values of T_{neutron} , so as to give approximately the same value for $\sigma(\delta\theta)$ ($T_{\text{neutron}} \sim 900^\circ \text{ K}$ for the pressurized water reactor).

The parameter n_{sp} is the number of ζ steps used for a flux-time fit step, where ζ was the spacing for the solution of the differential nuclide concentration equations:

$$(\delta\theta)_{\text{fit}} = n_{\text{sp}} \zeta \tag{10}$$

The degree of the fit polynomial is then given by,

$$\text{degree} = \frac{n_{\xi} - 1}{n_{\text{sp}}} \quad (11)$$

which must be an integer.

3. Errors in the Spatial Calculation

3.1 The Condensed Two Group Equation. In the condensed two group equation, Eq. (4.30), the assumption is made that the fast flux is given by,

$$\phi_1 \sim \frac{(\Sigma + \Sigma_w) \phi}{p\Sigma_1} \quad (12)$$

rather than the true value, from Eq. (4.27), of,

$$\phi_1 = \frac{(\Sigma + \Sigma_w) \phi - D\nabla^2 \phi}{p\Sigma_1} \quad (13)$$

The error occurs in the fast leakage term, $-D_1\nabla^2\phi$. An expression for the relative error (defined as ("true" - "approximate") / "true") in this fast leakage term, F_1 , can be obtained from Eqs. (12) and (13),

$$F_1 = \frac{-\nabla^2 \left(\frac{D}{p\Sigma_1} \right) \nabla^2 \phi}{\nabla^2 \left[\frac{(\Sigma + \Sigma_w)}{p\Sigma_1} \phi \right] - \nabla^2 \left(\frac{D}{p\Sigma_1} \right) \nabla^2 \phi} \quad (14)$$

For simplification, consider the case where $\frac{D}{p\Sigma_1}$ and $\frac{\Sigma + \Sigma_w}{p\Sigma_1}$ are constant. In this case Eq. (14) for the relative error in the fast leakage reduces to,

$$F_1 = \frac{L^2 \nabla^4 \phi}{\nabla^2 \phi - L^2 \nabla^4 \phi} \sim \frac{-L^2 \nabla^4 \phi}{\nabla^2 \phi} \quad (15)$$

which is very small for a power reactor. In particular, $F_1 \sim B_g^2 L^2$ for a bare uniformly loaded reactor and $F_1 = 0$ for a flat thermal flux region.

3.2 The Estimate for the Control Poison. In Batch irradiation an estimate is made for the amount of control poison required to just keep the reactor critical. The deviation of this estimate, Σ_w , from the true value, Σ'_w is also a source of error in the fast group leakage term,

$$-D_1 \nabla^2 \frac{(\Sigma + \Sigma_w)}{p\Sigma_1} \phi \quad (\text{In addition to its effect on the thermal flux,}$$

which was discussed in Section IV.A.2.5). The expression for the relative error, due to the control poison, in the fast leakage term is seen to be,

$$F_w = 1 - \frac{\nabla^2 \left[\frac{(\Sigma + \Sigma_w)}{p\Sigma_1} \phi \right]}{\nabla^2 \left[\frac{(\Sigma + \Sigma'_w)}{p\Sigma_1} \phi \right]} \quad (16)$$

where prime denotes the true value. For the case where $-\nabla^2 = B_g^2$ and also $p\Sigma_1$ is constant, Eq. (16) reduced to,

$$F_w = 1 - \frac{\Sigma + \Sigma_w}{\Sigma + \Sigma'_w} \quad (17)$$

The criticality factor with control poison, C_w , is printed out by the code and for the uniform loaded case, with no resonance fissions, is defined by,

$$C_w = \frac{\epsilon v \Sigma_f P_1 p}{\Sigma + \Sigma_w + DB_g^2} \sim \frac{\epsilon v \Sigma_f P_1 p}{\Sigma + \Sigma_w} \quad (18)$$

where for the correct value of control poison the criticality factor would be unity,

$$1 \sim \frac{\epsilon v \Sigma_f P_1' p}{\Sigma + \Sigma_w'} \quad (19)$$

For power reactors the non-leakage probably, P_1 , is large compared to $(1 - P_1)$ so small changes in the fast leakage produce negligible changes in the non-leakage probability and we can set P_1' in Eq. (19) equal to P_1 . Eqs. (18) and (19) can then be combined to give,

$$C_w \sim \frac{\Sigma + \Sigma_w'}{\Sigma + \Sigma_w} \quad (20)$$

Inserting this result into Eq. (17) gives the following convenient estimate for the relative error in fast leakage, due to errors in the control poisoning,

$$F_w = \frac{C_w - 1}{C_w} \sim C_w - 1 \quad (21)$$

This error is negligible.

3.3 The Spatial Flux-Distribution. The error involved in approximating the second-order differential diffusion equation, Eq. (4.30), by a difference equation can be estimated as follows. Consider the axial direction, where the differential term $\partial^2 \phi / \partial z^2$ will be abbreviated as ϕ_z'' . The symbol δ^2 will be used to represent the central difference operator, where

$$\delta^2 \phi_z \equiv \phi_{z+1} - 2\phi_z + \phi_{z-1} \quad (22)$$

$\delta^2 \phi_z$ is related to ϕ_z'' , H27, p. 146, by,

$$\delta^2 \phi_z = h^2 \left(1 + \frac{1}{12} \delta^2 - \frac{1}{240} \delta^4 + \dots \right) \phi_z^n \quad (23)$$

where, h is the spacing in the axial direction. The approximation used here was to retain only the first term in Eq. (23) giving the familiar relationship,

$$\phi_z^n = \frac{\delta^2 \phi_z}{h^2} + F_T \quad (24)$$

where the truncation error F_T is given by,

$$F_T = -\frac{h^2}{12} \phi_\xi^{IV}, \quad (z-1) < \xi < (z+1) \quad (25)$$

the relative error in ϕ_z^n , F_z , is then

$$F_z = \frac{F_T}{\phi_z^n} = -\frac{h^2}{12} \frac{\phi_\xi^{IV}}{\phi_z^n} \sim -\frac{h^2}{12} \frac{\phi_z^{IV}}{\phi_z^n} \quad (26)$$

For the bare uniformly loaded case

$$\phi_z = \cos \frac{\pi z'}{2Z} \quad (27)$$

$$\phi_z^n = -\left(\frac{\pi}{2Z}\right)^2 \cos \frac{\pi z'}{2Z} \quad (28)$$

and

$$\phi_z^{IV} = \left(\frac{\pi}{2Z}\right)^4 \cos \frac{\pi z'}{2Z} \quad (29)$$

where, $2Z = (H + 2\delta_H)$. Taking h as Z/z_L , where z_L is the number of axial regions, and inserting Eqs. (29) and (28) into Eq. (26), gives, for the relative truncation error in the leakage,

$$F_z \sim \frac{\pi^2}{48z_L^2} \sim \frac{0.2}{z_L^2} \quad (30)$$

The total relative error for radial leakage would be expected to be of the same order of magnitude. For $r_L = z_L$ this gives the general estimate for the relative errors in the leakage terms,

$$F_n \sim \frac{0.2}{n} \quad (31)$$

where n is the number of mesh points ($n = r_L z_L$).

The validity of Eq. (31) was verified for FUELCYC calculations of the relative errors in $DB^2\phi$ (and ϕ) for mesh spacings of 3×3 , 5×5 , and 10×10 .

The relative error in the initial criticality factor, F_c , is roughly that due to the fast nonleakage probability and therefore estimated by,

$$F_c \sim \frac{(1-P_1)}{P_1} F_n \quad (32)$$

since F_n gives the relative error in $(1-P_1)$.

3.4 Spatial Averaging. In averaging the reactor properties it is assumed that the flux is constant in each region. This assumption introduces the largest errors of the numerical methods since it effectively flattens the flux as the number of regions is decreased and affects the values for maximum to average power density, the average burnup, the final nuclide concentrations, and the fuel cycle cost. The error introduced depends upon the irradiation history but, for the pressurized water reactor the magnitude of the relative error in the above values was approximately 12% for a 3×3 mesh, 3% for a 5×5 mesh and 1% for a 7×7 mesh.

Since the parameters considered in the previous section can be calculated so accurately with coarse meshes, the trend of the spatial average parameters, as changes are made in physical parameters (enrichment, for instance), is correct even for coarse meshes. For this reason, if computer time is an important consideration, the bulk of the calculations can be run using a 3×3 mesh followed by normalization to correct values by a few runs at a 7×7 mesh.

3.5 Flux-time Settings for Fuel Scheduling Methods. The flux-time step for Batch fuel scheduling, ζ_2 , should be such that the flux shape changes only slightly during a step. However, the error in the criticality factor becomes less as flux-time progresses. A reasonable rule has been found to take $\zeta_2 = 0.1$ n/kb unless the final flux time exceeds 1 n/kb, for which cases $\zeta_2 = 0.2$ n/kb was used.

For the steady state fuel scheduling methods, where no control poison is added, the flux iteration will not converge if the criticality factor for the estimated flux-time distribution is too much less than unity (roughly it must be greater than $\frac{1 + P_1}{2}$ for convergence). For this reason it is good to choose the initial central flux-time estimates θ_1 and θ_2 so that the resulting criticality factor is greater than or approximately equal to, unity. θ_2 is reused for the second interpolation so should be the better estimate.

F. TABULATED RESULTS FOR THE PRESSURIZED LIGHT-WATER REACTOR

Tables F1 through F7 list local properties of the fuel which are dependent on the flux-time for enrichments from 2.876 a/o U235 to 6.452 a/o U235. These tables are analogous to Table 6.1 which was presented in Section VI. A.1 for the 3.441 a/o U235 case.

Tables F8 through F25 are cost results for different enrichments, fuel scheduling methods and price bases. These tables are analogous to Table 6.6 of Section VI. A.3, which was for Batch fuel scheduling in the 3.441 a/o U235 variation. (All values were rounded from more accurate data, so the net fuel cycle cost will not necessarily agree exactly with the sum of the component costs.)

Tabulated results for final nuclide concentrations and other results of runs were listed in Tables 6.2 to 6.5 of Section VI. A.2.

Table F1 Local Properties of Fuel Dependent on Initial Enrichment and Flux-Time.

Initial Enrichment: 2.876 a/o U235

Runs No. 4

Property	Flux-Time (n/kb)					
	0	0*	0.2	0.4	0.6	0.8
Cross Sections (b)						
$\sigma_{5,f}$	267.6	264.5	262.7	261.5	260.6	260.0
$\sigma_{9,f}$	882.3	891.7	898.0	902.4	905.6	908.0
$\sigma_{11,f}$	839.3	839.7	838.0	836.6	835.5	834.6
σ_5	320.8	317.1	315.0	313.6	312.6	311.8
σ_6	3.546	3.508	3.485	3.469	3.458	3.451
σ_8	1.373	1.358	1.349	1.343	1.339	1.336
σ_9	1425.	1443.	1455.	1463.	1469.	1473.
σ_{10}	190.4	189.5	189.2	189.0	188.9	188.9
σ_{11}	1155.	1156.	1154.	1152.	1150.	1149.
σ_{12}	16.01	15.86	15.77	15.71	15.67	15.64
Atoms/b cm (of fuel)						
N_5	7.300 E-4	7.300 E-4	6.681 E-4	6.105 E-4	5.573 E-4	5.083 E-4
N_6	0	0	1.198 E-5	2.303 E-5	3.311 E-5	4.221 E-5
N_{FP}	0	0	5.852 E-5	1.202 E-4	1.841 E-4	2.493 E-4
N_8	2.465 E-2	2.465 E-2	2.461 E-2	2.456 E-2	2.451 E-2	2.446 E-2
N_9	0	0	3.423 E-5	6.088 E-5	8.136 E-5	9.692 E-5

*With equilibrium Xenon and "Samarium Group" poison.

Table F1 (Cont.)

Property	Flux-Time (n/kb)					
	0	0*	0.2	0.4	0.6	0.8
N_{10}	0	0	1.838 E-6	5.882 E-6	1.078 E-5	1.588 E-5
N_{11}	0	0	3.059 E-7	1.904 E-6	4.930 E-6	8.972 E-6
N_{12}	0	0	6.261 E-9	8.137 E-8	3.326 E-7	8.458 E-7
Space Properties						
$\Sigma_{Xe, max}$, cm^{-1} (fuel)	0	0.01795	0.01884	0.01934	0.01963	0.01974
$(\Sigma_{fl} - \Sigma_{Xe})$, cm^{-1} (fuel)	0.2680	0.2700	0.3026	0.3276	0.3475	0.3631
$\Sigma_f V_{fl}$, cm^{-1}	0.06643	0.06565	0.07035	0.07357	0.07586	0.07741
$v \Sigma_f V_{fl}$, cm^{-1}	0.1641	0.1622	0.1783	0.1900	0.1990	0.2056
$(1-p)/(1+\alpha)$	0.09923	0.09923	0.09658	0.09369	0.09080	0.08798
$(1-p)\eta$	0.2450	0.2450	0.2409	0.2359	0.2307	0.2255
p	0.6225	0.6225	0.6180	0.6082	0.5983	0.5901
Inverse Mod. Ratio, $\frac{\Sigma}{\xi \Sigma_g}$						
Velocity Step,** 4	0.7317	0.7744	0.7758	0.7715	0.7664	0.7604
9	0.2978	0.3167	0.3197	0.3242	0.3256	0.3261
14	0.1802	0.1924	0.1997	0.2159	0.2238	0.2301
19	0.1652	0.1742	0.2285	0.3567	0.4198	0.4692
24	0.09056	0.09768	0.1019	0.1115	0.1161	0.1195

*With equilibrium Xenon and "Samarium Group" poison.

**The step number is proportional to velocity where step 24 corresponds to an energy of 0.45 ev.

Table F2 Local Properties of Fuel Dependent on Initial Enrichment and Flux-Time

Initial Enrichment: 3.105 a/o U235

Runs. No. 7

Property	Flux-Time (n/kb)					
	0	0*	0.4	0.8	1.2	1.6
Cross Sections (b)						
$\sigma_{5,f}$	264.9	261.7	258.7	257.2	256.8	257.0
$\sigma_{9,f}$	890.1	899.8	910.6	916.2	918.5	918.5
$\sigma_{11,f}$	839.6	839.9	836.5	834.3	832.9	832.1
σ_5	317.6	313.9	310.3	308.6	308.1	308.4
σ_6	3.513	3.474	3.436	3.417	3.410	3.413
σ_8	1.360	1.345	1.330	1.323	1.320	1.321
σ_9	1440.	1459.	1478.	1488.	1493.	1492.
σ_{10}	189.6	188.7	188.3	188.1	188.2	188.3
σ_{11}	1156.	1156.	1152.	1148.	1147.	1145.
σ_{12}	15.88	15.72	15.57	15.50	15.48	15.49
Atoms/b cm (of Fuel)						
N_5	7.9000 E-4	7.900 E-4	6.583 E-4	5.459 E-4	4.512 E-4	3.736 E-4
N_6	0	0	2.565 E-5	4.688 E-5	6.380 E-5	7.689 E-5
N_{FP}	0	0	1.321 E-4	2.733 E-4	4.169 E-4	5.585 E-4
N_8	2.465 E-2	2.465 E-2	2.455 E-2	2.444 E-2	2.433 E-2	2.422 E-2
N_9	0	0	6.516 E-5	1.032 E-4	1.241 E-4	1.345 E-4

*With equilibrium Xenon and "Samarium Group" poison.

Table F2 (Cont.)

Property	Flux-Time (n/kb)					
	0	0*	0.4	0.8	1.2	1.6
N_{10}	0	0	6.296 E-6	1.678 E-5	2.691 E-5	3.568 E-5
N_{11}	0	0	2.169 E-6	1.005 E-5	2.013 E-5	2.944 E-5
N_{12}	0	0	9.687 E-8	9.709 E-7	3.149 E-6	6.522 E-6
Space Properties						
$\Sigma_{Xe, max}$, cm^{-1} (fuel)	0	0.01971	0.02124	0.02156	0.02124	0.02049
$(\Sigma_{fl} - \Sigma_{Xe})$, cm^{-1} (fuel)	0.2845	0.2866	0.3492	0.3864	0.4071	0.4157
$\Sigma_f V_{fl}$, cm^{-1}	0.07116	0.07030	0.07887	0.08275	0.08386	0.08295
$v \Sigma_f V_{fl}$, cm^{-1}	0.1758	0.1736	0.2038	0.2199	0.2271	0.2279
$(1-p)/(1+a)$	0.1067	0.1067	0.1004	0.09397	0.08784	0.08193
$(1-p)\eta$	0.2635	0.2635	0.2528	0.2409	0.2289	0.2167
p	0.6139	0.6139	0.5993	0.5815	0.5706	0.5647
Inverse Mod. Ratio, $\frac{\Sigma}{\xi \Sigma_s}$						
Velocity Step, ** 4	0.7726	0.8178	0.8118	0.7982	0.7810	0.7614
9	0.3137	0.3338	0.3406	0.3420	0.3401	0.3358
14	0.1896	0.2025	0.2269	0.2416	0.2499	0.2533
19	0.1749	0.1842	0.3791	0.4976	0.5669	0.6036
24	0.09479	0.1023	0.1168	0.1251	0.1293	0.1308

*With equilibrium Xenon and *Samarium Groupⁿ poison.

**The step number is proportional to velocity where step 24 corresponds to an energy of 0.45 ev.

Table F3 Local Properties of Fuel Dependent on Initial Enrichment and Flux-Time

Initial Enrichment: 3.711 a/o U235

Runs No. 6

Property	Flux-Time (n/kb)					
	0	0*	0,8	1,6	2,4	3,2
Cross Sections (b)						
$\sigma_{5,f}$	258.2	254.9	250.4	250.9	253.7	257.4
$\sigma_{9,f}$	909.9	920.2	936.8	936.9	929.4	919.1
$\sigma_{11,f}$	840.1	840.5	833.2	830.8	830.7	831.4
σ_5	309.8	305.9	300.6	301.2	304.5	308.8
σ_6	3.431	3.391	3.333	3.338	3.372	3.417
σ_8	1.328	1.313	1.290	1.292	1.306	1.323
σ_9	1478.	1497.	1527.	1527.	1513.	1493.
σ_{10}	187.7	186.8	186.4	186.8	187.6	188.6
σ_{11}	1156.	1157.	1147.	1144.	1143.	1144.
σ_{12}	15.55	15.39	15.17	15.20	15.33	15.51
Atoms/b cm (of fuel)						
N_5	9.500 E-4	9.500 E-4	6.427 E-4	4.308 E-4	2.911 E-4	1.995 E-4
N_6	0	0	6.026 E-5	9.703 E-5	1.166 E-4	1.259 E-4
N_{FP}	0	0	3.409 E-4	6.883 E-4	1.002 E-3	1.273 E-3
N_8	2.465 E-2	2.465 E-2	2.440 E-2	2.413 E-2	2.389 E-2	2.367 E-2
N_9	0	0	1.197 E-4	1.519 E-4	1.525 E-4	1.427 E-4

*With equilibrium Xenon and "Samarium Group" poison.

Table F3 (Cont.)

Property	Flux-Time (n/kb)					
	0	0*	0.8	1.6	2.4	3.2
N_{10}	0	0	1.919 E-5	3.956 E-5	5.316 E-5	6.138 E-5
N_{11}	0	0	1.319 E-5	3.587 E-5	4.887 E-5	5.327 E-5
N_{12}	0	0	1.355 E-6	8.394 E-6	1.854 E-5	2.8419 E-5
Space Properties						
$\Sigma_{Xe, max}$, cm^{-1} (fuel)	0	0.02475	0.02665	0.02458	0.02125	0.01793
$(\Sigma_{fl} - \Sigma_{Xe})$, cm^{-1} (fuel)	0.3270	0.3299	0.4477	0.4748	0.4597	0.4295
$\Sigma_f V_{fl}$, cm^{-1}	0.08340	0.08233	0.09661	0.09525	0.08715	0.07716
$v \Sigma_f V_{fl}$, cm^{-1}	0.2060	0.2034	0.2572	0.2621	0.2442	0.2187
$(1-p)/(1+a)$	0.1261	0.1261	0.1093	0.19361	0.07940	0.06714
$(1-p)\eta$	0.3115	0.3115	0.2803	0.2477	0.2151	0.1852
p	0.5914	0.5914	0.5598	0.5469	0.5466	0.5507
Inverse Mod. Ratio, $\frac{\Sigma}{\xi \Sigma_s}$						
Velocity Step,** 4	0.8813	0.9334	0.8985	0.8435	0.7839	0.7292
9	0.3560	0.3791	0.3843	0.3718	0.3517	0.3306
14	0.2143	0.2292	0.2725	0.2818	0.2743	0.2606
19	0.2000	0.2110	0.5735	0.6814	0.6837	0.6464
24	0.1060	0.1147	0.1400	0.1444	0.1405	0.1342

*With equilibrium Xenon and "Samarium Group" poison.

**The step number is proportional to velocity where step 24 corresponds to an energy of 0.45 ev.

Table F4 Local Properties of Fuel Dependent on Initial Enrichment and Flux-Time

Initial Enrichment: 4.272 a/o U235

Runs No. 5

Property	Flux-Time (n/kb)					
	0	0*	1.0	2.0	3.0	4.0
Cross Sections (b)		*				
$\sigma_{5,f}$	252.5	249.2	244.5	247.5	252.9	258.2
$\sigma_{9,f}$	927.0	937.9	955.3	947.8	932.5	917.0
$\sigma_{11,f}$	840.6	841.0	830.9	829.3	830.4	831.8
σ_5	303.2	299.2	293.7	297.2	303.5	309.8
σ_6	3.362	3.321	3.260	3.296	3.361	3.427
σ_8	1.302	1.286	1.262	1.276	1.301	1.327
σ_9	1510.	1531.	1562.	1547.	1518.	1489.
σ_{10}	186.2	185.3	185.1	186.1	187.5	188.8
σ_{11}	1157.	1158.	1144.	1142.	1143.	1145.
σ_{12}	15.28	15.12	14.89	15.03	15.29	15.55
Atoms/b cm (of fuel)						
N_5	1.100E-3	1.100E-3	6.547E-4	3.888E-4	2.373E-4	1.491E-4
N_6	0	0	8.7657E-5	1.299E-4	1.460E-4	1.502E-4
N_{FP}	0	0	5.155E-4	1.005E-3	1.406E-3	1.724E-3
N_8	2.465E-2	2.465E-2	2.428E-2	2.391E-2	2.360E-2	2.334E-2
N_9	0	0	1.496E-4	1.685E-4	1.547E-4	1.357E-4

*With equilibrium Xenon and "Samarium Group" poison.

Table F4 (Cont.)

Property	Flux-Time (n/kb)					
	0	0*	1.0	2.0	3.0	4.0
N_{10}	0	0	2.766 E-5	5.107 E-5	6.355 E-5	6.924 E-5
N_{11}	0	0	2.364 E-5	4.993 E-5	5.781 E-5	5.642 E-5
N_{12}	0	0	3.338 E-6	1.594 E-5	2.959 E-5	4.039 E-5
Space Properties						
$\Sigma_{Xe, \max}$, cm^{-1} (fuel)	0	0.02997	0.03123	0.02615	0.02058	0.01616
$(\Sigma_{ff} - \Sigma_{Xe})$, cm^{-1} (fuel)	0.3656	0.3692	0.5183	0.5185	0.4723	0.4219
$\Sigma_f V_{ff}$, cm^{-1}	0.09445	0.09319	0.1097	0.1011	0.08586	0.07142
$v\Sigma_f V_{ff}$, cm^{-1}	0.2333	0.2302	0.2958	0.2814	0.2429	0.2041
$(1-p)/(1+\alpha)$	0.1438	0.1438	0.1178	0.09458	0.07528	0.06030
$(1-p)\eta$	0.3550	0.3550	0.3049	0.2537	0.2067	0.1685
p	0.5711	0.5711	0.5364	0.5325	0.5397	0.5490
Inverse Mod. Ratio, $\frac{\Sigma}{\xi\Sigma_s}$						
Velocity Step,** 4	0.9830	1.042	0.9727	0.8770	0.7876	0.7170
9	0.3955	0.4217	0.4196	0.3905	0.3563	0.3269
14	0.2374	0.2542	0.3055	0.3022	0.2809	0.2580
19	0.2237	0.2361	0.6910	0.7536	0.7006	0.6258
24	0.1165	0.1263	0.1560	0.1539	0.1439	0.1337

*With equilibrium Xenon and "Samarium Group" poison.

**The step number is proportional to velocity where step 24 corresponds to an energy of 0.45 ev.

Table F5 Local Properties of Fuel Dependent on Initial Enrichment and Flux-Time

Initial Enrichment: 4.383 a/o U235

Runs No. 9

Property	Flux-Time (n/kb)					
	0	0*	0.6	1.2	1.8	2.4
Cross Sections (b)						
$\sigma_{5,f}$	251.5	240.1	243.9	243.7	245.7	248.8
$\sigma_{9,f}$	930.3	941.3	956.2	958.2	953.0	944.3
$\sigma_{11,f}$	840.6	841.0	833.2	829.9	829.1	829.4
σ_5	301.9	298.0	293.1	292.8	295.1	298.7
σ_6	3.349	3.308	3.254	3.250	3.274	3.312
σ_8	1.297	1.281	1.260	1.258	1.268	1.282
σ_9	1516.	1537.	1564.	1567.	1557.	1541.
σ_{10}	185.9	185.0	184.7	185.0	185.6	186.4
σ_{11}	1157.	1158.	1147.	1142.	1141.	1142.
σ_{12}	15.23	15.06	14.86	14.85	14.95	15.09
Atoms/b cm (of fuel)						
N_5	1.130 E-3	1.130 E-3	8.277 E-4	6.009 E-4	4.381 E-4	3.227 E-4
N_6	0	0	6.121 E-5	1.029 E-4	1.285 E-4	1.429 E-4
N_{FP}	0	0	3.158 E-4	6.403 E-4	9.430 E-4	1.212 E-3
N_8	2.465 E-2	2.465 E-2	2.443 E-2	2.419 E-2	2.396 E-2	2.376 E-2
N_9	0	0	1.188 E-4	1.622 E-4	1.718 E-4	1.668 E-4

*With equilibrium Xenon and "Samarium Group" poison.

Table F5 (Cont.)

Property	Flux-Time (n/kb)					
	0	0*	0.6	1.2	1.8	2.4
N_{10}	0	0	1.538 E-5	3.399 E-5	4.815 E-5	5.793 E-5
N_{11}	0	0	1.004 E-5	3.152 E-5	4.757 E-5	5.590 E-5
N_{12}	0	0	7.917 E-7	5.575 E-6	1.354 E-5	2.224 E-5
Space Properties						
$\Sigma_{Xe, max}$, cm^{-1} (fuel)	0	0.03111	0.03316	0.03137	0.0280	0.02431
$(\Sigma_{fl} - \Sigma_{Xe})$, cm^{-1} (fuel)	0.3731	0.3770	0.4963	0.5370	0.5341	0.5102
$\Sigma_f V_{fl}$, cm^{-1}	0.09661	0.09531	0.1102	0.1115	0.1057	0.09668
$\nu \Sigma_f V_{fl}$, cm^{-1}	0.2386	0.2354	0.2904	0.3034	0.2929	0.2712
$(1-p)/(1+a)$	0.1472	0.1472	0.1307	0.1151	0.1006	0.08759
$(1-p)\eta$	0.3635	0.3635	0.3323	0.3004	0.2683	0.2374
p	0.5671	0.5671	0.5433	0.5305	0.5292	0.5326
Inverse Mod. Ratio, $\frac{\Sigma}{\xi \Sigma_s}$						
Velocity Step,** 4	1.003	1.064	1.025	0.9702	0.9092	0.8497
9	0.4034	0.4302	0.4333	0.4220	0.4030	0.3812
14	0.2420	0.2593	0.3001	0.3131	0.3098	0.2983
19	0.2284	0.2411	0.5964	0.7365	0.7682	0.7488
24	0.1186	0.1287	0.1530	0.1596	0.1576	0.1520

*With equilibrium Xenon and "Samarium Group" poison.

**The step number is proportional to velocity where step 24 corresponds to an energy of 0.45 ev.

Table F6 Local Properties of Fuel Dependent on Initial Enrichment and Flux-Time

Initial Enrichment: 5,592 a/o U235

Runs No. 8

Property	Flux-Time (n/kb)					
	0	0*	0.6	1.2	1.8	2.4
Cross Sections (b)						
$\sigma_{5,f}$	241.0	237.4	232.9	233.7	237.3	241.8
$\sigma_{9,f}$	963.7	975.8	990.9	989.2	979.1	965.9
$\sigma_{11,f}$	841.3	841.7	830.1	826.1	826.0	827.3
σ_5	289.6	285.5	280.2	281.2	285.3	290.5
σ_6	3,220	3,176	3,119	3,128	3,170	3,225
σ_8	1,247	1,230	1,207	1,211	1,227	1,249
σ_9	1579.	1602.	1629.	1625.	1606.	1581.
σ_{10}	183.1	182.2	182.1	182.7	183.7	184.8
σ_{11}	1158.	1159.	1143.	1137.	1137.	1139.
σ_{12}	14.72	14.55	14.33	14.37	14.54	14.76
Atoms/b cm (of fuel)						
N_5	1.460 E-3	1.460 E-3	1.022 E-3	7.113 E-4	5.020 E-4	3.667 E-4
N_6	0	0	9.160 E-5	1.482 E-4	1.784 E-4	1.928 E-4
N_{FP}	0	0	4.532 E-4	8.990 E-4	1.291 E-3	1.621 E-3
N_8	2.465 E-2	2.465 E-2	2.435 E-2	2.404 E-2	2.375 E-2	2.351 E-2
N_9	0	0	1.533 E-4	1.993 E-4	2.018 E-4	1.887 E-4

*With equilibrium Xenon and "Samarium Group" poison.

Table F6 (Cont.)

Property	Flux-Time (n/kb)					
	0	0*	0.6	1.2	1.8	2.4
N_{10}	0	0	1.959 E-5	4.131 E-5	5.680 E-5	6.668 E-5
N_{11}	0	0	1.578 E-5	4.361 E-5	6.054 E-5	6.707 E-5
N_{12}	0	0	1.413 E-6	8.645 E-6	1.896 E-5	2.892 E-5
Space Properties						
$\Sigma_{Xe, max}$, cm^{-1} (fuel)	0	0.04503	0.04674	0.04184	0.03523	0.02910
$(\Sigma_{fl} - \Sigma_{Xe})$, cm^{-1} (fuel)	0.4536	0.4597	0.6197	0.6574	0.6346	0.5892
$\Sigma_f V_{fl}$, cm^{-1}	0.1196	0.1179	0.1372	0.1358	0.1247	0.1107
$\Sigma_f V_{fl}$, cm^{-1}	0.2954	0.2911	0.3637	0.3715	0.3471	0.3112
$(1-p)/(1+a)$	0.1837	0.1837	0.1592	0.1366	0.1163	0.09890
$(1-p)\eta$	0.4537	0.4537	0.4056	0.3576	0.3110	0.2686
p	0.5251	0.5251	0.5037	0.4980	0.5032	0.5119
Inverse Mod. Ratio, $\frac{\Sigma}{\xi \Sigma_s}$						
Velocity Step,** 4	1.226	1.302	1.229	1.135	1.038	0.9504
9	0.4900	0.5240	0.5192	0.4943	0.4607	0.4269
14	0.2926	0.3145	0.3630	0.3707	0.3570	0.3355
19	0.2803	0.2964	0.7525	0.8977	0.9011	0.8491
24	0.1416	0.1543	0.1834	0.1872	0.1802	0.1701

*With equilibrium Xenon and "Samarium Group" poison.

**The step number is proportional to velocity where step 24 corresponds to an energy of 0.45 ev.

Table F7 Local Properties of Fuel Dependent on Initial Enrichment and Flux-Time

Initial Enrichment: 6.452 a/o U235

Runs No. 3

Property	Flux-Time (n/kb)					
	0	0*	0.6	1.2	1.8	2.4
Cross Sections (b)						
$\sigma_{5,f}$	234.5	230.8	226.2	227.9	232.6	238.0
$\sigma_{9,f}$	985.2	998.2	1013.	1001.	993.8	977.5
$\sigma_{11,f}$	841.6	841.9	827.1	823.1	823.9	825.9
σ_5	282.1	277.8	272.3	274.3	279.8	286.2
σ_6	3.140	3.095	3.035	3.055	3.112	3.179
σ_8	1.216	1.198	1.175	1.183	1.205	1.231
σ_9	1620.	1644.	1670.	1660.	1634.	1603.
σ_{10}	181.4	180.5	180.6	181.4	182.6	183.9
σ_{11}	1158.	1159.	1139.	1133.	1134.	1137.
σ_{12}	14.40	14.22	14.00	14.09	14.31	14.58
Atoms/b cm (of fuel)						
N_5	1.700E-3	1.700E-3	1.143E-3	7.685E-4	5.302E-4	3.769E-4
N_6	0	0	1.186E-4	1.852E-4	2.167E-4	2.294E-4
N_{FP}	0	0	5.747E-4	1.116E-3	1.570E-3	1.936E-3
N_8	2.465E-2	2.465E-2	2.428E-2	2.391E-2	2.359E-2	2.332E-2
N_9	0	0	1.810E-4	2.257E-5	2.206E-4	2.008E-4

*With equilibrium Xenon and "Samarium Group" poison.

Table F7 (Cont.)

Property	Flux-Time (n/kb)					
	0	0*	0.6	1.2	1.8	2.4
N_{10}	0	0	2.302 E-5	4.709 E-5	6.340 E-5	7.308 E-5
N_{11}	0	0	2.092 E-5	5.268 E-5	6.898 E-5	7.348 E-5
N_{12}	0	0	2.063 E-6	1.133 E-5	2.308 E-5	3.350 E-5
Space Properties						
$\Sigma_{Xe, max}$, cm^{-1} (fuel)	0	0.05776	0.05813	0.04946	0.03978	0.03172
$(\Sigma_{fl} - \Sigma_{Xe})$, cm^{-1} (fuel)	0.5095	0.5180	0.7110	0.7398	0.6973	0.6348
$\Sigma_f V_{fl}$, cm^{-1}	0.1355	0.1334	0.1563	0.1516	0.1359	0.1180
$\nu \Sigma_f V_{fl}$, cm^{-1}	0.3348	0.3295	0.4162	0.4165	0.3792	0.3325
$(1-p)/(1+\alpha)$	0.2087	0.2087	0.1773	0.1490	0.1246	0.1044
$(1-p)\eta$	0.5153	0.5153	0.4526	0.3914	0.3341	0.2839
p	0.4966	0.4966	0.4781	0.4782	0.4881	0.5003
Inverse Mod. Ratio, $\frac{\Sigma}{\xi \Sigma_s}$						
Velocity Step,** 4	1.387	1.4771	1.369	1.240	1.115	1.008
9	0.5526	0.5926	0.5793	0.5413	0.4957	0.4531
14	0.3293	0.3549	0.4084	0.4092	0.3861	0.3570
19	0.3180	0.3369	0.8729	1.010	0.9838	0.9050
24	0.1581	0.1731	0.2055	0.2057	0.1944	0.1807

*With equilibrium Xenon and "Samarium Group" poison.

**The step number is proportional to velocity where step 24 corresponds to an energy of 0.45 ev.

Table F8 Partial and Net Fuel Cycle Costs, in mills/kwhe, Depending on Enrichment, Fuel Scheduling Procedure, and Unit Price Basis.

Enrichment: 2.876 a/o U235

Fuel Scheduling Method: Batch

Average Burnup: 1654. (MWD/ton)

Run No. 4.1

Fuel Cycle Step		Unit Price Set No.			
No.	Process	1	2	3	4
2	UF ₆ from A. E. C., mills/kwhe	32.19	*	21.48	25.27
6	UF ₆ → UO ₂	1.71	3.42	*	*
8	Physical Fabrication	8.13	*	2.71	4.06
9	Shipping	0.81	*	0.45	*
10	Solvent Extraction	1.82	*	*	*
11	UO ₂ (NO ₃) ₂ → UF ₆	0.50	*	*	*
12	Pu(NO ₃) ₄ → Pu	0.15	*	*	*
13	UF ₆ to A. E. C.	-28.64	*	-19.11	-22.41
14	Pu to A. E. C.	-1.20	*	-3.00	*
16	UF ₆ Lease Charge	2.50	7.51	1.67	1.96
17	Working Capital Charge	0.53	0.62	0.24	0.31
	Net Fuel Cycle Cost	18.49	25.30	8.61	12.99

* An asterisk means same value as given for Cost Set No. 1

Table F9 Partial and Net Fuel Cycle Costs, in mills/kwhe, Depending on Enrichment, Fuel Scheduling Procedure, and Unit Price Basis.

Enrichment: 4.383 a/o U235

Fuel Scheduling Method: Batch

Average Burnup: 20510. (MWD/ton)

Run No. 9.1

Fuel Cycle Step		Unit Price Set No.			
No.	Process	1	2	3	4
2	UF ₆ from A. E. C., mills/kwhe	4.36	*	2.91	3.49
6	UF ₆ → UO ₂	0.21	0.42	*	*
8	Physical Fabrication	0.66	*	0.22	0.33
9	Shipping	0.07	*	0.04	*
10	Solvent Extraction	0.15	*	*	*
11	UO ₂ (NO ₃) ₂ → UF ₆	0.04	*	*	*
12	Pu(NO ₃) ₄ → Pu	0.09	*	*	*
13	UF ₆ to A. E. C.	-2.17	*	-1.45	-1.70
14	Pu to A. E. C.	-0.70	*	-1.76	*
16	UF ₆ Lease Charge	0.89	2.68	0.60	0.71
17	Working Capital Charge	0.17	0.21	0.08	0.10
	Net Fuel Cycle Cost	3.76	5.79	1.12	2.78

* An asterisk means same value as given for Cost Set No. 1

Table F10 Partial and Net Fuel Cycle Costs, in mills/kwhe, Depending on Enrichment, Fuel Scheduling Procedure, and Unit Price Basis.

Enrichment: 5.592 a/o U235

Fuel Scheduling Method: Batch

Average Burnup: 35380. (MWD/ton)

Run No. 8.1

Fuel Cycle Step		Unit Price Set No.			
No.	Process	1	2	3	4
2	UF ₆ from A. E. C., mills/kwhe	3.37	*	2.25	2.71
6	UF ₆ → UO ₂	0.16	0.31	*	*
8	Physical Fabrication	0.38	*	0.13	0.19
9	Shipping	0.04	*	0.02	*
10	Solvent Extraction	0.08	*	*	*
11	UO ₂ (NO ₃) ₂ → UF ₆	0.02	*	*	*
12	Pu(NO ₃) ₄ → Pu	0.07	*	*	*
13	UF ₆ to A. E. C.	-1.28	*	-0.85	-1.00
14	Pu to A. E. C.	-0.57	*	-1.42	*
16	UF ₆ Lease Charge	1.04	3.11	0.69	0.83
17	Working Capital Charge	0.17	0.22	0.09	0.11
	Net Fuel Cycle Cost	3.48	5.75	1.23	2.64

* An asterisk means same value as given for Cost Set No. 1

Table F11 Partial and Net Fuel Cycle Costs, in mills/kwhe, Depending on Enrichment, Fuel Scheduling Procedure, and Unit Price Basis.

Enrichment: 6.452 a/o U235
Average Burnup: 45420. (MWD/ton)

Fuel Scheduling Method: Batch
Run No. 3.1

Fuel Cycle Step		Unit Price Set No.			
No.	Process	1	2	3	4
2	UF ₆ from A. E. E., mills/kwhe	3.09	*	2.06	2.50
6	UF ₆ → UO ₂	0.14	0.28	*	*
8	Physical Fabrication	0.30	*	0.10	0.15
9	Shipping	0.03	*	0.02	*
10	Solvent Extraction	0.07	*	*	*
11	UO ₂ (NO ₃) ₂ → UF ₆	0.02	*	*	*
12	Pu(NO ₃) ₄ → Pu	0.06	*	*	*
13	UF ₆ to A. E. C.	-1.02	*	-0.68	-0.80
14	Pu to A. E. C.	-0.51	*	-1.27	*
16	UF ₆ Lease Charge	1.17	3.52	0.78	0.95
17	Working Capital Charge	0.17	0.23	0.09	0.11
	Net Fuel Cycle Cost	3.52	6.06	1.39	2.71

* An asterisk means same value as given for Cost Set No. 1

Table F12 Partial and Net Fuel Cycle Costs, in mills/kwhe, Depending on Enrichment, Fuel Scheduling Procedure, and Unit Price Basis.

Enrichment: 2.876 a/o U235
Average Burnup: 5326. (MWD/ton)

Fuel Scheduling Method: Inout
Run No. 4.2

Fuel Cycle Step		Unit Price Set No.			
No.	Process	1	2	3	4
2	UF ₆ from A. E. C., mills/kwhe	9.99	*	6.67	7.85
6	UF ₆ → UO ₂	0.53	1.06	*	*
8	Physical Fabrication	2.52	*	0.84	1.26
9	Shipping	0.25	*	0.14	*
10	Solvent Extraction	0.56	*	*	*
11	UO ₂ (NO ₃) ₂ → UF ₆	0.15	*	*	*
12	Pu(NO ₃) ₄ → Pu	0.13	*	*	*
13	UF ₆ to A. E. C.	-7.35	*	-4.91	-5.71
14	Pu to A. E. C.	-1.06	*	-2.64	*
16	UF ₆ Lease Charge	1.02	3.06	0.68	0.80
17	Working Capital Charge	0.25	0.29	0.11	0.14
	Net Fuel Cycle Cost	7.01	9.62	2.28	4.92

* An asterisk means same value as given for Cost Set No. 1

Table F13 Partial and Net Fuel Cycle Costs, in mills/kwhe, Depending on Enrichment, Fuel Scheduling Procedure, and Unit Price Basis.

Enrichment: 3.105 a/o U235

Fuel Scheduling Method: Inout

Average Burnup: 14090. (MWD/ton)

Run No. 7.2

Fuel Cycle Step		Unit Price Set No.			
No.	Process	1	2	3	4
2	UF ₆ from A. E. C., mills/kwhe	4.16	*	2.78	3.28
6	UF ₆ → UO ₂	0.22	0.43	*	*
8	Physical Fabrication	0.95	*	0.32	0.48
9	Shipping	0.09	*	0.05	*
10	Solvent Extraction	0.21	*	*	*
11	UO ₂ (NO ₃) ₂ → UF ₆	0.06	*	*	*
12	Pu(NO ₃) ₄ → Pu	0.10	*	*	*
13	UF ₆ to A. E. C.	-2.06	*	-1.37	-1.57
14	Pu to A. E. C.	-0.82	*	-2.04	*
16	UF ₆ Lease Charge	0.67	2.00	0.45	0.53
17	Working Capital Charge	0.17	0.20	0.08	0.10
	Net Fuel Cycle Cost	3.77	5.35	8.50	2.68

* An asterisk means same value as given for Cost Set No. 1

Table F14 Partial and Net Fuel Cycle Costs, in mills/kwhe, Depending on Enrichment, Fuel Scheduling Procedure, and Unit Price Basis.

Enrichment: 3.441 a/o U235

Fuel Scheduling Method: Inout

Average Burnup: 25580. (MWD/ton)

Run No. 1.2

Fuel Cycle Step		Unit Price Set No.			
No.	Process	1	2	3	4
2	UF ₆ from A. E. C., mills/kwhe	2.61	*	1.74	2.06
6	UF ₆ → UO ₂	0.13	0.26	*	*
8	Physical Fabrication	0.53	*	0.18	0.26
9	Shipping	0.05	*	0.03	*
10	Solvent Extraction	0.12	*	*	*
11	UO ₂ (NO ₃) ₂ → UF ₆	0.03	*	*	*
12	Pu(NO ₃) ₄ → Pu	0.08	*	*	*
13	UF ₆ to A. E. C.	-0.81	*	-0.54	-0.60
14	Pu to A. E. C.	-0.63	*	-1.58	*
16	UF ₆ Lease Charge	0.62	1.85	0.41	0.49
17	Working Capital Charge	0.15	0.18	0.07	0.09
	Net Fuel Cycle Cost	2.88	4.28	0.67	2.08

* An asterisk means same value as given for Cost Set No. 1

Table F15 Partial and Net Fuel Cycle Costs, in mills/kwhe, Depending on Enrichment, Fuel Scheduling Procedure, and Unit Price Basis.

Enrichment: 4.272 a/o U235

Fuel Scheduling Method: Inout

Average Burnup: 49320. (MWD/ton)

Run No. 5.2

Fuel Cycle Step		Unit Price Set No.			
No.	Process	1	2	3	4
2	UF ₆ from A. E. C., mills/kwhe	1.76	*	1.17	1.40
6	UF ₆ → UO ₂	0.09	0.17	*	*
8	Physical Fabrication	0.27	*	0.09	0.14
9	Shipping	0.03	*	0.02	*
10	Solvent Extraction	0.06	*	*	*
11	UO ₂ (NO ₃) ₂ → UF ₆	0.02	*	*	*
12	Pu(NO ₃) ₄ → Pu	0.05	*	*	*
13	UF ₆ to A. E. C.	-0.23	*	-0.15	-0.16
14	Pu to A. E. C.	-0.42	*	-0.11	*
16	UF ₆ Lease Charge	0.70	2.10	0.47	0.56
17	Working Capital Charge	0.15	0.18	0.07	0.09
	Net Fuel Cycle Cost	2.47	4.00	0.83	1.85

* An asterisk means same value as given for Cost Set No. 1

Table F16 Partial and Net Fuel Cycle Costs, in mills/kwhe, Depending on Enrichment, Fuel Scheduling Procedure, and Unit Price Basis.

Enrichment: 2.876 a/o U235

Fuel Scheduling Method: Outin

Average Burnup: 3817. (MWD/ton)

Run No. 4.3

Fuel Cycle Step		Unit Price Set No.			
No.	Process	1	2	3	4
2	UF ₆ from A. E. C., mills/kwhe	13.95	*	9.30	10.95
6	UF ₆ → UO ₂	0.74	1.48	*	*
8	Physical Fabrication	3.52	*	1.17	1.76
9	Shipping	0.35	*	0.20	*
10	Solvent Extraction	0.79	*	*	*
11	UO ₂ (NO ₃) ₂ → UF ₆	0.22	*	*	*
12	Pu(NO ₃) ₄ → Pu	0.14	*	*	*
13	UF ₆ to A. E. C.	-11.08	*	-7.39	-8.63
14	Pu to A. E. C.	-1.12	*	-2.79	*
16	UF ₆ Lease Charge	1.28	3.85	0.86	1.01
17	Working Capital Charge	0.30	0.35	0.13	0.17
	Net Fuel Cycle Cost	9.08	12.44	3.36	6.38

*An asterisk means same value as given for Cost Set No. 1

Table F17 Partial and Net Fuel Cycle Costs, in mills/kwhe, Depending on Enrichment, Fuel Scheduling Procedure, and Unit Price Basis.

Enrichment: 3.105 a/o U235

Fuel Scheduling Method: Outin

Average Burnup: 10010. (MWD/ton)

Run No. 7.3

Fuel Cycle Step		Unit Price Set No.			
No.	Process	1	2	3	4
2	UF ₆ from A. E. C., mills/kwhe	5.86	*	3.91	4.62
6	UF ₆ → UO ₂	0.30	0.61	*	*
8	Physical Fabrication	1.34	*	0.45	0.67
9	Shipping	0.13	*	0.07	*
10	Solvent Extraction	0.30	*	*	*
11	UO ₂ (NO ₃) ₂ → UF ₆	0.08	*	*	*
12	Pu(NO ₃) ₄ → Pu	0.11	*	*	*
13	UF ₆ to A. E. C.	-3.53	*	-2.35	-2.73
14	Pu to A. E. C.	-0.91	*	-2.28	*
16	UF ₆ Lease Charge	0.78	2.34	0.52	0.62
17	Working Capital Charge	0.19	0.23	0.09	0.11
	Net Fuel Cycle Cost	4.67	6.57	1.21	3.31

* An asterisk means same value as given for Cost Set No. 1

Table F18 Partial and Net Fuel Cycle Costs, in mills/kwhe, Depending on Enrichment, Fuel Scheduling Procedure, and Unit Price Basis.

Enrichment: 3.441 a/o U235

Fuel Scheduling Method: Outin

Average Burnup: 17800. (MWD/ton)

Run No. 1.3

Fuel Cycle Step		Unit Price Set No.			
No.	Process	1	2	3	4
2	UF ₆ from A. E. C., mills/kwhe	3.75	*	2.50	2.97
6	UF ₆ → UO ₂	0.19	0.38	*	*
8	Physical Fabrication	0.75	*	0.25	0.38
9	Shipping	0.08	*	0.04	*
10	Solvent Extraction	0.17	*	*	*
11	UO ₂ (NO ₃) ₂ → UF ₆	0.05	*	*	*
12	Pu(NO ₃) ₄ → Pu	0.09	*	*	*
13	UF ₆ to A. E. C.	-1.68	*	-1.12	-1.29
14	Pu to A. E. C.	-0.75	*	-1.88	*
16	UF ₆ Lease Charge	-0.69	2.08	0.46	0.55
17	Working Capital Charge	0.16	0.20	0.08	0.10
	Net Fuel Cycle Cost	3.50	5.11	0.83	2.52

* An asterisk means same value as given for Cost Set No. 1

Table F19 Partial and Net Fuel Cycle Costs, in mills/kwhe, Depending on Enrichment, Fuel Scheduling Procedure, and Unit Price Basis

Enrichment: 3.711 a/o U235

Fuel Scheduling Method: Outin

Average Burnup: 24120. (MWD/ton)

Run No. 6.3

Fuel Cycle Step					
No.	Process	1	2	3	4
2	UF ₆ from A. E. C., mills/kwhe	3.04	*	2.02	2.41
6	UF ₆ → UO ₂	0.15	0.30	*	*
8	Physical Fabrication	0.56	*	0.19	0.28
9	Shipping	0.06	*	0.03	*
10	Solvent Extraction	0.12	*	*	*
11	UO ₂ (NO ₃) ₂ → UF ₆	0.03	*	*	*
12	Pu(NO ₃) ₄ → Pu	0.08	*	*	*
13	UF ₆ to A. E. C.	-1.10	*	-0.73	-0.84
14	Pu to A. E. C.	-0.66	*	-1.66	*
16	UF ₆ Lease Charge	0.69	2.07	0.46	0.55
17	Working Capital Charge	0.16	0.19	0.07	0.10
	Net Fuel Cycle Cost	3.13	4.69	0.78	2.28

* An asterisk means same value as given for Cost Set No. 1

Table F20 Partial and Net Fuel Cycle Costs, in mills/kwhe, Depending on Enrichment, Fuel Scheduling Procedure, and Unit Price Basis.

Enrichment: 4.272 a/o U235

Fuel Scheduling Method: Outin

Average Burnup: 36180. (MWD/ton)

Run No. 5.3

Fuel Cycle Step		Unit Price Set No.			
No.	Process	1	2	3	4
2	UF ₆ from A.E.C., mills/kwhe	2.40	*	1.60	1.92
6	UF ₆ → UO ₂	0.12	0.23	*	*
8	Physical Fabrication	0.37	*	0.12	0.19
9	Shipping	0.04	*	0.02	*
10	Solvent Extraction	0.08	*	*	*
11	UO ₂ (NO ₃) ₂ → UF ₆	0.02	*	*	*
12	Pu(NO ₃) ₄ → Pu	0.07	*	*	*
13	UF ₆ to A.E.C.	-0.61	*	-0.41	-0.46
14	Pu to A.E.C.	-0.54	*	-1.35	*
16	UF ₆ Lease Charge	0.74	2.23	0.50	0.59
17	Working Capital Charge	0.15	0.19	0.08	0.09
	Net Fuel Cycle Cost	2.84	4.48	0.85	2.12

* An asterisk means same value as given for Cost Set No. 1

Table F21 Partial and Net Fuel Cycle Costs, in mills/kwhe Depending on Enrichment, Fuel Scheduling Procedure, and Unit Price Basis.

Enrichment: 2.876 a/o U235
Average Burnup: 4420. (MWD/ton)

Fuel Scheduling Method: Graded
Run No. 4.4

Fuel Cycle Step		Unit Price Set No.			
No.	Process	1	2	3	4
2	UF ₆ from A. E. C., mills/kwhe	12.04	*	8.03	9.45
6	UF ₆ → UO ₂	0.64	1.28	*	*
8	Physical Fabrication	3.04	*	1.01	1.52
9	Shipping	0.30	*	0.17	*
10	Solvent Extraction	0.68	*	*	*
11	UO ₂ (NO ₃) ₂ → UF ₆	0.19	*	*	*
12	Pu(NO ₃) ₄ → Pu	0.14	*	*	*
13	UF ₆ to A. E. C.	-9.28	*	-6.19	-7.21
14	Pu to A. E. C.	-1.09	*	-2.73	*
16	UF ₆ Lease Charge	1.16	3.47	0.77	0.91
17	Working Capital Charge	0.27	0.32	0.12	0.16
	Net Fuel Cycle Cost	8.09	11.09	2.83	5.68

* An asterisk means same value as given for Cost Set No. 1

Table F22 Partial and Net Fuel Cycle Costs, in mills/kwhe Depending on Enrichment, Fuel Scheduling Procedure, and Unit Price Basis.

Enrichment: 3.105 a/o U235

Fuel Scheduling Method: Graded

Average Burnup: 12560. (MWD/ton)

Run No: 7:4

Fuel Cycle Step		Unit Price Set No.			
No.	Process	1	2	3	4
2	UF ₆ from A. E. C., mills/kwhe	4.67	*	3.12	3.68
6	UF ₆ → UO ₂	0.24	0.49	*	*
8	Physical Fabrication	1.07	*	0.36	0.53
9	Shipping	0.11	*	0.06	*
10	Solvent Extraction	0.24	*	*	*
11	UO ₂ (NO ₃) ₂ → UF ₆	0.06	*	*	*
12	Pu(NO ₃) ₄ → Pu	0.11	*	*	*
13	UF ₆ to A. E. C.	-2.49	*	-1.66	-1.91
14	Pu to A. E. C.	-0.85	*	-2.12	*
16	UF ₆ Lease Charge	0.70	2.10	0.47	0.55
17	Working Capital Charge	0.18	0.21	0.08	0.10
	Net Fuel Cycle Cost	4.04	5.72	0.95	2.87

*An asterisk means same value as given for Cost Set No. 1

Table F23 Partial and Net Fuel Cycle Costs, in mills/kwhe Depending on Enrichment, Fuel Scheduling Procedure, and Unit Price Basis.

Enrichment: 3.441 a/o U235

Fuel Scheduling Method: Graded

Average Burnup: 22820. (MWD/ton)

Run No. 1.4

Fuel Cycle Step		Unit Price Set No.			
No.	Process	1	2	3	4
2	UF ₆ from A. E. C., mills/kwhe	2.92	*	1.95	2.31
6	UF ₆ → UO ₂	0.15	0.30	*	*
8	Physical Fabrication	0.59	*	0.20	0.29
9	Shipping	0.06	*	0.03	*
10	Solvent Extraction	0.13	*	*	*
11	UO ₂ (NO ₃) ₂ → UF ₆	0.04	*	*	*
12	Pu(NO ₃) ₄ → Pu	0.08	*	*	*
13	UF ₆ to A. E. C.	-1.04	*	-0.69	-0.78
14	Pu to A. E. C.	-0.67	*	-1.68	*
16	UF ₆ Lease Charge	0.64	1.92	0.43	0.51
17	Working Capital Charge	0.16	0.19	0.07	0.09
	Net Fuel Cycle Cost	3.06	4.51	0.71	2.21

* An asterisk means same value as given for Cost Set No. 1

Table F24 Partial and Net Fuel Cycle Costs, in mills/kwhe, Depending on Enrichment, Fuel Scheduling Procedure, and Unit Price Basis.

Enrichment: 3.711 a/o U235

Fuel Scheduling Method: Graded

Average Burnup: 30450. (MWD/ton)

Run No. 6.4

Fuel Cycle Step		Unit Price Set No.			
No.	Process	1	2	3	4
2	UF ₆ from A. E. C., mills/kwhe	2.40	*	1.60	1.91
6	UF ₆ → UO ₂	0.12	0.24	*	*
8	Physical Fabrication	0.44	*	0.15	0.22
9	Shipping	0.04	*	0.02	*
10	Solvent Extraction	0.10	*	*	*
11	UO ₂ (NO ₃) ₂ → UF ₆	0.02	*	*	*
12	Pu(NO ₃) ₄ → Pu	0.07	*	*	*
13	UF ₆ to A. E. C.	-0.65	*	-0.43	-0.48
14	Pu to A. E. C.	-0.58	*	-1.45	*
16	UF ₆ Lease Charge	0.65	1.95	0.43	0.52
17	Working Capital Charge	0.15	0.18	0.07	0.09
	Net Fuel Cycle Cost	2.78	4.23	0.72	2.03

* An asterisk means same value as given for Cost Set No. 1

Table F25 Partial and Net Fuel Cycle Costs, in mills/kwhe, Depending on Enrichment, Fuel Scheduling Procedure, and Unit Price Basis.

Enrichment: 4.272 a/o U235

Fuel Scheduling Method: Graded

Average Burnup: 44720. (MWD/ton)

Run No. 5.4

Fuel Cycle Step		Unit Price Set No.			
No.	Process	1	2	3	4
2	UF ₆ from A. E. C., mills/kwhe	1.94	*	1.29	1.55
6	UF ₆ → UO ₂	0.09	0.19	*	*
8	Physical Fabrication	0.30	*	0.10	0.15
9	Shipping	0.03	*	0.02	*
10	Solvent Extraction	0.07	*	*	*
11	UO ₂ (NO ₃) ₂ → UF ₆	0.02	*	*	*
12	Pu(NO ₃) ₄ → Pu	0.06	*	*	*
13	UF ₆ to A. E. C.	-0.32	*	-0.22	-0.24
14	Pu to A. E. C.	-0.46	*	-1.15	*
16	UF ₆ Lease Charge	0.71	2.14	0.48	0.57
17	Working Capital Charge	0.15	0.19	0.07	0.09
	Net Fuel Cycle Cost	2.59	4.14	0.83	1.93

* An asterisk means same value as given for Cost Set No. 1

G. NOMEMCLAUTRE

The text references give the location of a section that contains a more detailed definition of the symbol or of an equation that uses the symbol. Equation numbers are placed in parenthesis. A set of compatible units for input data for FUELCYC is given in Appendix D. 1. Section 1. of this Appendix defines English letters; Section 2., Greek letters; Section 3., subscripts; and Section 4., superscripts.

1. English Letters

<u>Text Symbol</u>	<u>Fortran Symbol</u>	<u>Definition</u>	<u>Text Reference</u>
A(x)	A(I)	Inverse of the moderating ratio.	(4. 4)
a _k	A(K)	Constants in Wilkins equation startup series.	IX. A.
a _{Lag}	ALAG	Denominator of Lagrangian fit coefficient.	IX. C. 23.
a _{Lag2}	ALAG2	Lagrangian fit coefficient.	IX. C. 23.
a _m	A(M)	Constants in Nuclide concentration equations.	IX. C. 14.
B _g	—	Geometric buckling.	V. A. 2.
b	B	Term for evaluating reprocessing rate.	(4. 130)
b	—	Westcott parameter $\left(br = \frac{n_e}{n} \right)$.	V. B. 2.
b _j	B(J)	Constants in Wilkins equation startup series.	IX. A.
C	C	Criticality factor for the reactor in the absence of control poison.	(4. 76)

<u>Text Symbol</u>	<u>Fortran Symbol</u>	<u>Definition</u>	<u>Text Reference</u>
$C_{r, z}$	C50(I, J)	Local (or regional) criticality factor in the absence of control poison.	IV. B. 2. 7.
C_w	C52	Criticality factor for the reactor with control poison.	IV. C. 2. 1.
C_E	CE	Unit price of separative work.	(4. 119)
C_F	-	Unit price of the UF_6 cascade feed material.	(4. 120)
C_P	CP	Unit price for enriched uranium.	(4. 119)
$\bar{C}_{i, j}$	CA(I, J)	Partial fuel-cycle cost for cost step i, cost set j.	(4. 104)
\bar{C}_{mt}	EDS(1)	Material partial fuel-cycle cost.	(4. 144)
\bar{C}_{fb}	EDS(2)	Fabrication partial fuel-cycle cost.	(4. 145)
\bar{C}_{rp}	EDS(3)	Reprocessing partial fuel-cycle cost.	(4. 146)
C_{cp}		Capital charge	(6. 3)
$C_{i, j}$	C(I, J)	Unit price for cost step i, cost set j.	(4. 104)
C_k	CK	Constant K in the reactor-physics equations; e. g., see following seven definitions.	-
C_1	C1	Constant terms in resonance escape probability exponent $(V_{fl}/\xi \sum_s V_{md})$.	(4. 8)
$C_{2, r, z}$	$\frac{C2(I, J)}{P(I, J)}$	Reactor-physics constants No. 2. $\left(\frac{1}{1 - \epsilon[\eta(1-p)]_{r, z}} \right)$	(4. 26)
$C_{3, r, z, u}$	-	Reactor-physics constants No. 3.	(4. 41)
$C_{4, r, z, u}$	-	Reactor-physics constants No. 4.	(4. 42)

<u>Test Symbol</u>	<u>Fortran Symbol</u>	<u>Definition</u>	<u>Text Reference</u>
C ₅	C5	Ratio of average to maximum Xe poisoning.	IX. C. 14.
C _{7,r}	C7(I)	Reactor-physics constant No. 7.	(4. 47)
C _{8,z}	C8(J)	Reactor-physics constant No. 8.	(4. 49)
c _n	C(N)	"Source" terms for flux-shape iteration.	IX. B. (17)
c	-	Matrix of the above terms.	IX. B. (1)
D	D	Diffusion coefficient.	(4. 27)
d _{r,z,u}	D(I, J, K) or DL(I, J, K)	"∇ ² " terms in the spatial flux-shape equations.	(4. 39)
d	-	Matrix of the above coefficients.	(4. 56)
d _i	DI	Price for use in cost step i.	IV. B. 2.
E	E	Energy.	(4. 2)
E	E	Burnup (MWD/ton).	(4. 79)
e _{r,z}	E(I, J) or EL(I, J)	Non-"∇ ² " terms in the spatial flux-shape equations.	(4. 39)
e	-	Matrix of the above terms.	(4. 56)
F	-	Relative error; used with various subscripts.	IX. E.
F _{T,i}	FT(i)	Truncation error in i th stop of Wilkins equation solution.	IX. A. (22)
F _I		Fract. chg. on cap. invest.	(6. 3)
F _N	FN	Lease charge on UF ₆ (fraction of initial cost per year).	(4. 142)
F _W	FW	Working capital charge rate (fraction year).	(4. 143)
F _{cum, i}	FCUM(I)	Cumulative truncation error in Wilkins equation solution.	IX. A. (24)

<u>Text Symbol</u>	<u>Fortran Symbol</u>	<u>Definition</u>	<u>Text Reference</u>
f	-	Number of flux-time points included in polynomial fit, $f = \left(\frac{n_g - 1}{n_{sp}} \right) + 1.$	(4. 158)
f _d	DAMP 1	Damping factor in criticality iteration.	(4. 151A)
f _i	F(I)	Material adjustment factor for cost step i.	(4. 104)
f _{nat}	FNAT	Fraction of the fresh U235 obtained from natural uranium.	(4. 106)
f _{recy}	FRECY	Fractional recovery term for Pu recycle.	Fig. 4. 7.
f(θ)	-	One of the seven "space properties".	(4. 156)
G	G	Inverse energy yield term.	(4. 103)
G	-	Coefficient matrix.	(4. 53)
G ₂	-	Coefficient matrix No. 2.	(4. 55)
g	GL	Radial spacing between mesh points.	(4. 36)
g	-	Westcott factor (g = 1 for 1/v material).	V. B. 2.
H	H	Height of core.	IX. C. 18.
h	HL	Axial spacing between mesh points.	(4. 36)
I	-	Capital investment	(6. 3)
I	-	Integral.	IX. C. 26.
I _m [∞]	RI(M)	Infinite dilution resonance integral for nuclide m.	(4. 7)
I _m ^{eff}	-	Effective resonance integral for nuclide m.	(4. 8A)

<u>Text Symbol</u>	<u>Fortran Symbol</u>	<u>Definition</u>	<u>Text Reference</u>
i	(I)	Velocity index, in steps of x (or V for WILK2).	IX. A(5)
i _{cst}	INPCST	Designator for cost input data.	Table D3.
icr	—	Initial conversion ratio.	V. B.
j	—	Loop count of SPACFX iterations.	(4. 158)
j	(J)	Index for b _j .	IX. A.
j	(J)	Index for cost input set.	(4. 104)
j _{cst, L}	JCOSTL	Number of cost input data sets.	Table D3.
K(r)	—	Slowing down kernel.	IV. A. 2. 2.
k	—	Infinite multiplication factor.	(4. 61)
k	—	Boltzmann constant.	IV. A. 1. 1.
k	(K)	Diagonal (or second) index for Crout reduction.	IX. B.
k	—	Index for "a".	IX. A. (8)
L	FLOAD	Load factor.	(4. 142)
M	—	Migration length.	(4. 61)
M	—	Max.-to-avg. power-den. ratio	(6. 3)
m	(M)	Nuclide index; see listings under subscripts for special values.	IV. A. 3.
m	—	Number of passes through NUCON.	(4. 158)
N _m	N(M)	Concentration of nuclide m.	IV. A. 3.
N _{c, m}	—	Central concentration of nuclide m.	IX. C. 30.
N _{R, m}	—	Recycled concentration of nuclide m.	IX. B. 2.

<u>Text Symbol</u>	<u>Fortran Symbol</u>	<u>Definition</u>	<u>Text Reference</u>
n	(N)	Row (or first) index for Crout reduction.	IX. B.
n	-	Neutron density.	IV. A. 1.
n _{th}	-	Thermal neutron density.	V. B. s
n _e	-	Epithermal neutron density (total less thermal).	V. B. 2.
n _L	NL	Number of mesh points.	(4. 158)
n _ξ	NUMPOZ	The number of flux-time points at which nuclide concentrations are calculated (including the zero flux-time point).	IX. D.
n _{sp}	NUMSPA	The spacing in the above points for a flux-time fit; see definition of f.	IX. D.
P _d	POWERD	Average power density in the core.	(4. 78)
P ₁	P1	Fast non-leakage probability.	(4. 31)
p _c	-	Initial resonance escape probability for structural and coolant material.	V. A. 2.
P _u	-	Thermalization probability for normalized radius u.	IV. A. 2. 2.
p	PL or PTOT	Total resonance escape probability.	(4. 102)
$\frac{1-p}{1+\alpha}$	C54	Resonance fission probability.	(4. 100)
p _m	PL(M)	Resonance escape probability for nuclide m.	(4. 7)
(1-p)η	C11	"Resonance production" probability.	(4. 101)

<u>Text Symbol</u>	<u>Fortran Symbol</u>	<u>Definition</u>	<u>Text Reference</u>
Q	-	"Source" matrix in flux-shape iteration.	(4. 55)
q	-	Slowing-down density just below the fast fission group.	(4. 23)
q/φ	QOPHI	Slowing-down density per unit thermal flux.	(4. 34)
R	R	Radius of core.	IX. C. 18.
R. c. r.		Reactivity-change ratio	(6. 18)
r	(I)	Radial index.	(4. 36)
r	-	Radial length from origin.	IV. A. 2. 2.
r	R	Reprocessing rate.	(4. 129)
r	-	Read-in time for FUELCYC.	(4. 158)
r'	-	Radial length from origin.	Fig. 4. 4
S	-	Flux ratio.	(4. 68)
s	-	Square root of x.	IX. A. (6)
s	-	Westcott factor for epithermal absorption.	V. B. 2.
s	-	Number of passes through spacial subroutine (SPACE2).	(4. 158)
T	-	Temperature.	IV. A. 1. 1.
T _o	-	Room temperature, 293. 6° K.	IX. C. 9.
T _{md}	-	Moderator temperature,	(4. 2)
$\left(\frac{T_o}{T_{md}}\right)^{1/2}$	T	Conversion variable for velocity normalization.	IX. C. 9.
t	-	Time.	(4. 58)
t _L	TL	Lease charge time for enriched uranium excluding the time spent in the reactor.	(4. 142)

<u>Text Symbol</u>	<u>Fortran Symbol</u>	<u>Definition</u>	<u>Text Reference</u>
t_R	TR	Average time the fuel spends in the reactor if operated at full power (on stream time).	(4. 142)
t_v	TV	Time per unit volume, or inverse volumetric flow rate constant, for Inout and Outin.	(4. 146A)
t_W	TW	Working capital charge time excluding reactor time.	(4. 143)
u	-	Lethargy.	IV. A. 1. 3.
u	-	Normalized radius, $r\tau^{-1/2}$	(4. 17)
u	-	Neighbor mesh point identification index.	(4. 39)
v_{T_0}	V	Velocity normalized to v_0 : $\left(\frac{E}{kT_0}\right)^{1/2}$	IX. 6. 7.
V_{fl}	VFL	Volume fraction of fuel in the core.	(4. 8)
V_{md}	-	Volume fraction of moderator ($1 - V_{fl}$).	(4. 8)
V_r	C13(I)	Volume of region (r, z) (normalized to $V_1 = 1$).	(4. 146A)
v	-	Neutron velocity.	IV. A. 1. 2.
v_0	-	Velocity of 2200 m/s.	IV. A. 1.
W_i	W(I)	Weight of required material upon which unit cost i is based to the weight of fuel entering the reactor.(ratio of).	(4. 104)
W_d	WD	Term used in above weight ratios that is proportional to the weight of fuel fed to the reactor.	(4. 105)

<u>Text Symbol</u>	<u>Fortran Symbol</u>	<u>Definition</u>	<u>Text Reference</u>
W_{fl}	WFL	Weight of fuel fed to the reactor.	(4. 129)
X	-	Excess absorption term for resonance region due to the higher value of the average moderator flux to that of the fuel-moderator interface.	IV. A. 1. 3.
x	X	Velocity normalized to that corresponding to kT_{md} $(E/kT_{md})^{1/2}$.	(4. 2)
x_F	-	Weight fraction of U235 in the feed for the UF_6 diffusion cascade.	(4. 120)
x_P	XP	Weight fraction of U235 in product UF_6 .	(4. 119)
x_o	XO	Optimum weight fraction of U235 in the waste stream from the diffusion cascade.	(4. 119)
Y(x)	Y(I) or DPDX(I)	Flux per unit velocity, $d\phi/dx$.	(4. 1)
y(x)	Y(I)	Modified Y term used in solution of Wilkins equation $(x^{-3/2} e^{x^2/2} Y(x))$	IX. A. (3)
y	-	Fission yield.	(4. 92)
Z_{sym}	ZSYM	Designator for axial symmetry.	IX, D.
z	(J)	Axial index.	(4. 36)
z'	-	Axial length from origin.	Fig. 4.4

2. Greek Letters

<u>Text Symbol</u>	<u>Fortran Symbol</u>	<u>Definition</u>	<u>Text Reference</u>
α_m	ALPHA(M)	Average ratio of capture cross section to fission cross section for nuclide m in the resonance region.	(IV. A. 3)
β	-	Beta particle decay.	IV. A. 3.
γ	-	Eigenvalue for flux-shape iteration.	(4. 59)
γ	GAMMA	Net thermal efficiency.	(4. 103)
γ	-	Gamma ray.	IV. A. 3.
Δ	-	Spectrum parameter for Wilkins Equation; $4 \times A(x)$.	(4. 5)
δ	-	Small increment.	IX. A.
δ^2	-	Central difference operator.	IX. E. 3. 3.
δ_H	DELH	Axial extrapolation distance to zero flux (axial reflector savings when only core regions are specified).	(4. 49)
δ_R	DELR	Radial extrapolation distance to zero flux (radial reflector savings when only core regions are specified).	(4. 47)
δ_i	-	Print option designator.	(4. 158)
$\delta(k)$	-	Option designator.	IX. B. (11)
ϵ	EPSI	Fast fission factor.	(4. 23)
ζ	ZETA	Spacing in flux-time.	IX. C. 14.
η_m	ETA(M)	Fission neutrons produced per resonance absorption in nuclide m.	(4. 101)

<u>Text Symbol</u>	<u>Fortran Symbol</u>	<u>Definition</u>	<u>Text Reference</u>
θ	THETA or TH	Flux-time.	(4. 81)
θ_c	THETAC	Flux-time of central axial portion of fuel.	(4. 146B)
$\theta_{r, z}$	THETA(I, J)	Flux-time of fuel in region (r, z).	(4. 150)
$\theta_{r, z, L}$	THETAL(I, J)	Flux-time of fuel leaving region (r, z).	(4. 148)
κ	-	Reciprocal diffusion length.	(4. 15)
λ_{Xe}	XELAM	Beta-decay constant of Xenon.	(4. 91)
λ_{11}	ALAM11	Beta-decay constant of Pu241.	(4. 87)
λ	-	$(1/\bar{v})$ times the inverse reactor period.	(4. 57)
μ	AMU	Spacing in x velocity (δx).	IX. A. (5)
μ_v	AMUV	Spacing in v_{T_0} velocity (δv_{T_0}).	IX. C. 7.
ν_m	ANU(M)	Neutrons produced per fission in nuclide m.	(4. 99)
ξ	-	Average logarithmic energy decrement.	(4. 8)
$(\xi \Sigma_s)$	SDP	Slowing-down power.	(4. 4)
ρ	-	Convergence factor.	(4. 71)
Σ	SIGMA	Macroscopic cross section for thermal absorption excluding control poison, (when not otherwise subscripted).	(4. 27)
Σ_1	-	Macroscopic fast removal cross section.	(4. 22)
$(\Sigma_{ff} - \Sigma_{Xe})$	SIGMA1	Macroscopic thermal absorption cross section for the fuel excluding Xenon absorptions.	(4. 97)

<u>Text Symbol</u>	<u>Fortran Symbol</u>	<u>Definition</u>	<u>Text Reference</u>
Σ_w	SIGMAW	Macroscopic thermal absorption cross section for control poison.	(4. 27)
$\nu\Sigma_f$	C10	"Thermal production" cross section.	(4. 99)
Σ_f	C53	Macroscopic thermal fission cross section.	(4. 98)
$\Sigma_{Xe, max}$	SGXEMX	Maximum macroscopic Xe cross section (high flux).	(4. 92)
σ_m	SIG(M) or CSF2	Average thermal microscopic cross section for nuclide m.	(4. 82)
σ_{FP}	SIG(7)	Average cross section for low cross section fission product pairs.	(4. 90)
$\sigma_{i, m}$	SIGX(I, M)	Microscopic cross section for nuclide m at velocity, v_{T_0} , step i.	IX. C. 7.
τ	TAU	Fermi age.	IV. A. 2. 2
ϕ	PHI or FLF2	Thermal neutron flux.	(4. 27)
ψ	PSI	Thermal disadvantage factor (n_{md}/n_{fl}).	IX. C. 8.
$\psi_{1, m}$	PSI1(M)	Resonance disadvantage factor for nuclide m.	(4. 7)

3. Subscripts

<u>Text Symbol</u>	<u>Fortran Symbol</u>	<u>Definition</u>	<u>Text Reference</u>
c	C	Central value.	(4. 146B)
c	-	See p_c .	-
cst	CST	Cost.	Table D3.
d	-	See P_d , W_d .	-
e	-	Epithermal.	IV. B. 2.
E	-	See C_E .	-
eff	-	Effective value.	(4. 8A)
F	-	See C_F .	-
FP	(7)	Fission products group having cross sections less than 10,000 b.	(4. 90)
f	-	Fission.	(4. 98)
fb	-	See C_{fb} .	-
fl	FL	Fuel.	(4. 8)
i	(I)	Velocity index, x or v_{T_0} .	IX. A(5)
j	(J)	b index.	IX. A.
j	(J)	Cost set index.	IV. B. 2.
k	(K)	Diagonal or second index for Crout reduction.	IX. B.
Lag	LAG	Lagrangian coefficient.	IX. C. 23.
L	L	Last (i. e., final) value.	(4. 47)
L	-	See t_L .	-
m	(M)	Nuclide index.	IV. A. 3.
max	-	Maximum value.	(4. 92)

<u>Text Symbol</u>	<u>Fortran Symbol</u>	<u>Definition</u>	<u>Text Reference</u>
md	-	Moderator.	(4. 8)
mt	-	See \bar{C}_{mt} .	-
N	N	See F_N .	-
n	(N)	Row (or first) index for Crout reduction.	IX. B.
nat	-	See f_{nat} .	-
P	P	Product (U235), see C_P and x_P .	(4. 119)
R	R	Recycled (in $N_{m,R}$).	IV. B. 2.
R	R	See t_R .	-
r	(I)	Radial index.	(4. 36)
recy	RECY	See f_{recy} .	-
rp	-	See \bar{C}_{rp} .	-
Sm	SM	Samarium group of fission products with cross section greater than 10,000 b excluding Xe 135.	(4. 93)
s	-	Scattering (for cross sections).	(4. 4)
th	-	Thermal.	IV. B. 2.
sp	SP	See n_{sp} .	-
T_o	-	See v_{T_o} .	-
u	-	Neighbor mesh point identification index.	(4. 39)
V	-	See t_V .	-

<u>Text Symbol</u>	<u>Fortran Symbol</u>	<u>Definition</u>	<u>Text Reference</u>
v	V	See μ_v .	-
W	W	Working capital.	(4. 143)
w	W	Control poison.	(4. 27)
Xe	XE	Xenon 135.	(4. 92)
z	(J)	Axial index.	(4. 36)
ζ	-	Flux-time step.	IX. C. 14.
θ	-	Flux-time.	IX. C. 14.
o	-	2200 m/s value, v_o , T_o .	-
o	-	See x_o .	-
1	-	Fast group index.	(4. 22)
8	(1)	Fast fission terms for U238 (a_8 , η_8 , $y_{Xe, 8}$, $y_{Sm, 8}$).	IV. A. 3.
5	(2)	Fission terms for U235 ($\sigma_{f, 5}$, ν_5 , a_5 , η_5 , $y_{Xe, 5}$, $y_{sm, 5}$).	"
9	(3)	Fission terms for Pu239..	"
11	(4)	Fission terms for Pu241.	"
5	(5)	U235 (other than fission terms).	"
6	(6)	U236.	"
FP	(7)	Low cross section fission products.	"
8	(8)	U238 (other than fast fission terms).	"
9	(9)	Pu239 (other than fission terms).	IV. A. 3.
10	(10)	Pu240.	"

<u>Text Symbol</u>	<u>Fortran Symbol</u>	<u>Definition</u>	<u>Text Reference</u>
11	(11)	Pu241 (other than fission terms).	IV. A. 3.
12	(12)	Pu242.	"

4. Superscripts

eff	—	Effective value, see I_m^{eff} .	—
(i)	—	Value for i^{th} iteration.	IX. E. 1.
o	—	2200 m/s value.	(5. 9)
o	—	Initial value.	IV. B. 2.
'	—	To distinguish a length from an index, see z' .	—
'	—	To distinguish the true value from the approximate value.	IX. E. 3. 2.
∞	—	Infinite dilution value, see I_m^{∞} .	—
\wedge	—	Effective cross section for 2200 m/s flux.	(5. 20)

H. BIBLIOGRAPHY

1. Index

The references are listed in alphabetical groups by author or, if no authors were indicated, by report title. For convenience the references will be indexed below under various topics related to fuel cycles. Only a few of the general fuel cycles references have been indexed, and these were chosen because they are the more basic or comprehensive of the numerous references cited.

- 1) Blackness Theory: G11, K11, S10, T2.
- 2) Blending of UF with natural U: B7, H7, K2.
- 3) Burnable poisons: B8, D8, W2.
- 4) Cladding material for fuel elements: A3, B6, G3, L18.
- 5) Computer codes, nuclear: A4, A16, B14, C1, C3, C16, G6, G10, H5, H11, H12, K12, L25, L26, M2, R1, W16.
- 6) Costs: A7, A12, B1, B22, C8, C14, E5, E7, E8, F1, J1, J3, L1, L2, N5, P1, P3, R7, S4, T4, T6, U4-17, W3, Z1, R12.
- 7) Cross sections: A4, A5, A6, A13, C13, D6, H29, P2, W11.
- 8) Experimental data: A9, C11, D4, H15, H20, H28, K8, K11, L5, L23, L24, W17.
- 9) Fission products: B12, B13, B15, B21, B23, C11, C12, D1, D5, D7, G12, H16, H18, H21, J2, O1, O2, R4, S1, S3, W4, W6.
- 10) Fuel cycles, general: B4, D10, F2, L20, L24, P3, S6.
- 11) Flux spatial distribution (regional) and fuel scheduling: D3, G8, G15, H11, H13, L14, L18, M8, M7.
- 12) Local flux distribution: A14, H20, H26, K7, K10, K11, S10.

- 13) Power requirements: B3, D2, E4, G5, H8, H10, R6.
- 14) Plutonium recycle: A2, B2, H25, P3,
- 15) Resonance absorptions: A1, C13, D9, G14, G11, I1, R9.
- 16) Temperature coefficients: G1.
- 17) Thermalization: A4-6, B16-20, C5-7, C9, C10, D12, G11,
G13, H24, K9, L3, N1-4, P4, P5, T7, W13, W14.

2. Reference Citations

In the following listings "PICG(1) n(1955)" will be used as an abbreviation for "Proceedings of the International Conference on the Peaceful Uses of Atomic Energy, in Geneva, 1955, Vol. n." "ICG(2), P/n(1958)" will be used as an abbreviation for "International Conference on the Peaceful Uses of Atomic Energy, in Geneva, 1958, Paper No. n."

- A1 Adler, F. T., G. W. Hinman, and L. W. Nordheim: The Quantitative Evaluation of Resonance Integrals, ICG(2), P/1988(1958).
- A2 Albaugh, F. W., and R. M. Fryar: Program Study Report on Plutonium Fuel Cycles, HW-44703, 1956.
- A3 Albrecht, W. L.: Effect on the Power Cost of the Substitution of Al for Zr Cladding in Boiling Water Reactors, CF-58-7-86, 1958.
- A4 Amster, H., and R. Suarez: The Calculation of Thermal Constants Averaged over a Wigner-Wilkins Flux Spectrum: Description of the SUFOCATE code, WAPD-TM-39, 1957.
- A5 Amster, H. J.: Wigner-Wilkins Calculated Thermal Neutron Spectra Compared with Measured in a Water Moderator, Nuclear Sci. and Eng. 2, 394(1957).
- A6 Amster, H. J.: A Compendium of Thermal Neutron Cross Sections Averaged over the Spectra of Wigner and Wilkins, WAPD-185, 1958.
- A7 Anderson, E. L.: Nuclear Fuel Reprocessing - Its Status and Direction, Chem. Engr. Progr. 53, 19(1957).
- A8 Arnold, E. D.: Effect of Uranium Recycle on Transuranium Element Buildup, Nuclear Sci. and Eng. 3, 707(1958).
- A9 Arnold, W. H., Jr.: Analysis of Experimental Data on Reactivity for Plutonium Bearing Fuel Rods, YAEC-57, 1958.
- A10 Arnold, W. H., Jr.: Private communications of March 23 and February 26, 1959.
- A11 The Canadian Study for a Full-Scale Nuclear Power Plant, AECL-557.
- A12 Comparison of Calder Hall and PWR Reactor Types, AECU-3398.

- A13 Reactor Physics Constants, ANL-5800.
- A14 Astley, E. R.: Energy Generation and Fission Isotope Distribution as a Function of Radius for High Exposures, HW-52274, 1957.
- A15 Guide to Abstracts and Manuals for Computer Program Interchange, Amer.Inst.Ch. E., 1959.
- A16 Archibald, J. A., Jr.: CUREBO: A Generalized Two Space Dimensional Coding with Cross Section and Depletion Calculations for the IBM 704, KAPL-1885, 1959.
-
- B1 Babcock, D. F., and ...: ICG(2), P/610 (1958).
- B2 Barbieri, L. J., J. W. Webster, and K. T. Chow: Plutonium Recycle in the Calder Hall Type Reactor, ASAE-S-8, 1958.
- B3 Baumiester, T.: Power Generation, "Nuclear Engineering," Chapt. 13, McGraw-Hill Book Company, Inc., New York, 1957.
- B4 Benedict, M., and T. H. Pigford: "Nuclear Chemical Engineering," McGraw-Hill Book Company, Inc., New York, 1957.
- B5 Benedict, M., and T. H. Pigford: Fuel Cycles in Single Region Thermal Reactors, Chem. Eng. Progr. 53, 96F and 145M(1957).
- B6 Benedict, M.: Summary Report on the Economic Comparison of Zircaloy and Stainless Steel in Nuclear Power Reactors, COLN-Y-1.
- B7 Benedict, M.: Teaching Notes, M.I.T., unpublished.
- B8 Benumof, R., and Nestor: Fuel Exposures in U-Th Reactors with Boric Acid Control, CF-57-9-68, 1957.
- B9 Benumof, R.: Reactivity Lifetime of a U-Th Bare Slab Reactor, CF-57-8-83, 1957.
- B10 Beyer: Average Properties for Fast Fission in U235 and U238, PICG(1) 5, 345(1955).
- B11 Bilodeau and Hageman: A Survey of Numerical Methods in Solution of Diffusion Problems, WAPD-TM-64, 1957.
- B12 Blomeke, J. O.: Nuclear Properties of U235 Fission Products, ORNL-1783, 1955.
- B13 Blomeke, J. O., and M. F. Todd: U235 Fission Product Production as a Function of the Thermal Neutron Flux, Irradiation Time, and Decay Time: 1) Atomic Concentrations and Gross Totals, ORNL-2127, 1957.
- B14 Bohl, H., E. Gelbard, and Ryan, MUFT-4-Fast Neutron Spectrum Code for the IBM-704, WAPD-TM-72, 1957.
- B15 Booth, A. K., and D. Schweitzer: Accumulation of Fission Products from U235, BNL-407, 1956.

- B16 Brockhouse, B. N.: "Proceedings of the Uarena Conference of the Condensed State of Simple Systems," Acta. Cryst. 10, 827(1957).
- B17 Brown, H. D., and D. S. St. John: Neutron Energy Spectrum in D_2O , DP-33, 1954.
- B18 Brown, H. D.: Neutron Energy Spectra in Water, DP-64, 1956.
- B19 Brown, H. D.: Tables of Effective Neutron Cross Sections in Water Moderated Reactors (D_2O and H_2O), DP-194, 1957.
- B20 Brown, H. D.: A Monte Carlo Study of Neutron Thermalization, J. Nuclear Energy 8, No. 4(1959).
- B21 Busimaro, U. L., S. Gallone, and D. Morgan: On the Dependence upon Energy of the Fission Product Poisoning of U235, J. Nuclear Energy 4, 319.
- B22 Butterworth, A. V.: Private communication on costs.
- B23 Bolles, and N. E. Ballou: Calculated Activities and Abundances of U235 Fission Products, Nuclear Sci. and Eng. 5, 156(1959).
- B24 Bigham, C. B., G. C. Hanna, P. R. Tunnicliffe, P. J. Champion, and M. Lounsbury: The Slow Neutron Fission Cross Sections of the Common Fissile Nuclides, ICG(2), P/204(1958).
- C1 Callaghan, J. B., et al: TURBO-A Two Dimensional Few-Group Depletion Code for the IBM-704, WAPD-TM-95, 1957.
- C2 Carter, J. C., and J. M. West: Reactivity as a Function of Irradiation Time in Thermal Reactors, ANL-5186, 1958.
- C3 Clendinning, O. A.: TRIXY, A Three Dimensional Multigroup Code: Input Preparation, KAPL-M-OAC-1, 1958.
- C4 Cohen, E. R., and R. H. Sehnert: Long Term Irradiation of Nuclear Fuels, TID-10066, 1954.
- C5 Cohen, E. R.: PICG(1)5, 405(1955).
- C6 Cohen, E. R.: The Neutron Velocity Spectrum in a Heavy Moderator, Nuclear Sci. and Eng. 2, 227(1957).
- C7 Cohen, E. R., and M. S. Nelkin: Recent Work in Neutron Thermalization, ICG(2), P/1839(1958).
- C8 Cohen, K: Nucleonics 16, 66(1958).
- C9 Corngold: Neutron Thermalization Conference, Gatlinburg, Tenn., 1958.
- C10 Coveyou, R. R., R. R. Bate, and R. K. Osborn: J. Nuclear Energy 2, 153(1956).
- C11 Craig, D. S., G. C. Hanna, D. G. Hurst, S. A. Kushneriuk, W. B. Lewis, and A. G. Ward: Long Irradiation of Natural Uranium, ICG(2), P/205(1958).
- C12 Crouch, E. G. H.: Calculation of Fission Product Accumulation, AERE-T/M-159, 1958.

- C13 Crowther, R. L., and J. W. Weil: The Effective Cross Section of Pu240 in Long Term Reactivity Calculations, GEAP-2058, 1957.
- C14 Culler, R. L., Jr.: General Economics of Chemical Reprocessing Using Solvent Extraction Processing, Preprint 22, Session XXXVII, Nuclear Sci. and Eng. Conference, 1958.
- C15 Cunningham, J. P.: Fuel Burnup Studies for a Pressurized Water Reactor, M.I.T. Masters Thesis, 1958.
- C16 Culpepper, L. M.: CANDLE 3, WAPD-TM-53 (Add. 2), 1957.
- C17 Coen, I. H., and R. W. Garbe: Quarterly Progress Report, April 1 to June 30, 1958, YAEC-87, 1958.
- C18 Colmer, F. C. W., and D. J. Littler: GLEEP: Design, Construction, and Use, Nucleonics 8, 3(1951).
-
- D1 Davidge, P. C., and C. J. Lock: Neutron Poisoning by Gaseous Fission Products, J. Nuclear Energy 6, 191(1958).
- D2 Davis, W. K., and U. M. Staebler: Highlights on Nuclear Power Development in the United States, ICG(2), P/1076(1958).
- D3 Davison, B., and H. H. Clayton: The Enrichment Cost of Power Increments Gained by Flattening and by Close Rod Spacing, AECL-446.
- D4 de Boisblanc, P., et al: The RMF and Its Application, ICG(2), P/1842(1958).
- D5 Deutsch, R. W.: Fission Product Buildup in Enriched Thermal Reactors, Nucleonics 14, No. 9(1956).
- D6 Deutsch, R. W.: Computing Three Group Constants for Neutron Diffusion, Nucleonics 15(1957).
- D7 Dillon, I. G., and L. Burns, Jr.: Estimation of Fission Product Spectra in the Discharged Fuel from Fast Reactors, Nuclear Sci. and Eng. 2, 567(1957).
- D8 Dodson, W. J.: A Survey of Burnable Poisons to be Used in Structural Material of Core, KAPL-M-WJD-2, 1954.
- D9 Dresner, L.: Tables for Computing Effective Resonance Integrals, Including the Doppler Broadening of Nuclear Resonances, CF-55-9-74, 1955.
- D10 Dunworth, J. V.: Fuel Cycles and Types of Reactors, PICG(1) 3, 14(1955).
- D11 Dunworth, J. V.: The Methods of Using Fuels in a Nuclear Power Program, Acta. Phys. Austriaca 11, 452(1958).
- D12 de Sobrino, L. G.: Seminar at M.I.T. on Thermalization, 1959.

- D13 Davidson, J. K., R. S. Miller, and D. J. Smith: Fast Oxide Breeder, ICG(2), P/2027(1958).
- E1 Edlund, M. C., and G. K. Rhode: Spectral Shift Control, Nucleonics 16, 80(1958).
- E2 Egelstaff, P. A., and J. H. Tait: Some Developments in Reactor Calculations, Atomics 8, 251(1957).
- E3 Ehrlich, and Hurwitz: on multigroup methods, Nucleonics 12, No. 2, 23(1954).
- E4 Emelyanov, V. S.: The Future of Atomic Energetics in the USSR, ICG(2), P/2027(1958).
- E5 Ernst, W., Norton Company: private communication of March 1958, on fabrication costs.
- E6 Eschbach, E. A., D. P. Granquist, and M. Lewis: The Comparative Economics of Plutonium Fuel Utilization and U235 Fuel Utilization in Thermal Power Reactors, ICG(2), P/1068(1958).
- E7 Status and Prospects of Nuclear Power, An Interim Survey, Report of the Technical Appraisal Task Force on Nuclear Power to the Board of Directors of the Edison Electric Institute, 1958.
- E8 Survey of Initial Fuel Costs of Large U.S. Nuclear Power Stations, A Report of the Technical Appraisal Task Force on Nuclear Power to the Board of Directors of the Edison Electrical Institute, 1958.
- F1 Feinberg, S. M., and S. A. Skvortsov: The Economics of Atomic Power, J. Nuclear Energy 3, 383(1956).
- F2 Feinberg, S. M., et al: Burnup of Fuel in Water-Moderated and Water-Cooled Power Reactors and Uranium Water Lattice Experiments, ICG(2), P/2145(1958).
- F3 Fox, R. H.: Reactivity Lifetime Calculations for Large One-Region, Homogeneous, Fixed Fuel, Thermal Breeders, UCID-4002, 1958.
- F4 Fromheld, A., Jr.: Reactivity Lifetimes with Non-Uniform Burnup, CF-57-9-92, 1957.
- G1 Gast, P. F.: Reactivity Temperature Coefficient of High Exposure Piles, HW-34082, 1954.

- G2 Gill, S. : A Process for the Step by Step Integration of Differential Equations in an Automatic Digital Computing Machine, Proc. Cambridge Phil. Soc. 47, 96 (1951).
- G3 Glass, J. Y.: Contribution to Power Cost by Sheathing Materials, AECL-547, 1957.
- G4 Glasstone, S., and M. C. Edlund: "The Elements of Nuclear Reactor Theory," D. Van Nostrand Company, Inc., New York, 1952.
- G5 Goodman, C., L. H. Roddis, and W. H. Zinn: Experience with United States Power Reactors, ICG(2), P/1075(1958).
- G6 Goto, M., et al: Burnup Calculations of Natural-Uranium Graphite Moderated Power Reactors by Using Digital Computers, ICG(2), P/1339(1958).
- G7 Goller, K. R.: "Engineering and Cost Analysis of Fuel Cycles in a Zirconium-Clad Pressurized-Water Reactor," S.M. Thesis, M.I.T., 1958.
- G8 Grant, P. J.: Fuel Cycling in Nuclear Power Reactors, G.E.C. Atomic Energy Review, 1958.
- G9 Graves, H. W., Jr.: Determination of the Reactivity Lifetime for Low Enrichment, Light-Water Moderated Power Reactors, WIAP-NM-16, 1954.
- G10 Graydon, R. J.: Nuclear Codes, Nu 15, No. 5, 1957.
- G11 Greebler, P., W. H. Harker, J. M. Harriman, and E. L. Zebroski: Recycle of Plutonium in Low-Enrichment Light Water Reactors, ICG(2), P/2167(1958).
- G12 Greebler, P., H. Hurwitz, and Storm: Statistical Evaluation of Fission Products Cross Sections at Intermediate and High Energies, Nuclear Sci. and Eng. 2, 334(1957).
- G13 Greebler, P., W. H. Harker, and J. M. Harriman: Neutron Thermalization Calculations in Heterogeneous Lattices Containing U and Pu Fuel in Water, VAL-67.
- G14 Gurevich, I. I., and I. Y. Pomeranchouk: The Theory of Resonance Absorptions in Heterogeneous Systems, PICG(1) 5, 466(1955).
- G15 Graves, H. W., Jr., W. H. Arnold, Jr., W.J. Eich, G. M. Minton, R. E. Wolf: A Study of Loading Configurations for the Yankee Reactor, YAEC-114, 1959.
- H1 Hall, D, and J. Hall: Effect of Temperature and Reactivity Changes in the Operation of the Los Alamos Plutonium Reactor, LAMS-733, 1948.
- H2 Hall, D. B.: Plutonium Fuels for Fast Reactors, ICG(2), P/2021(1958).

- H3 Halperin, J., and R. W. Stoughton: Heavy Isotope Build-up in the Core of the U233 Breeder, ORNL-1567(del), 1953.
- H4 Halperin, J., and J. O. Blomeke: Effective Reactor Cross Sections for MTR Fuel Assemblies, Nuclear Sci. and Eng. 3, 395(1958).
- H5 Hellens, R. L., B. H. Mount, and W. R. Long: Multi-Group Fourier Transform Calculation: Description of MUFT-3 code, WAPD-TM-4, 1956.
- H6 Herron, D. P., W. H. Newkirk, and A. Puishes: An Evaluation of Heavy Water Reactors for Power, ASAE-S-3, 1957.
- H7 Herron, D. P., D. R. Mash, and J. W. Webster: Fuel Cycles for Nuclear Power Reactors, ICG(2), P/1044(1958).
- H8 Hillberry, N.: Report on Full Scale Power Reactor Projects in the U.S.A., ICG(2), P/2447(1958).
- H9 Hinman, G.: Calculation of the Effect of Fuel Burnup on Fuel and Poison Distributions in the Marine Reactor, AECU-3596.
- H10 Hinton, C.: The Outlook for Economic Nuclear Power, At. Nuc. Eng. 9, 224(1958).
- H11 Hitchcock, A. J. M., V. E. Price, and J. Shenton: Flux Changes in a Thermal Reactor under Long-Term Irradiation, IGR-R/R-208, 1957.
- H12 Hoffman, G. W.: One Dimensional Few Group Burnout Code and Isotropic Density Equations, WAPD-TM-2, 1956.
- H13 Hofmann, P. L., and H. Hurwitz: Application of Minimum Loading Conditions to Enriched Lattices, Nuclear Sci. and Eng. 2, 461(1957).
- H14 Howerton, R. J.: Pile Production of Plutonium Irradiated under Time Variable Flux Conditions, IDO-16405, 1957.
- H15 Hurst, D. G.: Experiments on Some Characteristics of the NRX Reactor: Part 1, Methods and Prolonged Fuel Irradiation, AECL-204, 1955.
- H16 Hurst, D. G.: An Estimate of Total Cross Sections of Accumulated Fission Products, AECL-248, 1951.
- H17 Hurst, D. G., and H. Gellman: Calculated Cross Sections of Irradiated Thorium, AECL-250.
- H18 Hurst, D. G.: Calculation of the Cross Sections of Irradiated Fission Products, AECL-346, 1956.
- H19 Hurst, D. G.: Calculated Cross Section of Irradiated Thorium (revised), AECL-364, 1956.
- H20 Hurst, D. G., A. H. Booth, M. Lounsbury, and G. C. Hanna: NRX Rod 683: Analysis of Irradiated Uranium and Estimation of Effective Cross Sections, AECL-447, 1957.
- H21 Hurst, D. G., Kennedy, and W. H. Walker: Cross Sections and Yields of Pseudo Fission Products, AECL-715, 1958.

- H22 Deleted
- H23 Hurwitz, H., and R. Ehrlich; on multi-group methods, PICG(1) 5, 423(1955).
- H24 Hurwitz, H., M. S. Nelkin, and G. J. Habetler: Neutron Thermalization 1. Heavy Gaseous Moderator, Nuclear Sci. and Eng. 1, 280(1956).
- H25 The Plutonium Recycle Program – A Resume of the Concept, Progress, and Facilities, HW-50700, 1957.
- H26 Honeck, H. C.: A Method for Computing Thermal Neutron Distributions in Reactor Lattices as Functions of Space and Energy, M.I.T. Sc.D. Thesis, 1959.
- H27 Hildebrand, F. B.: "Introduction to Numerical Analysis," McGraw-Hill Book Company, Inc., New York, 1956.
- H28 Hone, D. W., E. Critoph, M. F. Curet, R. E. Green, A. Okazaki, R. M. Pearce, and L. Pearce: Natural Uranium Heavy Water Lattices, Experiment and Theory, ICG(2), P/212(1958).
- H29 Hughes, D. J., and R. B. Schwartz: Neutron Cross Sections, Second Edition, BNL-325, 1958.
- I1 Ioffe, B. L., and L. B. Okun: Effect of Long Term Irradiation, Soviet J. Atomic Energy 4, 80(1956).
- J1 Jealous, A. C., and R. J. Klotzbach: Reprocessing Costs for Fuel from a Single Region Aqueous Homogeneous Reactor, Nuclear Eng. and Sci. Conference, Chicago, 1958.
- J2 Johnson, B. W., and H. L. McMurry: Reactivity Effects of Xe135 and Sm149 for MTR with U235 and Pu239 Fuels, IDO-16398, 1957.
- J3 Judkins, M. F.: Price of Reactor Materials, Nucleonics, No. 1, 1958.
- K1 Kallman, D.: Heat Transfer Economics as Related to Design of Nuclear Fuel Elements, Chem. Eng. Progr. 53, 289(1957).
- K2 Kallman, D., and Brennan: Blending versus Re-enrichment, Nucleonics 16, 101(1958).
- K3 Kasten, P. R., and H. C. Claiborne: Fuel Costs in Homogeneous U235 Burners, Nucleonics 14 (1956).

- K4 Kasten, P. R., T. B. Fowler, and M. P. Lietzke: Fuel Costs in Single Region Homogeneous Power Reactors, ORNL-2341, 1957.
- K5 Kazachkovsky, O. D.: The Economics of Fast Power Reactor Nuclear Fuel, ICG(2), P/2028(1958).
- K6 Klahr, C.: Limitations of Multigroup Calculations, Nuclear Sci. and Eng. 1, 253(1956).
- K7 Klein, D., W. Baer, and G. G. Smith: Spatial Distribution of U238 Resonance Neutron Capture in Uranium Metal Rods, Nuclear Sci. and Eng. 3, 698(1958).
- K8 Kouts, H. J., and K. W. Downes: Reactivity Coefficient Measurement of Buckling, BNL-1785, 1954.
- K9 Krieger, T. J., P. F. Zweifel, M. L. Storm, and D. M. Keaveney: The Influence of Non-1/v Absorbers on Reactor Parameters, Gatlinburg Conference on Neutron Thermalization, 1958.
- K10 Kushneriuk, S. A.: Neutron Capture by Long Cylindrical Bodies Surrounded by Predominantly Scattering Media, AECL-462, 1957.
- K11 Kushneriuk, S. A.: Effective Cross Sections and Neutron Flux Distribution in a Natural Uranium Rod. Applications to Rod 683, AECL-497, 1957.
- K12 CURE: A Generalized Two Dimension Coding for the IBM-704, KAPL-1724, 1957.
-
- L1 Lane, J. A.: on fuel cycle costs, PICG(1) 1, 309(1955).
- L2 Lane, J. A., et al: Homogeneous Reactor Cost Studies, "Fluid Fuel Reactors," Atoms for Peace Series, Addison-Wesley Press, Inc., Cambridge, Mass., 1958.
- L3 Leibfried, G.: A Remark on Neutron Thermalization Theory, Nuclear Sci. and Eng. 4, 570(1958).
- L4 Lewis, W. B.: Possibilities of Generating Atomic Electric Power at Competitive Rates, AECL-178, 1955.
- L5 Lewis, W. B.: Reactivity Changes Expected and Observed in the Long Irradiation of Natural Uranium in the NRX Reactor, AECL-187, 1952.
- L6 Lewis, W. B.: Calculated Reactivity Changes in the Long Term Irradiation of Natural Uranium, AECL-188, 1953.
- L7 Lewis, W. B.: Note on Possibilities of Uranium-Plutonium Regenerative Thermal Neutron Reactors, AECL-189, 1953.
- L8 Lewis, W. B.: Cost of Light Water as a Coolant for Enriched Power Reactors, AECL-190, 1954.
- L9 Lewis, W. B.: Economic Aspects of Nuclear Fuel Cycles, AECL-203.

- L10 Lewis, W. B.: Economic Power Fuelling without U235 Enrichment, AECL-265.
- L11 Lewis, W. B.: Attainable Burnup of Uranium with Plutonium Recycle, AECL-285.
- L12 Lewis, W. B.: The Heavy Water Reactor for Power, AECL-319, 1956.
- L13 Lewis, W. B.: Low Cost Fuelling without Recycling, AECL-382, 1956.
- L14 Lewis, W. B.: Fuelling System for a Natural Uranium Reactor with Long Rods for High Burnup without Recycling, AECL-436, 1957.
- L15 Lewis, W. B.: Comment on American Standards "An Evaluation of D₂O Reactors for Power," Project Sizeup Report ASAE-3, AECL-527, 1957.
- L16 Lewis, W. B.: High Burnup from Fixed Fuel, AECL-531, 1957.
- L17 Lewis, W. B.: UO₂ Fuel of Low Cost, AECL-568, 1958.
- L18 Lewis, W. B.: Cost Comparisons for Enriched versus Natural Uranium Fuel and for Zirconium versus Stainless Steel in Bidirectional Fuelled Reactors, AECL-651, 1958.
- L19 Lewis, W. B.: Initial Fuelling of Power Reactors, AECL-696, 1958.
- L20 Lewis, W. B.: Some Economic Aspects of Nuclear Fuel Cycles, PICG(1) 3, 3(1955).
- L21 Lewis, W. B.: Enriched or Natural Uranium, Nuclear Power 2, 340(1957).
- L22 Lewis, W. B.: Is Fuel Reprocessing Necessary? For Canada the Answer Seems to be No, Nuclear Power 3, 69(1958).
- L23 Littler, D. J.: Measurements of the Change in Cross Section of Irradiated Uranium Made by Modulating the Power of a Nuclear Reactor, AERE-RS/R-2092, 1956.
- L24 Littler, D. J.: Long Term Reactivity Changes in Natural Uranium Reactors, PICG(1) 5, 141(1955).
- L25 Leffert, C. B.: Instruction Manual for the Nuclear Reactor Code System Magnum, GMR-100, 1958.
- L26 Leshan, E. J., J. R. Burr, R. Morrison, M. Temme, G. T. Thompson, and J. R. Triplett: RBU, Calculation of Reactor History Including the Details of Isotropic Concentration, Part 1: The Method, ASAE-34, 1958.
- M1 Mandl, M. E., and J. Howlett: A Method of Calculating Critical Mass for Intermediate Reactors, PICG(1) 5, 433(1955).

- M2 Marlowe, O. L., and R. A. Ombrellav; CANDLE-A One Dimension Few Group Depletion Code for the IBM-704, WAPD-TM-53, 1957.
- M3 McKay, C. D.: Some Reactivity Effects of Irradiation in NRU, AECL-405, 1957.
- M4 McMurry, H. L.: MTR Charge Life with Mixtures of U235 and Pu239, IDO-16420, 1957.
- M5 McMurry, H. L., et al: Estimation of Charge Life for Reactors with Small Cores, Nuclear Sci. and Eng. 3, 38(-958).
- M6 Merriman, F. C.: Long Term Reactivity Changes in Medium Enrichment Reactors, KAPL-MLFCM-1, 1957.
- M7 Minton, G. H.: Nuclear Characteristics of Multi-Region Reactor Cores, YAEC-46.
- M8 Minton, G. H.: Two Dimension Diffusion Theory Studies of Flux Peaking and Control Rod Worths in the Yankee Reactor, YAEC-85, 1958.
- M9 Mooradian, A. J.: Canada's Approach to the Economic Fuelling of Power Reactors, AECL-528, 1957.
- M10 Mummery, P. W., and J. J. Syrett: Fuel Recycling in Equilibrium Uranium-Plutonium Thermal Reactors, AERE-R/R-1915, 1956.
- M11 Murray, R. L., and A. W. Banister: Calculating Burnout Effect, Nucleonics 15, No. 6, 129(1957).
-
- N1 Nelkin, M. S.: Neutron Thermalization II. Heavy Crystalline Moderator, Nuclear Sci. and Eng. 2, 199(1957).
- N2 Nelkin, M. S.: The Thermal Spectrum of an Intermediate Assembly, Nuclear Sci. and Eng. 2, 373(1957).
- N3 Nelkin, M. S.: Chemical Binding Effects in Hydrogen-Moderated Reactors, Gatlinburg Conference, 1958.
- N4 Nelkin, M. S., and E. R. Cohen: Recent Work in Neutron Thermalization, GA-351, 1958.
- N5 Nuclear Power Costs, Special Report, Nucleonics, No. 1, 1958.
- N6 Nuclear Reactor Data 2, Raytheon, 1956.
-
- O1 Obenshain, F. E., and B. D. O'Reilly: Distribution of Fission Product Gases in PWR Type Reactor Systems, WAPD-TN-522, 1955.
- O2 Old, C. C.: Fast Reactor Poisoning by Fission Products, LWS-24612, 1952.

- P1 Perez-Belles, R.: on the breakeven price of Plutonium as a function of isotopic composition, M.S. Thesis, M.I.T., 1958.
- P2 Petrie, Storm, and Zweifel: Calculation of Thermal Group Constants for Mixtures Containing Hydrogen, Nuclear Sci. and Eng. 2, 728.
- P3 Pigford, T. H., M. Benedict, R. T. Shanstrom, C. C. Loomis, and B. Van Ommeslaghe: Fuel Cycles in Single-Region Thermal Power Reactors, ICG(2), P/1016(1958).
- P4 Poole, M. J.: J. Nuclear Energy 5, 325(1957).
- P5 Poole, M. J., M. S. Nelkin, and R. S. Stone: Measurement and Theory of Reactor Spectra, "Progress in the Peaceful Uses of Atomic Energy," Vol. II, Series 1, Physics and Mathematics, Pergamon Press.
- P6 Prince, B. E.: Permissible Exposure of U233-Th Fuel Elements in Reactors Having Continuous Fuel Feed, CF-57-9-95, 1957.
-
- R1 Radowsky, and Brodsky: A Bibliography of Available Digital Computer Codes for Nuclear Reactor Problems, AECU-3078, 1955.
- R2 Rae, H. K.: A Preliminary Cost Estimate for Fuel Recycling, AECL-418.
- R3 Rae, H. K.: Fuel Processing and Recycling for Natural Uranium Power Reactors, 2nd Nuclear Eng. and Sci. Conference.
- R4 Robb, W. L., J. B. Sampson, Stehn, and Davidson: Fission Product Buildup in Long-Burning Thermal Reactors, Nucleonics 13, No. 12, 30(1955).
- R5 Roberts, F., and K. Towers: Fast Reactor Fuel Processing - The Economic Importance of Cooling Time, RCTC/P-92, 1957.
- R6 Roberts, H. E.: Trends in Power Generation, Nucleonics 16, 7(1958).
- R7 Roboff, S., and L. Smiley: Sylvania Corning Nuclear Corporation, private communication of March 1958 on fabrication costs.
- R8 Roddis, L. H., Jr.: How Nuclear Power Cost Estimates Are Made, A.E.C. speech released March 18, 1958.
- R9 Roe, G. M.: The Absorption of Neutrons in Doppler Broadened Resonances, KAPL-1241, 1954.
- R10 Rosenthal, Tobias, and Fowler: Fuel Costs in Spherical Slurry Reactors, ORNL-2313, 1957.
- R11 Radiation Effects in UO₂, Reactor Core Materials 1, No. 1, 12(1958).
- R12 Reactor Fuel Processing 1, No. 3 (1958).

- S1 Sampson, J. B., W. L. Robb, J. R. Stehn, and J. K. Davidson: Poisoning in Thermal Reactors Due to Stable Fission Products, KAPL-1226.
- S2 Shanstrom, R. T., C. T. McDaniel, and M. Benedict: Progress Report on MIT Fuel Cycle Study Project, Sept., 1957 - March, 1958, NYO-2128, 1958.
- S3 Shanstrom, R. T.: Gross Fission Product Cross Sections, GAMD-444, 1958.
- S4 Smith, R. J.: Economics of Nuclear Power: A Literature Search, TID-3510, 1957.
- S5 Sola, J. P. A.: Mathematical Treatment of Batch Irradiation of Nuclear Fuels in a Non-Uniform Neutron Flux, M.S. Thesis, M.I.T., 1957.
- S6 Spinrad, Carter, and Egger: Reactivity Changes and Reactivity Lifetimes of Fixed Fuel Elements in Thermal Reactors, PICG(1) 5, 125(1955).
- S7 Sporn, P.: Power Reactors 4. Outlook for Utilities, Nucleonics, 15, No. 9, 104(1957).
- S8 Starr, C.: Power Reactors. 2. Economic Trends, Nucleonics 15, No. 9, 94(1957).
- S9 Starr, C.: Fuel Enrichment and Reactor Performance, ICG(2), P/1078(1958).
- S10 Stuart, G. W.: on Blackness Theory, Nuclear Sci. and Eng. 2, 617(1957).
- S11 Syrett, J. J., and J. A. Dyson: Fuel Recycling in Equilibrium Thorium Single Region Thermal Reactors, AERE-R/R-2167, 1957.
- S12 Shanstrom, R. T., C. T. McDaniel, and M. Benedict: Progress Report on MIT Fuel Cycle Study Project, April 1 - October 1, 1958, NYO-2129, 1959.
- S13 Shanstrom, R. T., C. T. McDaniel, and M. Benedict: Progress Report on MIT Fuel Cycle Study Project, October, 1958 - April, 1959, NYO-2130, 1959.
- T1 Triplett, J. R.: Reactivity Changes and Isotope Yields at High Temperatures, HW-33912, 1955.
- T2 Triplett, J. R.: Proceedings of the Brookhaven Conference on Resonance Absorption of Neutrons in Nuclear Reactors, Sept. 1956, BNL-433, p. 79, 1957.
- T3 Triplett, J. R.: Nuclear Problems Associated with Plutonium Fuel Cycles and with the Experimental Reactor, Paper at Session 13, New York, Amer. Inst. Ch. E.

- T6 Topical Law Reports, Atomic Energy Issues.
- T7 Takahashi, H.: The Thermal Neutron Spectrum in a Heterogeneous Reactor, Nuclear Sci. and Eng. 5, 338(1959).
- T8 Tattersall, R. B., W. A. Cooper, D. Jowitt, and S. K. Pattendon; Oscillator Measurements of Some Major Fission Product Poisons, A.E.R.E. - R/R-2459, 1958.
- U1 Ulmann, J. W.: Effect of Plant Size on Costs of Purex Processing of Heterogeneous Power Reactor Fuel, ORNL-2020, 1956.
- U2 Ullman, J. W.: Heavy Element Isotopic Build-Up, Symposium of Reprocessing Irradiated Fuels, Brussels, 1957.
- U3 Ullman, J. W.: Economics of Nuclear Power, Science 127, 739(1958).
- U4 USAEC Press Release on the price of natural uranium metal and of heavy water, August 8, 1955.
- U5 USAEC Press Release on the price of enriched uranium as UF_6 , Nov. 18, 1956.
- U6 U.S. Federal Register Notice of Commission Service in the Chemical Processing of Spent Fuels, March 8, 1957.
- U7 U.S. Federal Register Notice on plutonium guaranteed fair prices, Vol. 22, 395, June 6, 1957.
- U8 U.S. Federal Register Notice on Uranyl-233 Nitrate prices, Vol. 22, 251, 10965, Dec. 28, 1957.
- U9 USAEC Press Release A-45 on Commission Service in the Chemical Processing of Spent Fuels, March 7, 1958.
- U10 USAEC Press Release on the prices for the conversion of $UO_2(NO_3)_2$ to UF_6 and for the conversion of $Pu(NO_3)_4$ to metal, March 17, 1958.
- U11 USAEC Press Release A-92 on the distribution policy for U235, April 25, 1958.
- U12 USAEC Announcement No. A-107 on natural uranium from private producers, May 8, 1958.
- U13 USAEC Press Release No. A-145 on Boron-10 Distribution, June 17, 1958.
- U14 USAEC Press Release, Memo of Understanding to Euratom, June 23, 1958.
- U15 USAEC Announcement No. A-158 on depleted uranium and price schedules for UF_6 , June 27, 1958.
- U16 USAEC Press Release No. TI-5 on the price of heavy water, July 3, 1958.
- U17 USAEC Press Release No. A-198 on "Plutonium: Foreign Critical Assemblies and Training Programs," Aug. 1, 1958.

- V1 Van Ommeslaghe, B.: "Fuel Cycles in a Heavy Water Moderated Natural Uranium Fueled Reactor," M.S. Thesis, M.I.T., 1958.
- V2 Vance, P.: Equations for the MTR Burnup Apportionment, IDO-16367, 1956.
- V3 Volpe, J. J., and G. G. Smith: Two Region Studies in Slightly Enriched Water Moderated, U and UO₂ Lattices, WAPD-TM-119, 1958.
- W1 Wachspress, E. L.: Two-Space-Dimension Multigroup Analysis of a Moving Fuel Reactor, KAPL-1642, 1955.
- W2 Wachspress, E. L.: A Burnable Poison Optimization Study, KAPL-M-ELW-6, 1957.
- W3 Wade, F. J.: private communication on conversion and fabrication prices, Mallinckrodt Chemical Works, Dec. 12, 1958.
- W4 Walker, W. H.: Fission Product Accumulation, AECL-309, 1956.
- W5 Webster, J. W.: Reactivity Losses in the First 3 x 9 Loading of MTR, IDO-16026, 1952.
- W6 Webster, J. W.: The Low Cross Section Fission Product Poisons, IDO-16100, 1953.
- W7 Weinburg, A. M.: Survey of Fuel Cycles and Reactor Types, PICG(1) 3, 19(1955).
- W8 Weinberg, A. M., and E. P. Wigner: "The Physical Theory of Neutron Chain Reactors," The University of Chicago Press, 1958.
- W9 Westcott, C. H.: on neutron cross sections, AECL-352.
- W10 Westcott, C. H.: Effective Cross Section Values for Well Moderated Thermal Reactor Spectra, AECL-407, 1957.
- W11 Westcott, C. H.: Effective Cross Sections for Well-Moderated Thermal Reactor Spectra (1958 Revision), AECL-670, 1958.
- W12 Westcott, C. H., W. H. Walker, and T. K. Alexander: Effective Cross Sections and Cadmium Ratios for Neutron Spectra of Thermal Reactors, ICG(2), P/202(1958).
- W13 Wigner, E. P., and J. E. Wilkins, AECD-2275.
- W14 Wilkins, J. E., R. Hellens, and Zweifel: Status of Experimental and Theoretical Information on Neutron Slowing Down Distribution in Hydrogenous Media, PICG(1) 5, 62(1955).
- W15 The Effect of Buckling on Multigroup Diffusion Theory Group Constants Calculated by MUFT Code, WAPD-TM-50, 1957.
- W16 PDQ-An IBM 704 Code to Solve the Two Dimensional, Few Group, Neutron Diffusion Equation, WAPD-TM-70, 1957

- W17 Ward, A. G., and D. S. Craig: Measurement of the Reactivity Change with Irradiation for Natural Uranium Samples Irradiated in NRX, CRRP-761-A, AECL-812, 1959.
- Y1 "Yankee Atomic Electric Company Research and Development Program, Reference Design," YAEC-1, 1957.
- Z1 Zebroski, E. L.: private communication on fabrication costs, Jan. 6, 1959.